



**You have downloaded a document from  
RE-BUŚ  
repository of the University of Silesia in Katowice**

**Title:** Procesy utleniania i redukcji dla pochodnych 1,10-fenantroliny oraz ich analogów = Oxidation and reduction processes for 1,10-phenanthroline derivatives and their analogs

**Author:** Jakub Wantulok

**Citation style:** Wantulok Jakub. (2021). Procesy utleniania i redukcji dla pochodnych 1,10-fenantroliny oraz ich analogów = Oxidation and reduction processes for 1,10-phenanthroline derivatives and their analogs. Praca doktorska. Katowice : Uniwersytet Śląski

© Korzystanie z tego materiału jest możliwe zgodnie z właściwymi przepisami o dozwolonym użytku lub o innych wyjątkach przewidzianych w przepisach prawa, a korzystanie w szerszym zakresie wymaga uzyskania zgody uprawnionego.



UNIwersytet śląski w Katowicach  
Wydział Nauk ścisłych i Technicznych



## ROZPRAWA DOKTORSKA

Procesy utleniania i redukcji dla pochodnych  
1,10-fenantroliny oraz ich analogów

**Jakub Wantulok**

*Promotor:*

**Dr hab. inż. Jacek Nycz**

*Promotor pomocniczy:*

**Dr Romana Sokolová**

**Katowice 2021**

*Jakub  
Wantulok*

UNIVERSITY OF SILESIA IN KATOWICE  
FACULTY OF SCIENCE AND TECHNOLOGY



## **DOCTORAL DISSERTATION**

**Oxidation and reduction processes for 1,10-phenanthroline  
derivatives and their analogs**

**Jakub Wantulok**

*Supervisor:*

**PhD DSc Eng. Jacek Nycz**

*Co-supervisor:*

**PhD MSc Romana Sokolová**

**Katowice 2021**

## Acknowledgments

I would like to sincerely thank my supervisors **Dr. Jacek Nycz** and **Dr. Romana Sokolová** for the guidance, patient supervision, and encouragement throughout the course of my research.

I would also like to thank **Dr. Maria Książek**, **Prof. Jan Grzegorz Malecki** and **Prof. Joachim Kusz** for making X-ray measurements.

I'd like to thank all the academic and technical staff, especially **Ms Danuta Kwapulińska** for making NMR measurements.

## Table of contents

<b>1. GENERAL INTRODUCTION</b> .....	<b>7</b>
<b>2. ABSTRACT IN ENGLISH</b> .....	<b>10</b>
<b>3. ABSTRACT IN POLISH</b> .....	<b>14</b>
<b>4. ACRONYMS AND ABBREVIATIONS</b> .....	<b>18</b>
<b>4.1 Abbreviations of compounds used in Results and discussion and Experimental:</b> .....	<b>19</b>
<b>5. LITERATURE REVIEW</b> .....	<b>21</b>
<b>5.1 The <i>N</i>-heterocyclic compounds - introduction</b> .....	<b>21</b>
<b>5.2 Phenanthroline: a brief history</b> .....	<b>22</b>
<b>5.3 Methods of synthesis of 1,10-phenanthrolines and their derivatives</b> .....	<b>23</b>
5.3.1 Synthesis of 1,10-phenanthroline derivatives by the modified Skraup methods	23
5.3.2 Synthesis of 1,10-phenanthroline derivatives based on Meldrum acids .....	26
<b>5.4 Applications of selected 1,10-phenanthroline and their metal complexes</b> .....	<b>32</b>
<b>5.5 Theoretical calculation of 1,10-phenanthroline</b> .....	<b>34</b>
<b>5.6 Functionalization of selected 1,10-phenanthroline</b> .....	<b>35</b>
5.6.1 Oxidation of 1,10-phenanthroline derivatives .....	35
5.6.2 Selected acids derivatives of 1,10-phenanthroline .....	41
<b>5.7 Synthesis of substituted 1,10-phenanthroline derivatives</b> .....	<b>43</b>
5.7.1 Nucleophilic Aromatic Substitution.....	43
5.7.2 Synthesis of mono- and disubstituted 1,10-phenanthroline by selected amines in ortho and para position .....	46
5.7.3 Optical properties and applications of mono and disubstituted-1,10- phenanthrolines .....	49
<b>5.8 Quinoline derivatives: introduction</b> .....	<b>53</b>
<b>5.9 The use of Skraup reaction and reaction using Meldrum acid transformation of     selected quinolines</b> .....	<b>55</b>

<b>5.10</b>	<b>Functionalization of selected quinolines .....</b>	<b>58</b>
5.10.1	Formylation of quinoline derivatives via Electrophilic Aromatic Substitution .	58
5.10.2	The preparation of selected quinoline carboxylic acids .....	61
<b>5.11</b>	<b>Electrochemical properties of selected <i>N</i>-heterocycles.....</b>	<b>62</b>
5.11.1	Electrochemical properties of 1,10-phenanthroline .....	63
5.11.2	Electrochemical behavior of chlorinated aromatic compounds .....	64
5.11.3	Electrochemical properties of pyrrolidine, 9 <i>H</i> -carbazole, and 10 <i>H</i> -phenothiazine derivatives .....	65
<b>6.</b>	<b>RESULTS AND DISCUSSION .....</b>	<b>69</b>
<b>6.1</b>	<b>Introduction .....</b>	<b>69</b>
<b>6.2</b>	<b>Synthesis, functionalization and oxidation, and reduction processes of 1,10-phenanthroline derivatives .....</b>	<b>71</b>
6.2.1	Syntheses of symmetrical and unsymmetrical 1,10-phenanthroline derivatives based on synthesis with Meldrum acid .....	71
6.2.2	Electrochemical and spectroelectrochemical studies of selected 4,7-dichloro-1,10-phenanthroline.....	74
6.2.3	Functionalization of selected 1,10-phenanthrolines with pyrrolidine, 9 <i>H</i> -carbazole and 10 <i>H</i> -phenothiazine substituents. ....	85
6.2.4	Electrochemical and spectroelectrochemical studies of selected 4,7-di(pyrrolidin-1-yl)-1,10-phenanthroline.....	89
6.2.5	Electrochemical and spectroelectrochemical studies of 4,7-di(9 <i>H</i> -carbazol-9-yl)-1,10-phenanthroline.....	104
6.2.6	Electrochemical and spectroelectrochemical studies of selected 4,7-di(10 <i>H</i> -phenothiazine-10-yl)-1,10-phenanthroline.....	112
6.2.7	Oxidation and hydrolysis reactions of selected 1,10-phenanthroline.....	126
<b>6.3</b>	<b>Symmetrical and unsymmetrical 1,10-phenanthroline derivatives .....</b>	<b>137</b>
<b>6.4</b>	<b>Synthesis and functionalization of selected mono and diformyl quinolines.....</b>	<b>142</b>
6.4.1	Synthesis of selected mono and diformyl quinolines in the Reimer-Tiemann, Vilsmeier-Haack, and Duff reactions .....	142
6.4.2	Oxidation of selected diformyl quinolines. Hydroxy dicarboxylic acids.....	150
<b>6.5</b>	<b>VNS reaction in electron-deficient nitroquinolines .....</b>	<b>152</b>

<b>7. EXPERIMENTAL .....</b>	<b>159</b>
<b>7.1 Experimental techniques and computational methods .....</b>	<b>159</b>
<b>7.2 Materials.....</b>	<b>160</b>
<b>7.3 General Procedures for Synthesis of 4,7-dichloro-1,10-phenanthrolines.....</b>	<b>161</b>
7.3.1 Step A.....	161
7.3.2 Step B .....	166
7.3.3 Step C .....	170
<b>7.4 Synthesis of selected 4,7-di(pyrrolidin-1-yl)-1,10-phenanthrolines .....</b>	<b>174</b>
<b>7.5 Synthesis of 4,7-di(9<i>H</i>-carbazol-9-yl)-1,10-phenanthrolines derivatives.....</b>	<b>177</b>
<b>7.6 Synthesis of 4,7-di(10<i>H</i>-phenothiazin-10-yl)-1,10-phenanthrolines derivatives ....</b>	<b>179</b>
<b>7.7 Oxidation and hydrolysis reaction of selected 1,10-phenanthroline products. 181</b>	
7.7.1 Oxidation of 4,7-dichloro-1,10-phenanthroline .....	181
7.7.2 Procedures for Oxidation of 2,9-dimethyl-1,10-phenanthroline .....	182
7.7.3 Hydrolysis of 4,7-dichloro-1,10-phenanthroline-5-carbonitrile.....	183
7.7.4 Hydrolysis of 4,7-disubstituted-9-oxo-9,10-dihydro-1,10-phenanthroline-5-carbonitrile .....	183
<b>7.8 Symmetrical and unsymmetrical quinoline and 1,10-phenanthroline derivatives 185</b>	
7.8.1 General Procedures for Synthesis 4-chloro-2-methyl-1,10-phenanthroline.....	185
7.8.2 General Procedures for Synthesis of 4-chloro-8-nitroquinoline .....	187
7.8.3 Preparation of 4-chloro-8-aminoquinoline.....	189
7.8.4 General Procedures for Synthesis of 4,7-dichloro-2-methyl-1,10-phenanthroline .....	189
7.8.5 General Procedures for Synthesis of 7-chloro-2-methyl-1,10-phenanthrolines.....	191
<b>7.9 Synthesis of selected Quinolinecarbaldehydes .....</b>	<b>193</b>
7.9.1 Synthesis of selected Quinolinecarbaldehydes based on Reimer-Tiemann reaction .....	193
7.9.2 Synthesis of selected Quinolinecarbaldehydes based on Vilsmeier Haack reaction .....	195

7.9.3	Synthesis of selected Quinolinecarbaldehydes based on the Duff reaction .....	197
<b>7.10</b>	<b>Oxidation of selected dicarbaldehydes .....</b>	<b>199</b>
<b>7.11</b>	<b>Synthesis of selected nitroquinolines; VNS reaction.....</b>	<b>200</b>
7.11.1	Synthesis of nitroquinolines .....	200
7.11.2	VNS reaction .....	201
<b>8.</b>	<b>CONCLUSIONS .....</b>	<b>203</b>
8.1	Other research achievements .....	208
<b>9.</b>	<b>SUMMARY .....</b>	<b>208</b>
<b>10.</b>	<b>MAIN ACHIEVEMENTS .....</b>	<b>209</b>
<b>11.</b>	<b>SCIENTIFIC ACHIEVEMENTS AND SCIENTIFIC INTERNSHIPS .....</b>	<b>209</b>
11.1	Publications .....	209
11.2	Patents .....	210
11.3	Proceedings .....	210
11.4	Patent applications .....	211
11.5	Participation in national and international conferences .....	211
11.5.1	National conferences .....	211
11.5.2	International conferences .....	212
11.6	Scientific internships.....	212
<b>12.</b>	<b>LITERATURE .....</b>	<b>213</b>



# 1. General introduction

Oxidation and reduction reactions are an integral part of our lives. Thanks to these reactions, life on earth, plants, and animals' development and all changes in the inanimate matter are possible. Burning fuels provide energy to maintain civilization, and food metabolism provides energy to keep us alive, all of which are oxidation and reduction reactions. Moreover, antibiotics, drugs, vaccines containing various chemical compounds, whether through metabolism or reactions with air can be oxidized and reduced. Hence, it is essential to study the mechanisms of oxidation or reduction of chemical compounds. This type of research may predict an improvement/deterioration in anti-cancer, bactericidal, or virucidal properties. Knowledge about the products of oxidation or reduction can predict the toxicity of compounds and their stability. It allows for the design and functionalization of new compounds that exhibit new properties or improve the existing ones. Redox reactions are crucial for organic chemistry, organometallic chemistry, and biochemistry.

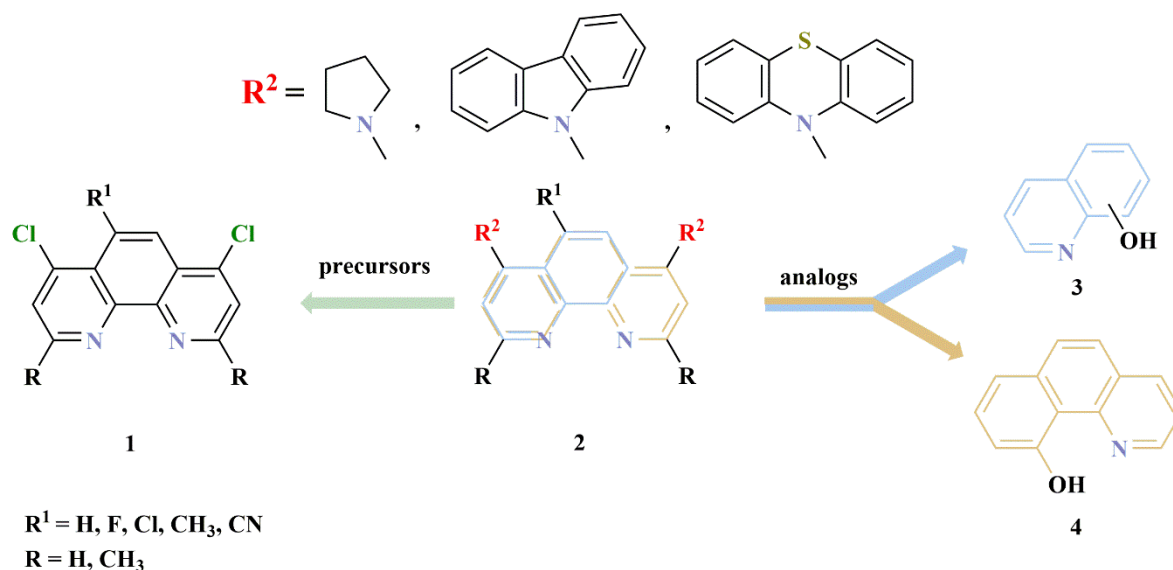
In addition to carrying out the reactions themselves, electrochemical studies are a valuable source of information. Such studies allow us to clarify the electrochemical properties or characterize the redox reaction's resulting products. This type of data makes it possible to exclude and notice how the oxidation and reduction reactions take place, which is a valuable aid in designing new syntheses or chemical compounds.

The main aim of this dissertation was to obtain new symmetrical and unsymmetrical 1,10-phenanthroline derivatives as model compounds to study oxidation-reduction processes. These molecules were selected for their possible wide range of applications, mainly due to their optical properties and metal coordination abilities. One of the target groups were amino-1,10-phenanthrolines which are promising compounds for a broad range of applications, mostly due to their metal coordination abilities and luminescence properties<sup>1,2,3,4</sup>. The functionalization of 1,10-phenanthroline derivatives was made mainly using amination reaction with selected amines is investigated in terms of their oxidation and reduction processes, whether in chemical reactions or electrochemical tests. The research was extended to precursors of 1,10-phenanthroline and their analogs, such as quinoline and benzo[*h*]quinoline derivatives, due to their structural similarities and potentially chemical similarities (Scheme 1). To prove the presence of some expected 1,10-phenanthroline oxidation products obtained during electrochemical processes, these chemicals were synthesized newly developed chemical transformations. However, reactions occur not always as known as chemical pathways. The goal was to obtain oxidation products of selected 1,10-

phenanthroline derivatives to be used as authentic samples. Oxidation processes can lead to a wide range of compounds such as ethers, epoxides, alcohols, aldehydes, or acids, hence the need for such research. The reduction processes are not so interesting in terms of synthesis for 1,10-phenanthrolines and their analogs. These processes are largely dependent on the substituents present. In the case of halogen derivatives, elimination of the halogen is expected to result. In turn, reducing the *N*-heterocycle backbones leads to a loss of aromaticity through the introduction of hydrogen, where other reactions can obtain these products.

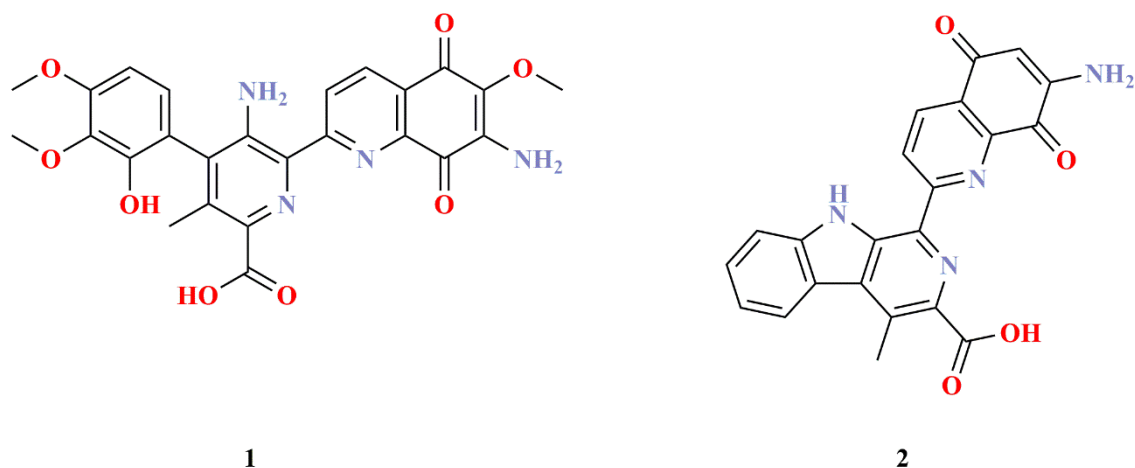
An important element of the work was the performance of DFT calculations, which allowed for deepening the interpretation of the experimental results (spectroscopic and electrochemical measurements).

The new idea was to conduct initial studies for quinoline (Scheme 1, **3**) and benzo[*h*]quinoline (Scheme 1, **4**) derivatives. Due to the complexity of the oxidation of selected 4,7-disubstituted-1,10-phenanthrolines (Scheme 1, **2**), the first step was the synthesis and oxidation of quinoline and benzo[*h*]quinoline derivatives. It is easier to understand the oxidation and reduction processes by studying simplified analogs. Importantly, this mode of operation allows to speed up and reduce the cost of research. The first phase of the research was the reactions to obtain selected carbaldehyde of quinolines and benzo[*h*]quinolines. Then the obtained compounds were used for their further functionalization, i.e., oxidation to acid and reduction to alcohols. Getting quinoline acid allows authenticating part of electrochemical tests in which the oxidation of their precursor's process may lead to acid. Based on previously developed procedures for quinoline derivatives oxidation, the oxidation of selected 1,10-phenanthrolines substituted by functional groups were studied, supported by electrochemical tests. Research performed on the oxidation of compounds is also enriched with hydrolysis reactions. Besides, electrochemical studies for 1,10-phenanthrolines were carried out for all groups of compounds obtained by their substitution as well as for their precursors.



**Scheme 1.** Structures of 4,7-disubstituted-1,10-phenanthrolines **2**, their analogs **3**, **4**, and precursors.

The *N*-heterocycles are interesting due to their wide application in the pharmaceutical and agrochemical industries. The worldwide annual production of quinoline derivatives is more than 2000 tonnes, of which 8-hydroxyquinoline makes up the main part<sup>5</sup>. They are common in many natural products. They attract considerable attention due to their biological activity, including anti-malarial<sup>6</sup>, anti-fungal<sup>7</sup>, anti-bacterial<sup>8</sup>, anti-asthmatic<sup>9</sup>, and anti-inflammatory properties<sup>10</sup>. They are also important synthetic intermediates for the production of various biologically active compounds. Some of them also show coordination properties, acting as a nitrogen atom donor for metal chelating, thanks to which they are used for metal identification or homogeneous catalysis. They are used in supramolecular chemistry as luminescent agents and photosensitizers in solar cells. The well-known streptonigrin (Scheme 2, **1**, also known as rufochromomycin and bruneomycin), lavendamycin (Scheme 2, **2**), and other similar compounds possess an *N*-heterocycle subunit.



**Scheme 2.** Structures of streptonigrin **1**, and lavendamycin **2**.

## 2. Abstract in English

This thesis report results in fourth areas: (i) the synthesis and functionalization of selected 1,10-phenanthrolines, (ii) oxidation of selected 1,10-phenanthrolines, (iii) electrochemical, spectroelectrochemical studies extended with DFT calculations, and (iv) the synthesis and functionalization of quinoline and benzo[*h*]quinoline derivatives.

In the first part, the synthesis of 4,7-dichloro-1,10-phenanthroline and their unsymmetric derivatives, including examples of compounds with only one chlorine atom, is presented.

The multi-step synthesis of 4,7-dichloro-1,10-phenanthroline derivatives was based on the reaction of Meldrum's acid with selected analogs of 1,2-diaminobenzene, known in the literature. In the case of the synthesis of monochloro derivatives of 1,10-phenanthroline, both the Skraup–Doebner–Miller reaction and the previously mentioned cyclization with the use of Meldrum's acid were used.

In part devoted to the synthesis of 4,7-disubstituted-1,10-phenanthrolines, the functionalization of some of their precursors is discussed. One of the chemical transformations that were used to accomplish this task was the aromatic nucleophilic substitution of chlorine atoms using amines such as pyrrolidine, 9*H*-carbazole, and 10*H*-phenothiazine. 5-Fluoro-4,7-di(pyrrolidin-1-yl)-1,10-phenanthroline, was determined by single-crystal X-ray diffraction measurements.

At this stage of the study, reactions to obtain monosubstituted 1,10-phenanthrolines were conducted. As a result of a series of reactions, several examples of 1,10-phenanthroline

derivatives containing a chlorine atom in different positions were obtained. The structure of the three precursors was determined using single-crystal X-ray diffraction measurements.

To obtain monosubstituted amine derivatives of 1,10-phenanthroline, a multi-stage synthesis was used, which due to the VNS substitution competitive reaction, was not successful in obtaining the expected above-mentioned compounds. The VNS reaction was investigated so as to eliminate or reduce it or to use it in the synthesis of the previously discussed compounds. To this end, a series of reactions using nitroquinolines as the precursors of 1,10-phenanthrolines as electrophiles, and 9*H*-carbazole as the nucleophilic reagent were performed. As a result of research, several products with 9*H*-carbazole in their structure were obtained. Two of the products have been determined using single-crystal X-ray diffraction measurements.

The second stage of research was studying the oxidation and hydrolysis of selected substituted 1,10-phenanthrolines. The model compounds selected for oxidation studies were derivatives of 1,10-phenanthroline with methyl and chloro substituents located at C2, C4, C5, C7, and C9 positions. Besides, oxidation reactions of 2,9-dimethyl-1,10-phenanthroline by two different methods were carried out. The first procedure was based on a developed method for the oxidation of dicarbalddehyde derivatives of quinoline and benzo[*h*]quinoline. The second method was based on the use of nitric acid and sodium bromide. However, for application reasons, these two oxidation methods have synthetic limitations. In this work, the oxidation reactions with transition metal salts were excluded due to potential metal complexation reactions by 1,10-phenanthrolines, which are excellent *N,N*-donor ligands. Also, the use of strong oxidants, such as potassium manganate(VII), has been rejected due to its destructive oxidizing properties, which many times lead to the opening of aromatic rings<sup>11</sup>.

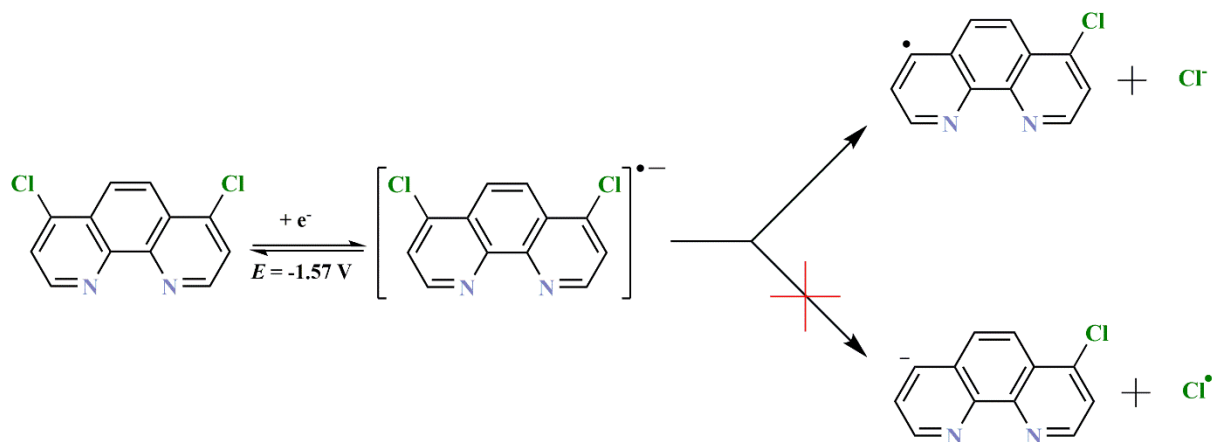
For the hydrolysis reaction, nitrile derivatives such as 4,7-dichloro-1,10-phenanthroline-5-carbonitrile, 4,7-di(9*H*-carbazol-9-yl)-1,10-phenanthroline and 4,7-di(10*H*-phenothiazin-10-yl)-1,10-phenanthroline-5-carbonitrile were selected as model compounds. In the chemical literature, there are many examples of the hydrolysis of the nitrile group leading to the synthesis of carboxylic acids or aldehydes depending on the reaction conditions used, including in particular the pH of the transformation medium<sup>12,13,14</sup>.

As a result of the conducted reactions, two groups of products were synthesized. As a result of the hydrolysis of 4,7-dichloro-1,10-phenanthroline-5-carbonitrile, 7-chloropyrrolo[2,3,4-*de*][1,10]phenanthroline-5(4*H*)-one product was obtained, most probably as a result of hydrolysis the nitrile group and the subsequent substitution of the chlorine atom

in the pyridine ring of the 1,10-phenanthroline. The second group of products is based on the NOSH reaction (Oxidative Nucleophilic Aromatic Substitution of Hydrogen). For both products, the structures were determined by single-crystal X-ray diffraction measurements.

The third stage of this research was to conduct electrochemical tests for selected compounds that were obtained as a result of the previously described reactions. The reduction and oxidation mechanism of each of the studied groups of compounds was proposed from obtained results. Spectroscopic measurements, including in particular mass spectrometry, confirmed the formation of the described products. Groups, which have been examined are derivatives of 4,7-dichloro-1,10-phenanthroline, 4,7-di(pyrrolidin-1-yl)-1,10-phenanthroline, 4,7-di(9*H*-carbazol-9-yl)-1,10-phenanthroline and 4,7-di(10*H*-phenothiazine-10-yl)-1,10-phenanthroline. A series of electrochemical and spectroelectrochemical studies for each group, supported by theoretical DFT calculations, was performed.

In the reduction processes in electrochemical studies, a selective elimination of chlorine atoms for 4,7-dichloro-1,10-phenanthrolines was shown (Scheme 3). This cleavage of chloro substituent is a well-known process<sup>15,16</sup>; however, no systematic studies have been performed for 1,10-phenanthroline derivatives.



**Scheme 3.** The proposition of reduction mechanism of 4,7-dichloro-1,10-phenanthroline.

The knowledge of the reducing potential for selected chloro derivatives of 1,10-phenanthrolines can select the best-reducing agents for use in the chlorine atom elimination reactions in the abovementioned compounds. The electrochemical studies were performed in acetonitrile as a solvent. It is worth noting that under different conditions, the redox potential has a different value.

Electrochemical knowledge of the reductive pathways for the elimination of one or two chloro substituents can help to predict reduction-based synthesis experiments.

In the case of reduction of 4,7-disubstituted-1,10-phenanthroline compounds, the subsequent reductive cleavage of the amino substituent located on C4 and C7 position was confirmed. The measurements were carried out for substituents such as pyrrolidine, 9*H*-carbazole, and 10*H*-phenothiazine. This process was interesting because the selectivity of reduction led exclusively to monosubstituted amine derivative of 1,10-phenanthroline.

There are various basic methods of eliminating halogens<sup>17,18</sup> and amine substituents, including pyrrolidine<sup>19</sup> or 9*H*-carbazole<sup>20</sup>. Still, there are no systematic studies that would show their selective removal. For this reason, electrochemical reduction studies have been performed for selected 4,7-dichloro-1,10-phenanthroline and 4,7-disubstituted-1,10-phenanthrolines.

Selective elimination of the amino substituent may be an interesting direction of further research due to the preparation of monosubstituted derivatives of 1,10-phenanthroline. From an organic synthesis point of view, the synthesis of these compounds often involves complicated series of reactions. Additionally, selected metal complexes with 1,10-phenanthroline derivatives can participate in a number of catalytic reactions, including the reduction and oxidation type<sup>21</sup>. The research of the electrochemical properties of studied compounds leads to the determination of their reduction and oxidation effects.

The doctoral dissertation's last stage presents the results of studies for the formylation of selected quinoline and benzo[*h*]quinoline molecules. The number of carbaldehydes and several dicarbaldehydes through three different formylation methods i.e., Reimer-Tiemann, Vilsmeier-Haack, and Duff reaction, were obtained. The structure of 8-hydroxy-2-methyl-quinoline-5,7-dicarbaldehyde was determined by single-crystal X-ray diffraction measurements determined.

A new procedure for the oxidation of dicarbaldehydes based on reactions with sodium hypochlorite was developed. The oxidation reactions for selected dicarbaldehydes of quinoline derivatives and benzo[*h*]quinoline were performed. As a result of the conducted reactions, the 10-hydroxybenzo[*h*]quinoline-7,9-dicarboxylic acid was obtained.

### 3. Abstract in Polish

Niniejsza praca dyplomowa obejmuje cztery obszary: (i) syntezę i funkcjonalizację wybranych 1,10-fenantrolin, (ii) utlenianie wybranych 1,10-fenantrolin, (iii) badania elektrochemiczne, spektroelektrochemiczne rozszerzone o obliczenia DFT oraz (iv) synteza i funkcjonalizacja pochodnych chinoliny i benzo[*h*]chinoliny, jako związków pomocniczych.

W pierwszej części przedstawiono syntezę 4,7-dichloro-1,10-fenantroliny i ich niesymetrycznych pochodnych, w tym przykłady związków posiadających tylko jeden atom chloru. Wieloetapowa synteza pochodnych 4,7-dichloro-1,10-fenantroliny oparta była na znanej w literaturze reakcji kwasu Meldruma z wybranym analogiem 1,2-diaminobenzenu. W przypadku syntezy monochlorowych pochodnych 1,10-fenantroliny wykorzystano zarówno reakcję Skraupa-Doebnera-Von Millera oraz uprzednio wspomnianą cyklizację z wykorzystaniem kwasu Meldruma. W części poświęconej syntezie 4,7-dipodstawionych-1,10-fenantrolin omówiono również funkcjonalizację wybranych ich prekursorów. Jedną z ważniejszych transformacji chemicznych, którą wykorzystano w realizacji tego zadania było aromatyczne podstawienie nukleofilowe atomów chloru, z wykorzystaniem amin takich jak piroolidyna, 9*H*-karbazol i 10*H*-fenotiazyna. 5-Fluoro-4,7-di(piroolidyn-1-yl)-1,10-fenantrolina została scharakteryzowana za pomocą analizy rentgenostrukturalnej.

Na tym etapie badań przeprowadzono również reakcje mające na celu otrzymanie monopodstawionych 1,10-fenantrolin. W wyniku szeregu przemian chemicznych otrzymano kilka pochodnych 1,10-fenantroliny zawierających atom chloru w różnych położeniach. Strukturę trzech ich prekursorów określono za pomocą analizy rentgenostrukturalnej. W celu otrzymania monopodstawionych aminowych pochodnych 1,10-fenantroliny zastosowałem wieloetapową syntezę, która ze względu na zajście reakcji konkurencyjnej jaką była reakcja VNS nie zezwoliła mi na otrzymanie oczekiwanych ww. związków.

Substytucja VNS była badana w celu jej wyeliminowania lub ograniczenia jako reakcji konkurencyjnej, bądź wykorzystać w syntezie uprzednio omówionych związków. W tym celu przeprowadzono serię reakcji z wykorzystaniem nitrochinolin jako prekursorów 1,10-fenantrolin jako elektrofilu, oraz 9*H*-karbazol jako odczynnik nukleofilowy. W wyniku badań uzyskano kilka produktów posiadających w swej strukturze 9*H*-karbazol. Dwa z otrzymanych produktów zostały scharakteryzowane za pomocą analizy rentgenostrukturalnej.

Drugim etapem pracy doktorskiej było poznanie procesów utleniania i hydrolizy wybranych podstawionych 1,10-fenantrolin. Jako modelowe związki wybrano pochodne 1,10-fenantroliny z podstawnikami metylowymi i chlorowymi zlokalizowanymi w pozycjach C2,



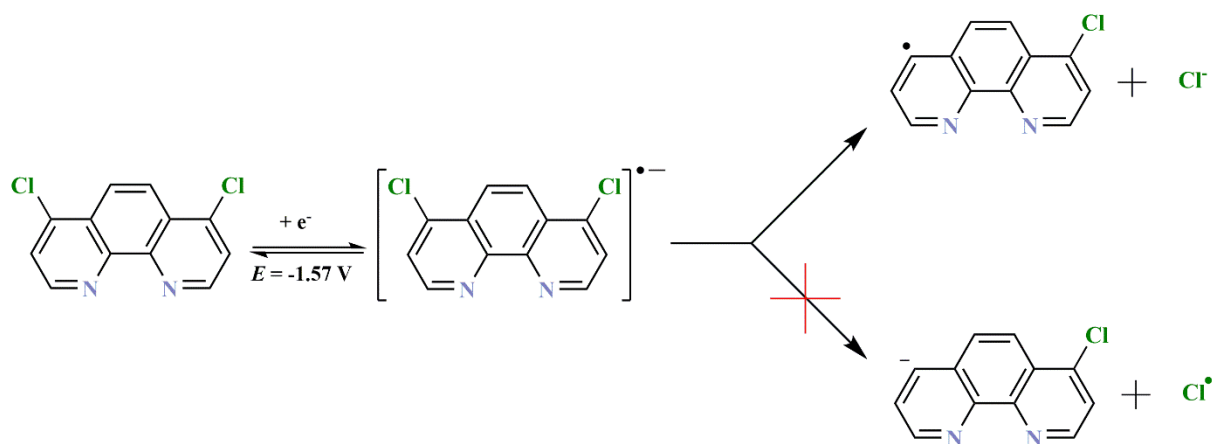
C4, C5, C7 i C9. Przeprowadzono także reakcje utleniania 2,9-dimetylo-1,10-fenantroliny za pomocą dwóch metod. Pierwsza procedura została oparta na nowo opracowanej metodzie utleniania dialdehydów pochodnych chinoliny oraz benzo[h]chinoliny. Druga metoda polegała na reakcji z wykorzystaniem kwasu azotowego oraz bromku sodu. Jednak ze względów aplikacyjnych te dwie metody utleniania mają znaczne ograniczenia syntetyczne. W pracy doktorskiej wykluczono reakcje utleniania z zastosowaniem soli metali przejściowych ze względu na potencjalne reakcje kompleksowania metali przez 1,10-fenantroliny, które są bardzo dobrymi ligandami *N,N*-donorowymi. Dodatkowo zastosowanie niektórych z nich będących silnymi utleniaczami, takich jak manganian potasu(VII), jest bardzo ograniczone ze względu na jego destrukcyjne właściwości utleniające, które wielokrotnie prowadzą do otwarcia pierścieni aromatycznych<sup>11</sup>.

Do reakcji hydrolizy wybrano pochodne nitrylowe 1,10-fenantrolin, a jako modelowe związki wybrano 4,7-dichloro-1,10-fenantrolino-5-karbonitryl, 4,7-di(9*H*-karbazol-9-ilo)-1,10-fenantrolino-5-karbonitryl i 4,7-di(10*H*-fenotiazyn-10-ylo)-1,10-fenantrolino-5-karbonitryl. W literaturze chemicznej istnieje wiele przykładów hydrolizy grupy nitrylowej prowadzące do syntezy kwasów karboksylowych lub aldehydów w zależności od zastosowanych warunków reakcji, a w tym przede wszystkim pH środowiska przemiany<sup>12,13,14</sup>.

W wyniku przeprowadzonych reakcji uzyskano dwie grupy produktów. W wyniku hydrolizy 4,7-dichloro-1,10-fenantrolino-5-karbonitrylu otrzymano 7-chloropirolo [2,3,4-de][1,10]fenantrolin-5(4*H*)-on, produkt powstały najprawdopodobniej w wyniku hydrolizy grupy nitrylowej oraz następczej reakcji substytucji atomu chloru w pierścieniu pirydynowym 1,10-fenantroliny. Druga grupa produktów powstała w oparciu o reakcję NOSH (oksydatywne nukleofilowe podstawienie wodoru, ang. *Oxidative Nucleophilic Aromatic Substitution of Hydrogen*). Dla obu produktów struktury zostały scharakteryzowane za pomocą analizy rentgenostrukturalnej.

Trzecim etapem badań było przeprowadzenie pomiarów elektrochemicznych dla wybranych związków, które otrzymano w wyniku wcześniej opisanych reakcji. Dla każdej z badanych grup związków zaproponowano możliwe mechanizmy towarzyszące ich redukcji i utlenianiu. Pomiar spektroskopowy, w tym przede wszystkim spektroskopia mas potwierdziła powstanie opisywanych produktów. Badanymi grupami były pochodne 4,7-dichloro-1,10-fenantroliny, 4,7-di(pirolidyn-1-ylo)-1,10-fenantroliny, 4,7-di(9*H*-karbazol-9-ylo)-1,10-fenantrolina i 4,7-di(10*H*-fenotiazyn-10-ylo)-1,10-fenantroliny.

Przeprowadzono serię badań elektrochemicznych i spektroelektrochemicznych dla każdej z grup związków, które zostały dodatkowo poparte obliczeniami teoretycznymi DFT. W procesach redukcji w badaniach elektrochemicznych wykazano selektywną eliminację atomów chloru dla 4,7-dichloro-1,10-fenantroliny (patrz Schemat 3). Eliminacja podstawnika chlorowego jest dobrze poznanym procesem<sup>15,16</sup>; jednak nie przeprowadzono systematycznych badań dla pochodnych 1,10-fenantroliny.



**Schemat 3.** Propozycja mechanizmu redukcji 4,7-dichloro-1,10-fenantroliny.

Znając potencjał redukcyjny wybranych chloro pochodnych 1,10-fenantroliny możliwe jest zaproponowanie, które odczynniki najlepiej zastosować jako reduktory w reakcjach eliminacji atomu chloru w ww. związkach. Badania elektrochemiczne przeprowadzono z użyciem acetonitrylu jako rozpuszczalnika. Warto zauważyć, że w różnych warunkach potencjał redox będzie posiadał odmienną wartość. Znajomość potencjału wielu reduktorów może być wykorzystana w doborze odpowiedniego środka redukującego. Znajomość elektrochemiczna dróg redukcyjnej eliminacji jednego lub dwóch podstawników chlorowych może pomóc w przewidywaniu eksperymentów w syntezie opartej na procesach redukcji.

W przypadku redukcji wybranych pochodnych 4,7-diamino-1,10-fenantroliny potwierdzono redukcyjną eliminację podstawnika aminowego znajdującego się w pozycji C4 lub/oraz C7. Badania przeprowadzono dla podstawników takich jak pirolidyna, 9*H*-karbazol i 10*H*-fenotiazyna. Proces ten był interesujący ze względu na zaobserwowaną selektywność redukcji prowadzącą wyłącznie do monopodstawionej pochodnej aminowej 1,10-fenantroliny.

W literaturze chemicznej istnieją różne podstawowe metody eliminacji podstawników halogenowych<sup>17,18</sup> i aminowych w tym pirolidyny<sup>19</sup> lub 9*H*-karbazolu<sup>20</sup>. Nie ma jednak

systematycznych badań w ww. grupie związków. Z tego powodu przeprowadzono badania redukcji elektrochemicznej dla wybranych 4,7-dichloro-1,10-fenantrolin i 4,7-dipodstawionych-1,10-fenantrolin.

Selektywna eliminacja podstawnika aminowego może być interesującym kierunkiem dalszych badań ze względu na otrzymywanie monopodstawionych pochodnych 1,10-fenantroliny. Z punktu widzenia syntezy organicznej otrzymywanie monopodstawionych pochodnych 1,10-fenantroliny często obejmuje znacznie bardziej złożone serie reakcji. Dodatkowo wybrane kompleksy metali z pochodnymi 1,10-fenantroliny mogą uczestniczyć w szeregu reakcji katalitycznych, w tym typu redukcji czy utleniania<sup>21</sup>. Przeprowadzone badania elektrochemiczne mogą być pomocne wskazując ograniczenia zastosowania kompleksów metali z pochodnymi 1,10-fenantroliny, gdyż same mogą ulegać reakcjom eliminacji, redukcji czy utleniania.

Ostatni etap pracy doktorskiej przedstawia wyniki badań nad formylowaniem wybranych cząsteczek chinoliny i benzo[*h*]chinoliny. Szereg aldehydów i dialdehydów uzyskano trzema różnymi metodami formylowania, tj. z zastosowaniem reakcji Reimer-Tiemanna, Vilsmeier-Haacka i Duffa. Strukturę 8-hydroksy-2-metylochinolino-5,7-dikarboaldehydu scharakteryzowano za pomocą analizy rentgenostrukturalnej.

Opracowano również nową procedurę utleniania dialdehydów opartą na reakcji z podchlorynem sodu. Dla wybranych dialdehydów pochodnych chinoliny i benzo[*h*]chinoliny przeprowadzono reakcje ich utleniania. W wyniku przeprowadzonych reakcji otrzymano z dobrą wydajnością kwas 10-hydroksybenzo[*h*]chinolino-7,9-dikarboksylowy.

## 4. Acronyms and abbreviations

• ACN	Acetonitrile
• CP MAS	Cross polarization magic angle spinning
• CV	Cyclic voltammetry
• CCDC	The Cambridge Crystallographic Data Centre
• DIPEA	<i>N,N</i> -Diisopropylethylamine
• DME	Dimethoxyethane
• DMF	<i>N,N</i> -Dimethylformamide
• DMSO	Dimethylsulfoxide
• DPV	Differential pulse voltammetry
• EDG	Electron-donating group
• EI	Electron ionization
• ESI	Electrospray ionization
• EWG	Electron-withdrawing group
• Fc	Ferrocene
• HMTA	1,3,5,7-Tetraazatricyclo[3.3.1.1 <sup>3,7</sup> ]decane
• HOMA	Harmonic oscillator measure of aromaticity
• HOMO	Highest occupied molecular orbital
• HR-MS	High resolution mass spectrometry
• LUMO	Lowest unoccupied molecular orbital
• Meldrum acid's	2,2-Dimethyl-1,3-dioxane-4,6-dione
• MO	Molecular orbital
• MW	Microwave irradiation
• NHE	Normal hydrogen electrode
• OLED	organic light-emitting diode
• ORTEP	Oak ridge thermal ellipsoid plot
• Pd(dba) <sub>3</sub>	Tris(dibenzylideneacetone)dipalladium
• PHEN	1,10-phenanthroline
• PHEN-2CH <sub>3</sub>	2,9-dimethyl-1,10-phenanthroline, neocuproine
• PPA	Phenylpropanolamine
• SCE	Saturated calomel electrode
• S <sub>N</sub> Ar	Aromatic nucleophilic substitution
• TBAOH	Tetrabutylammonium hydroxide
• TBAPF <sub>6</sub>	Tetrabutylammonium hexafluorophosphate
• TEA	Triethylamine
• TEOA	Triethyl orthoacetate, 1,1,1-Triethoxyethane
• TEOF	Triethyl orthoformate, Triethoxymethane

- TFA Trifluoroacetic acid
- THF Tetrahydrofuran
- TMOA Trimethyl orthoacetate, 1,1,1-Trimethoxyethane
- TMOF Trimethyl orthoformate, Trimethoxymethane
- UV Ultraviolet
- VNS Vicarious nucleophilic substitution
- ONSH Oxidative nucleophilic aromatic substitution of hydrogen
- Xantphos 4,5-Bis(diphenylphosphino)-9,9-dimethylxanthene

## 4.1 Abbreviations of compounds used in Results and discussion and Experimental:

### Derivatives of 1,10-phenanthrolines:

- 1 – 3a – l, n – p substrates at successive stages of preparation of selected  
(e.g., **1c**, **2a**, **3g**, **3o**) mono and dichloro-1,10-phenanthroline
- 4a – l derivatives of 4,7-dichloro-1,10-phenanthroline  
(e.g., **4c**)
- 4n – p derivatives of mono-chloro-1,10-phenanthroline  
(e.g., **4o**)
- 5a – m derivatives of 4,7-disubstituted-1,10-phenanthroline  
(e.g., **5g**)
- 4a – h-P1 – P7 product of reduction or oxidation of selected  
(e.g., **4b-P1**) 4,7-dichloro-1,10-phenanthrolines in the part of the  
research devoted to electrochemical properties
- 5a – l-P1 – P8 product of reduction or oxidation of selected  
(e.g., **5c-P1**) 4,7-disubstituted-1,10-phenanthroline in the part of the  
research devoted to electrochemical properties

Ox-4 – 5a – l oxidation product of selected 1,10-phenanthrolines  
(e.g., **Ox-4a**, **Ox-5l**)

Hyd-4 – 5e, i, m product of hydrolysis reaction of selected  
(e.g., **Hyd-4e**) 1,10-phenanthrolines

**Phen-F** 5-fluoro-1,10-phenanthroline

Ox1 – 2-Phen-2CH<sub>3</sub> oxidation products of 2,9-dimethylo-1,10-phenanthroline  
(e.g., **Ox2-Phen-2CH<sub>3</sub>**)

#### Derivatives of quinolines and benzo[*h*]quinolines:

1 – 3m substrates at successive stage to preparation of  
(e.g., **2m**) 5-chloroquinolin-8-amine

**4m** 5-chloroquinolin-8-amine

Q1a – l substrates of dicarbaldehydes of selected  
(e.g., **Q1c**) quinolines and benzo[*h*]quinolines

Q2a – l derivatives of dicarbaldehydes of quinolines and  
(e.g., **Q2g**) benzo[*h*]quinolines

**Ox-Q2b -l** oxidation products of  
8-hydroxyquinoline-5,7-dicarbaldehyde

**Ox-Q2l** oxidation product of  
10-hydroxybenzo[*h*]quinoline-7,9-dicarbaldehyde

Q3a – d derivatives of nitro-quinolines  
(e.g., **Q3d**)

Q4a – d product of vicarious nucleophilic substitution of selected (e.g., **Q4b**)  
nitro-quinolines

## 5. Literature review

### 5.1 The *N*-heterocyclic compounds - introduction

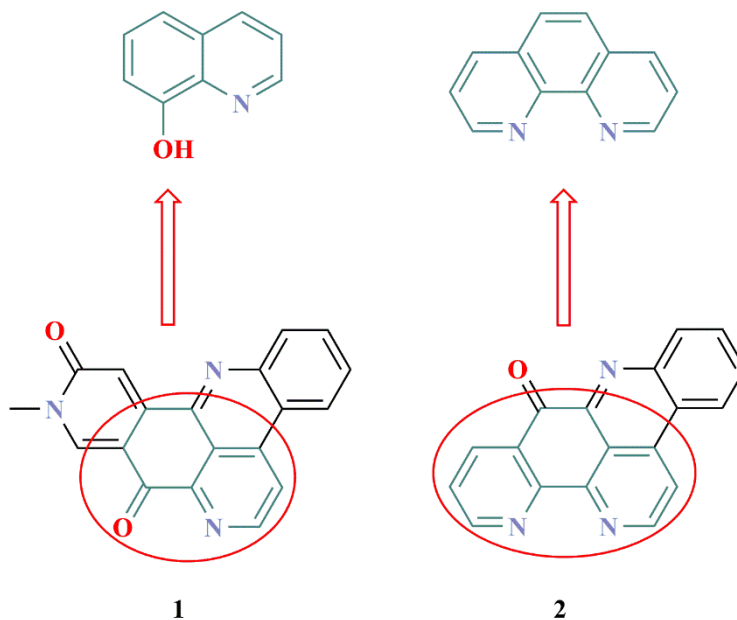
Heterocyclic compounds have a wide range of applications but are of particular interest in medicinal chemistry, and this has catalyzed the discovery and development of much heterocyclic chemistry and methods. According to the Golden Book of IUPAC, heterocyclic compounds are described as cyclic compounds containing at least two atoms of different elements in the ring<sup>22</sup>. In the case of *N*-heterocycles, the atom in addition to carbon that is in the ring is a nitrogen atom. Such compounds include quinolines, benzo[*h*]quinolines and phenanthrolines, and many other more complex compounds. The applications in the industry like metal complexes of 8-hydroxyquinoline derivatives for dyeing wool can be found. Also, to check the iron content of sodium sulfate for industrial use is photometry with 1,10-phenanthroline<sup>23</sup>. The nitrogen atom is an important factor affecting the properties of molecules. For aromatic systems, the nitrogen atoms are involved in the  $\pi$ -bonding aromatic system using its unhybridized p orbital. The lone pair is in an  $sp^2$  orbital, projecting outward from the ring in the same plane as the  $\sigma$  bonds. As a result, the lone pair does not contribute to the aromatic system but significantly influences the chemical properties, as it easily supports bond formation via an electrophilic attack<sup>24</sup>.

The nitrogen atom's influence is analyzed in heterocyclic compounds by the index of aromaticity (HOMA, Harmonic Oscillator Measure of Aromaticity). Based on that geometric criterion, can compare the aromaticity of pyridine and benzene. This method's reference value is the structure of aromatic benzene, where the HOMA value equals 1 according to the literature<sup>25</sup>. In the case of pyridine on theoretical calculation, the HOMA value equals 0.944 according to the literature<sup>26</sup>. The lower value of HOMA for pyridine determines weaker aromaticity. It can be explain by the difference in electronegativity of a nitrogen atom to carbon atoms.

Although most living organisms cannot directly utilize nitrogen, they use access to their compounds. Interest in organic nitrogen compounds is because most of them exhibit physiological activity<sup>27</sup>, which also includes *N*-heterocyclic compounds.

An exciting example is *N*-heterocyclic compounds isolated from marine organisms. Compounds such as amphimedine (Scheme 4, 1) and ascididemin (Scheme 4, 2) were

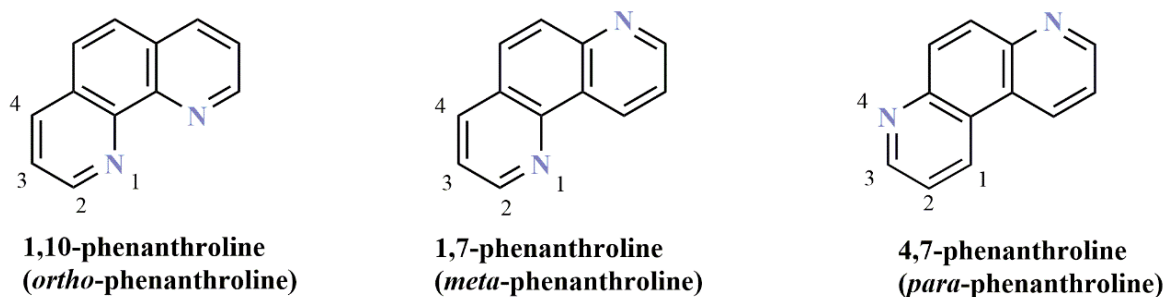
isolated, respectively, from sponge (*Amphimedon sp.*) and tunicate (*Didemnum sp.*). They exhibit, among other things, cytotoxic and anticancer properties. These compounds were reconstructed through chemical synthesis, and the research is still extended by obtaining their new derivatives and discovering their unique uses.



**Scheme 4.** Structure of amphimedine (1) and ascididemin (2). The 8-hydroxyquinoline and 1,10-phenanthroline component parts are marked grey-green.

## 5.2 Phenanthroline: a brief history

In 1883, Skraup and Vortmann received the first isomer (1,7) from a new group of compounds, which they called phenanthroline<sup>28</sup>. By proving that it had an angular structure of phenanthrene and not a linear anthracene, they called it phenanthroline. In 1909, Kaufmann and Radosevic proposed a nomenclature distinguishing ortho, meta, and para regioisomers, but this naming system becomes forgotten<sup>29</sup>. Currently, a numerical system is used to distinguish the three regioisomers shown in Scheme 5.



**Scheme 5.** Structures of selected phenanthroline regioisomers.



Gerdeissen received the first derivative of 1,10-phenanthroline (2-methyl-1,10-phenanthroline)<sup>30</sup>. In turn, the first 1,10-phenanthroline was received by F. Blau<sup>31</sup>, calling it  $\alpha$ -phenanthroline. He also noted the formation of their complexes with metal salts. In the case of 1,10-phenanthroline, the numerical nomenclature and its symmetry are still used today.

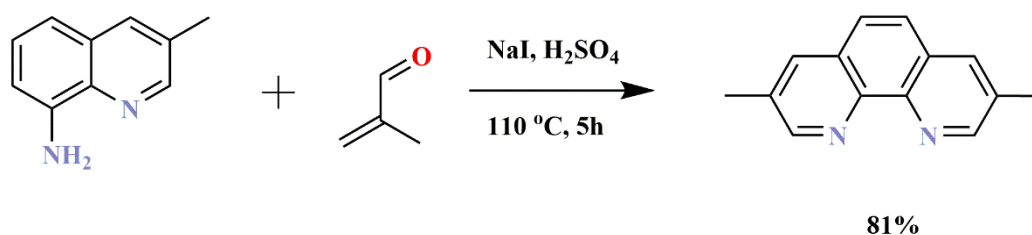
### 5.3 Methods of synthesis of 1,10-phenanthrolines and their derivatives

The preparation of 1,10-phenanthroline derivatives can be divided into multi-stage and single-stage protocols. One-stage transformations include the Skraup method and its modifications, while multi-stage ones include syntheses based on Meldrum acids.

#### 5.3.1 Synthesis of 1,10-phenanthroline derivatives by the modified Skraup methods

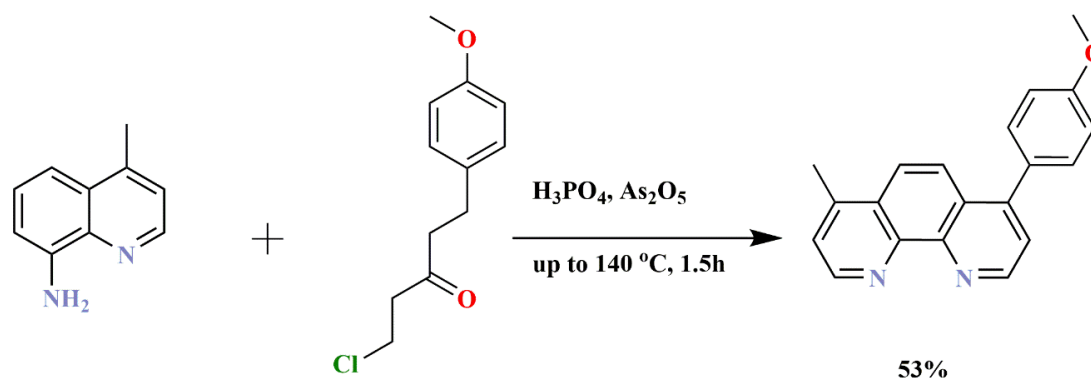
Several syntheses of 1,10-phenanthroline derivatives are collected using modified Skraup's methods. The Dobner-Von Miller reaction relies on the reaction of aniline derivatives with  $\alpha$ ,  $\beta$ -unsaturated carbonyl compounds in an acidic environment (Lewis's acid or protic acid). An oxidizing agent may be use ions like Fe(III), 1,2-dihydrolepidine-HCl (disproportionation), oxygen from air, nitrobenzene, and a mixture of nitrobenzene with hydrochloric acid (HCl) or trifluoroacetic acid (TFA)<sup>32</sup>.

One of the examples is a synthesis of 3,8-dimethyl-1,10-phenanthroline choose by Belser et al.<sup>33</sup>. They received a compound with 81% yield (Scheme 6). The disadvantage of the described method is the difficulty in determining the 1,10-phenanthroline derivatives from reaction separations.



**Scheme 6.** Synthesis of 3,8-dimethyl-1,10-phenanthroline<sup>33</sup>.

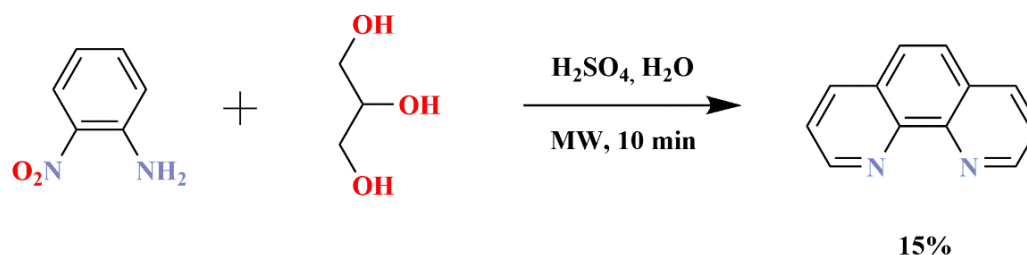
In analogous syntheses,  $\alpha,\beta$ -unsaturated carbonyl compounds are not always used. An interesting example, Pomeranc et al. described in their article<sup>34</sup>. Where the reaction of 4-methyl-8-aminoquinoline with 3-chloro-1-(4-methoxyphenyl) propan-1-one (Scheme 7) leads to obtain 4-methyl-7-anisyl-1,10-phenanthroline with a good yield. The 4-methyl-8-aminoquinoline was obtained from the same procedure starting from nitroaniline with but-3-en-2-one in the 87% solution of sulphuric acid in the presence of arsenic pentoxide to obtain 4-methyl-8-nitroquinoline. Finally, compound 4-methyl-8-nitroquinoline was reduced with stannous chloride to give the amino derivative of quinoline.



**Scheme 7.** Synthesis of 4-methyl-7-methoxyphenyl-1,10-phenanthroline<sup>34</sup>.

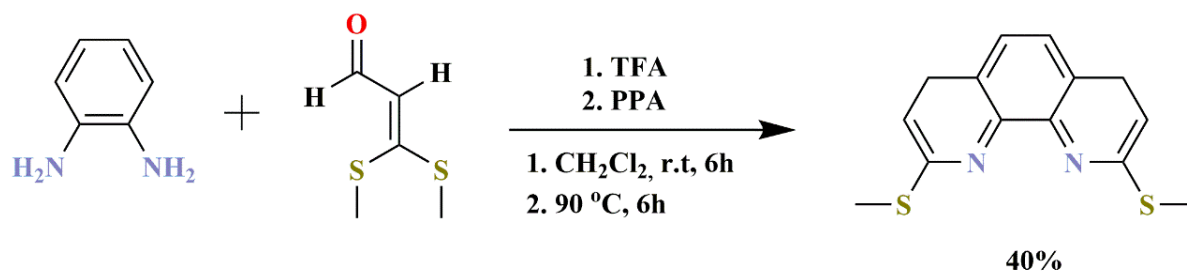
Another interesting variation of the Skraup method is its modification with a microwave irradiation. H. Sagadii et al.<sup>35</sup> shown an efficient “green” reaction in water using glycerol under microwave irradiation conditions.

Using aniline derivatives, they obtain various selected quinolines with their by-products. The 4,7-; 1,7-; and 1,10-phenanthroline were obtained regioselectivity, starting from 4-, 3-, 2- nitroanilines regioisomers. Reactions were carried out in sulfuric acid solution where the mixture was irradiated with power high enough to reach the predicted temperature with a heating ramp of 36 °C min<sup>-1</sup>, then 200 °C for 10 min. They have shown that first cyclization was realized with the amino group and reduction of the nitro group to the amino start second Skraup reaction (Scheme 8).



**Scheme 8.** Modified Skraup reaction of 2-nitroaniline with glycerol obtaining 1,10-phenanthroline<sup>35</sup>.

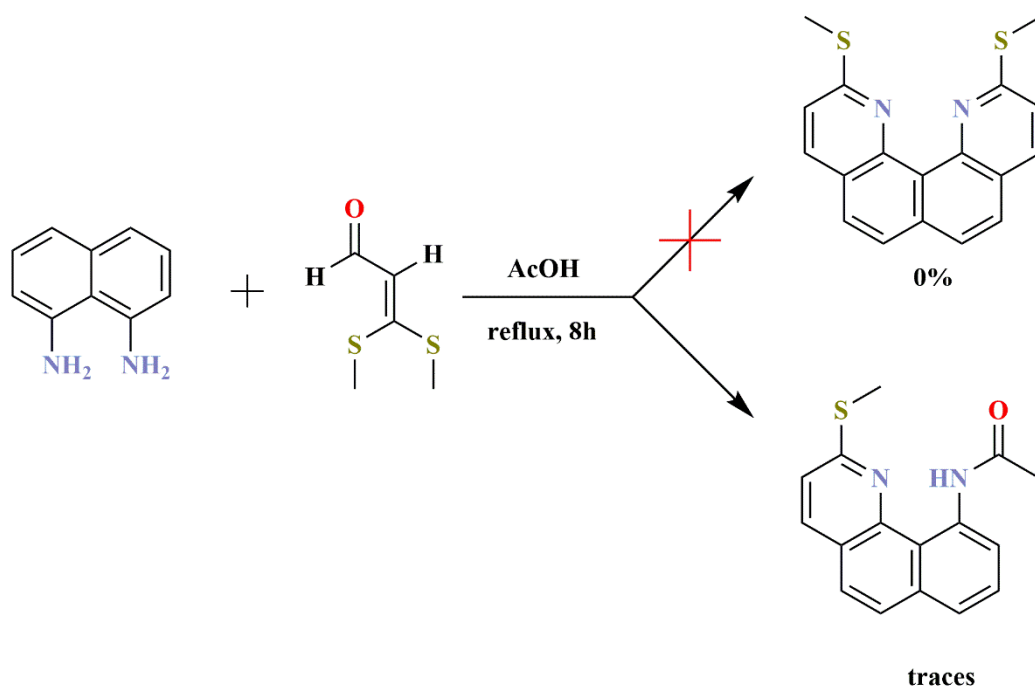
K. Panda et al.<sup>36</sup> describe the synthesis of 2,9-bis(methylthio)-1,10-phenanthroline by Skraup reaction. Where the solution of 3-bis(methylthio)acrolein was added 1,2-diamine in dichloromethane was added in room temperature TFA. The crude iminoenamine was used for further reactions where it was dissolved in PPA (phenylpropanolamine) and heated for 6 hours. The crude product was obtained with a yield of 40% (Scheme 9).



**Scheme 9.** Synthesis of 2,9-bis(methylthio)-1,10-phenanthroline<sup>36</sup>.

The Skraup synthesis has many advantages, which include its low cost and ease of the procedure. Its additional advantage is that it takes place in one reaction vessel. Hence other groups of scientists tried to repeat this methodology. On the other hand, in literature, the use of orthodiaminobenzene derivatives as an example of aniline derivative raises controversies.

K. J. Shaffer et al. criticized the earlier work of K. Panda et al.<sup>37</sup>. They repeated one of the procedures. They reacted 1,8-diaminonaphthalene with 3,3-bis-(thiomethyl) acrolein in an acetic acid medium. As a result of the transformation, the authors did not receive the expected 2,11-bis(methylthio)quinolino[7,8-h]quinoline. Instead, they obtained and fully confirmed trace amounts of *N*-[2-(methylthio)benzo[*h*]quinolin-10-yl]acetamide (Scheme 10). Reaction conditions with other simple anilines of K. Panda et al. gave the expected quinolines.



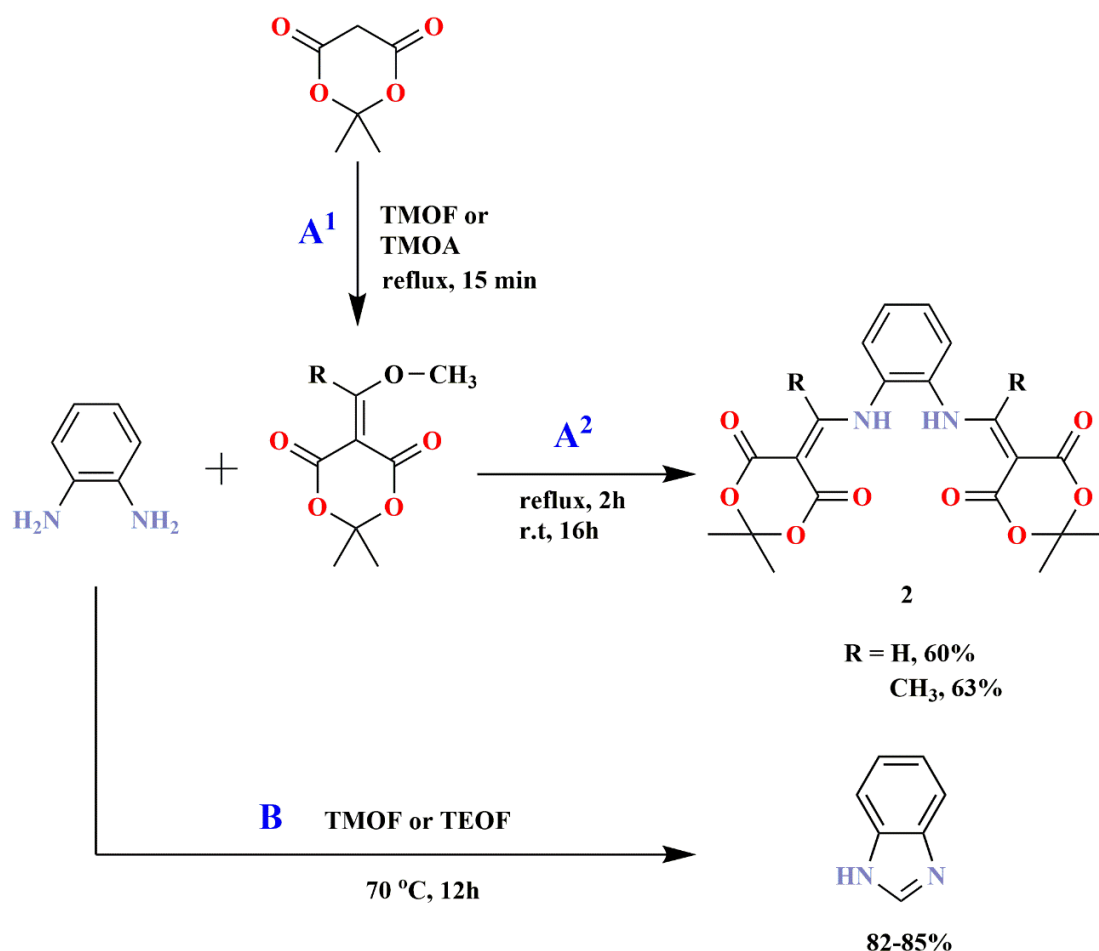
**Scheme 10.** Synthesis quinoline derivatives by K.J. Shaffer et al.<sup>37</sup>.

### 5.3.2 Synthesis of 1,10-phenanthroline derivatives based on Meldrum acids

Halogenated derivatives of 1,10-phenanthroline are common starting reagents for the synthesis of more elaborate structures. A well-known method for obtaining such phenanthrolines is a synthesis based on Meldrum acids, which can be used to obtain also quinoline derivatives<sup>38</sup>.

A derivative of 8-aminoquinoline or 1,2-diaminobenzene can be used for the obtained 1,10-phenanthroline derivative<sup>39,40</sup>. In the case of 8-aminoquinoline through one nucleophilic center in the form of an amino group, there is a 3-stage synthesis leading to the formation of one phenyl ring<sup>41</sup>. When 1,2-diaminebenzene is used, these syntheses can include two nucleophilic centers leading to the formation of two phenyl rings. In order to approximate this method, the three stages of synthesis with 1,2-diaminebenzene are presented below.

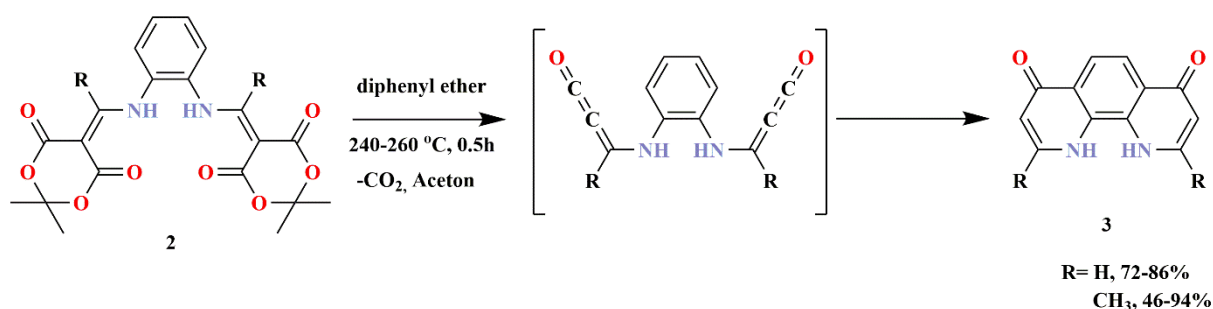
In the first stage of this synthesis, the condensation product of Meldrum acid with trimethyl orthoformate (TMOF)<sup>39</sup> or trimethyl orthoacetate (TMOA)<sup>40</sup> is obtained *in situ* (Scheme 11, path A<sup>1</sup>), and then 1,2-diaminobenzene is added to obtain compound **2** shown in Scheme 11, path A<sup>2</sup>.



**Scheme 11.** Path A (A<sup>1</sup> and A<sup>2</sup>): Adduct synthesis **2**. The first step in the synthesis of 1,10-phenanthroline derivatives<sup>39,40</sup>. Path B: Synthesis of benzimidazole as a possible side reaction<sup>42</sup>.

Depending on whether it was (type of used orthoester) an orthoformate or orthoacetate, 1,10-phenanthroline type of compounds is obtained without or with a methyl group at the C2 and C9 positions. Also, triethyl orthoformate or triethyl orthoacetate can also be used in this reaction<sup>43</sup>. It is noteworthy that the orthoesters may reduce reaction efficiency by their side reaction with 1,2-diaminobenzene, forming by-products like benzimidazole. In the work of Kaboudin et al.<sup>43</sup> they present treatment of 1,2-diaminobenzene with TMOF or TEOF (triethyl orthoformate) were without any additional reagent, their reactions afforded the benzimidazoles (Scheme 11, path B).

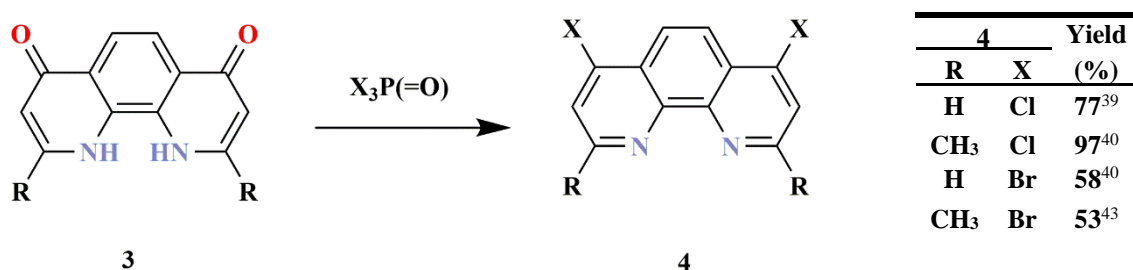
In the next stage of the synthesis of 1,10-phenanthroline derivatives, product **2** undergoes thermal cyclization by decarboxylation. The reaction generates very reactive ketene, which is cyclized to form two outer 1,4-dihydropyridine rings in a diphenyl ether medium. As a result of this synthesis, 1,10-dihydro-1,10-phenanthroline-4,7-dione derivative (**3**) is obtained (Scheme 12)<sup>44,45,46,47</sup>.



**Scheme 12.** Synthesis of 1,10-dihydro-1,10-phenanthroline-4,7-diones<sup>39,40,44,45,46,47</sup>.

Ketene generation *in situ* in reactions has its own limitation. The main disadvantage of this type of reaction is the requirement to use additional reagents. Often, these reagents are not chemically inert and can interfere with the reaction by forming by-products or reducing the efficiency of the reaction. Reducing the impact of such a defect allows the production of ketene as a result of a thermally or photolytically induced intramolecular reaction. They allow ketene to be obtained where by-products are gases or easily volatile compounds<sup>48</sup>. Ketene and by-products are formed using thermal cyclization (Scheme 12).

In the final step, selected 1,10-dihydro-1,10-phenanthroline-4,7-dione (**3**) is treated with phosphoryl trichloride<sup>39,40</sup> or tribromide<sup>40,43</sup> to give selected 4,7-dihalogenated-1,10-phenanthroline (**4**, Scheme 13).



**Scheme 13.** Synthesis of 4,7-dichloro or 4,7-dibromo-1,10-phenanthroline derivatives.

Depending on the type of used substituents in the constitution of molecule **3**, it is observed differences in yield for the reaction with phosphorus trichloride/tribromide.

The disadvantage of synthesis by using Meldrum acid is the high cost of the used reagents and their multi-stage nature. At each of the three stages, an intermediate product is isolated, which significantly extends the entire synthesis time<sup>33</sup>. Currently, there are reports on the preparation of 1,10-phenanthroline derivatives based on Meldrum acids and their further modifications<sup>49</sup>.

For any possible reaction, substituents are an important factor affecting its yield by changing the electron density and/or conformation or steric reasons. This is also the case for the preparation of selected 1,10-phenanthroline with the use of Meldrum's acid.

Many factors can influence the effect of the substituent where they are briefly described below. A substituent can cause a polarization of electron density through the  $\pi$  system in both the reactant and the product. This directly affects the balance position. One such effect that affects charge redistribution is the resonance effect, also called the mesomeric effect<sup>50</sup>.

There is also an effect that originates with the bond dipoles between groups of differing electronegativity. Substituents that are more electronegative than aromatic carbon will place a positive charge on the substituted carbon atom. In contrast, atoms less electronegative than aromatic carbon will have the opposite effect. The presence of the charge separation will influence the energy associated with the development of charge elsewhere in the molecule. This is the result of electrostatic interaction in space and is called the field effect. Depending on the dipole orientation and the charge developing at the reaction site, a substituent can be either favor or disfavor the reaction<sup>50</sup>.

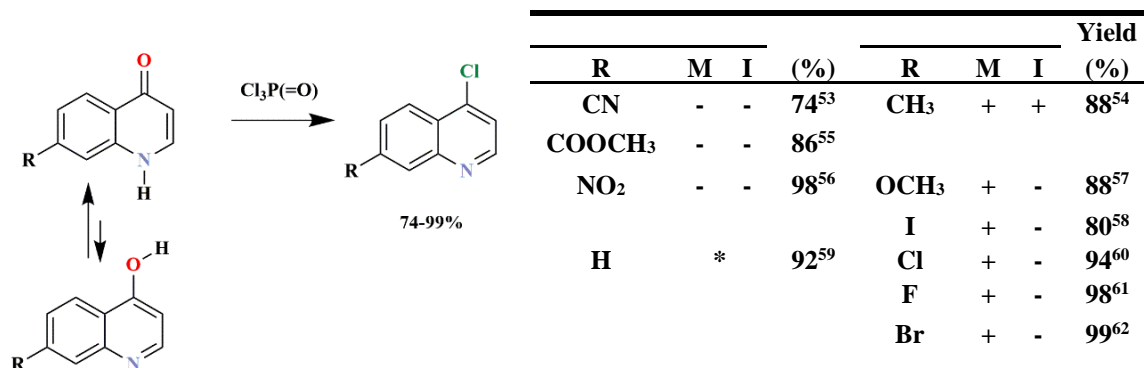
Another possible means of interaction of a substituent and reaction site is called the inductive effect. This effect is the transmission of bond dipoles through the intervening bonds by successive polarization of each bond. Field effects and inductive effects can be considered together as polar effects that originate from bond dipoles<sup>50</sup>.

Another effect related to the used substituent is the solvent effect. Depending on the substituent used, the compound may dissolve better or worse depending on the interaction with the solvent<sup>51</sup>. Thus, it directly affects the duration of the reaction as well as its efficiency. The dissolution process depends on the free energy change of both the solute and the solvent.

The last effect discussed, which is influenced by a substituent, is the steric effect. It refers to the influence on interactions unrelated to the kinetics or thermodynamics of a chemical reaction. It is relatively easy on a qualitative level to identify a substituent with a large or a small steric effect by examining the degree of substitution and their volume. However, actually determining their magnitude and effect on a given reaction is quite difficult because steric effects rarely occur in the absence of other types of substituent effects<sup>52</sup>.

To approximate this effect, a comparison of the reaction yield to different substituents was presented for the reactions of selected quinoline-4-(1*H*)-one with phosphorus trichloride (Scheme 14). Differences in the reaction duration and the temperature at which the reactions

were carried out have been ignored. It is worth noting that there is no systematic research in which were studied how the use of a specific substituent affects the yield of the reaction (Scheme 14).



**Scheme 14.** Synthesis to obtain 4-chloroquinoline derivatives. **M** – mesomeric effect; **I** – inductive effect; \*- as reference for mesomeric and inductive effect<sup>53-62</sup>.

The presented in Scheme 14 the influence of used substituent on the synthesis of 4-chloroquinoline derivatives show that the highest yield of the reaction was obtained in the case of used bromine atom (99%), followed by the nitro group (98%) and fluorine atom (98%). Interestingly, halogen atoms (except iodine) show better yields (94-99%) if it is a compound without a substituent, as a reference example (92%). This may be explained by the high electromagnetic force of the halogen atoms. For the iodine atom, the inferior performance may be due to chlorine's reactivity, which can displace the iodine atom in the reaction. In addition, a large impact on the yield of compounds with the presence of iodo substituent is their instability, which makes it possible to break the C-I bond when exposed to light (even visible light<sup>63</sup>). In the case of fluoro substituent, displace of fluorine group by chlorine atom is also possible as a side reaction, which was confirmed by Z. Wang et al.<sup>64</sup>. By the same reaction shown in Scheme 14 for the 7-fluoroquinolin-4(1H)-one, they obtained 4,7-dichloroquinoline in an 85% yield.

In turn, for the nitro group, its high efficiency can be explained by the resonance structures of the compound that improve the stability of the product and thus the efficiency of the reaction.

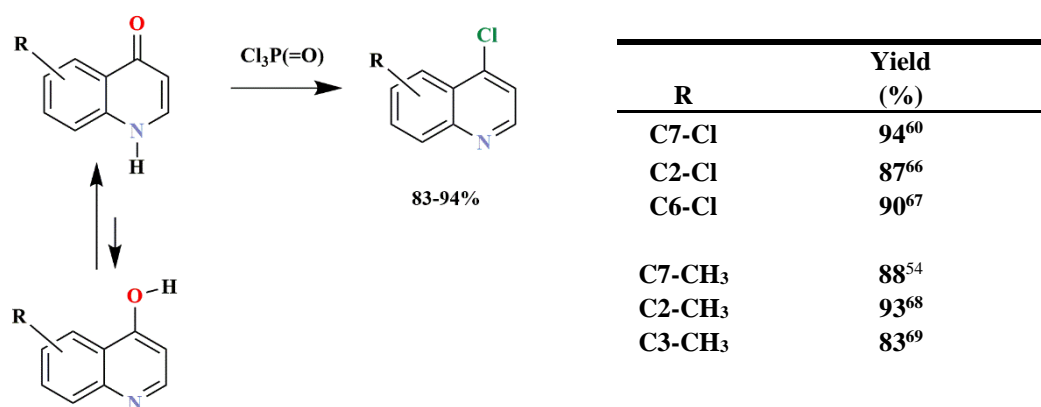
Mostly all of the groups mentioned are electron-withdrawing groups. However, they differ in their steric effect and electronegativity. For the nitrile and ester groups, their inferior yield reaction may result from their sensitivity to water, where, as a result of the reaction, they



may lead to by-products that are difficult to isolate. An example of a hydrolysis reaction of nitrile group is the studies by G.-J. ten Brink et al. where 1,10-phenanthroline-2-carbonitrile were hydrolyzed in an acidic environment to give 1,10-phenanthroline-2-carboxylic acid<sup>65</sup>.

The previously mentioned steric effect can also significantly influence the yield of the reaction. It is worth noting that there are no systematic studies in which the steric effect would be tested for 1,10-phenanthroline or quinoline analogs.

To approximate the steric effect, a comparison of the reaction yield for different positions of substituents was also presented for the reactions of selected quinoline-4-(1*H*)-one with phosphorus trichloride (Scheme 15). Differences in the duration of the reaction and the temperature at which the reactions were carried out have been ignored.



**Scheme 15.** Synthesis of 4-chloro-quinoline derivatives<sup>54,60,66-69</sup>.

On the above Scheme 15, there is a list of the methyl and chloro substituent at different positions in the quinoline constitution with recorded yields. In the case of the chlorine atom, the highest efficiency of the reaction was obtained for the C7 position on the phenyl ring in the quinoline skeleton. In turn, the C2 position in the pyridine ring showed the lowest yield.

In the case of the chloro substituent, its position in the molecule affects the yield of the reaction through a negative induction effect (-I) and a positive mesomeric effect (+M) (these effects are presented for selected substituents. Scheme 14). Depending on whether it is in the C2, C6, or C7 position, the inductive effect may improve or degrade the yield of the reaction.

For the methyl substituent, as an example of an electron-donating group, the C2 position on the pyridine ring showed the highest yield, while the C3 position showed the lowest yield.

A positive effect on the yield of the reaction is the presence of a methyl group in position C2 also can be observed for the reaction of receiving 4,7-dichloro-1,10-phenanthroline and 2,9-dimethyl-4,7-dichloro-1,10-phenanthroline (Scheme 13).

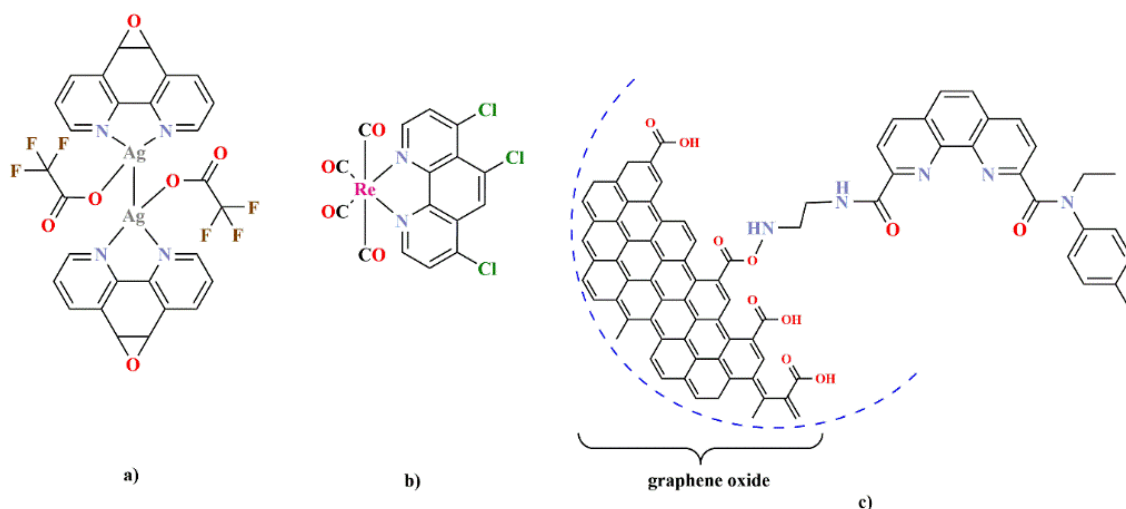
An additional aspect is the limitations of reaction with phosphoryl trichloride, which is presented in the work of C. Perez et al., in which in order to obtain acid derivatives, they had to block the carboxyl group of the initial reagent 5-amino-nicotinic acid. This type of action avoided by-products and maintained better reaction efficiency<sup>70</sup>.

## 5.4 Applications of selected 1,10-phenanthroline and their metal complexes

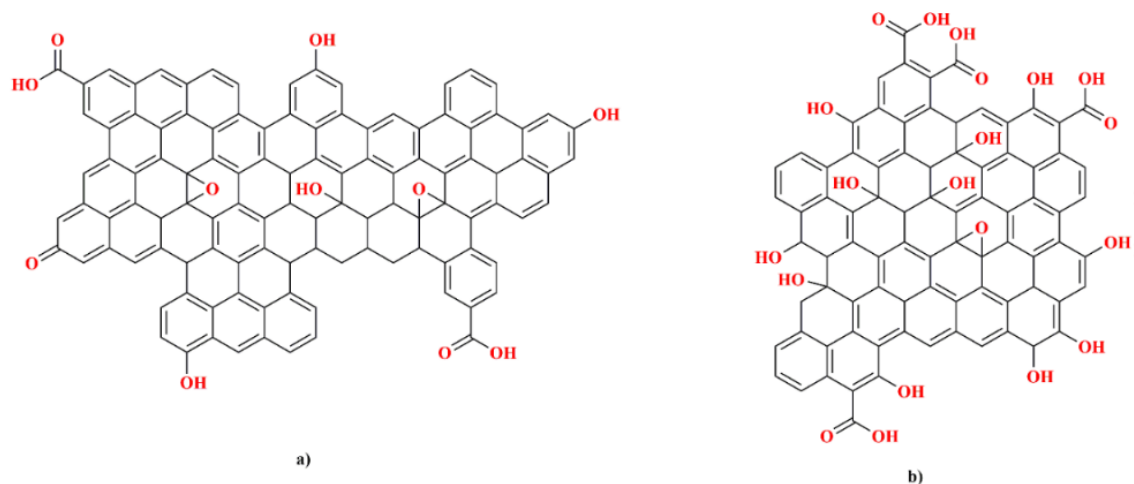
The 1,10-phenanthroline is a ligand and is one of the most explored chelate systems in *N*-heterocyclic compounds due to its robust redox stability, a wide range of complexing properties<sup>71</sup>. This ligand played a vital role in the development of coordination chemistry. Thanks to two nitrogen atoms are always in juxtaposition, and being more rigid imposed by the central ring has better coordination properties than bipyridine<sup>72</sup>. It is worth noting that 1,10-phenanthroline as *N*-heterocycle is an electron-deficient aromatic system and is predetermined for  $\pi$ - $\pi$  stacking formation as  $\pi$ -acceptors<sup>73</sup>. Therefore, compounds of this type are also interesting from the supramolecular chemistry point of view. The 1,10-phenanthroline is capable of forming stable complexes with various metal ions in different configurations at their various oxidation states depending up on conditions<sup>74,75</sup>. These complexes have characteristic electronic<sup>76</sup> and antimicrobial<sup>77</sup> properties which are being continuously exploited in various fields like physics, chemistry, biology, biochemistry, crystallography, and medicine. The 1,10-phenanthroline complexes have found numerous applications due to their excellent ability to coordinate many metal ions. Selected compounds with 1,10-phenanthroline structure due to the angular arrangement of the rings also show biological properties like complexing porphyrins<sup>78</sup>. Many articles are devoted to research on selected 1,10-phenanthrolines and their metal complexes in biology and medicine. Where the anti-fungal, anti-cancer properties of 1,10-phenanthroline are still being studied and developed<sup>79,80</sup>. In the article of S. Z. Duric et al.<sup>81</sup> they present complexes with significant antifungal and

anticancer activity. The silver complex of 1,10-phenanthroline-5,6-epoxy could be examined for combination therapy combating fungal infections in relation to cancer (Scheme 16, a).

Selected 1,10-phenanthroline complexes have also been tested for their luminescent properties<sup>82</sup>. In work, Świetlicka et al.<sup>83</sup> were presented ruthenium complexes with electroluminescence properties. Also, it was found that the number and type of phenanthroline substituents impact the thermal behavior of the complexes (Scheme 16, b). The complexes of 1,10-phenanthrolines also found use as organic semiconductors used in OLEDs<sup>84</sup>. Selected 1,10-phenanthrolines were also studied for their sorption properties<sup>85</sup>. In the work of F. Li et al.<sup>86</sup>, the 2,9-diamide-1,10-phenanthroline were used to functionalized graphene oxide (GO-PDA, Scheme 16, c). This sorbent allows for selective absorption of transition metals as uranium (U(VI)) and thorium (Th(IV)) from rare earth elements in a strongly acidic solution. For this purpose, scheme 10-c shows a simplified structure of graphene oxide based on the structure presented by the Sigma-Aldrich company. In the literature, there are reported structures of graphene oxide containing various functional groups, such as epoxy, hydroxy, or carbonyl groups, nor is it a fully aromatic system. With this in mind, the structure of graphene oxide presented in Scheme 16 is simplified. Structures for graphene oxide are shown in Scheme 17, which was also suggested by researchers<sup>87,88</sup>. For graphene oxide as a material, it is impossible to determine its exact structure.



**Scheme 16.** Structures of selected 1,10-phenanthroline derivatives and their metal and nonmetal complexes<sup>81,83,86</sup>. In example c) the structure of graphene oxide, modeled on the diagram from the Sigma-Aldrich website, has been additionally simplified by cutting out a part of the structure.



**Scheme 17.** Suggested structures of graphene oxide based on a) A. T. Smith et al.<sup>87</sup> b) R. Saito et al.<sup>88</sup>.

## 5.5 Theoretical calculation of 1,10-phenanthroline

Computational modeling with a variety of basis sets has been used to predict some of the properties of 1,10-phenanthroline. These include geometry<sup>89</sup>, MO types<sup>90</sup>, and vibrational spectra<sup>91</sup>.

The dipole moment  $\mu$  of the 1,10-phenanthroline molecule, calculated from the electron density distribution, is 3.8 D (the experimental value is 3.64 D<sup>92</sup>). The low energy of electron removal from the highest occupied molecular orbital (HOMO), equal to 6.49 eV, is also favorable for donor properties of 1,10-phenanthroline. The 1,10-phenanthroline has been studied for the distribution of  $\pi$ -electrons by Longuet et al.<sup>93</sup>. Using molecular orbital and first-order perturbation, they present the relative net charge ( $\pi$ -electrons density) in various external positions (Figure 1b). The nitrogen atoms bear negative charges, making this molecule attractive from the viewpoint of complexation with metal ions.

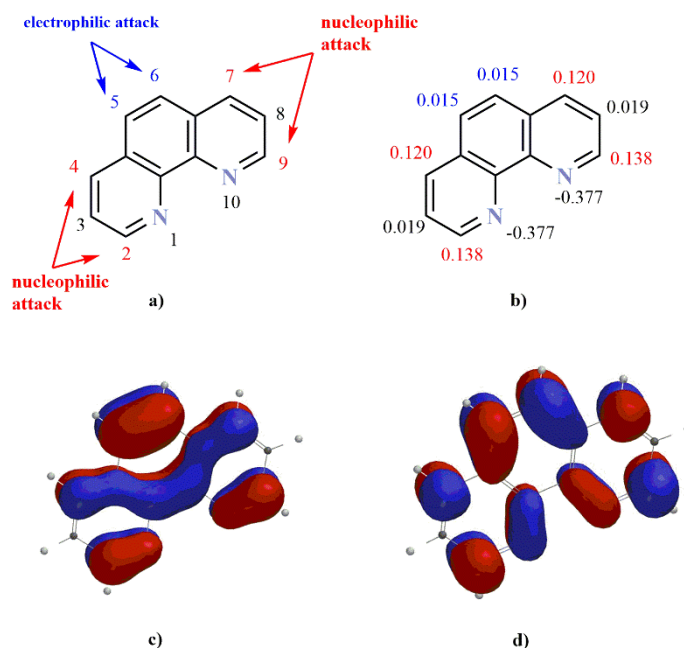


**Figure 1.** a) numbered position of atoms b)  $\pi$ -electrons density<sup>93</sup> c) HOMO base on S.S. Tan et al.<sup>90</sup> d) LUMO base on S.S. Tan et al.<sup>90</sup> of 1,10-phenanthroline.

Due to electron density calculations on the related system were found to be closely correlated with chemical behavior in reactivity. Thanks to these calculations and their correlations, a number of prognostic rules for 1,10-phenanthroline were formulated.

It was predicted that the C2-, C4-, C7-, and C9- positions in 1,10-phenanthroline prefer nucleophilic attack. In turn, the electrophilic attack should occur preferentially at the 5- and 6-positions<sup>30</sup>.

## 5.6 Functionalization of selected 1,10-phenanthroline

### 5.6.1 Oxidation of 1,10-phenanthroline derivatives

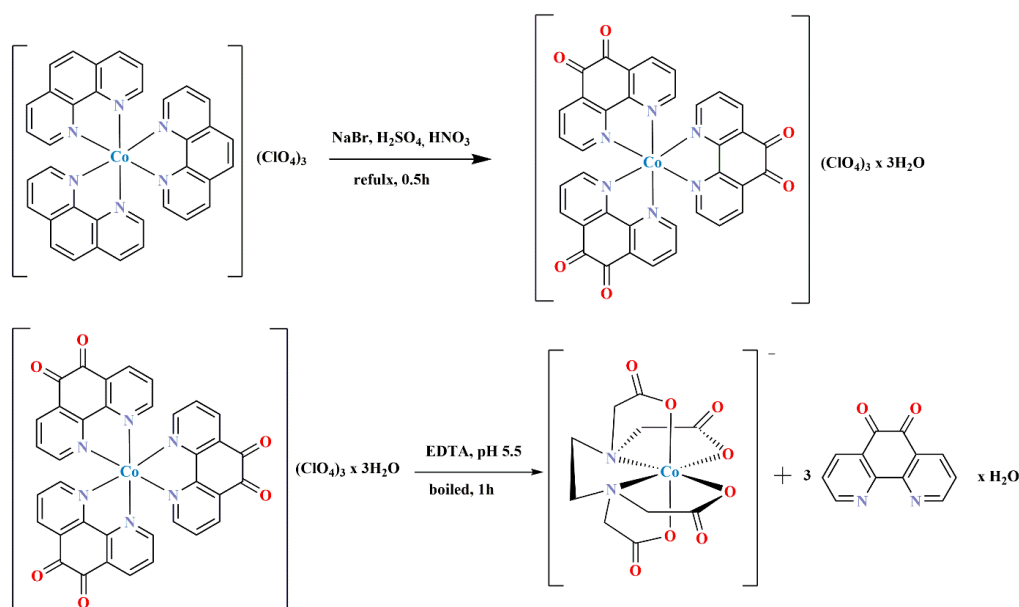
For 1,10-phenanthroline molecule, the double bond at position C5, C6 position is most susceptible to electrophilic attack, as presented in chapter 1.4. It can also explain this by the fact that pyridine rings are electron-poor (compared to the benzene ring) due to the presence of nitrogen, which attracts electrons to itself through an inductive effect, and therefore is not readily electrophilic.

The functionalization of 1,10-phenanthrolines at the C5 and C6 positions found its examples in the phase transfer reaction using commercially available bleaches. This reaction

yields 5,6-epoxy-1,10-phenanthroline, which is an intermediate for further functionalization of the 5-position in 1,10-phenanthroline<sup>94</sup>. Another practical solution is direct nitration of 1,10-phenanthroline by the HNO<sub>3</sub> and H<sub>2</sub>SO<sub>4</sub> mixture, and then the sequence of the 5-nitro-1,10-phenanthroline obtained to 5-amino-1,10-phenanthroline (the amino group allows for further functionalization)<sup>95</sup>. However, the nitration of 1,10-phenanthroline not only showed the possibility of functionalization of the C5-position but also the possibility of the oxidation of 1,10-phenanthroline itself.

The first mentions of 1,10-phenanthroline oxidation are derived from a nitration reaction where by-products were the result of substrate oxidation. Nitration of either 1,10-phenanthroline (**Phen**) or 2,9-dimethyl-1,10-phenanthroline (**Phen-2CH<sub>3</sub>**) leads to the 5-nitro-derivatives, generally accompanied by some of the 1,10-phenanthroline-5,6-dione, and the ratio of the two products can be partly controlled by careful choice of conditions<sup>96</sup>.

One of the procedures that describe the oxidation of the 1,10-phenanthroline derivative is the work of M. Yamada et al.<sup>97</sup>. This type of procedure is based on the work of Gillard et al.<sup>98</sup>. According to them, the cobalt(III) complex of 1,10-phenanthroline reacts with nitric acid, sodium bromide, and sulphuric acid. As a result of the reaction, the ligands were oxidized to obtain a 1,10-phenanthroline-5,6-dione. They also present the method this molecule isolation from cobalt complex (Scheme 18).



**Scheme 18.** Oxidation of tris(1,10-phenanthroline) cobalt(III) perchlorate and isolation of 1,10-phenanthroline-5,6-dione hydrate.

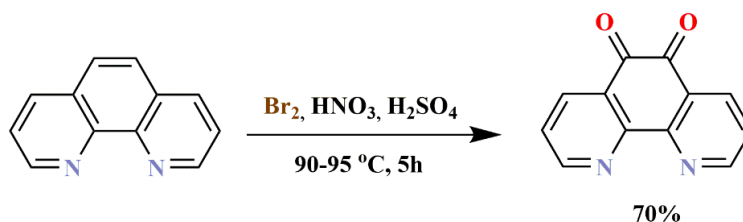
The work of M. Yamada et al.<sup>97</sup> has shown that by careful selection of reaction conditions, they are able to obtain 1,10-phenanthroline-5,6-dione from uncoordinated 1,10-phenanthroline (Scheme 19) where sulphuric acid and potassium bromide (bromine source) occurs as an oxidant.



**Scheme 19.** The preparation of 1,10-phenanthroline-5,6-dione is based on the work of M. Yamada et al.<sup>97</sup>.

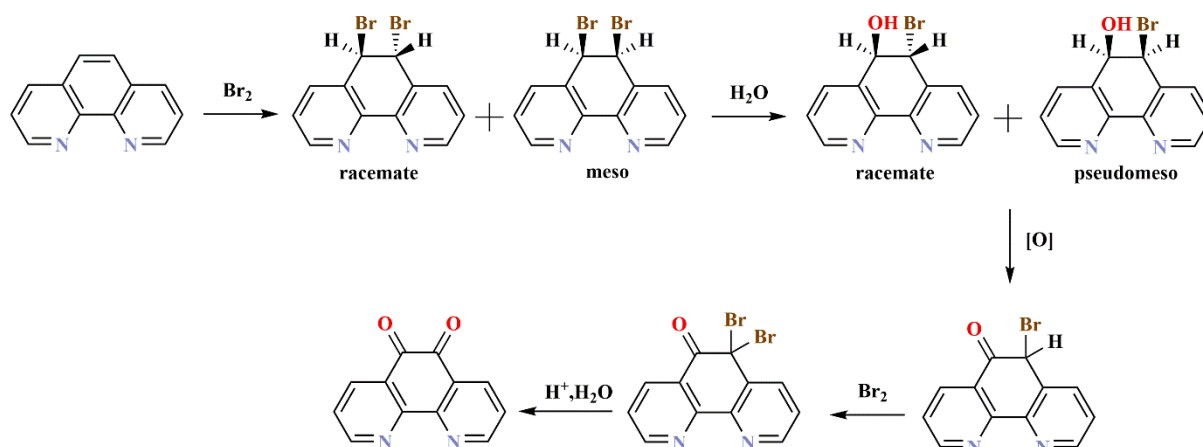
Even though the reaction mechanism has remained unclear, it is evident that potassium bromide and other *in situ* obtained bromic reagents act solely as a bromine source, whereas nitric acid is an oxidizer for its generation.

In view of that, Mitsov et al.<sup>99</sup> suggested the use of molecular bromine to obtain 1,10-phenanthroline-5,6-dione (Scheme 20). The reaction consisted of adding 1,10-phenanthroline and bromine in sequence at stirring to a mixture of H<sub>2</sub>SO<sub>4</sub> (96%) and HNO<sub>3</sub> (70%). The mixture was heated and stirred for 5 hours at 90 - 95 °C. After 2 hours of heating, an additional amount of bromine was introduced. The mixture was then poured onto the ice and neutralized with 30% NaOH solution. The product was extracted with methylene chloride and dried. The product has been recrystallized in methanol.



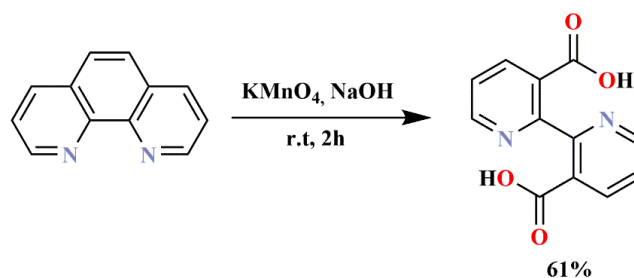
**Scheme 20.** The oxidation of 1,10-phenanthroline is based on the work of S. A. Mitsov et al.<sup>99</sup>.

Based on the observations collected by S. A. Mitsov et al., they suggested the following mechanism of 1,10-phenanthroline oxidation into 1,10-phenanthroline-5,6-dione (Scheme 21).



**Scheme 21.** Mechanism of 1,10-phenanthroline oxidation into 1,10-phenanthroline-5,6-dione presented by Mitsov et al.<sup>99</sup>. Hydrogen atoms were added to the mechanism to visualize compound transformations better. Racemates and meso (pseudomeso<sup>100</sup>) forms have been distinguished.

Oxidation of 1,10-phenanthroline derivatives can also lead to breaking the bond between carbon atoms on the phenyl ring, resulting in the formation of bipyridine derivatives. In the work of A.S Denisova et al.<sup>11</sup> in addition to receiving 1,10-phenanthroline-5,6-dione according to the procedure of M. Yamada et al., other oxidation reactions of 1,10-phenanthroline derivatives were also carried out, including obtaining bipyridine derivatives (Scheme 22). The use of potassium manganate(VII) in an alkaline environment as an oxidant led to the C = C bond breaking. Further oxidation of the compound led to obtaining selected selectively [2,2'-bipyridine]-3,3'-dicarboxylic acid dicarboxylic acid.

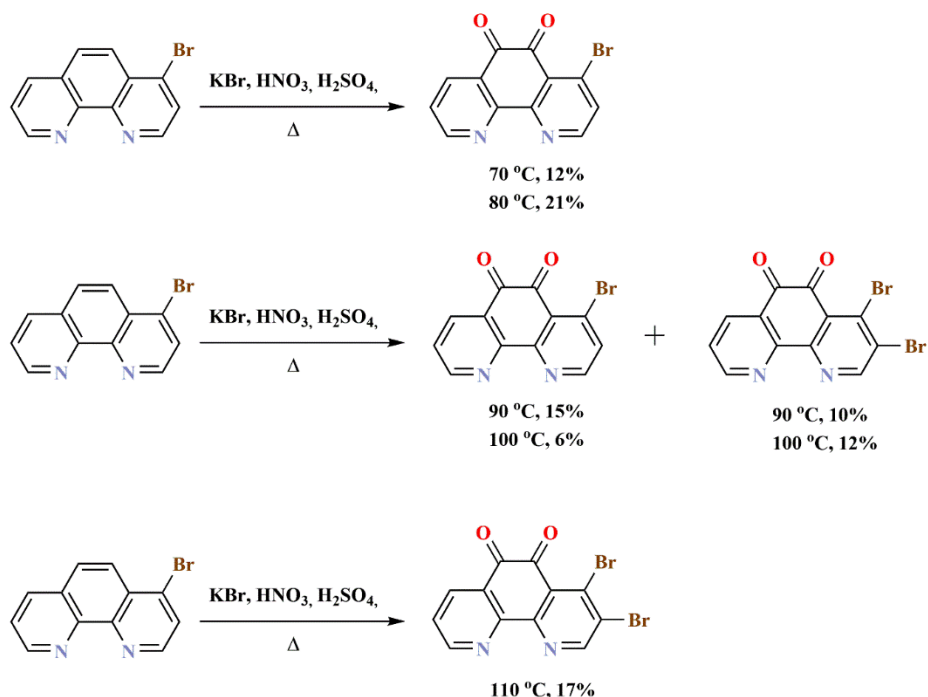


**Scheme 22.** Synthesis of [2,2'-bipyridine]-3,3'-dicarboxylic acid<sup>11</sup>.

Oxidation of selected halogenated 1,10-phenanthroline was shown in work Peng et al.<sup>101</sup>. In their work, they present by-products based on the reaction by M. Yamada et al. Peng et al. reported an interesting effect of temperature on reaction products was observed. In the case of 4-bromo-1,10-phenanthroline, the reaction in 70 - 80 °C results in a 4-bromo-phenanthroline-5,6-dione product. In turn, when the reaction proceeds at higher temperatures

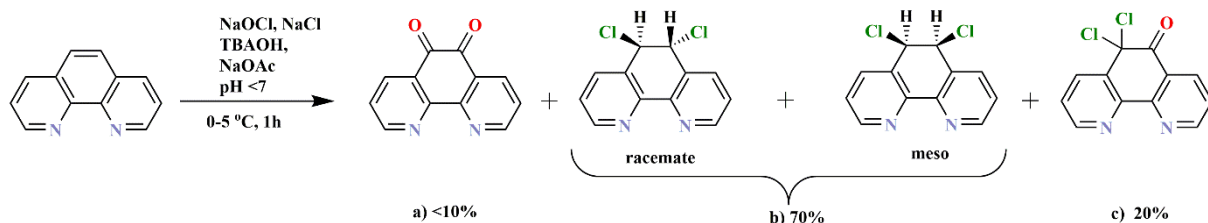


of 90 - 100 °C, a byproduct of 3,4-dibromo-1,10-phenanthroline-5,6-dione is formed. And for a temperature of 110 °C, the product is only a 3,4-dibromo derivative (Scheme 23).



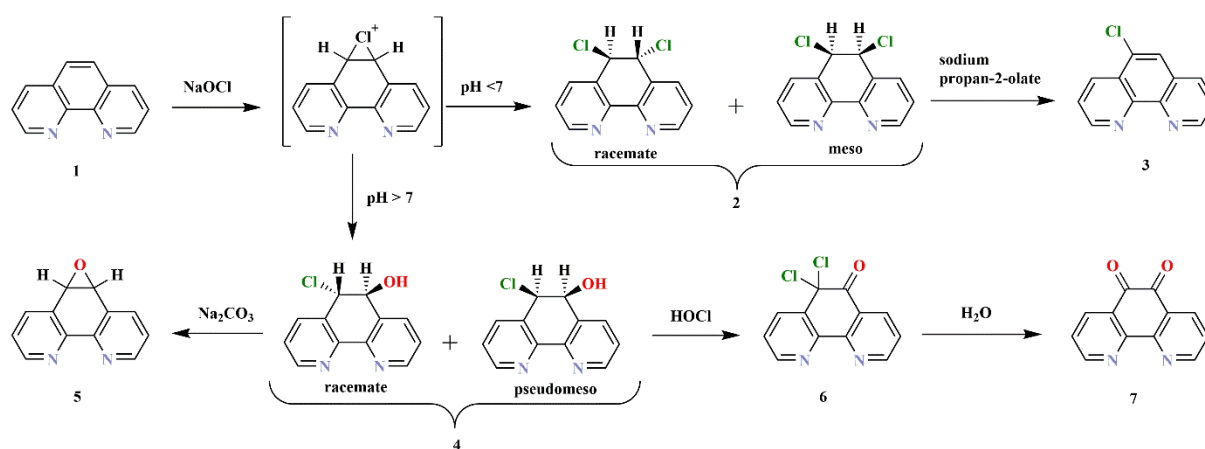
**Scheme 23.** Oxidation of 4-bromo-1,10-phenanthroline, the influence of temperature on the course of the reaction<sup>101</sup>.

Another exciting example shown in W.Z Antkowiak and R. Antkowiak's article is obtaining 1,1-phenanthroline-5,6-dione by reaction with an aqueous solution of hypochlorite<sup>102</sup>. Despite the desired product being obtained, the reaction showed a better yield for chloro derivatives. The article presents the influence of pH on the obtained products. It has been shown that at acidic pH, they received three products. One of them is the 1,10-phenanthroline-5,6-dione (Scheme 24, a), due to the ongoing hydrolysis of 6,6-dichloro-1,10-phenanthroline-5(6*H*)-one (Scheme 24, c).



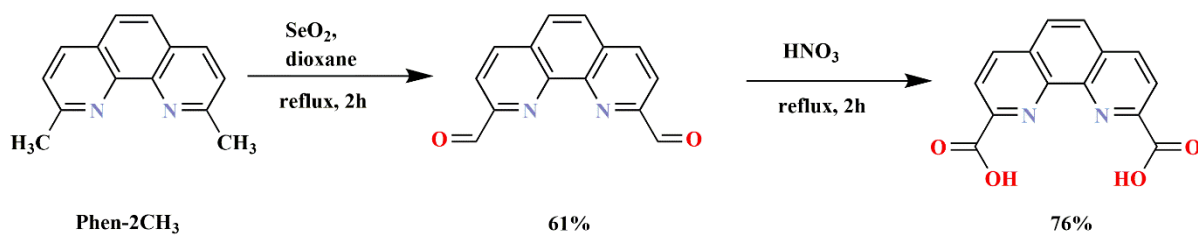
**Scheme 24.** The preparation of 1,10-phenanthroline-5,6-dione is based on the work of the Antkowiak group<sup>102</sup>.

Interestingly, they have shown that the treatment of chlorohydrine (**4**, Scheme 25) with sodium carbonate forms the corresponding epoxide (**5**), which can be omitted. In the case of different environments, a more acidic solution provides to obtain dichloro ketone (**6**) from chlorohydrine (**4**), which is already contaminated by 1,10-phenanthroline-5,6-dione (**7**) (Scheme 25). An additional element important from this point of view of the isolation of compounds is their optical isomerism. For compounds **2** and **4** (Scheme 24 and Scheme 25), racemates and meso (pseudomeso<sup>100</sup>) forms have been distinguished. This clarifies that the reaction's yield has not been determined for a particular isomer but rather for a racemic mixture and/or a meso compound.



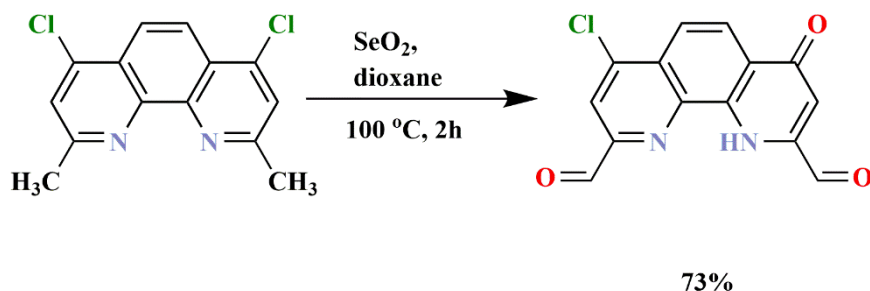
**Scheme 25.** Oxidation mechanism of the 1,10-phenanthroline base on the work Antkowiak et al.<sup>102</sup>.

Another example of the oxidation of selected 1,10-phenanthroline derivatives is the oxidation presented by A. De Cian et al.<sup>103</sup>. They presented the oxidation procedure of the 2,9-dimethyl-1,10-phenanthroline (**Phen-2CH<sub>3</sub>**) to obtain 1,10-phenanthroline-2,9-dicarbaldehyde in the first step and then 1,10-phenanthroline-2,9-dicarboxylic acid. The first step was to add selenium dioxide (SeO<sub>2</sub>) to a solution of 2,9-dimethyl-1,10-phenanthroline in dioxane at room temperature. After heating under reflux for 2 hours, the mixture was cooled, and the formed precipitate was collected and washed with diethyl ether. At the second stage, the obtained dicarbaldehyde was dissolved in a 70% solution of nitric acid. After reflux for 2 hours, a solution was cooled to 0 °C, and then water was added in portions until a precipitate formed. The residue was collected and washed with diethyl ether. After drying in vacuo, the crude 1,10-phenanthroline-2,9-dicarboxylic acid was recrystallized from methanol. (Scheme 26).



**Scheme 26.** Synthesis of 1,10-phenanthroline-2,9-dicarboxylic acid by A. De Cian et al.<sup>103</sup>.

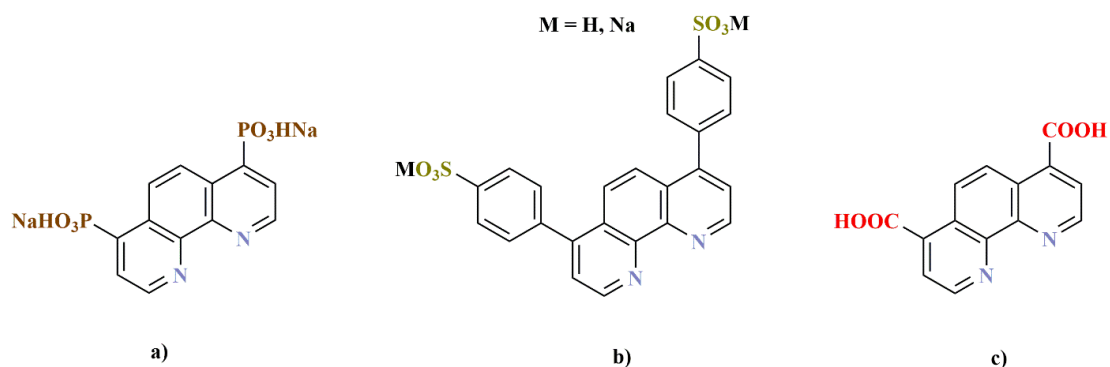
It is worth mentioning that in the case of oxidation of 4,7-dichloro-2,9-dimethyl-1,10-phenanthroline with SeO<sub>2</sub> in 1,4-dioxane the desired dialdehyde has not been afforded as the major product which was presented in work Larsen et al.<sup>104</sup>. The product was the unsymmetrical partially hydrolyzed 7-chloro-4-oxo-1,4-dihydro-1,10-phenanthroline-2,9-dicarbaldehyde in good yields (Scheme 27). Thus, although this compound was not the desired product from the reaction, it provides a valuable entry into unsymmetrical 4,7-disubstituted-1,10-phenanthroline-2,9-dicarboxylate derivatives.



**Scheme 27.** Preparation of 4-chloro-7-hydroxy-1,10-phenanthroline-2,9-dicarbaldehyde by oxidation with SeO<sub>2</sub>.

### 5.6.2 Selected acids derivatives of 1,10-phenanthroline

Substituted 1,10-phenanthrolines which are water-soluble, were sought as a means to extend their usefulness as indicators. Water-soluble 1,10-phenanthrolines are usually obtained by sulfonation, carboxylation or phosphorylation of 1,10-phenanthrolines or their derivatives. At present, there are already procedures in which water-soluble 1,10-phenanthroline derivatives are synthesized, permitting the preparation of metallic complexes that catalysis in water (Scheme 28).



**Scheme 28.** Examples of 1,10-phenanthroline acids base on literature a) sodium salt of 4,7-diphosphono-1,10-phenanthroline acid only claim in patent application<sup>105</sup>, b) 4,7-diphenyl-1,10-phenanthroline sulfonic acid and their sodium salts<sup>106</sup>, c) 1,10-phenanthroline-4,7-dicarboxylic acid<sup>107</sup>.

The soluble in water acids of 1,10-phenanthroline can be divided into three classes. The first class is derivatives of 1,10-phenanthroline phosphonic acids, which have not been characterized or described in spite of their description<sup>105</sup>. Next are derivatives of 1,10-phenanthroline sulfonic acids, which is also an interesting side of water-soluble compounds. There are not many descriptions of their preparation, but they are commercially available. They constitute a large field of their possible application like, for example, drug gradient challenge assay or measuring iron levels in the liver<sup>108,109</sup>.

The third class is derivatives of carboxylic acids. Despite the already existing publications or patents in which the synthesis of 1,10-phenanthroline-2,9-dicarboxylic acid (showed in chapter 5.6.1) or 1,10-phenanthroline-2-carboxylic acid has been described, the most frequently presented transformations are multistep and based on the use of toxic compounds like selenium dioxide and HNO<sub>3</sub>. An additional problem associated with the use of SeO<sub>2</sub> is the possibility of product contamination with selenium. An alternative method is the oxidation of commercially available 2,9-dimethyl-1,10-phenanthroline (**Phen-2CH<sub>3</sub>**, neocuproine) by means of CrO<sub>3</sub> or KMnO<sub>4</sub>. The 1,10-phenanthroline-2,9-dicarboxylic acid obtained in the reaction may be contaminated with 5,6-dihydro-5,6-dioxo-1,10-phenanthroline-2,9-dicarboxylic acid, which significantly limits the isolation yield<sup>110</sup>.

The described acids are bifunctional compounds that imitate amino acids or naturally occurring nicotinic acid (precursor of vitamin PP). This means that it or its derivatives can be used in medicine or the pharmaceutical industry.

For *N*-heterocyclic compounds with the carboxyl group, especially multi-carboxyl groups allow obtaining new properties. These types of compounds have been widely used to construct multifunctional coordination polymers because of the diverse coordination modes and the specific orientations<sup>111</sup>. The carboxyl group itself allows for coordination to the metal center through bridging/chelating modes; one carboxylic group could connect one, two, three, or even four metal centers. Additionally, the carboxyl groups could be partially or completely deprotonated where, depending on the acidity, different bonding modes can be expected<sup>112</sup>.

In acids or multi acids of 1,10-phenanthrolines, their possible coordination will be possible thanks to the known and characteristic angular system and through the carboxyl group or groups.

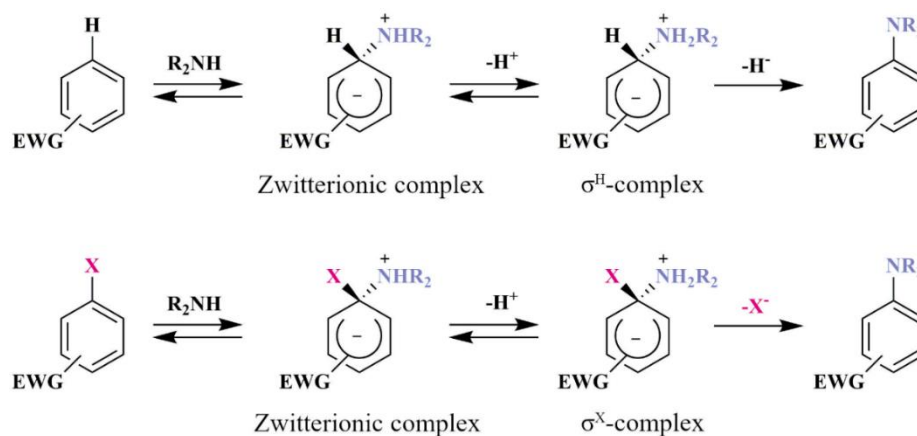
## 5.7 Synthesis of substituted 1,10-phenanthroline derivatives

The mechanism of substitution of 1,10-phenanthrolines will be briefly discussed in a separate section below.

### 5.7.1 Nucleophilic Aromatic Substitution

The mechanism of this type of reaction will be briefly discussed to proceed with the examples of the chemical transformation of 1,10-phenanthrolines.

In 1902 thanks to an article by Jakob Meisenheimer, nucleophilic substitution reactions in aromatic systems have been well known. In his work, he isolated an anionic  $\sigma$ -complex (Meisenheimer complex) between an alkoxide and a trinitrophenyl ether<sup>113</sup>. In turn, evidence from experiments generally points to a two-step process (addition-elimination) that depends on the nucleophile, the outgoing group, and the presence of electron-withdrawing substituents<sup>114</sup>. In the first step, the nucleophile would attack the position ipso to the electron-withdrawing group of the electron-deficient aromatic ring to yield an anionic sigma adduct intermediate. The tetrahedral carbon ( $sp^3$ ) intermediate is most often unstable, and the reaction may proceed further by reactivating to yield the substituted product or revert to previous reactants. It is possible to distinguish two types of Meisenheimer complex, the  $\sigma^H$ -complex or  $\sigma^X$ -complex, depending on the aromatic ring position attacked by the nucleophile (a non-substituted or substituted one, respectively) (Scheme 29). It is worth noting that when the  $\sigma^H$ -complex is formed, the reaction rarely proceeds spontaneously to the next stage<sup>115</sup>.



**Scheme 29.** Mechanism of nucleophilic aromatic substitution base on work R. O. Al-Kaysi et al.<sup>115</sup>.

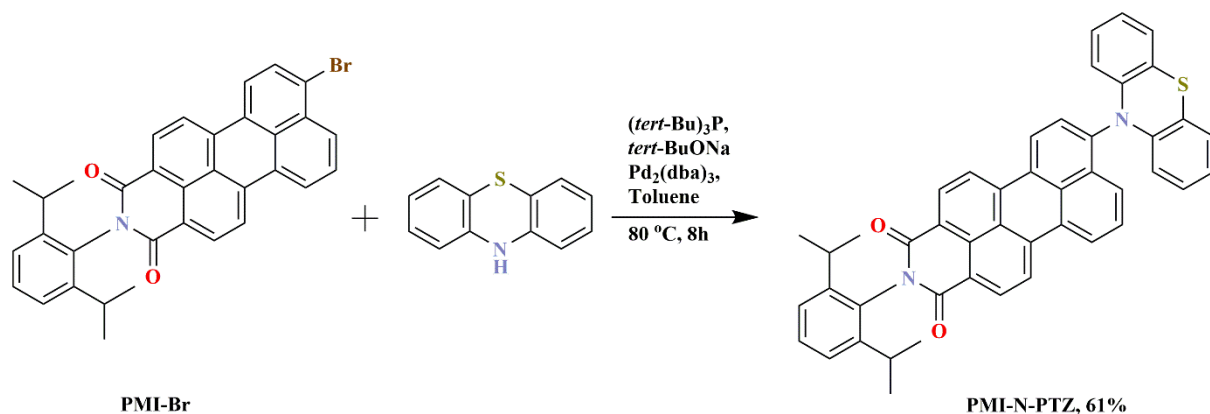
Reaction conditions employed to affect this reaction require anhydrous conditions, strong bases, or highly reactive aromatic coupling partners, especially when relatively bulky amines are used as nucleophiles. One of the varieties to overcome difficulties in this type of reaction is to use many artifices like electrochemistry, catalysis by transition metals using stronger nucleophiles, more polar solvents or using microwave irradiation.

G.V. Salmoria et al. study the microwave irradiation effect on nucleophilic aromatic substitution. They have shown the same substrate reactivity order to leaving group and the activating group as classical  $S_NAr$ . What was significant was the short reaction time with good yields<sup>116</sup>.

There are also other varieties of aromatic nucleophilic substitution in addition to the aforementioned substitution with the formation of the Meisenheimer complex. An interesting example is Buchwald-Hartwig amination where it forms a carbon-nitrogen bonding reaction by coupling aromatic halide with amines in the presence of a palladium catalyst. Y. Zhao et al.<sup>117</sup> presented this type of reaction with phenothiazine as amine (Scheme 30).

This reaction consisted of mixing PMI-Br, phenothiazine, and sodium *tert*-butoxide in toluene (previously dried) under a nitrogen atmosphere). Then Pd(dba)<sub>3</sub> (tris(dibenzylideneacetone)dipalladium) and (*tert*-Bu)<sub>3</sub>P were added and heated at 80 °C for 9 hours. Isolation consisted of adding water and dichloromethane and cooling the mixture. The limiting phase was separated and washed with brine and dried with sodium sulfate. The

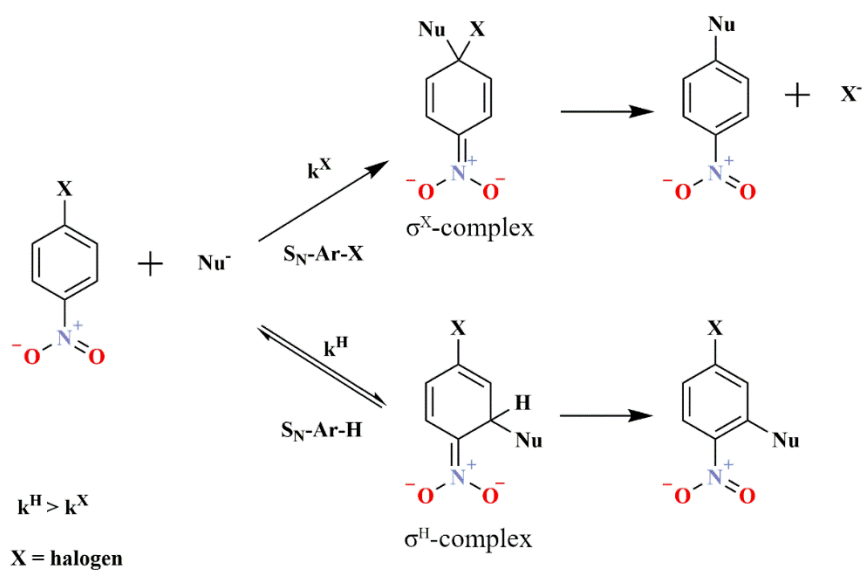
solvent was evaporated under reduced pressure. The crude product was purified by column chromatography.



**Scheme 30.** Buchwald-Hartwig reaction base on Y. Zhao et al.<sup>117</sup>.

For aromatic nucleophilic substitution in the case of compounds with an electron-withdrawing group, e.g., a nitro group, it is possible to observe two competing types of reactions  $S_NAr$  and VNS.

As mentioned before, when the  $\sigma^H$ -complex is formed, the reaction rarely proceeds spontaneously to the next stage, but in the case of compounds with the nitroaromatic ring, the next stage of the exchange of hydrogen atom is already present. This type of reaction is the nucleophilic substitution of hydrogen  $S_NAr\text{-}H$  (Scheme 31), which involves such reactions as the oxidative nucleophilic substitution of hydrogen (ONSH) and vicarious nucleophilic substitution (VNS)<sup>118</sup>.



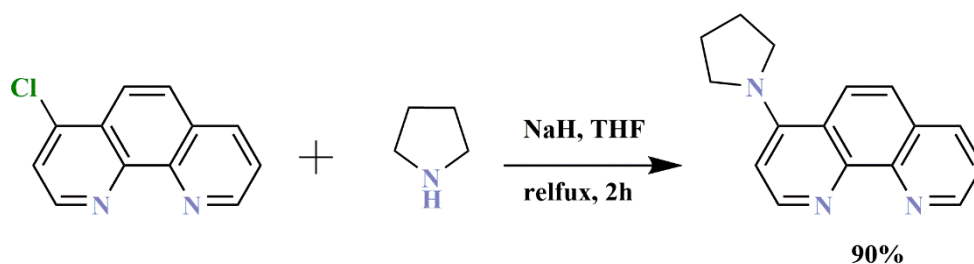
**Scheme 31.** Nucleophilic substitution of halogen  $S_NAr\text{-}X$  (a) and hydrogen  $S_NAr\text{-}H$  (b) in *para* substituted nitrobenzenes base on M. Małkosza et al.<sup>118, 119</sup>.

The aforementioned VNS reaction is one way to convert anion  $\sigma^H$ -complex into a product by indirectly removing the hydride anion in proton form. It is worth mentioning that the VNS reaction is faster than the typical nucleophilic substitution of the halogen atom. It is essential to mention that VNS reaction may compete with the aromatic nucleophilic substitution of halogen  $S_NAr$ . The substitution of the nitro substituent is also possible. According to Małosza et al., the VNS often proceeds much faster than  $S_NAr$  substitutions, as mentioned above<sup>120,121,122</sup>. The VNS reaction is usually intensively colored, which has diagnostic values<sup>120</sup>.

### 5.7.2 Synthesis of mono- and disubstituted 1,10-phenanthroline by selected amines in ortho and para position

In this chapter, the described substitutions will be based on the above-mentioned aromatic nucleophilic substitution  $S_NAr$ .

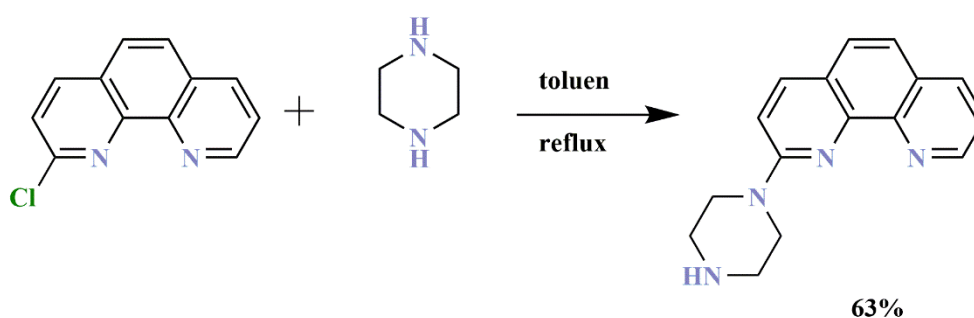
The first example of the synthesis of monosubstituted-1,10-phenanthrolines is the work of J. Engel-Andreasen et al. (Scheme 32)<sup>123</sup>. They received 4-pyrrolidine-1,10-phenanthroline starting from 4-chloro-1,10-phenanthroline substrate. The 4-chloro-1,10-phenanthroline with pyrrolidine was heated to reflux under nitrogen for 2 hours. Then they evaporate the excess solvent and washing crude products with water, and drying under reduced pressure. DIPEA was added to the filtrate to precipitate the rest. The reaction was carried out on a small scale of up to 100 mg. This is an example of the  $S_NAr$  mechanism discussed earlier, where the use of sodium hydride in the reaction allows the formation of a pyrrolidine anion that substitutes a halogen atom.



**Scheme 32.** Monosubstitution of 4-chloro-1,10-phenanthroline by J. Engel-Andreasen et al.<sup>123</sup>.

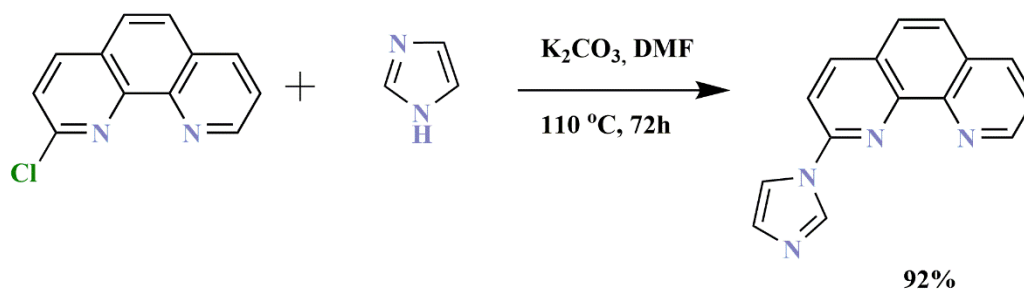


The interesting reaction was preparing the monosubstituted compound 2-(piperazin-1-yl)-1,10-phenanthroline, which was presented by a group of T.E. Kokina et al. (Scheme 33)<sup>124</sup>. The mixture of piperazine, 2-chloro-1,10-phenanthroline in toluene was boiled up until the disappearance of starting 2-chloro-1,10-phenanthroline, checked by TLC. Toluene was distilled off, and the residue was dissolved in chloroform and chromatographed on silica gel. The obtained product with piperazine group as a linker allows for its further functionalization. The reaction was carried out on a scale of up to a few grams. Despite the lack of an agent to deprotonate piperazine's acid proton, the reaction proceeded with good yield. The reaction mechanism is not presented in the article.



**Scheme 33.** The reaction of 2-chloro-1,10-phenanthroline with piperazine by T. E. Kokina et al.<sup>124</sup>.

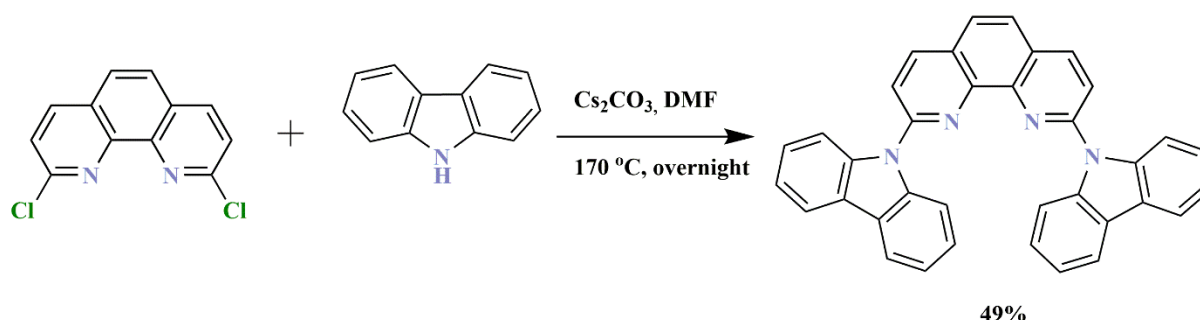
One of the proposed monosubstituted molecule present group of Zheng et al.<sup>125</sup>. The 2-((1*H*)-imidazol-1-yl)-1,10-phenanthroline was prepared according to the following method (Scheme 34). The 2-chloro-1,10-phenanthroline and imidazole were dissolved with DMF and potassium carbonate was added into the solution. After reflux for 72 h at 110 °C, the solvent was removed by distillation performed under reduced pressure. The yellow sediment appeared when ice/water mixture was added into the flask and fully stirred. The pale yellow solid 2-((1*H*)-imidazol-1-yl)-1,10-phenanthroline was obtained after the sediment was washed with iced water until the filtrate's pH value was neutral. The mechanism is also an S<sub>N</sub>Ar, which occurs through a proton elimination from piperazine, creating an anion that substitutes a chlorine atom. Potassium carbonate was used to deprotonate the acid proton of piperazine, enabling further reaction<sup>126</sup>.



**Scheme 34.** Preparation of 2-(1*H*-imidazol-1-yl)-1,10-phenanthroline by Zheng et al<sup>125</sup>.

In reactions with the substitution of two chlorine atoms, the reaction most often uses similar procedures to the previously presented examples. M. Sardini's doctoral thesis presents 2,9-di(9*H*-carbazol-9-yl)-1,10-phenanthroline obtained by substituting chlorine atoms (Scheme 35)<sup>127</sup>. The 2,9-dichloro-1,10-phenanthroline, 9*H*-carbazole, and dicesium carbonate were dissolved in DMSO. The dark red mixture was heated at  $170\text{ }^\circ\text{C}$  for several hours. After that time, it reduced the amount of DMSO. A precipitate formed by the addition of water was separated by filtration. The crude product was purified by column chromatography in methyl chloride as the eluent. The 2,9-di(9*H*-carbazol-9-yl)-1,10-phenanthroline was prepared by  $\text{S}_{\text{N}}\text{Ar}$  of deprotonated 9*H*-carbazole on 2,9-dichloro-1,10-phenanthroline.

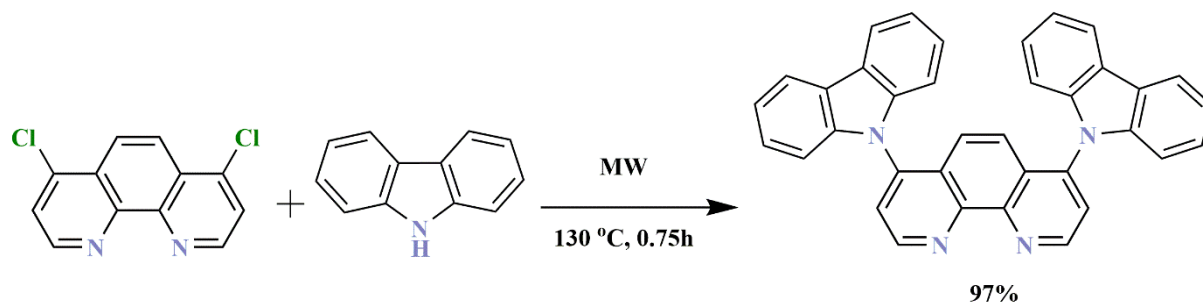
The dicesium carbonate used in the reaction was intended to deprotonate the 9*H*-carbazole molecules. The reaction of forming the C-N bond with cesium carbonate is known in the literature, most often with the addition of a catalyst, e.g., copper(I) iodide<sup>128</sup>. However, in the work of M. Sandroni, no additional catalyst was used.



**Scheme 35.** Substitution of the 2,9-dichloro-1,10-phenanthroline base on work M. Sandroni<sup>127</sup>.

Another example of the disubstitution of dichloro-1,10-phenanthrolines is described in the work of J. Engel-Andreasen et al. (Scheme 36)<sup>121</sup>. This work presents the effect of

microwave radiation mentioned in the previous chapter. The same order of reactivity of the leaving and activated group takes place as for the classical  $S_NAr$  reaction. A suspension of 4,7-dichloro-1,10-phenanthroline and pyrrolidine was heated in the microwave reactor at 130 °C for 45 min. The mixture was concentrated and washed with sodium hydrogen carbonate ( $NaHCO_3$ ) water solution followed by ice-cold water and dried under pressure to give a brown powder. Compared to the previous examples, the procedure using a microwave irradiation effect takes less than an hour to complete the reaction with a good yield.



**Scheme 36.** Preparation of 4,7-(dipyrrolidin-1-yl)-1,10-phenanthroline using a microwave reactor by J. Engel-Andreasen et al.<sup>132</sup>.

It is worth adding that the proton spectrum record in J. Engel-Andreasen et al.<sup>123</sup> lacks an additional aromatic signal in the form of a singlet corresponding to the protons at C5 and C6 positions.

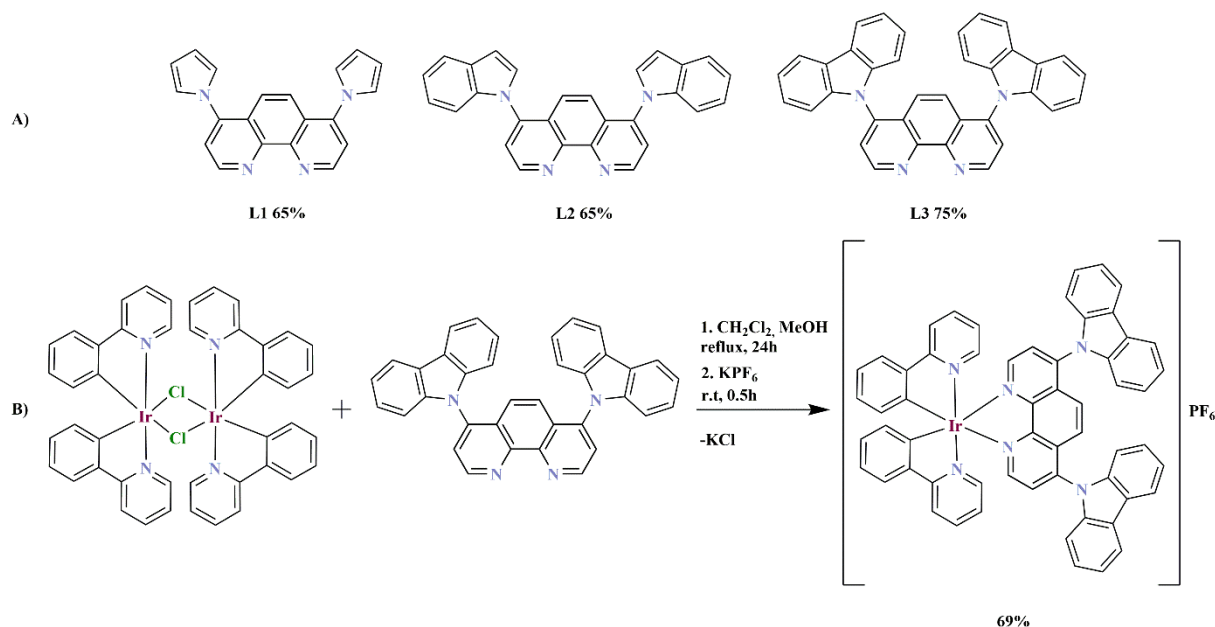
### 5.7.3 Optical properties and applications of mono and disubstituted-1,10-phenanthrolines

Many studies were dedicated to synthesizing 1,10-phenanthroline derivatives to obtain luminescence and fluorescence properties, where several examples are presented below. Selected phenanthroline substituents that differ in steric hindrance can evoke new properties. In turn, their good coordination properties make it possible to extend their potential applications.

In this section, applications will be presented for selected 4,7-disubstituted-1,10-phenanthrolines and their complexes reported in the literature.

The first example is Ir(III) based complexes of 4,7-di(1*H*-pyrrol-1-yl)-1,10-phenanthroline, 4,7-di (1*H*-indol-1-yl)-1,10-phenanthroline and 4,7-di(9*H*-carbazol-9-yl)-1,10-phenanthroline (Scheme 37, A) presented in work of G. -G. Shan et al.<sup>129</sup>. Compounds presented in Scheme 37A were obtained *via* aromatic nucleophilic substitution of 4,7-dichloro-1,10-phenanthroline. The obtained ligands were coordinated with organometal

dimers  $[\text{Ir}(\text{ppy})_2\text{Cl}]_2$ ,  $[\text{Ir}(\text{ppz})_2\text{Cl}]_2$  and  $[\text{Ir}(\text{dfppz})_2\text{Cl}]_2$  (one example of the reaction shown in Scheme 37, B).



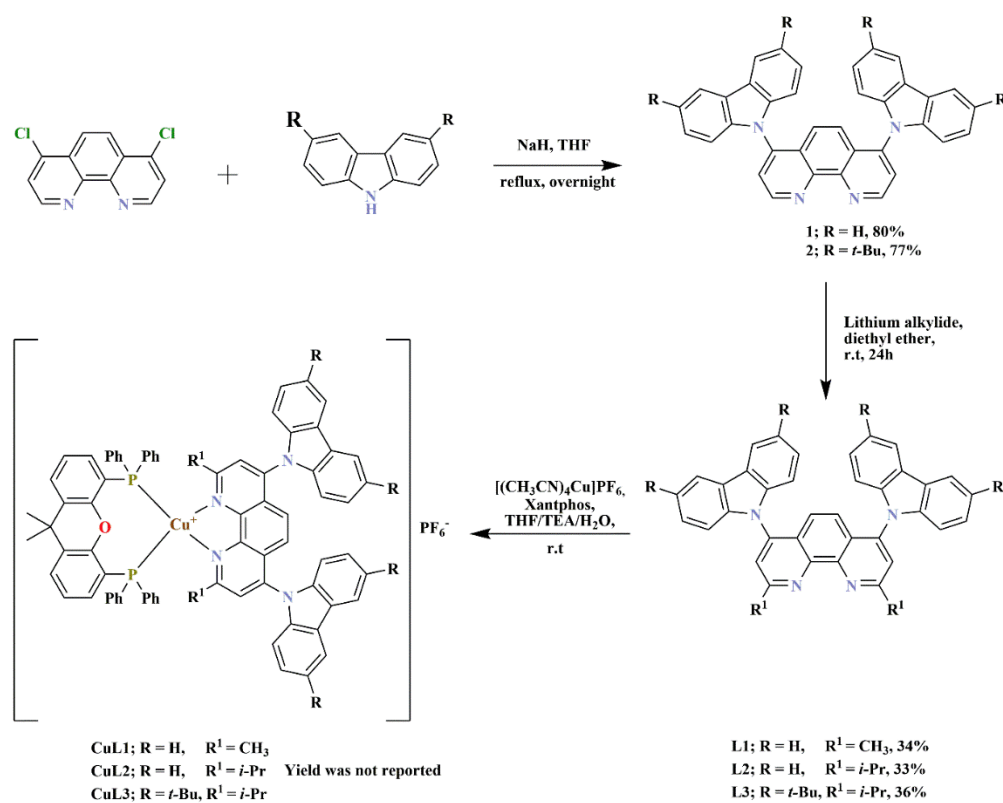
**Scheme 37. A)** The 4,7-disubstituted-1,10-phenanthroline by pyrrole (L1), indole (L2) and carbazole (L3) groups; **B)** Reaction of  $[\text{Ir}(\text{ppy})_2\text{Cl}]_2$  with 4,7-di(9*H*-carbazol-9-yl)-1,10-phenanthroline base on work G. -G. Shan et al.<sup>129</sup>.

The Ir(III) based complexes have shown a tendency to be highly appealing as triplet emitters in the organic light-emitting diodes (OLEDs) and light-emitting electro-chemical cells (LECs)<sup>130</sup>. Ir(III)-based LECs, a new type of organic electroluminescent devices, possess several advantages over conventional OLEDs such as simple device architecture, low turn-on voltage, and independent work function. In the work of G. -G. Shan et al.<sup>129</sup>, iridium(III) complexes with selected ligands (shown in Scheme 37, A) were tested for quantum photoluminescence efficiency (PLQY). It has been shown that the larger the steric hindrance, the higher the PLQY value. Additionally, in the case of complexes with 4,7-di(9*H*-carbazol-9-yl)-1,10-phenanthroline, the conducted studies showed high thermal stability. These types of properties are a valuable feature for the fabrication of efficient and stable LECs.

Due to the wide range of uses carbazole, for example, in the field of photoluminescence and electroluminescence, it arouses interest in examining the effectiveness of carbazole substituted dyes as photosensitizers. There were studied in the work of Z. -J. Yu

et al.<sup>131</sup>. Copper(I) complexes with carbazole-substituted 1,10-phenanthroline ligands were investigated as photosensitizers for water reduction. Synthesis of carbazole containing phenanthrolines was achieved by nucleophilic aromatic substitution using sodium hydride base similar to the procedure described in chapter 5.7.1 (Scheme 31).

The first step in obtaining the designed copper photosensitizers was the substitution of 4,7-dichloro-1,10-phenanthroline with the carbazole derivative. The ligand obtained earlier were transformed by their functionalization in the C2 and C9 positions by nucleophilic addition of lithium alkylide. The last step is an *in situ* synthesis method by reacting  $\text{Cu}(\text{CH}_3\text{CN})_4\text{PF}_6$ , Xantphos, and the selected 1,10-phenanthroline to form the desired complex (Scheme 38).

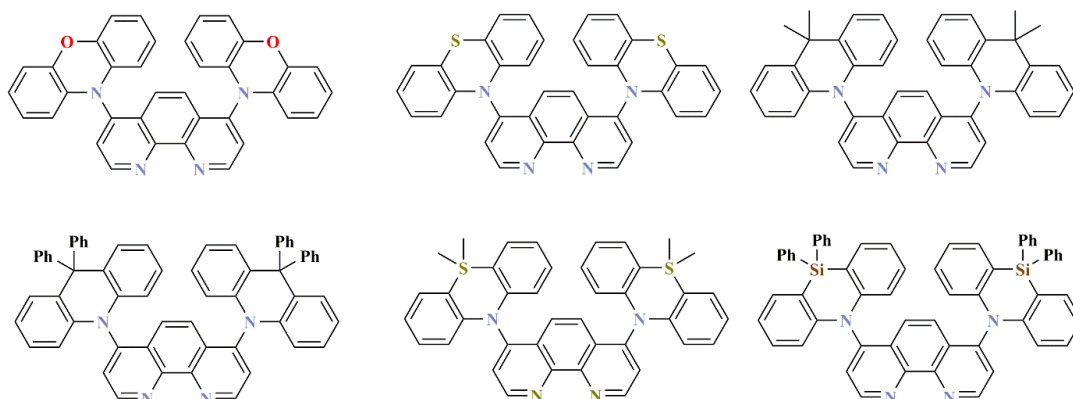


**Scheme 38.** The preparation of selected copper complexes presented in the work of Z. -J. Yu et al.<sup>131</sup>.

The copper complexes shown in Scheme 38 can be used for photocatalytic proton reduction using  $\text{Fe}_3\text{CO}_{12}$  as a water reduction catalyst.

Another example is substitution with aromatic diphenylamine derivatives. C. Yang et al. describe fluorescence material containing 4,7-disubstituted-1,10-phenanthrolines (Scheme 39)<sup>132</sup>. The invention provides a thermally-induced delayed fluorescence material and a preparation method of an organic electroluminescent device. The synthesis of 4,7-

disubstituted-1,10-phenanthrolines is based on aromatic nucleophilic substitution starting from 4,7-dichloro-1,10-phenanthroline.

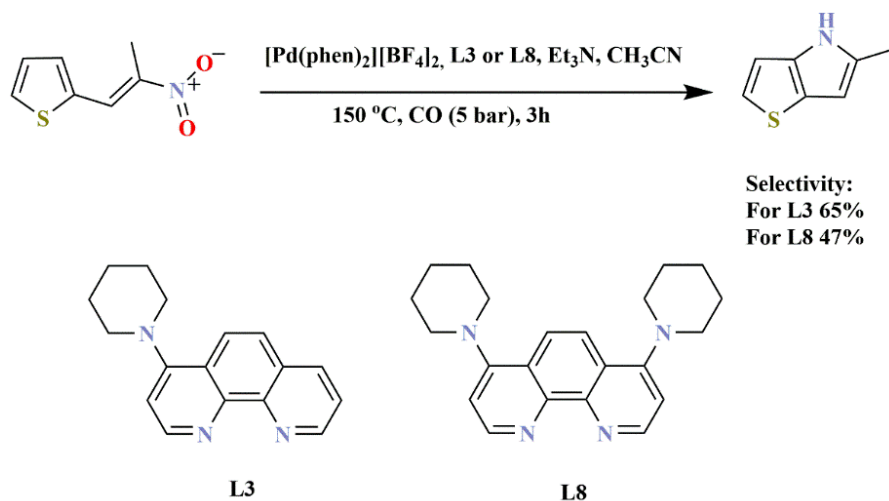


**Scheme 39.** The structures of the obtained 4,7-disubstituted-1,10-phenanthroline derivatives are based on C. Yang et al.<sup>132</sup>.

The obtained organic compounds showed in Scheme 39 can serve as a luminous layer material in OLEDs.

In the work of El-Atawy et al.<sup>133</sup> they used 4-piperidino-1,10-phenanthroline and 4,7-dipiperidino-1,10-phenanthroline to check the influence of the ligand on the palladium-catalyzed reductive cyclization of (*E*)-2-(2-nitropropenyl)thiophene to 5-methyl-4*H*-thieno[3,2-*b*]-pyrrole (Scheme 40). In their previous work, they showed that the ligand structure could strongly affect the activity of the catalytic system in the related reductive carbonylation of nitroarenes<sup>134,135</sup>.

For the reaction shown in Scheme 40, selectivity was determined by GC analysis with naphthalene as an internal standard.



**Scheme 40.** An example of a reducing cyclization of a thiophene derivative using a palladium catalyst and selected mono and disubstituted-1,10-phenanthroline<sup>133</sup>.

## 5.8 Quinoline derivatives: introduction

As shown in Scheme 1 in the General introduction, quinoline and benzo[*h*]quinoline are 1,10-phenanthroline analogs. The quinoline derivatives arouse interest due to their broad spectrum of activity. These compounds exhibit, for example, anti-inflammatory<sup>136</sup>, antipsychotic<sup>137</sup>, antioxidant<sup>138</sup>, antifungals<sup>139</sup>, or anti-HIV properties<sup>140</sup>. The quinoline structure includes a benzene ring fused to a pyridine ring, and the molecule is planar. Quinoline is a  $\pi$ -deficient heterocycle with a slightly lower pKa = 4.9 to related pyridine (pKa = 5.2). The  $\pi$ -electrons density for quinoline shows a strong negative charge on the nitrogen atom (similar to 1,10-phenanthroline)<sup>141</sup>. For nucleophilic activity, the C2 and C4 positions are more preferred on the electron-poor pyridine ring. In turn, the C8 and C5 positions will be preferred for electrophilic activity (Figure 2, a).

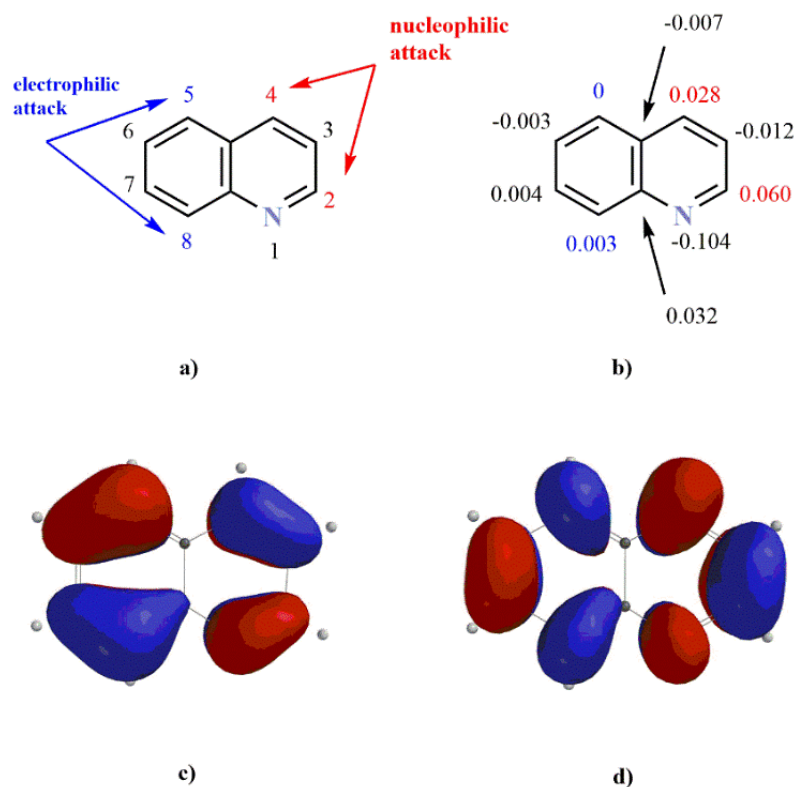
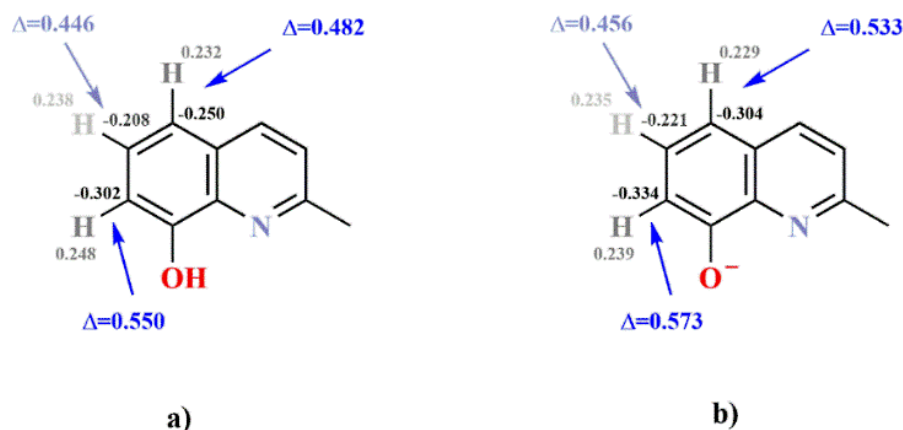


**Figure 2.** a) numbered position of atoms b)  $\pi$ -electrons density<sup>141</sup> c) HOMO base on A. A. Al-abbasi<sup>142</sup> d) LUMO base on A. A. Al-abbasi<sup>142</sup> of quinoline.

An interesting example of quinoline derivatives is 8-hydroxyquinoline. This compound, as monohydroxyquinoline, is one of eight possible regioisomers. It is the only one that allows to forming complexes with divalent metal ions through chelation<sup>143</sup>. It is one of the oldest antimicrobials with reported antiseptic activity dating back to 1895. Human anti-infective applications date back earlier than modern antibiotics<sup>144,145</sup>. In the 1940s, researchers recognized the strong affinity of 8-hydroxyquinoline to metal ions as giving the molecule strong antimicrobial properties against various bacterial pathogens in micromolar concentrations<sup>146</sup>. Interestingly, 8-hydroxyquinoline derivatives occur naturally. In an endemic deciduous tree native to Sri Lanka called *Broussonetia zeylanica*, 8-hydroxyquinoline-4-carbaldehyde and 8-hydroxyquinoline-4-carbaldehyde oxime were isolated<sup>147</sup>.



In the literature, it can be found the calculated natural atomic charge for 2-methyl-8-hydroxyquinoline<sup>148</sup>. Such data can predict substitution mechanisms, highlighting the preferred position in the molecule. By analyzing the atomic charge for 2-methyl-8-hydroxyquinoline, one can observe their compatibility with the electrophilic activity (Figure 2). The greatest potential differences occur at the C5 and C7 positions on the phenol ring



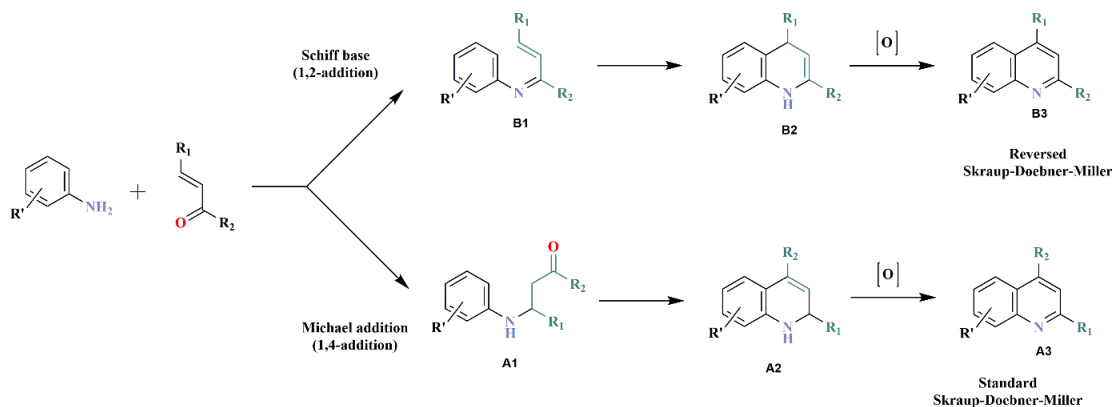
(especially under alkaline conditions, Figure 3, b).

**Figure 3.** Natural atomic charges of neutral (a) and anionic (b) 8-hydroxy-2-methylquinoline base on literature<sup>148</sup>.

For quinoline derivatives with an electron-withdrawing substituent at the C8 position, the position selection preference for  $S_{E}Ar$  changes for C5 and C7 position on the phenyl ring<sup>149</sup>.

## 5.9 The use of Skraup reaction and reaction using Meldrum acid transformation of selected quinolines

One of the methods allowing to obtaining quinoline derivatives is the Skraup-Doebner-Von Miller reaction<sup>150,151</sup>. It is based on the direct use of  $\alpha,\beta$ -unsaturated carbonyl, and aniline (example in Scheme 41).

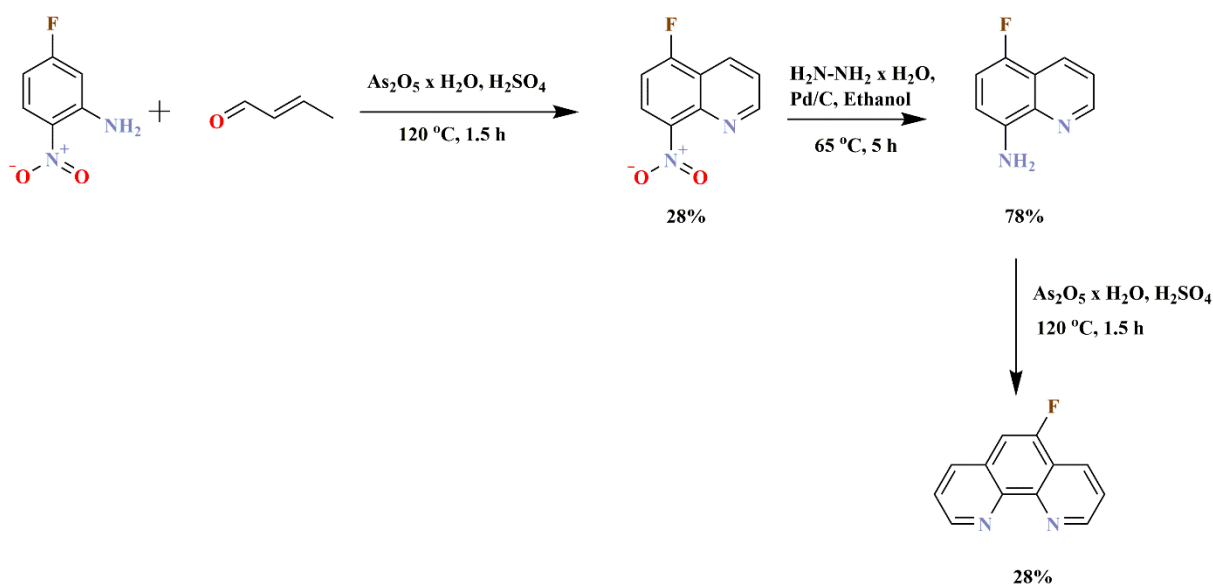


**Scheme 41.** Simplified mechanism of reversed and standard Skraup-Doebner-Miller reaction<sup>150</sup>. The main differences of the reaction are shown in gray-green.

This method also allows obtaining 1,10-phenanthroline derivatives by appropriate selection of the reagents.

For example, in the work of C. Ludtke et al.<sup>152</sup> was presented a synthesis of selected 1,10-phenanthroline using modified Skraup-Doebner-Miller reactions (Scheme 42). The products in the first reaction stage are quinoline derivatives, which take part in further reactions to form selected 1,10-phenanthrolines. In the first step selected nitroaniline derivative to react with arsenic pentoxide hydrate in a solution of sulfuric acid. The solution was then heated up to 70 °C, and crotonaldehyde was added dropwise. After completing the addition, the solution was heated up to 120 °C for 90 min with vigorous stirring. The mixture was poured onto an ice/water mixture, and the resulting suspension was separated by filtration. Dichloromethane was added, and the organic phase was washed with brine and extracted. A chromatography column purified the product, receiving the selected nitroquinoline.

The obtained selected nitroquinoline derivatives were reduced with a palladium-on-carbon catalyst. For the obtained aminoquinolines, the Skraup-Doebner-Miller reaction was performed again to obtain the selected 1,10-phenanthroline derivatives.

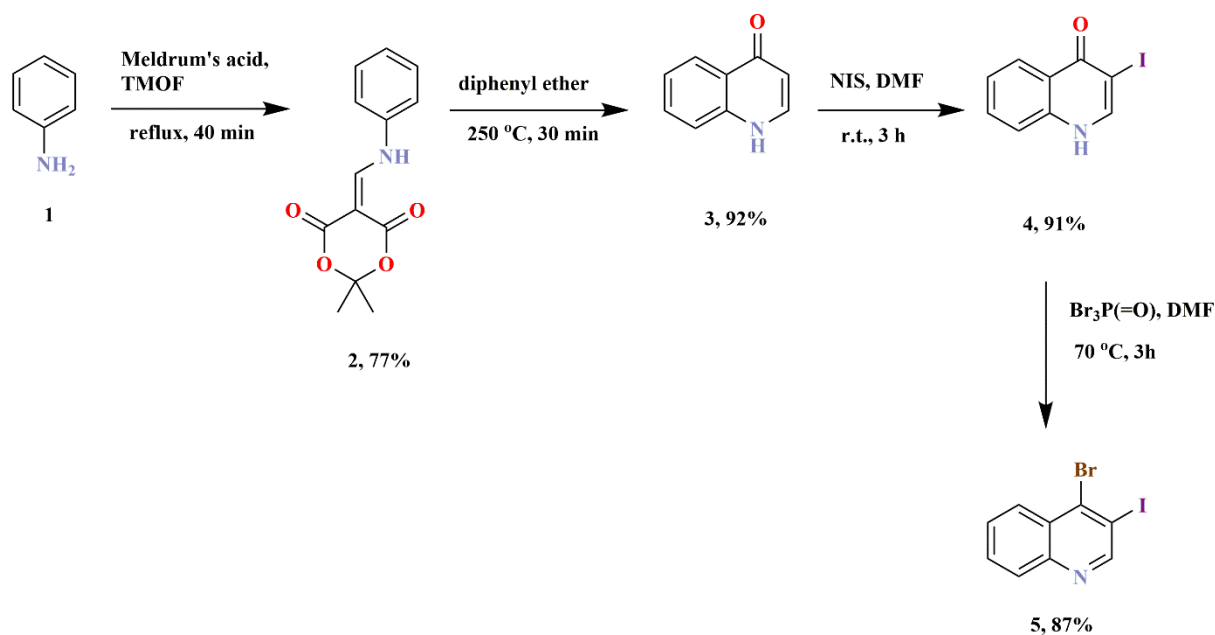


**Scheme 42.** Synthesis of 5-fluoro-8-nitroquinolines and 5-fluoro-1,10-phenanthroline derivatives via modified Skraup reaction based on C. Ludtke et al.<sup>152</sup>.

One of the methods of obtaining quinoline derivatives is the previously discussed method using Meldrum acids (chapter 5.3.2). In order to obtain the selected quinolines, aminobenzene (1,2-diaminobenzene in order to obtain 1,10-phenanthrolines) is used as a reagent. This reaction leads to the formation of 4-halogenated quinoline derivatives.

The work of B. Bohanyi and J. Kaman work presented a synthesis of 4-bromo-3-iodoquinoline (5) based on a method using Meldrum's acid (Scheme 43)<sup>153</sup>. The synthesis is based on the condensation of aniline (1) with Meldrum's acid in the presence of TMOF, followed by thermolysis with diphenyl ether. This procedure's modification is the additional step of direct halogenation before reaction with phosphoryl tribromide. For the preparation of 3-iodo-1*H*-quinoline-4-one (4) to the solution of 1*H*-quinolin-4-one (3) in DMF, *N*-iodosuccinimide was added dropwise. Reactions were carried out at room temperature for 3 hours. Then, after evaporation of the solvent, the precipitate was washed with water and dried in vacuo.

In the final step, treatment of 3-iodo-1*H*-quinoline-4-one (4) with phosphoryl tribromide gave the desired product 4-bromo-3-iodo-1*H*-quinoline (5) in high yield.



**Scheme 43.** Synthesis of the 4-bromo-3-iodoquinoline base on work of B. Bohanyi and J. Kaman<sup>153</sup>.

## 5.10 Functionalization of selected quinolines

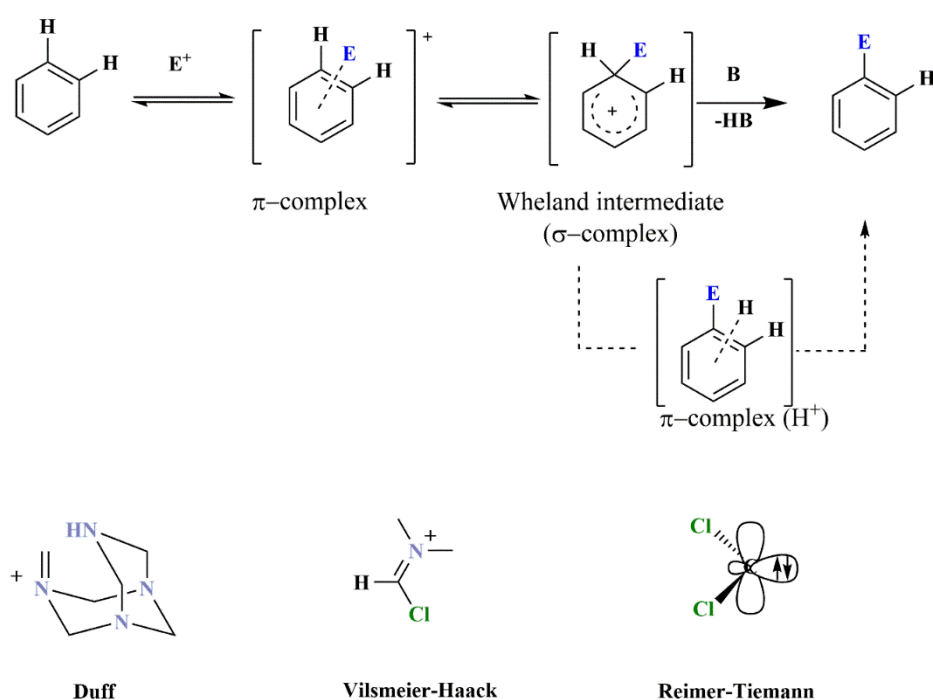
This chapter presents literature examples focused on the functionalization of quinoline derivatives through formylation. The possible mechanism of electrophilic aromatic substitution and its variations were also discussed. Selected methods of oxidation of quinoline derivatives with formyl groups are presented, receiving carboxylic acids.

### 5.10.1 Formylation of quinoline derivatives via Electrophilic Aromatic Substitution

Aldehydes are a class of compounds of great interest in organic chemistry due to their high chemical transformability. They can be converted into both the corresponding carboxylic acids and alcohols in redox reactions. Various methodologies and many synthetic protocols have been developed because of the aldehydes' importance, including the classical Reimer-Tiemann, Vilsmeier-Haack, and Duff reactions.

In the above-mentioned reactions, they proceed *via* electrophilic aromatic substitution ( $S_{EAr}$ ). There are several variations of this mechanism. Some of them have been described below.

The first example of such substitution is the reaction where a positively charged electrophile attaches one of the carbon atoms in the aromatic system (but dipolar groups or molecules may also initiate it). The initial interaction may lead to the formation of a  $\pi$ -complex or an encounter complex. The  $\pi$ -complex, as a result, the system loses its aromaticity, often form a delocalized carbocation (Wheland intermediate,  $\sigma$ -complex). These highly acidic species will donate the proton attached to the  $sp^3$  carbon to the solvent (or any other weak base, **B** in Scheme 44) to restore aromaticity. This mechanistic interpretation also allows for the formation of a second  $\pi$ -complex ( $H^+$ ) from the  $\sigma$ -complex intermediate, where the proton is loosely bound to the  $\pi$ -system. With the regeneration of the aromatic  $\pi$ -system, product stability typically leads to a fast reaction in the final step (Scheme 44)<sup>154,155</sup>. This type of substitution also includes the aforementioned nitration and halogenation reactions. Theoretical calculations help to define the  $S_{EAr}$  mechanism. They make it possible to predict which carbon in the aromatic system will be attacked by the electrophile.

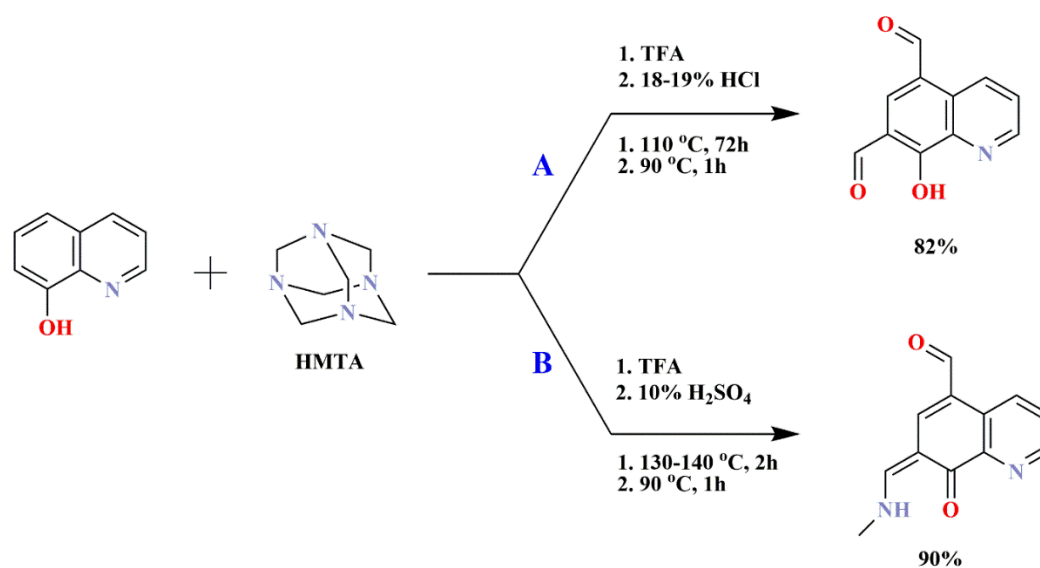


**Scheme 44.** Mechanism of electrophilic aromatic substitution (upper)<sup>154</sup>. Electrophilic groups involved in the Reimer Tiemann, Vilsmeier Haack, and Duff reaction (lower)<sup>154,156,157</sup>.

Another variation is the  $S_{EAr}$  mechanism of nitration. This mechanism results from a lot of evidence suggesting a single electron transfer between the nitronium cation ( $NO_2^+$ ) and the arene, followed by product radical coupling to form a  $\sigma$ -complex intermediate<sup>158</sup>.

There are also examples known involving the addition of radical species into the arene (such as  $\cdot NO_2$ ) as a route to substitution products<sup>159</sup>.

In the case of formylation by aromatic electrophilic substitution, the Duff reaction is one of the many examples of this type of substitution, which was presented in the work of Z. - N. Li et al.<sup>160</sup>. This reaction consisted of dissolving 8-hydroxyquinoline and 1,3,5,7-tetraazatricyclo[3.3.1.1<sup>3,7</sup>]decane (urotropine, HMTA, Scheme 45) in a trifluoroacetic acid environment under a nitrogen atmosphere. The solution was then heated at 110 °C for 72 hours. Then, after cooling to 80 °C, 10% hydrochloric acid solution was added to the system, and it was heated at this temperature for another hour. A tea-green product was filtered and washed several times with water. 8-Hydroxyquinoline-5,7-dicarbaldehyde was obtained in a yield of 82% (Scheme 45, A). In the case of the Duff reaction, an important factor influencing the reaction is its duration. One can observe this by comparing the previous reaction result with the work of K. V. Sashidhar et al.<sup>161</sup>. They also performed a Duff reaction for 8-hydroxyquinoline, but the procedure was changed by reducing the reaction time to two hours (Scheme 45, B). On the other hand, in the hydrolysis step, a 10% sulfuric acid solution was used instead of the hydrochloric acid solution. In this reaction, researchers did not isolate any byproducts, for example, dicarbaldehyde derivative, and the yield was 90% (Scheme 45, B).

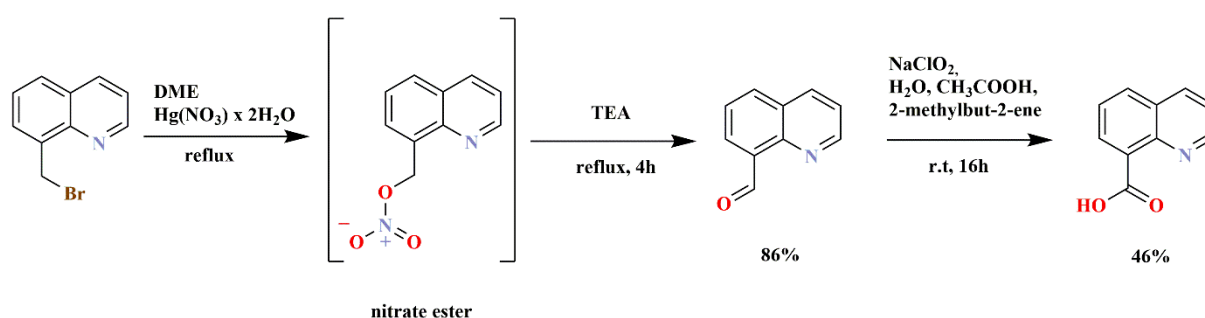


**Scheme 45.** Duff reaction of 8-hydroxyquinoline presented by A) Z.-N. Lu et al.<sup>160</sup> and B) K.V. Sashidhar et al.<sup>161</sup>.

### 5.10.2 The preparation of selected quinoline carboxylic acids

One of the methods of obtaining carboxylic acids of selected quinolines is the oxidation of their precursors containing formyl and/or methyl groups. There are many methods of their preparation in the literature; some of them are presented below.

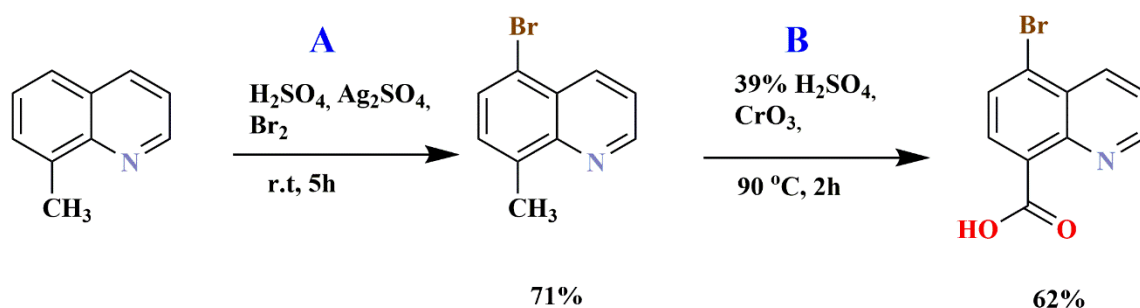
In the work of L.W. Deady et al.<sup>162</sup>, the aim was to obtain carboxylic acids in a two-step, one-pot reaction (Scheme 46). One of the couple examples was preparing quinoline-8-carboxylic acid starting from 8-(bromomethyl)quinoline. In the first step, mercury(I) nitrate dihydrate was added to the solution of 8-(bromomethyl)quinoline in dimethoxyethane (DME), and it was heated and stirred under reflux. The reaction time depended on the detection of the intermediate (nitrate ester, Scheme 46). To detection of the intermediate product, it is possible to check the characteristic chemical shift of the methyl group signal. It was checked on the <sup>1</sup>H NMR spectra (for the CH<sub>2</sub>Br group, it was approx. δ 5, and for the CH<sub>2</sub>ONO<sub>2</sub> group, it was approx. δ 6). Upon detection of **2**, triethylamine (TEA) was added to the mixture and heated under reflux for 4 hours. At this stage of the reactions, the researchers either isolated the resulting aldehyde or continued the reactions in the same vessel (Scheme 46). The researchers add water, acetic acid, and 2-methylbut-2-ene (as a chlorine scavenger) into the reaction mixture in the next step. Then an aqueous solution of sodium chlorite was added dropwise. The mixture was stirred for 16 hours at room temperature, then filtered, and the filtrate evaporated under reduced pressure. Water was added to the obtained crude product and basified with 10% sodium hydroxide to pH 12. Then quinoline-8-carboxylic acid was obtained after extraction with dichloromethane.



**Scheme 46.** Synthesis of 8-quinolinecarboxylic acid by L. W. Deady et al.<sup>162</sup>.

Another example is the work of S. Malancon et al.<sup>163</sup> in which they presented the oxidation reactions of the methyl group leading to 5-bromo-quinoline-8-carboxylic acid (Scheme 47).

The first step consisted of dissolving 8-methylquinoline in concentrated sulfuric acid and then adding silver(I) sulfate and bromine. The reaction mixture was stirred at room temperature for 5h, then poured into ice and filtered. The solution of saturated sodium carbonate was added to the resulting filtrate to increase pH of solution. The aqueous phase was extracted with ethyl acetate. The combined organic layers were evaporated, affording 5-bromo-8-methylquinoline (Scheme 47, A). In the next step, 5-bromo-8-methylquinoline was dissolved in 39% sulfuric acid. After heating the mixture to 90 °C, chromium trioxide was added. The solution was stirred for 2 hours at 90 °C. Afterwards, the mixture was poured into ice. The precipitated orange solid was filtered to give 5-bromoquinoline-8-carboxylic acid in 62% yield (Scheme 47, B).



**Scheme 47.** Preparation of 8-quinolinecarboxylic acid by S. Malancona et al.<sup>163</sup>.

In the case of the oxidation of carbonyl or methyl group for selected *N*-heterocycles, it is possible to use the developed methods for their analogs. An example is the oxidation of 4,7-dimethyl-1,10-phenanthroline and 4,4'-dimethyl-2,2'-bipyridine, where the reactants are concentrated sulfuric acid and chromium trioxide<sup>164,165</sup>.

## 5.11 Electrochemical properties of selected *N*-heterocycles

For organic chemistry, an important element in reaction design is understanding the possible constraints of new compounds, reactions, and mechanisms. When new organic compounds are developed, an important element influencing their attractiveness in terms of their later use and further functionalization is to learn about their possible transformations through reduction and oxidation processes. This allows to determine their possible oxidation metabolism of drugs<sup>166</sup> and detect additional properties, *i.e.*, electrochromism<sup>167,168</sup>. For this reason, electrochemical methods are increasingly used to study the oxidation and reduction products of new organic compounds, for example, *N*-heterocycles<sup>169</sup>.



Electrochemistry is also an excellent tool to obtain specific products within a “green chemistry” approach because the reaction conditions entail electrons as non-hazardous and clean reagents<sup>170</sup>. Nonetheless, to exploit electrochemistry as an alternative synthetic method, the knowledge of appropriate redox potentials is necessary to tune the presence or the absence of functional groups selectively.

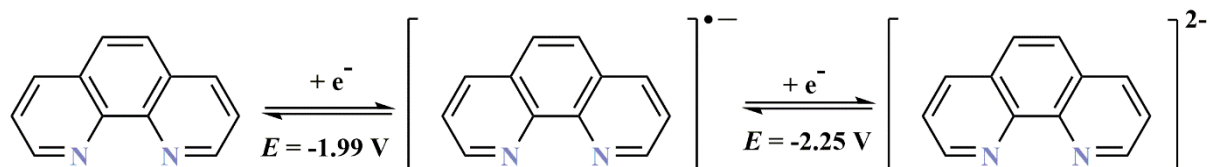
Electrochemical studies for *N*-heterocyclic compounds allow to discuss and confirm the ongoing reactions of their reduction and oxidation. They also describe the role of substituents, e.g., by determining their influence on the course of the reaction and the stability of the compounds. It is worth noting that the knowledge of the electrochemical properties of many characteristic groups, e.g., pyrrolidine, carbazoles, and phenothiazine, allows predicting possible processes for compounds in which they play the role of substituents.

This section provides a literature overview for the electrochemical processes of 1,10-phenanthroline, chlorinated aromatic compounds, pyrrolidine, carbazole, and phenothiazine derivatives.

### 5.11.1 Electrochemical properties of 1,10-phenanthroline

For 1,10-phenanthroline, there are many studies in the field of electrochemistry devoted to its complexes<sup>171</sup>. It is also worth presenting the behavior of the ligand itself in the oxidation and reduction processes, which makes it easier to determine the processes taking place in their complexes. The reduction and oxidation mechanisms of 1,10-phenanthroline determined by electrochemical studies are presented in this chapter.

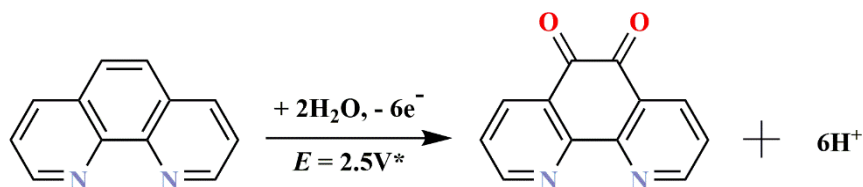
For the 1,10-phenanthroline, the electrochemical reduction proceeds in two one-electron steps at potentials  $-1.99$  V and  $-2.25$  V vs. SCE, where a radical anion and a dianion are formed, respectively<sup>172,173</sup> (Scheme 48).



**Scheme 48.** The proposition of reduction mechanism of 1,10-phenanthroline<sup>172,173</sup>.

In the case of the electrochemical oxidation of Phen proceeds in one irreversible anodic peak at ca.  $1.9$  V<sup>174</sup>. Mirifico et al. obtained 1,10-phenanthroline-5,6-dione (Phen-5,6-dione) by performing the electrooxidation of Phen by constant potential electrolysis at  $2.5$  V

vs. SCE in a solution composed of acetonitrile/water (4:1, v/v) (Scheme 49)<sup>174</sup>. Gayathri et al. obtained the oxidation of Phen to Phen-5,6-dione in an aqueous solution thanks to a glassy carbon electrode modified with nanotubes<sup>175</sup>.

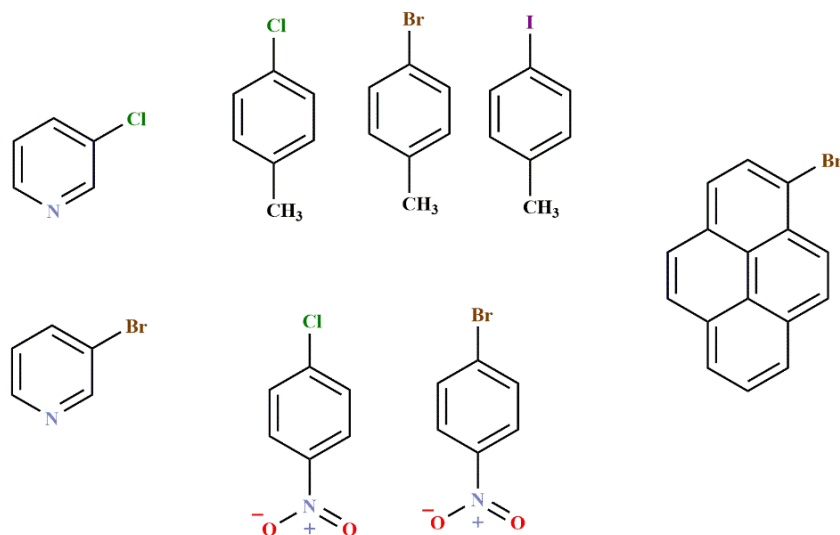
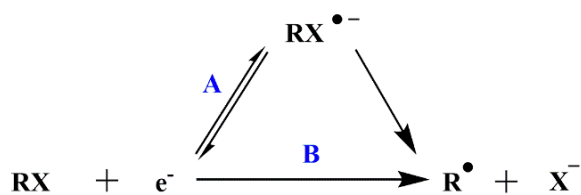


**Scheme 49.** Oxidation of 1,10-phenanthroline presented by Mirifico et al.<sup>174</sup>. \* - Potential for preparative electrolysis.

### 5.11.2 Electrochemical behavior of chlorinated aromatic compounds

Chlorinated aromatic compounds can be reduced to their radical anion, and then the cleavage of chloride from the molecule proceeds as reported for some halogenated derivatives<sup>176,177</sup>. The electrochemical reduction of halide derivatives may proceed through either of two principal mechanisms: a stepwise mechanism involving the intermediate formation of  $RX^{\bullet-}$ , followed by rupture of the carbon–halogen bond (Scheme 50, path A) and a concerted mechanism in which electron transfer (ET) and bond breaking occur in a single step (Scheme 50, path B)<sup>178</sup>.

The competition between stepwise and concerted mechanisms depends on various parameters such as molecular structure, nature of the halide leaving ion, the strength of the breaking bond, and reaction free energy. The case of aromatic halides mainly following a stepwise mechanism (Scheme 50, A)<sup>179</sup>. Extensive research is devoted to the application of electrochemical reduction of organic halides in synthesis<sup>180,181</sup> and pollution remedy<sup>182,183</sup>.



**Scheme 50.** The proposition of general mechanism of the electrochemical reduction of halogen derivatives. Example of organic halides following a stepwise mechanism presented by A.A. Isse et al.<sup>178</sup>.

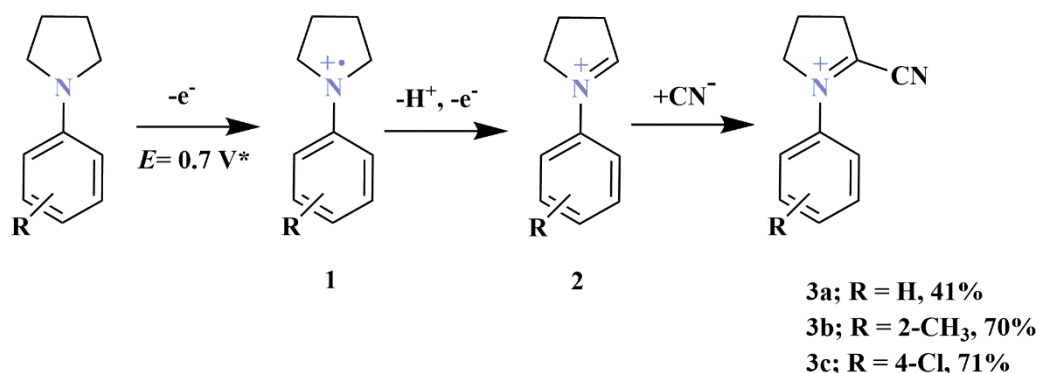
In the case of oxidation, the generation of hydroxyl group and its reaction with the aromatic ring was reported for the oxidation of chlorinated aromatic compounds in an aqueous solution<sup>184</sup>, while the formation of cation radical was found in a non-aqueous solution<sup>185</sup>.

### 5.11.3 Electrochemical properties of pyrrolidine, 9H-carbazole, and 10H-phenothiazine derivatives

This chapter presents the reduction and oxidation processes for selected groups of compounds, such as pyrrolidine, carbazole, or phenothiazine. These groups are successfully used as substituents in many types of compounds that are later tested for luminescent and biological properties<sup>186,187,188</sup>. Their derivatives are also tested for the study of electrochemical processes.

### Pyrrolidine derivatives

For pyrrolidine derivatives, the mechanism of their oxidation was presented in the work of W. Liu et al.<sup>189</sup>. Researchers have reported results on the anodic cyanation of 1-arylpyrrolidines. Based on a series of experiments, the mechanism of cyanation by anodic oxidation in the presence of nitrile ions has been proposed (Scheme 51).



**Scheme 51.** The proposition of electrocyanation mechanism of pyrrolidine derivatives presented by W. Liu et al.<sup>189</sup>. \* - Potential for preparative electrolysis.

In the first step, an adsorbed pyrrolidine derivative undergoes one-electron transfer to form a cation radical (1) followed by deprotonation and the second electron transfer to form the iminium cation (2). Then, the imine cation reacts with cyanide ion (sodium cyanide was dissolved in the solution) to give cyano derivatives formed in ortho position (3).

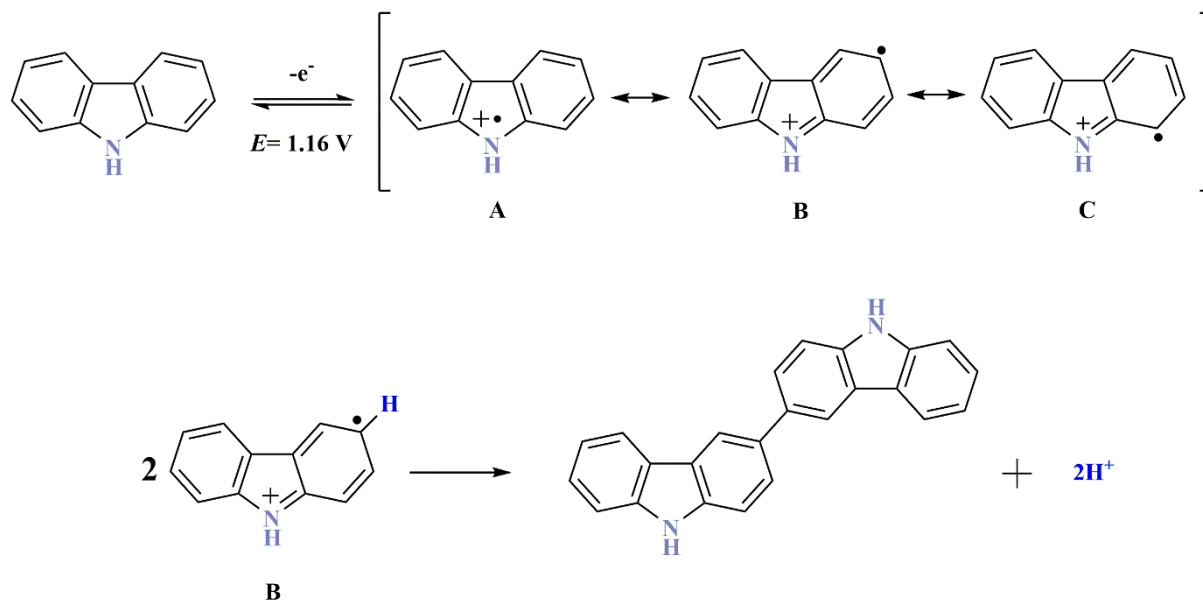
There is no systematic research for pyrrolidine derivatives or their analogs in the case of electrochemical reduction mechanisms.

### 9H-carbazole derivatives

Another group of compounds is 9H-carbazole and its derivatives. In the case of anodic oxidation of 9H-carbazole, it follows a classical ECE mechanism where each electrochemical step involves one electron per parent molecule. The first significant work on the electrochemical oxidation of 9H-carbazole was published by J. F. Ambrose et al.<sup>190</sup>. They explained and confirmed the presence of reaction products by comparing the CVs of compounds synthesized chemically.

The electrochemical oxidation of 9H-carbazole proceeds one electron process at potential 1.2 V vs. SCE, where cation radical is formed. As a cation radical is very unstable, it tends to couple with either another cation radical or with a parent molecule, forming the more stable di(9H-carbazole) (example presented in Scheme 52). This type of coupling leads to the

loss of two protons, one per *9H*-carbazole unit. Lost protons are further reduced in the cathodic cycle<sup>191</sup>.



**Scheme 52.** Oxidation of *9H*-carbazole by one electron process (upper); one example of forming dicarbazol by two cation radicals (lower)<sup>190,192</sup>.

Depending on the substituent and the position of its attachment to the *9H*-carbazole moiety, the oxidation potential may vary due to the inductive, mesomeric, or steric effects of a given substituent. In the absence of a slight steric hindrance, the molecule may undergo multi-stage oxidation to various subproducts. In this case, intermolecular coupling often occurs, leading to stable dication, which limits further reactions<sup>192</sup>.

There is no systematic research for *9H*-carbazole derivatives or their analogs in the case of electrochemical reduction mechanisms.

#### *10H*-phenothiazine derivatives

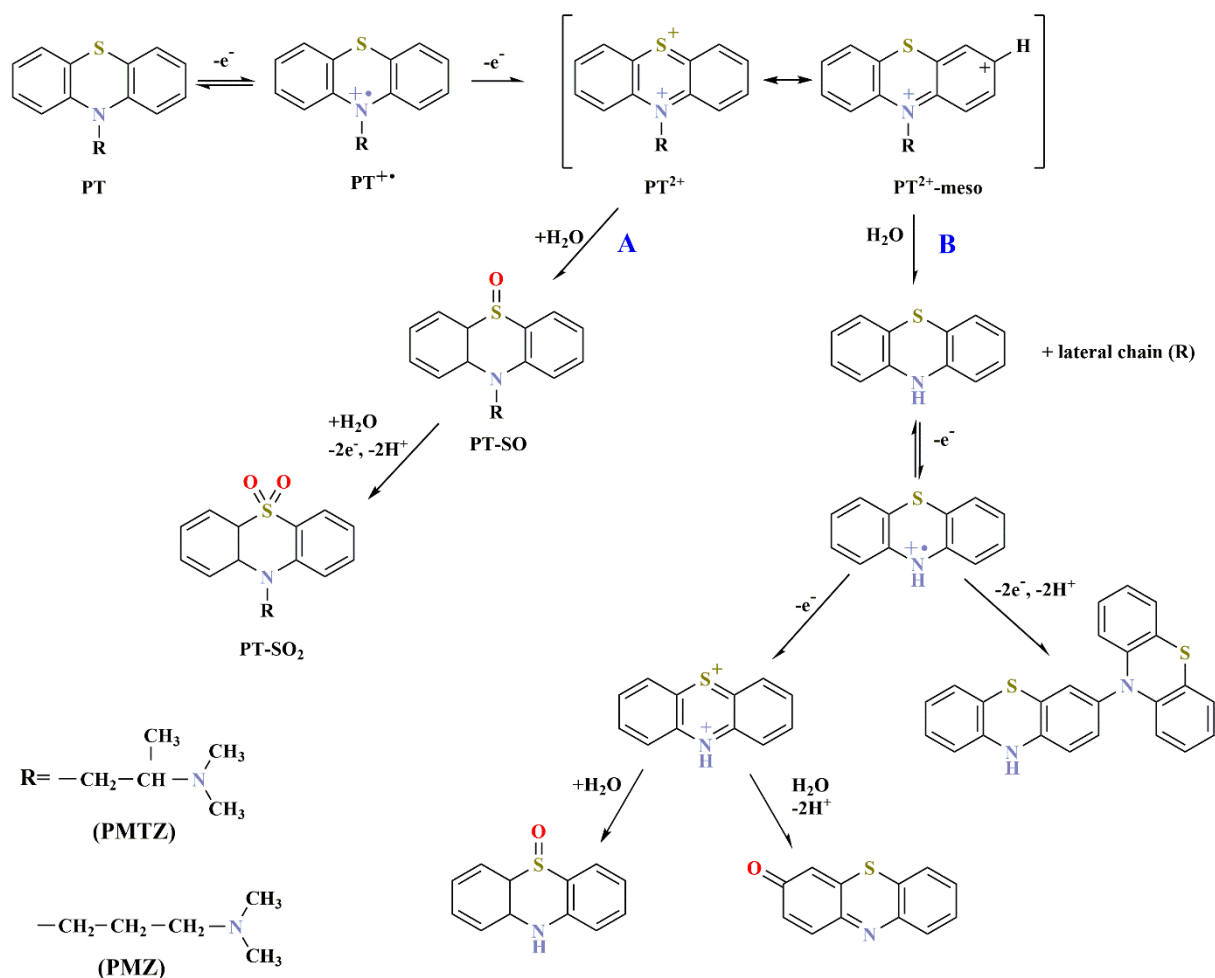
The last group of compounds discussed is *10H*-phenothiazine derivatives. As for the other groups (discussed in this chapter), there is no systematic research on the reduction mechanism of this group of compounds in the literature.

In the case of the oxidative processes of *10H*-phenothiazine derivatives, there are many studies devoted to their mechanisms<sup>193,194</sup>. In the work of B. Blankert et al.<sup>195</sup> the

pattern for the oxidation of 10*H*-phenothiazine derivatives has been presented for promethazine (PMTZ) and promazine (PMZ).

Scheme 53 illustrates the general trends regarding the oxidation of phenothiazines taking into account literature data<sup>195,196</sup>. The first stage of oxidation of phenothiazine derivatives (**PT**, Scheme 53), proceed one-electron process where cation radical is formed (**PT<sup>•+</sup>**). For 10*H*-phenothiazine without additional substituents, this process occurs at a potential of 0.69 V & Ag/AgCl<sup>207</sup>. Further oxidation leads to the formation of a dication (**PT<sup>2+</sup>**, Scheme 53). In the case of oxidation of **PT<sup>2+</sup>** in literature were showed upon enzymatic and electrochemical oxidation two possible parallel mechanisms, i.e., formation of the corresponding sulfoxide (**PT-SO**) or even dioxygenated sulfone (pathway A, **PT-SO<sub>2</sub>**), and other mechanism is the cleavage of the lateral chain (pathway B). For promethazine hydrochloride (PMTZ), it takes pathway B + A; and for promazine hydrochloride (PMZ) takes pathway A (Scheme 53).

Pathway B, after the cleavage of the lateral chain, obtained 10*H*-phenothiazine may proceed further oxidation already *via* pathway A. For 10*H*-phenothiazine, dimer formation is possible due to the forming of mesomeric structure (example shown in Scheme 53, **PT<sup>2+</sup> + meso**).



**Scheme 53.** Oxidation pattern of promethazine (PMTZ) and promazine (PMZ) presented by B. Blankert et al.<sup>195</sup>.

## 6. Results and discussion

### 6.1 Introduction

This chapter has been divided into three main thematic blocks focusing around the synthesis and functionalization of selected 1,10-phenanthrolines and their electrochemical, spectroelectrochemical tests extended with DFT calculations. An additional thematic block is a synthesis, functionalization, and oxidation reaction of selected 1,10-phenanthroline analogs.

The first main thematic block (Chapter 6.2) of the research is focused on the preparation of 4,7-dichloro-1,10-phenanthrolines derivatives. The scope and limitations of the reaction resulting from the used reagents, conditions, and substituents are also presented. The

next paragraph (Chapter 6.2.2) presents research on electrochemical processes of selected 4,7-dichloro-1,10-phenanthroline. In which the ongoing processes of reduction and oxidation of selected compounds are presented. The reaction mechanisms were also presented, and the influence of the substituent on the electrochemical properties of the compounds was compared.

The next paragraph (Chapter 6.2.3) describes the functionalization of selected 4,7-dichloro-1,10-phenanthrolines mentioned in the previous paragraph. Functionalization was based on the nucleophilic substitution in the C4 and C7 positions with selected amines such as pyrrolidine, 9*H*-carbazole, and 10*H*-phenothiazine. Several examples of derivatives are presented for each of the amines, where their reduction and oxidation mechanisms were also investigated through electrochemical studies. DFT calculations supported all electrochemical studies.

The following chapter 6.2.7 described the synthesis of selected 1,10-phenanthroline acids. Several possible oxidation and hydrolysis reactions were presented for selected derivatives, including commercially available neocuproine. The analysis of the obtained products was carried out, indicating the scope and limitations of the reaction resulting from many factors such as compound stability of compounds and the influence of the substituents and the reagents used. The research results confirmed the complexity and difficulty in the preparation of 1,10-phenanthroline acid derivatives, which suggested focusing on other reaction pathways for the preparation of acids, such as the oxidation of aldehydes.

The second main thematic block (Chapter 6.3) is devoted to obtaining unsymmetrical and symmetrical 1,10-phenanthroline derivatives based on Skraup-Doebner-Von Miller reaction and reaction based on using Meldrum acids. The first part of this block presents studies for the monochloro derivatives of 1,10-phenanthroline as reagents for the designed synthesis of monosubstituted 1,10-phenanthrolines. One of the final products required the  $S_NAr$  reaction, where the known competitive VNS reaction could also occur. An interesting result of this transformation was found. The product was obtained in the way of both competitive substitutions, which was a dead-end for further research. This finding resulted in the continuing of the research in the direction of VNS reactions development.

The third thematic block (Chapter 6.4) was devoted to the synthesis, functionalization, and oxidation reaction of quinoline and benzo[*h*]quinoline derivatives. Although this work focuses on 1,10-phenanthroline derivatives, the choice of this type of analogs resulted from simpler synthesis and cheaper reagents. This allowed the development of methods that may be used in the preparation of 1,10-phenanthrolines and their oxidation. This chapter describes the



simple and easily available molecules such as quinoline and benzo[*h*]quinoline derivatives. These compounds have been selected to help better understand described processes, and the knowledge was used in the synthesis of new 1,10-phenanthroline derivatives. These model molecules are an excellent way to understand the scope and limitations of the reaction, which may well be used for selected 1,10-phenanthrolines. It is mentioned in the chapter “Selected acids derivatives of 1,10-phenanthroline” (5.6.2) that until now, there is no reported easy and predictable synthesis of the carboxylic acid of 1,10-phenanthrolines. Because of this, simpler models such as quinoline and benzo[*h*]quinoline derivatives were chosen. The first two paragraphs present the methodology of synthesis and oxidizing dicarbaldehydes of quinolines and benzo[*h*]quinolines.

The third paragraph (Chapter 6.5) was devoted to the study of VNS reactions for selected nitroquinoline derivatives. This research direction was initiated during this work on the preparation of monosubstituted 1,10-phenanthroline derivatives, in the designed six-step procedure for the preparation of monoamine derivatives of 1,10-phenanthrolines, the fourth step of the procedure required an S<sub>N</sub>Ar transformation where the known competitive VNS reaction could also occur. An interesting result of this transformation turned out to be obtaining the product in the way of both competitive substitutions. The obtained result initiated the development of the research on VNS reactions.

## **6.2 Synthesis, functionalization and oxidation, and reduction processes of 1,10-phenanthroline derivatives**

This chapter presents studies on the preparation of 1,10-phenanthroline derivatives. In order to distinguish individual methods of obtaining them, each method has been discussed in a separate subsection.

### **6.2.1 Syntheses of symmetrical and unsymmetrical 1,10-phenanthroline derivatives based on synthesis with Meldrum acid**

The experimental work started by synthesis of 4,7-dichloro-1,10-phenanthroline derivatives **4** using a three-step condensation of 2,2-dimethyl-1,3-dioxane-4,6-dione (Meldrum's acid), orthoesters, and ortho-phenylenediamines **1** (Scheme 54) (each step

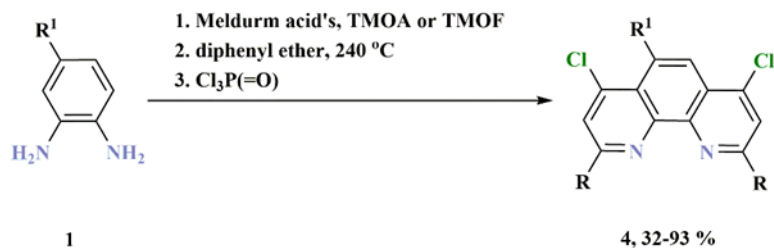
of reaction was discussed in chapter 5.3.2). Compounds **4** were prepared with high yield, even on the scale of several grams.

The main aim of the research was to obtain new 1,10-phenanthroline precursors for further functionalization. An additional aim was to demonstrate the limitations of the reactions and the improvement of available procedures.

The first step is the reaction of the selected diaminobenzene with Meldrum's acid and the selected orthoester (TMOA or TMOF). In addition to a decent product, by-products in the form of a benzimidazole derivative were isolated. The work of Kaboudin et al.<sup>42</sup> confirms this, where they present the reaction of diaminobenzene with an orthoester to form benzimidazole (Scheme 11, chapter 5.3.2). The formation of benzimidazole derivatives may result from carrying out the reaction in excess of an orthoester.

The next stage is internal cyclocondensation of *in situ* generating ketene. This reactive intermediate is thermally generating through acetone and CO<sub>2</sub> elimination in refluxing diphenyl ether. At this stage, no possible limitations were detected.

The final stage is the conversion of carbonyl groups at C4 and C7 by chlorine atoms into final chloro-compounds, *i.e.*, 4,7-dichloro-1,10-phenanthrolines with phosphoryl chloride. In this step, a great improvement in the isolation of the product is the evaporation of excess solvent after the conducted reaction. The received compounds were fully characterized, including spectroscopic methods and melting points measurements.



<b>4</b>			<b>Yield</b>				
<b>No.</b>	<b>R</b>	<b>R<sup>1</sup></b>	<b>(%)</b>	<b>No.</b>	<b>R</b>	<b>R<sup>1</sup></b>	<b>(%)</b>
<b>a</b>	H	H	84	<b>g</b>	CH <sub>3</sub>	F	93
<b>b</b>	H	F	85	<b>h</b>	CH <sub>3</sub>	Cl	78
<b>c</b>	H	Cl	75	<b>i</b>	CH <sub>3</sub>	Br	68
<b>d</b>	H	CH <sub>3</sub>	91	<b>j</b>	CH <sub>3</sub>	CH <sub>3</sub>	86
<b>e</b>	H	CN	48	<b>k</b>	CH <sub>3</sub>	CN	32
<b>f</b>	CH <sub>3</sub>	H	92	<b>l</b>	CH <sub>3</sub>	COOEt	38

**Scheme 54.** Synthesis of selected 4,7-dichloro-1,10-phenanthroline derivatives **4**.

By analyzing mass spectra for the prepared 4,7-dichloro-1,10-phenanthrolines (**4**), a fragmentation with the initial loss of chloride was observed, followed by the loss of a second chloride (Figure 4) and further decomposition, except for molecule **4i**, which first eliminates bromide (Figure 5).

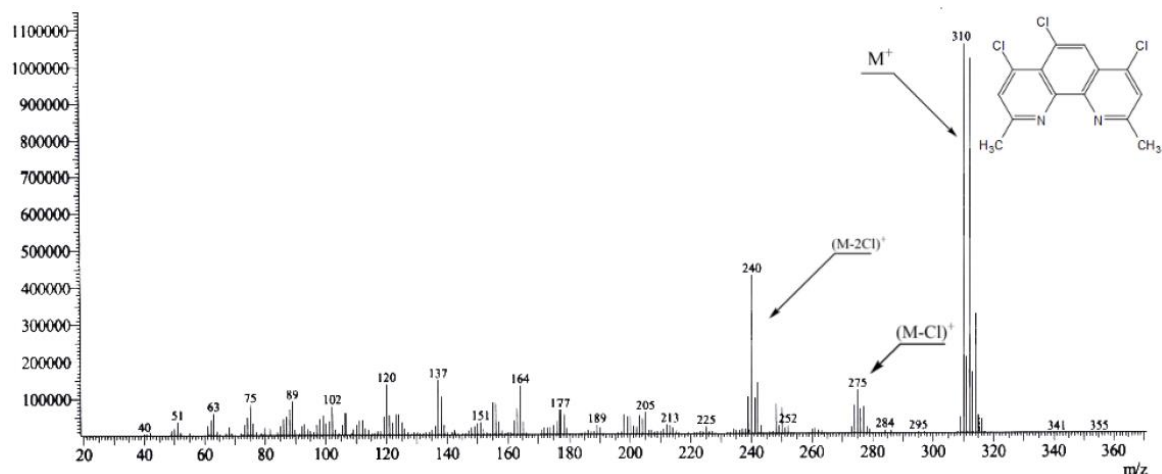


**Figure 4.** MS-EI spectrum for **4h**.

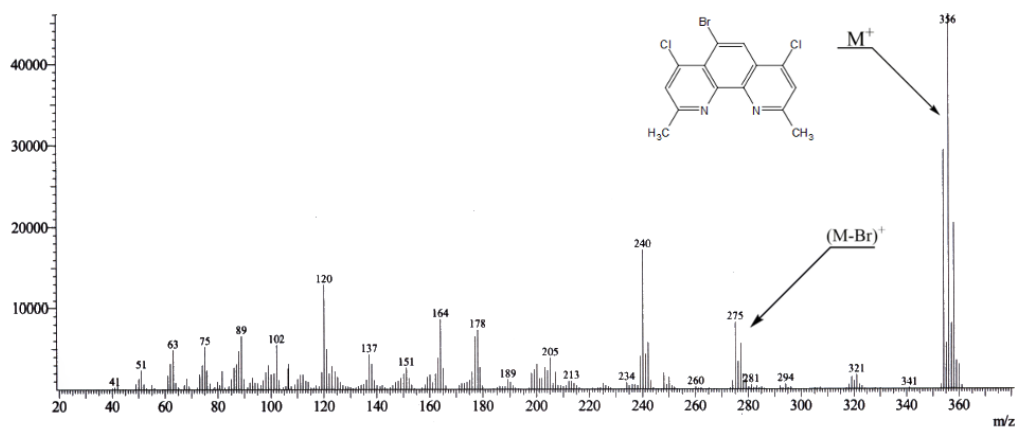


**Figure 5.** MS-EI spectrum for **4i**.

The research results in this chapter have been published in our paper<sup>197</sup>.

## 6.2.2 Electrochemical and spectroelectrochemical studies of selected 4,7-dichloro-1,10-phenanthroline

The electrochemical behavior of selected 4,7-dichloro-1,10-phenanthrolines was studied in non-aqueous solution using cyclic voltammetry (CV), controlled potential electrolysis, in-situ UV-Vis and IR spectroelectrochemistry, and HPLC-DAD (HPLC with diode array detector) and HPLC-MS/MS techniques. Additionally, the substitution of phenanthrolines at positions C2, C9, and C5 with methyl group, C5 for chlorine and/or fluorine atoms, was analyzed to check the influence on redox properties and the potential gap between the oxidation and reduction potentials.

The research results in this chapter have been published in our papers<sup>198,199</sup>.

### 6.2.2.1 Oxidation

Oxidation properties did not show significant differences in the number of oxidation waves and their potentials amongst the investigated compounds and correlate with the calculated HOMO energies. The cyclic voltammograms of compounds **4a**, **4b**, **4d**, **4f**, **4h** yield two oxidation waves similarly to **Phen** (1,10-phenanthroline) (Figure 6).

The oxidation of the target compounds most likely leads to a short living radical cation, and then a dimer can be formed (the first wave). The second oxidation wave, possibly assigned to the formation of a dication, occurs at a higher potential (around 2 V) and is poorly

developed. The oxidation of compound **4b**, which has one fluorine substituent at position C5, occurs at higher potentials than that of compound **4a**. Thus, compound **4b** is more stable against oxidation than compound **4a**, thanks to the presence of the fluorine substituent. This oxidation wave is no more present in the CV measured after the oxidative electrolysis performed at the potential of the second wave; nevertheless, the chromatograms before, during, and after the electrolysis did not feature any new peak. A dication was formed as a final product, which is then detected as a neutral species in the chromatogram performed in an aqueous solution; alternatively, the formed radical dimerizes in a species that is not stable and readily decomposes to the monomer, which is then detected in the chromatographic analysis.

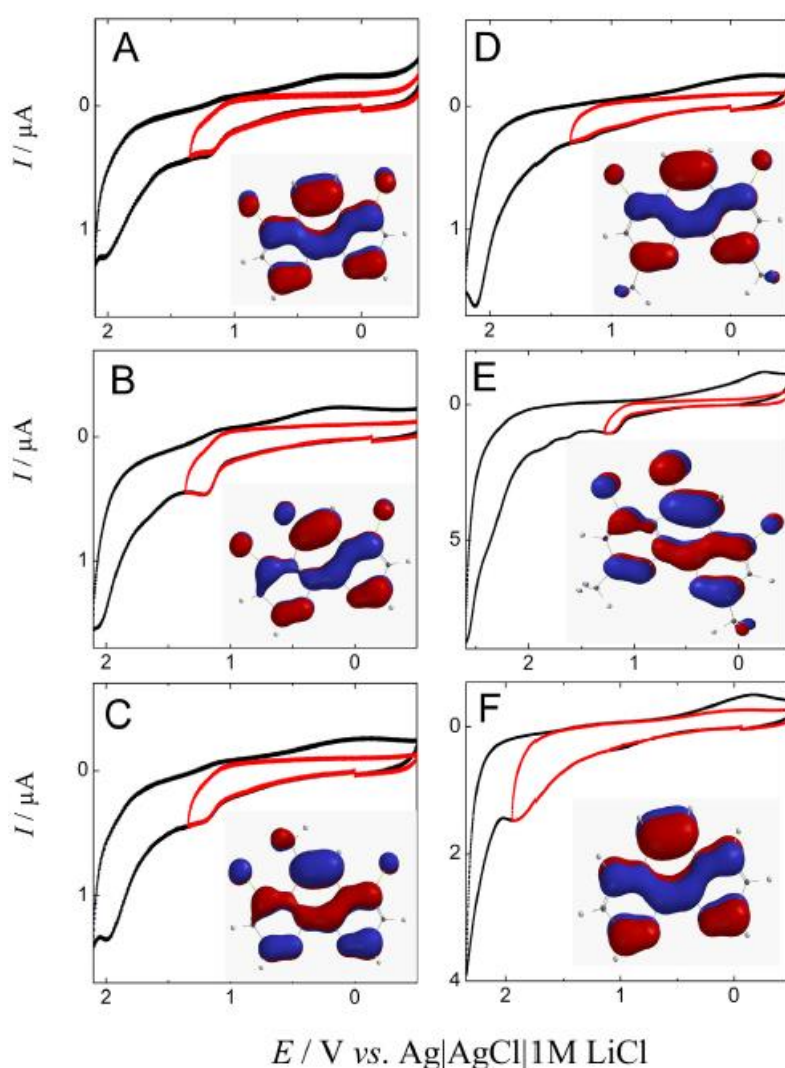


**Figure 6.** Cyclic voltammogram of 0.63mM **4a** (Panel A), 0.67mM **4b** (Panel B), 0.67mM **4d** (Panel C), 0.63mM **4f** (Panel D), 0.55mM **4h** (Panel E) and 0.63mM **Phen** (Panel F) in 0.1 M TBAPF<sub>6</sub> in acetonitrile. The scan rate was 0.1 V·s<sup>-1</sup>. The insets show the spatial distribution of HOMO orbitals for all the investigated molecules.

The UV-Vis spectroelectrochemistry at the potential of the first oxidation wave confirms that the reaction is indeed chemically reversible (Figure 7). A new wide absorption band at 344 nm increases, while the absorption band at 241 nm related to **Phen** moiety decreases. These changes are accompanied by an increase in the bands at 277 nm and 218 nm and a decrease in the band at 306 nm. During the rereduction, all mentioned changes reverse (Figure 7B). The absorption spectra do not show any changes in the region above 400 nm during oxidative electrolysis in the spectroelectrochemical cell. The identification of oxidation products was not successful. Chromatograms of solutions before and after electrolysis recorded using HPLC-DAD did not show any changes, no additional peaks were present, and no decrease of the peak of the starting compound was observed, even if cyclic voltammograms showed a decrease of its oxidation peak. Neither HPLC-MS/MS helped to find at least non stable intermediates, possibly because of difficulties with the composition of the analyzed solution containing high amounts of TBAPF<sub>6</sub>.

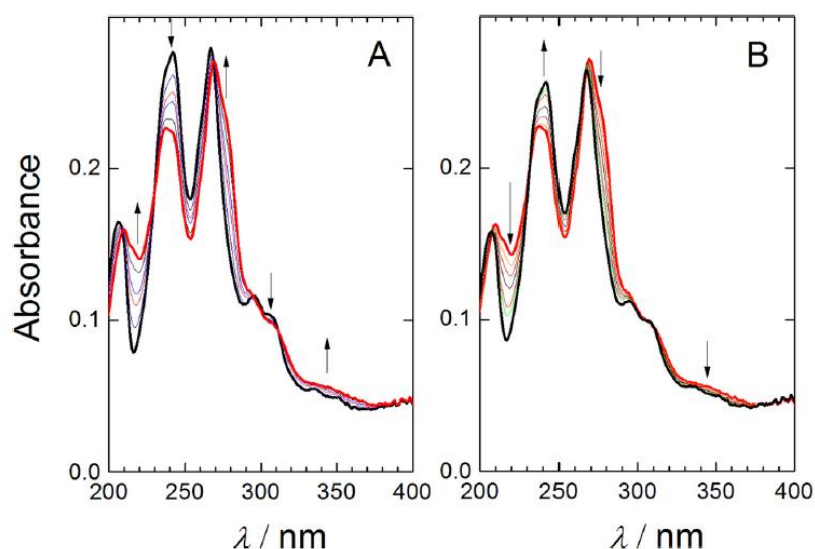


**Figure 7.** UV-Vis spectroelectrochemistry of compound **4b** at the first oxidation wave (Panel A) and the rereduction of the formed oxidation product (Panel B).

The chemical reversibility was also highlighted by IR spectroelectrochemistry (Figure 10). The minimal energy of three different dimer structures formed by the reaction of **4b** at positions C2, C3, and C9 was calculated. The results showed that the most favorable is the formation of a dimer C9-C9 (inset in Panel A of Figure 8) since the minimal energy calculated for this structure geometry is 441.3 kJ/mol, while the values for the minimal energy were higher for other structures (dimer C3-C3: 534.7 kJ/mol, dimer C2-C2: 442.7

kJ/mol). During oxidation, a decrease in the vibration bands belonging to compound **4b** occurred: 1628  $\text{cm}^{-1}$  (calculated value is 1622  $\text{cm}^{-1}$ ; partial decrease corresponds to presence of dimer with calculated value 1617  $\text{cm}^{-1}$ ), 1545  $\text{cm}^{-1}$  (1532  $\text{cm}^{-1}$ ), 1330  $\text{cm}^{-1}$  (1320  $\text{cm}^{-1}$ ), 1288  $\text{cm}^{-1}$  (1310  $\text{cm}^{-1}$ ), 1275  $\text{cm}^{-1}$  (1272  $\text{cm}^{-1}$ ), 1242  $\text{cm}^{-1}$  (1244  $\text{cm}^{-1}$ ), 1160  $\text{cm}^{-1}$  (1144  $\text{cm}^{-1}$ ), 1118  $\text{cm}^{-1}$  (1110  $\text{cm}^{-1}$ ), 1088  $\text{cm}^{-1}$  (1061  $\text{cm}^{-1}$ ) as shown in Figure 10A. Simultaneously, the vibration bands assigned to the suggested dimer increase: 1613  $\text{cm}^{-1}$  (1589  $\text{cm}^{-1}$ ), 1589  $\text{cm}^{-1}$  (1584  $\text{cm}^{-1}$ ), 1533  $\text{cm}^{-1}$  (1522  $\text{cm}^{-1}$ ), 1324  $\text{cm}^{-1}$  (1328  $\text{cm}^{-1}$ ), 1297  $\text{cm}^{-1}$  (1281  $\text{cm}^{-1}$ ), 1283  $\text{cm}^{-1}$  (1260  $\text{cm}^{-1}$ ), 1216  $\text{cm}^{-1}$  (1225  $\text{cm}^{-1}$ ), 1171  $\text{cm}^{-1}$  (1155  $\text{cm}^{-1}$ ), 1125  $\text{cm}^{-1}$  (1129  $\text{cm}^{-1}$ ). The calculated wavenumbers are in very good agreement with the experimental values. The IR spectrum obtained after the rereduction of the oxidation product is in agreement with the IR spectrum of compound **4b**.

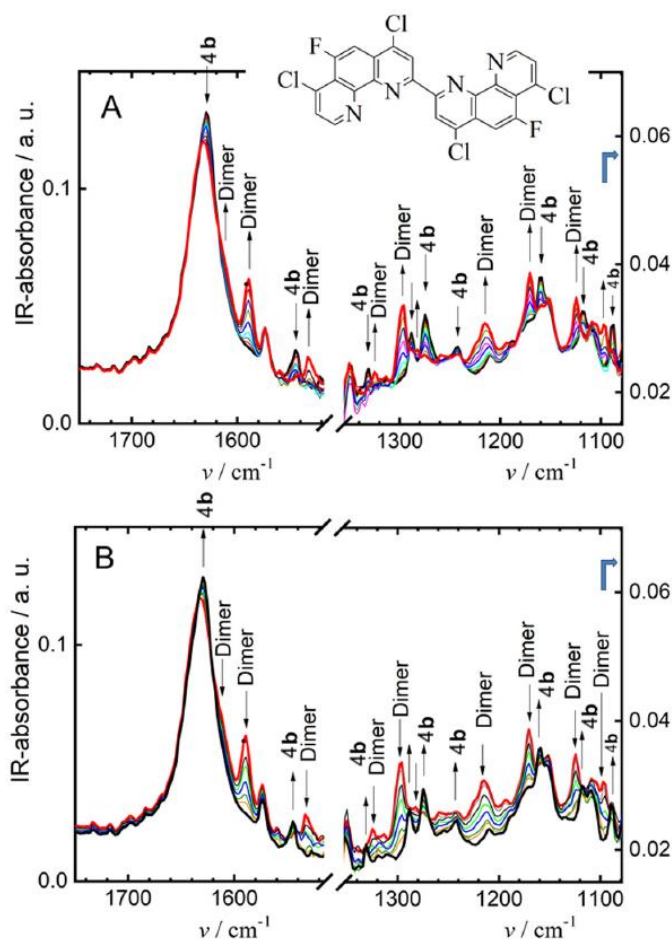


**Figure 8.** IR spectroelectrochemistry of compound **4b** at the first oxidation wave (Panel A) and IR spectroelectrochemistry during the rereduction of the formed oxidation product (Panel B) in the ranges 1750-1510 (on the left) and 1360-1080  $\text{cm}^{-1}$  (on the right). The inset of Panel A shows the chemical structure of the suggested dimer.

The formation of the suggested dimer structure is also in agreement with the literature on the ortho-ortho coupling of pyridinones<sup>200,201</sup>. Interestingly, in the acetonitrile solution of **4b** before electrolysis, small traces of a second compound were identified by chromatography interfaced with high resolution tandem mass spectrometry. This compound is characterized by the molecular formula  $C_{12}H_6ClFN_2O$ , identified by the detection in the full spectrum of ions at 249.0222 corresponding to  $[M + H]^+$ ; 271.0042 corresponding to  $[M + Na]^+$ ; and 519.0196 corresponding to  $[2 M + Na]^+$  (Figure 9). The tandem mass spectrum features ions at  $m/z$  229.0143, 207.099, 201.0193, 174.0087, and 166.0508. Although the interpretation of the tandem mass spectrum is not straightforward, based on the molecular formula, this species was tentatively interpreted as a hydroxylated derivative of **4b**.

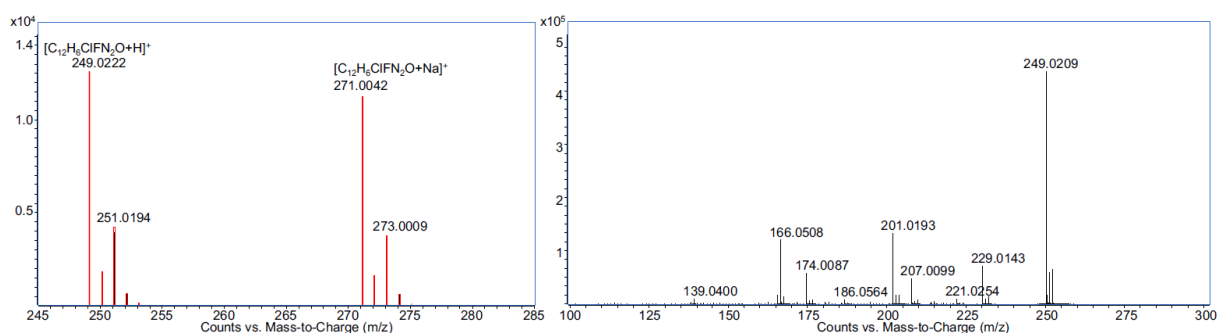


**Figure 9.** High resolution mass spectrum (on the left) and tandem mass spectrum (on the right) of the peak assigned to the hydroxylated derivative of **4b**. Positive acquisition mode, the voltage applied in the collision cell 30 V. The predicted exact mass and isotopic pattern for the species are shown in red, superimposed to the acquired data.

### 6.2.2.2 Reduction

A detailed analysis of the characteristics of the reduction peaks suggested that the first two reduction waves correspond to irreversible two-electron processes (Figure 10). This fact was confirmed by potentiostatic coulometry since the charge consumed at the potential behind the first reduction wave and the second reduction wave corresponded to two and four electrons, respectively. The first two reduction waves were thus attributed to the subsequent reductive cleavage of both chlorine substituents (Scheme 55). Since its peak current is linearly proportional to the scan rate and does not change with concentration, this peak is an adsorptive prepeak. The third and fourth reduction peaks are one-electron reductions of **Phen**



to its radical anion and dianion, as described in the literature<sup>202</sup> and confirmed by the CV of **Phen** measured under the same conditions (Fig. 10F). Insets in Fig. 10 show the dependence of peak current of the first wave on the square root of scan rate, which was linear for all compounds. It means that the reduction at the electrode was controlled by diffusion.

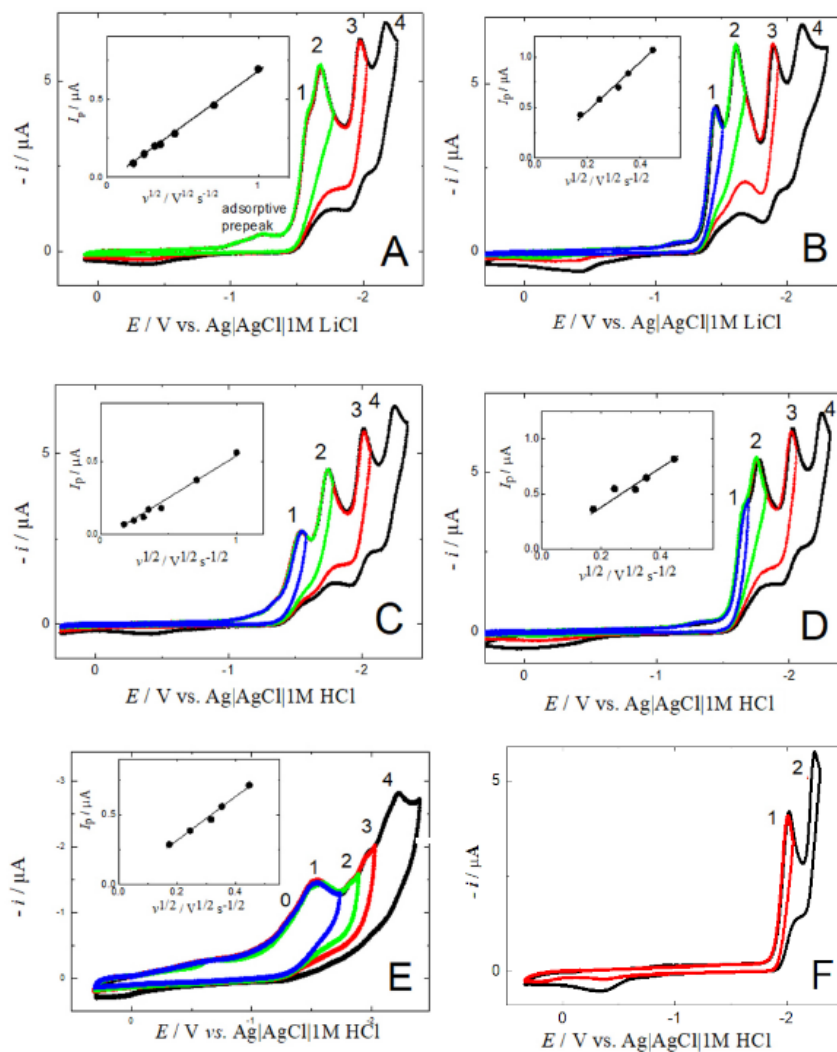
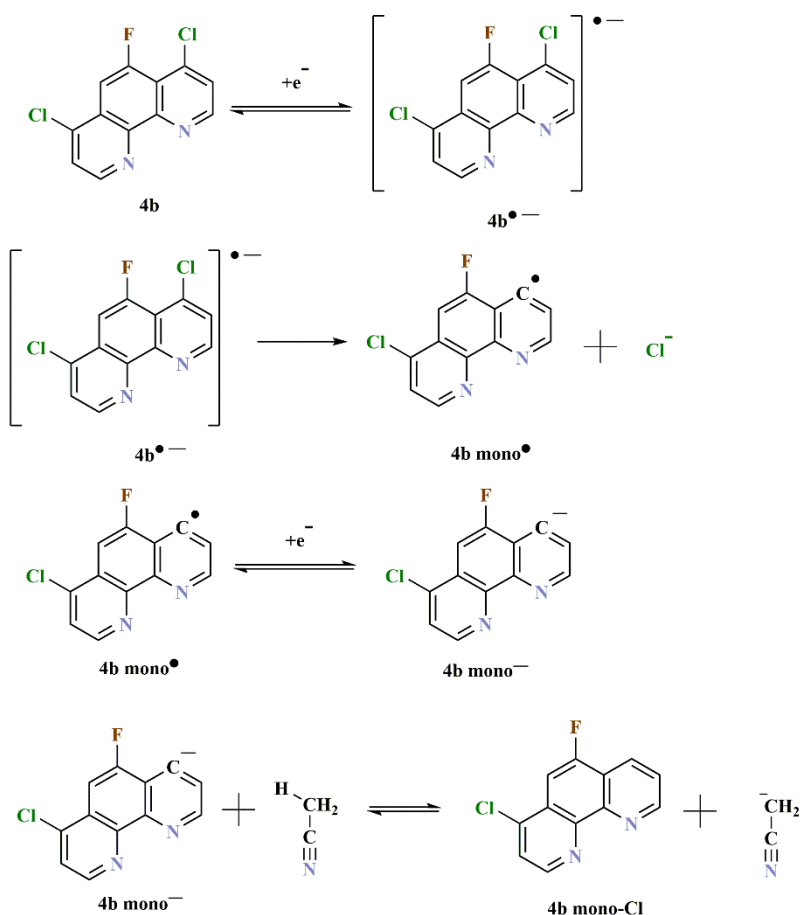


**Figure 10.** Cyclic voltammogram of 0.63mM **4a** (Panel A), 0.67 mM **4b** (Panel B), 0.67mM **4d** (Panel C), 0.63mM **4f** (Panel D), 0.19mM **4h** (Panel E) and 0.63 mM **Phen** (Panel F) in 0.1M TBAPF<sub>6</sub> in acetonitrile. The scan rate was 0.1 V·s<sup>-1</sup>. Insets show the dependence of peak current of the first reduction peak on the square root of scan rate.



**Scheme 55.** Proposition of reduction mechanism of 4,7-dichloro-5-fluoro-1,10-phenanthroline (**4b**).

The first reduction of **4b** is facilitated if compared to that of **4a** because of the pronounced inductive effect of the fluorine substituent. LUMO energies calculated for both compounds agree with this experimental finding:  $E_{\text{LUMO}}(\mathbf{4a}) = -1.89 \text{ eV} > E_{\text{LUMO}}(\mathbf{4b}) = -1.97 \text{ eV}$  (the calculated spatial distribution of LUMO orbitals for all studied compounds is shown in Fig. 11A). The cleavage of chloride from C4 position is suggested for molecule **4b** according to the higher difference in atomic charges compared to that of C7-chlorine (Fig. 11B). The presence of two methyl groups at C2, C9 positions (compound **4f**,  $E_1 = -1.68 \text{ V}$ ) caused a 110 mV shift in the reduction peak toward lower potentials if compared to **4a** ( $E_1 = -1.57 \text{ V}$ ) due to a contribution of a positive inductive effect of the methyl group (Figure 10A, D). Almost no influence of the methyl substitution at position C5 on peak potential was experimentally found comparing reduction potentials of **4a** and **4d** (Figure 10A, C). The calculated LUMO energies for the studied molecules in vacuum decrease in the following

order:  $E_{\text{LUMO}}(\mathbf{4f}) = -1.66 \text{ eV} > E_{\text{LUMO}}(\mathbf{4d}) = -1.79 \text{ eV} > E_{\text{LUMO}}(\mathbf{4a}) = -1.89 \text{ eV} > E_{\text{LUMO}}(\mathbf{4b}) = -1.97 \text{ eV}$ .

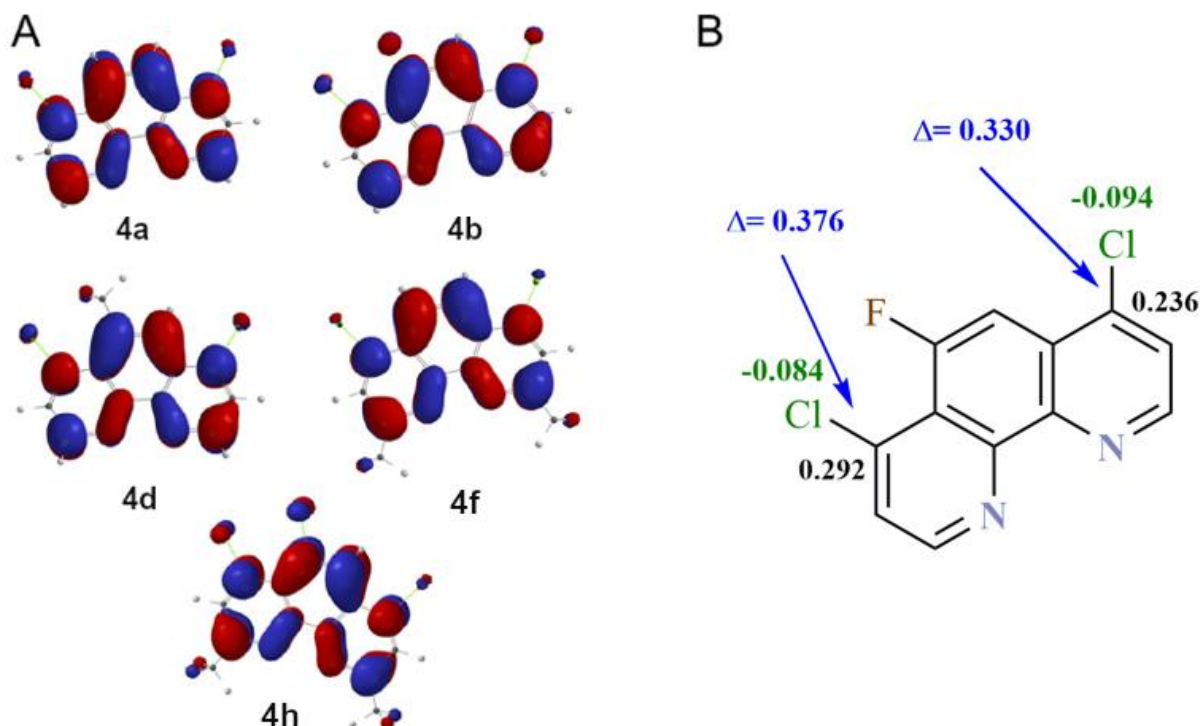


**Figure 11.** Theoretical calculations: Panel A shows the spatial distribution of the LUMO orbitals for molecules **4a**, **4b**, **4d**, **4f**, **4h**. Panel B shows the electrostatic potentials of the atoms participating in the CCl bond for compound **4b**.

Compound **4h** contains three chlorine atoms in the molecular structure, and its CV presents one additional reduction wave at  $-1.37 \text{ V}$  (labeled as 0 in Figure 10E). All of the chlorine substituents are reductively cleaved in three subsequent reduction steps. The reductive cleavage of this additional carbon-chlorine bond occurs more easily if compared to the dechlorinated molecule **4f** (specifically, at a higher potential, with a 310 mV difference). Such behavior is in accordance with the reduction of halogenated compounds containing a number of halogen atoms higher than one, as previously found and described for mono- and dichlorinated hydroxybenzonnitriles<sup>203</sup>, where the difference in the first reductions between mono- and dichlorinated compounds was equal to 855 mV. The calculated  $E_{\text{LUMO}}(\mathbf{4h}) = -1.90 \text{ eV}$  is considerably lower than that calculated for **4f**, in agreement with the difference observed for the reduction potential. The transfer coefficient  $\alpha$  was calculated using equation  $|E_{p/2} - E_p| = 1.857 RT/\alpha F$ <sup>204</sup> for all investigated compounds in this chapter. These values are all above 0.5 and point to a stepwise cleavage of a halide from the molecule.

The results of the UV-Vis spectroelectrochemistry experiments performed during the reductive electrolysis of **4b** at the potential of the first reduction wave are depicted in Figure 12A. A decrease in the absorption bands at 267 nm and bands at 295 and 307 nm belonging to **4b** is accompanied by the increase in the absorption at 219, 350, and 401 nm. The absorption band at 242 nm does not change its intensity but undergoes a slight bathochromic shift. When positive potential equal to 0.1 V was applied, no changes in the absorption spectrum were observed, indicating that the reaction was chemically irreversible. Scheme 55 shows the reduction mechanism assessed for compound **4b**. The radical anion formed after the uptake of the first electron by the molecule undergoes the cleavage of a chloride; an aryl radical is formed, and it is reduced by the second electron to give an aryl anion. The reaction is terminated by the reaction of the anion with a proton from the water traces present in the solvent. The occurrence of this reaction was proven by observing the apparent decrease of the two typical absorption bands of water during IR spectroelectrochemical experiments at the first reduction wave (data not shown). The changes in the IR spectra (Figure 12B and C) during the reductive electrolysis at the potential of the first reduction wave support the suggested reduction mechanism. Figure 12B and C show a decrease in the vibration bands belonging to compound **4b**: 1628  $\text{cm}^{-1}$  (calculated value is 1622  $\text{cm}^{-1}$ ), 1573  $\text{cm}^{-1}$  (1576  $\text{cm}^{-1}$ ), 1545  $\text{cm}^{-1}$  (1532  $\text{cm}^{-1}$ ), 1288  $\text{cm}^{-1}$  (1310  $\text{cm}^{-1}$ ), 1275  $\text{cm}^{-1}$  (1272  $\text{cm}^{-1}$ ), 1160  $\text{cm}^{-1}$  (1144  $\text{cm}^{-1}$ ), 1118  $\text{cm}^{-1}$  (1110  $\text{cm}^{-1}$ ), 1088  $\text{cm}^{-1}$  (1061  $\text{cm}^{-1}$ ). During the reduction, the vibration bands assigned to the reduction product 4-chloro-6-fluoro-1,10-phenanthroline containing only one chlorine substituent (labelled as **4b mono-Cl**) increase: 1639  $\text{cm}^{-1}$  (1630  $\text{cm}^{-1}$ ), 1608  $\text{cm}^{-1}$  (1603  $\text{cm}^{-1}$ ), 1586  $\text{cm}^{-1}$  (1583  $\text{cm}^{-1}$ ), 1343  $\text{cm}^{-1}$  (1339  $\text{cm}^{-1}$ ), 1307  $\text{cm}^{-1}$  (1321  $\text{cm}^{-1}$ ), 1261  $\text{cm}^{-1}$  (1252  $\text{cm}^{-1}$ ), 1246  $\text{cm}^{-1}$  (1234  $\text{cm}^{-1}$ ), 1137  $\text{cm}^{-1}$  (1126  $\text{cm}^{-1}$ ), 1103  $\text{cm}^{-1}$  (1078  $\text{cm}^{-1}$ ). Even if calculated for the molecule in a vacuum, the calculated wavenumbers are in very good agreement with the experimental values.

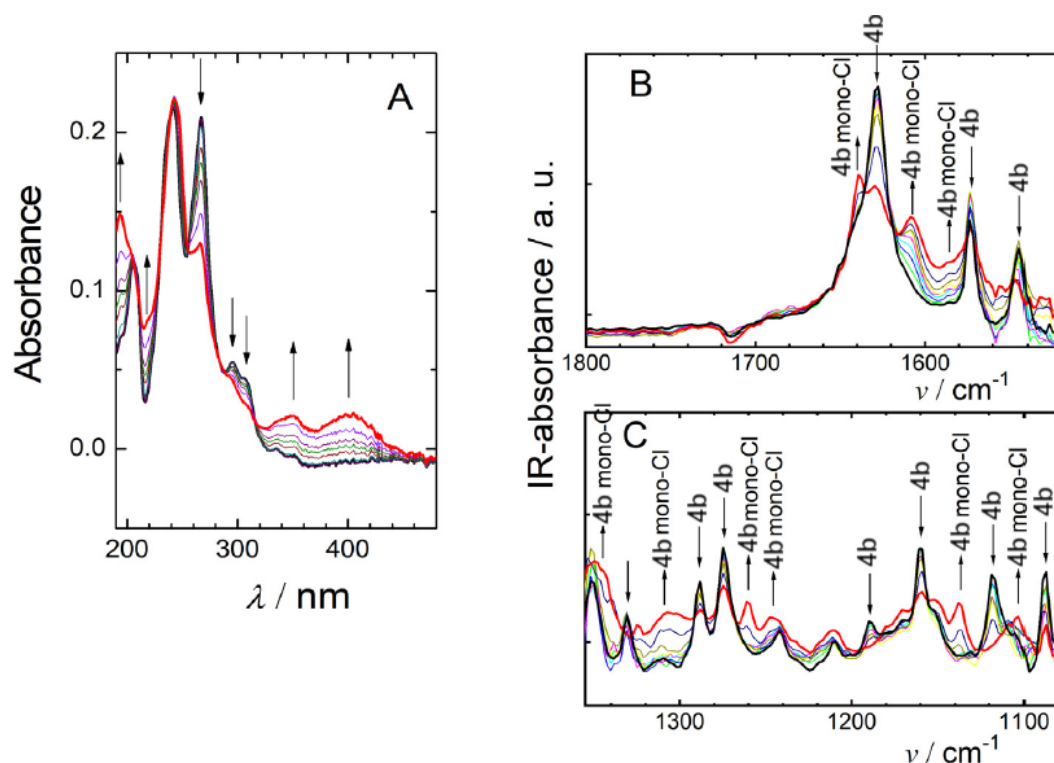


**Figure 12.** UV–Vis spectroelectrochemistry (Panel A) and IR spectroelectrochemistry in the ranges 1800–1520 and 1360–1080  $\text{cm}^{-1}$  (Panels B, C) at the first reduction wave of compound **4b**.

The solutions obtained during the reductive electrolysis were examined by chromatographic techniques such as HPLC-DAD and HPLC-MS/MS in +ESI positive mode. The chromatograms obtained by injecting the solution before, during, and after the reductive electrolysis of **4b** in acetonitrile are shown in Figure 13. The absorption spectrum of the resulting product obtained after subtraction of the background (inset on the left in Figure 13) is in good agreement with the absorption spectrum recorded during spectroelectrochemical experiments shown in Figure 12A. The cyclic voltammogram recorded in solution after the electrolysis shows a decrease in the first reduction wave and a new oxidation wave due to the resulting **4b mono-Cl** product (inset in Figure 13). The presence of the starting compound in the chromatogram in Figure 13D agrees with the cyclic voltammogram shown in the inset on the right of Figure 13. The oxidation of the formed chloride anion occurs in backward scan at 1.3 V<sup>205,206</sup>. This wave appears only when reaching the potential of the first reduction wave.

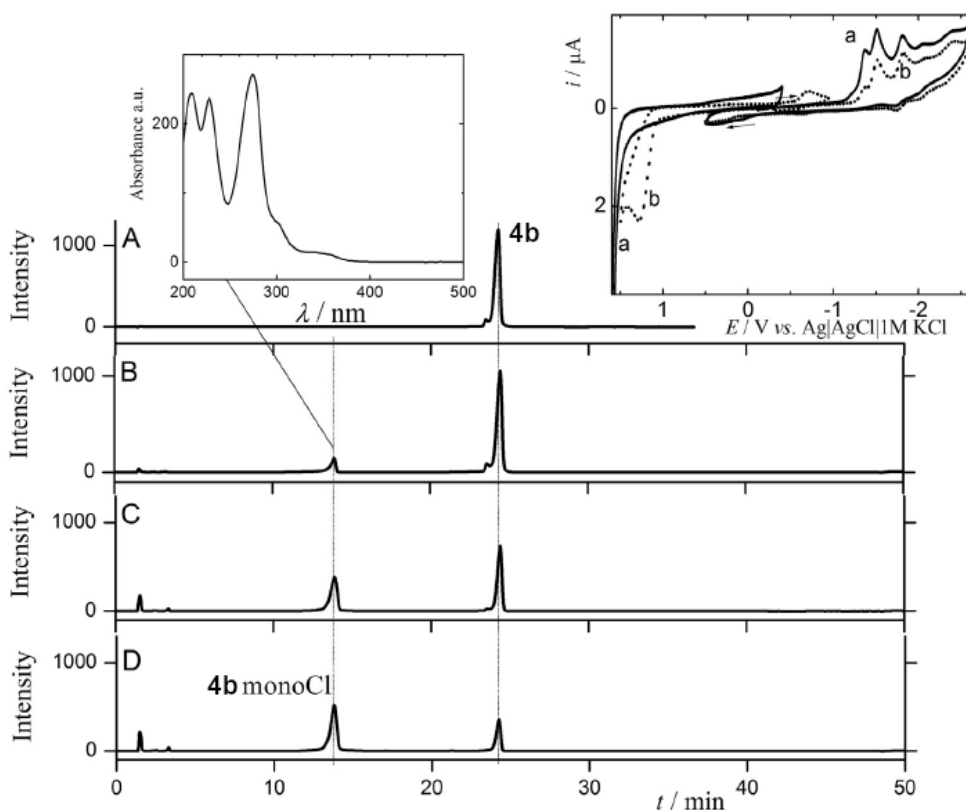


**Figure 13.** Chromatogram of the solution before (A), during (B, C), and after the 80% of the reductive electrolysis (D). The inset on the left shows the absorption spectrum registered for the peak at 13.8 min. The inset on the right reports the cyclic voltammograms before (a) and after the 80% of the electrolysis (b) of **4b** in 0.1 M TBAPF<sub>6</sub> in acetonitrile at  $-1.4$  V, recorded separately for reduction and oxidation as depicted by arrows.

Figure 14 shows the tandem mass spectrum of the ion characterized by  $m/z$  266.9894, corresponding to the molecular ion  $[M + H]^+$  of compound **4b**. The tandem mass spectrum features as main  $m/z$  product ions: 246.9816 corresponding to  $[M + H-HF]^+$  and 231.0119 corresponding to  $[M + H-HCl]^+$ . 7-Chloro-5-fluoro-1,10-phenanthroline (**4b mono-Cl**) was identified as the reduction product at the potential of the first reduction wave ( $-1.4$  V). Its  $[M + H]^+$  molecular ion at 233.0285  $m/z$  was fragmented and its tandem mass spectrum, depicted in Figure 14B, features as main  $m/z$  product ions: 197.0538  $[M + H-HCl]^+$  and 171.0485. The electrolysis at potential  $-2.0$  V resulted in the cleavage of both chlorines from the molecule, and 5-fluoro-1,10-phenanthroline (**Phen-F**) was identified ( $[M + H]^+$  at 199.0665). Figure 14C shows its main  $m/z$  product ions in the tandem mass spectrum: 172.0549  $[M + H-HCN]^+$ , 122.9475.

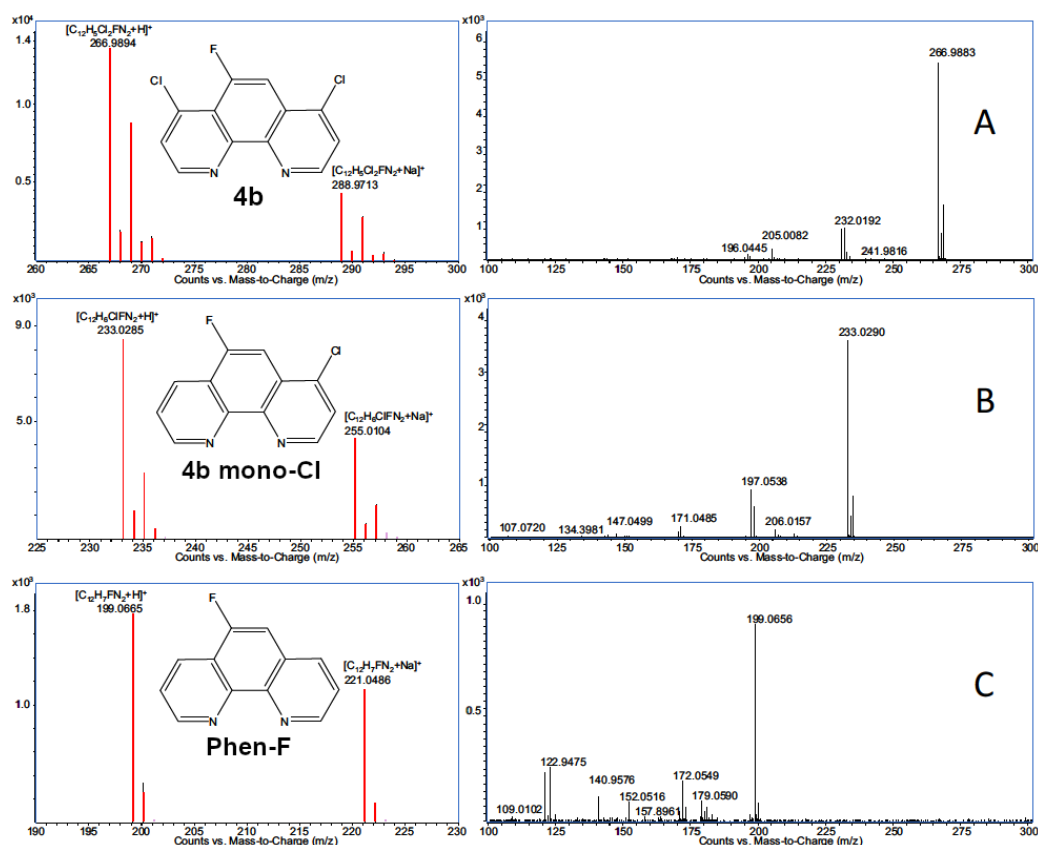


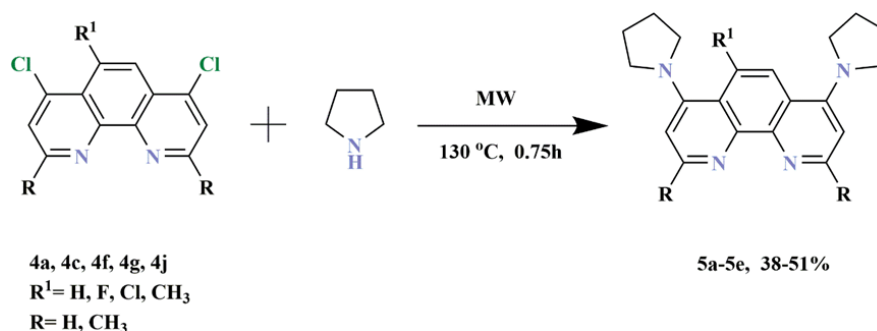
**Figure 14.** High resolution mass spectra (on the left) and tandem mass spectra (on the right) of the peaks assigned to (A) compound **4b**, (B) product of reduction after electrolysis of **4b** at the first reduction wave (**4b mono-Cl**) and (C) product of reduction after electrolysis of **4b** at the potential of the second reduction wave (**Phen-F**). Positive acquisition mode, voltage applied in the collision cell 30 V. The predicted exact mass and isotopic pattern for the three species are shown in red, superimposed to the acquired data.

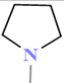
### 6.2.3 Functionalization of selected 1,10-phenanthrolines with pyrrolidine, 9H-carbazole and 10H-phenothiazine substituents.

In the current study, the functionalization of selected 1,10-phenanthroline derivatives at C4 and C7 positions was the focus, which has not been fully exploited and may serve as interesting building blocks for designing new catalyst or luminous layer material in OLEDs.

The introduction of the chlorine atom in the 1,10-phenanthroline skeleton opened opportunities for further functionalization. Five 4,7-dipyrrolidinyl-1,10-phenanthrolines (**5a-5e**) (Scheme 56) with four novel structures were synthesized from their precursors **4** by microwave-assisted nucleophilic aromatic substitution with a 10-fold excess of pyrrolidine. Reactions were carried out in a sealed vial in a microwave reactor at 130 °C (Scheme 56).

MW irradiation improves the reactivity of the substitutions, shortening the reaction time to give the substitution products better yields. In the absence of MW irradiation, the substitution reaction failed to initiate. The yields of products depend on the substituent R<sup>1</sup>, which may influence the outcome of the reaction through steric and/or electronic effects. Unexpectedly R<sup>1</sup> fluorine or chlorine atoms failed to undergo substitution. This phenomenon can be explained by a steric hindrance attributed to the already introduced pyrrolidinyl rings and too high an electron density on the carbon atom at C5 position. One of the obtained compounds, the 5-fluoro-4,7-di(pyrrolidin-1-yl)-1,10-phenanthroline **5b**, was determined by single-crystal X-ray diffraction measurements Figure 15.



Precursors		R	R <sup>1</sup>	Yield (%)
4a	5a	H	H	38
4c	5b	H	Cl	42
4f	5c	CH <sub>3</sub>	H	48
4g	5d	CH <sub>3</sub>	F	51
4j	5e	CH <sub>3</sub>	CH <sub>3</sub>	39

**Scheme 56.** Obtaining 4,7-dipyrolidine-1,10-phenanthroline derivatives.

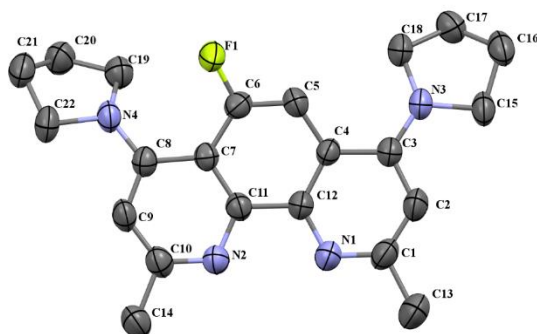
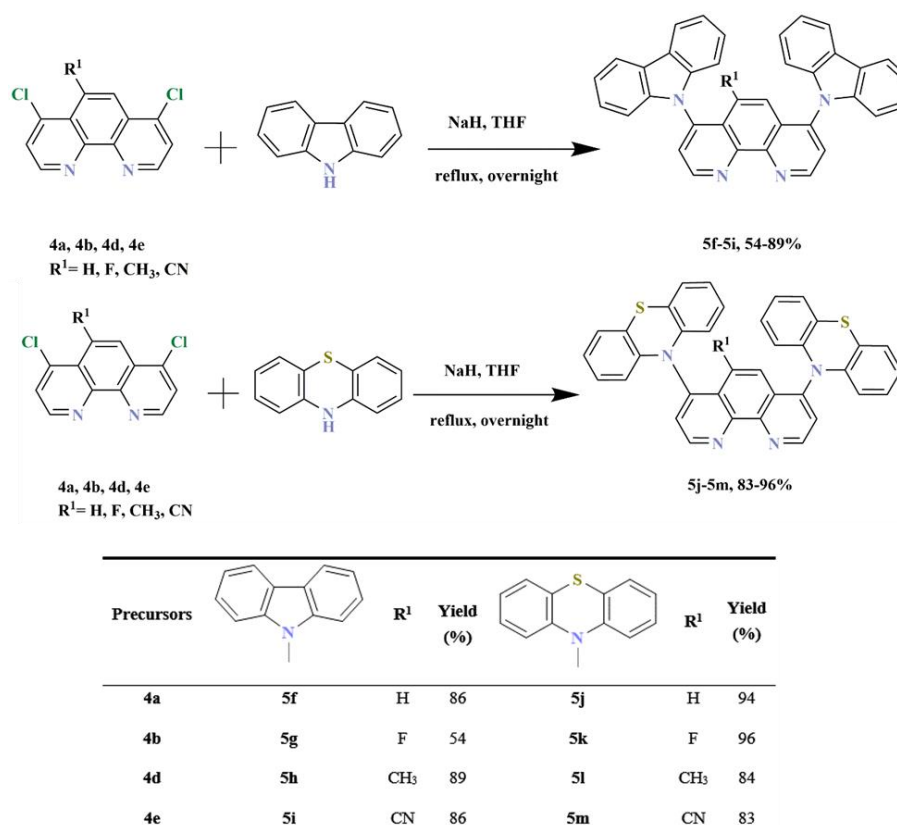


**Figure 15.** ORTEP drawing of compound **5d** with 30% probability. The solvent molecules and fluorine disorder were omitted for clarity.



Another part of this research was the further substitution of 4,7-dichloro-1,10-phenanthroline. Four 4,7-di(9*H*-carbazol-9-yl)-1,10-phenanthrolines and four 4,7-di(10*H*-phenothiazin-10-yl)-1,10-phenanthroline derivatives with seven novel structures which were synthesized from molecules **4** by nucleophilic aromatic substitution with 9*H*-carbazole and 10*H*-phenothiazine, respectively (Scheme 57). Reagents were stirred overnight under reflux. The chemistry was based on inexpensive, commercially available reagents and easily synthesized heterocycles **4**, which possess methyl, CN, fluorine, or hydrogen atom marked on Scheme 57 as R<sup>1</sup>.



**Scheme 57.** Synthesis of 4,7-di(9*H*-carbazol-9-yl)-1,10-phenanthroline (**5f-5i**) and 4,7-di(10*H*-phenothiazin-10-yl)-1,10-phenanthroline (**5j-5m**) derivatives.

The yields of 9*H*-carbazole derivatives **5** were lower than for 10*H*-phenothiazine derivatives. In all cases, the purification of 9*H*-carbazole derivatives **5** required chromatographic methods to receive pure products. However, the purification of 10*H*-phenothiazine could be carried out by crystallization from the mixture of CH<sub>2</sub>Cl<sub>2</sub> (or THF) and hexane to afford products even on a multigram scale. The highest yield and less complex reaction mixture of 10*H*-phenothiazine derivatives can be attributed to the better nucleophilic properties of 10*H*-phenothiazine anion than 9*H*-carbazole.

What is interesting K. Wu et al.<sup>207</sup> obtained the X-ray structure of 4,7-di(10*H*-phenoxazin-10-yl)-1,10-phenanthroline, which was cocrystallized with THF as a guest molecule located in the crystalline frameworks. The THF molecule is surrounded by two 10*H*-phenoxazine rings and a 1,10-phenanthroline core. This effect could explain that in <sup>1</sup>H-NMR and <sup>13</sup>C-NMR studies was a visible presence of signals from THF for 10*H*-phenothiazine derivatives **5j**, **5k**, and **5l** (for compound **5k**, Figure 16, 17).

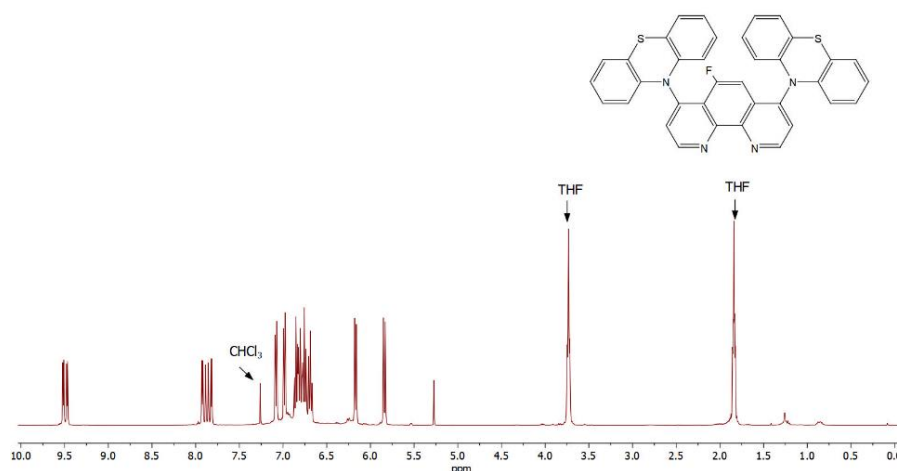


**Figure 16.** <sup>1</sup>H NMR (CDCl<sub>3</sub>; 500.2 MHz) for **5k**.

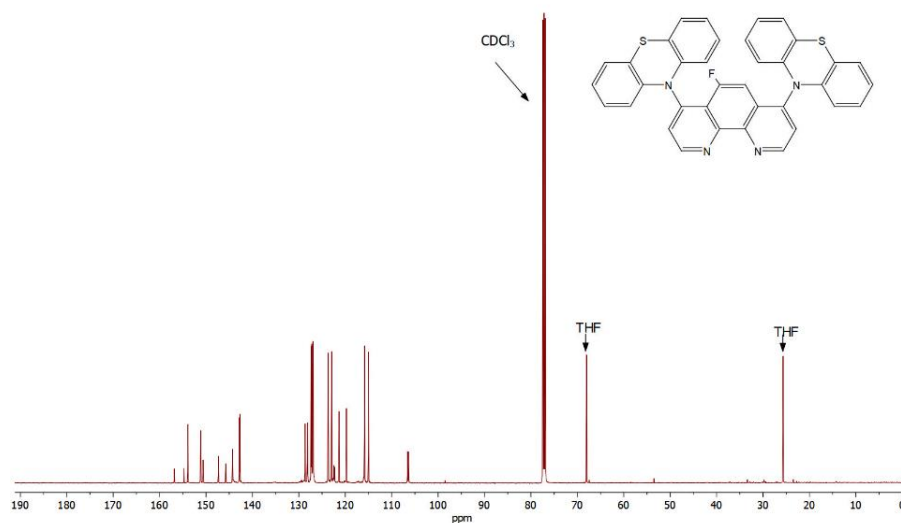


**Figure 17.** <sup>13</sup>C NMR (CDCl<sub>3</sub>; 500.2 MHz) for **5k**.

It is worth noting that in the case of molecule **5l**, with a methyl group marked as R<sup>1</sup>, no residual THF signals have been detected. 9*H*-Carbazole derivatives have shown similar supramolecular inclusion processes to compounds **5j**, **5k**, and **5l**, in which the solvent is located in a cage made by 1,10-phenanthroline derivatives, however, with smaller intensity on <sup>1</sup>H NMR spectrum.

The research results in this chapter have been published in our paper<sup>208</sup>.

## 6.2.4 Electrochemical and spectroelectrochemical studies of selected 4,7-di(pyrrolidin-1-yl)-1,10-phenanthroline

The reduction and oxidation mechanisms of selected 4,7-di(pyrrolidin-1-yl)-1,10-phenanthrolines were investigated in the non-aqueous environment using cyclic voltammetry (CV), controlled potential electrolysis, in-situ UV-Vis and IR spectroelectrochemistry, and HPLC-DAD (HPLC with diode array detector) and HPLC-MS/MS techniques.

The research results in this chapter have been published in our paper<sup>208</sup>.

### 6.2.4.1 Oxidation

Compound **5a** yields four oxidation waves labeled as Ox1 - Ox4 in the potential range from -0.5 V to 2.2 V (Figure 18). The first oxidation wave, Ox1, occurs at 1.02 V (for 2,9-dimethylated derivative **5c**: 0.930 V). The spatial distribution of HOMO orbitals in **5a** and **5c** shows the delocalization of HOMO on the conjugated aromatic rings and the nitrogen atom of the substituent (the inset of Figure 18 for **5a**, and Figure 19 for **5c**).

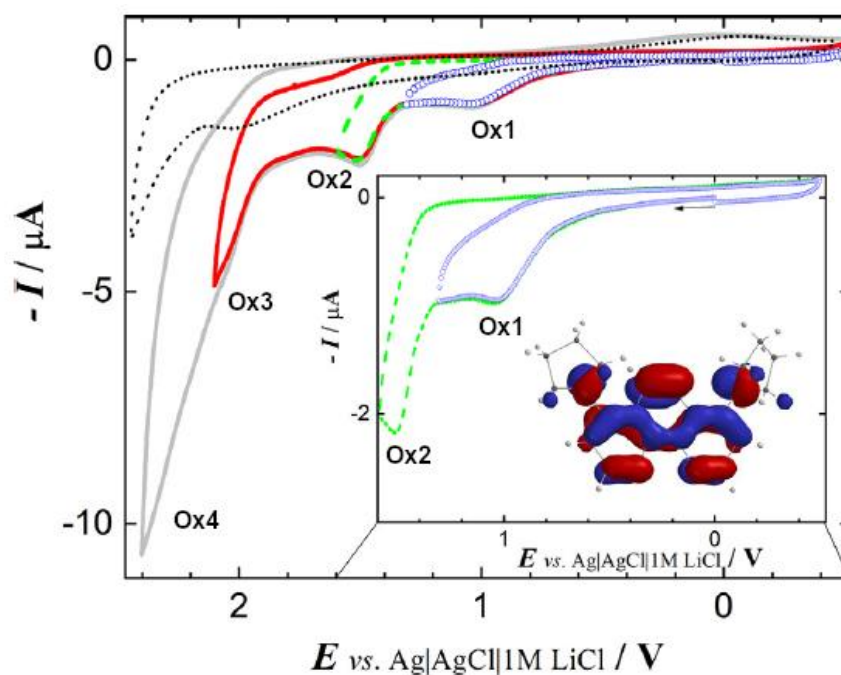


**Figure 18.** Cyclic voltammograms of 0.63 mM **5a** in 0.1 M TBAPF<sub>6</sub>/acetonitrile recorded at scan rate 0.1 V · s<sup>-1</sup> on glassy carbon electrode. The direction of polarity was changed behind the first (Ox1 - empty blue circles), second (Ox2 - dashed green curve), and third (Ox3 –solid red curve) oxidation wave. The dotted curve represents the cyclic voltammogram of 0.63 mM

1,10-phenanthroline (**Phen**) obtained at the same conditions. The inset shows an enlarged portion of the same CV depicting Ox1 and Ox2 peaks in detail and HOMO spatial distribution calculated for neutral **5a** molecule.

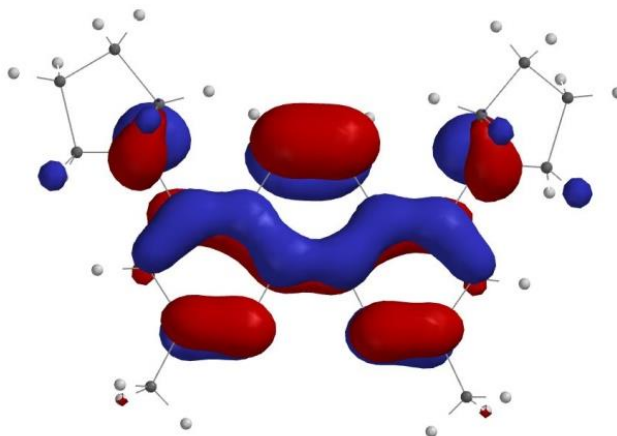
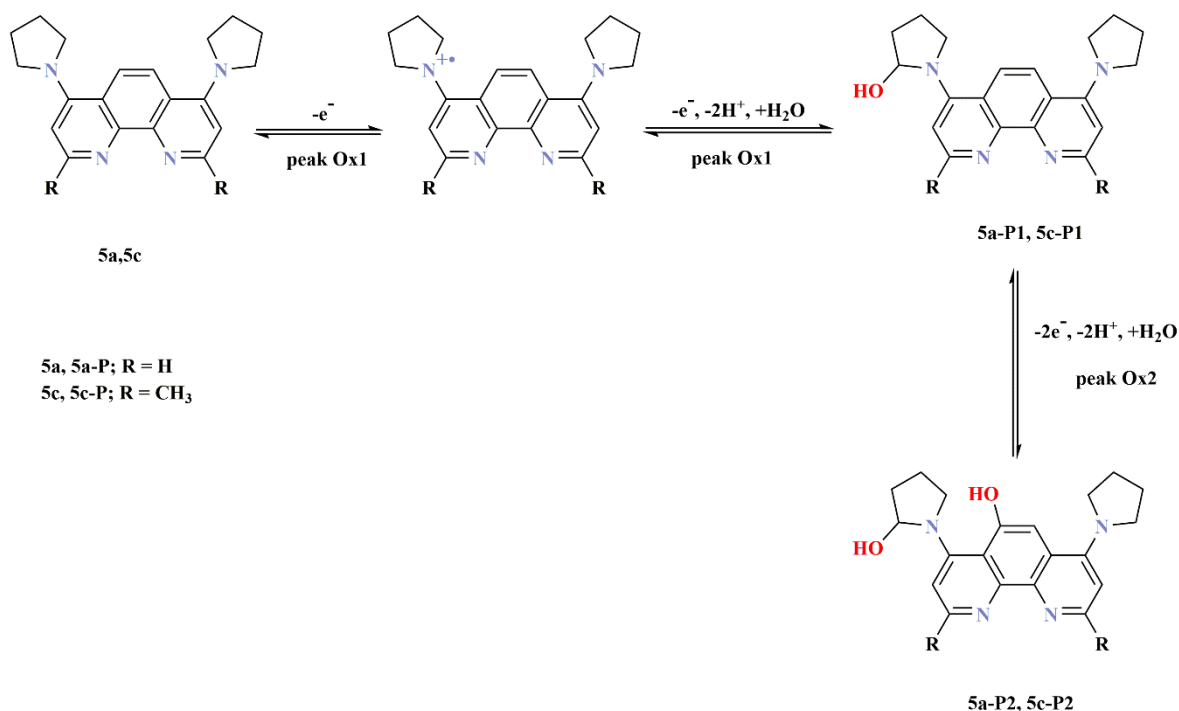


**Figure 19.** HOMO spatial distribution calculated for neutral **5c** molecule.

Since the non-substituted 1,10-phenanthroline molecule is not electroactive at the potential of Ox1, thus a radical cation is primarily formed on the nitrogen atom of the pyrrolidinyl group, as suggested in Scheme 58.



**Scheme 58.** The proposition of oxidation mechanism of molecules **5a** and **5c**.

The energy  $E_{\text{HOMO}}$  (**5a**) =  $-5.41$  eV is lower than  $E_{\text{HOMO}}$  (**5c**) =  $-5.30$  eV, and the values agree with those of peak potential experimentally obtained for both compounds. The second oxidation wave, Ox2 occurs at 1.50 V (for 2,9-dimethylated derivative **5c**: 1.36 V); the third oxidation wave was recorded at 2.06 V (for **5c**: 1.91 V), and the fourth wave at 2.35 V is poorly defined (for **5c**: 2.21 V). All the oxidation peaks current Ox1 - Ox4 are diffusion controlled, since the peak current depends linearly on the square root of scan rate (inset of Figure 20B for **5c**). All peak currents of processes Ox1 - Ox4 are linearly proportional to bulk concentration. The inset in Figure 20A shows the dependence of the peak current of the first oxidation wave of **5a** on its concentration. Interestingly, a small pre/post-peak labeled as Ads occurs at 1.279 V and its height remains constant at different concentration values above 0.28 mM (Figure 20A).

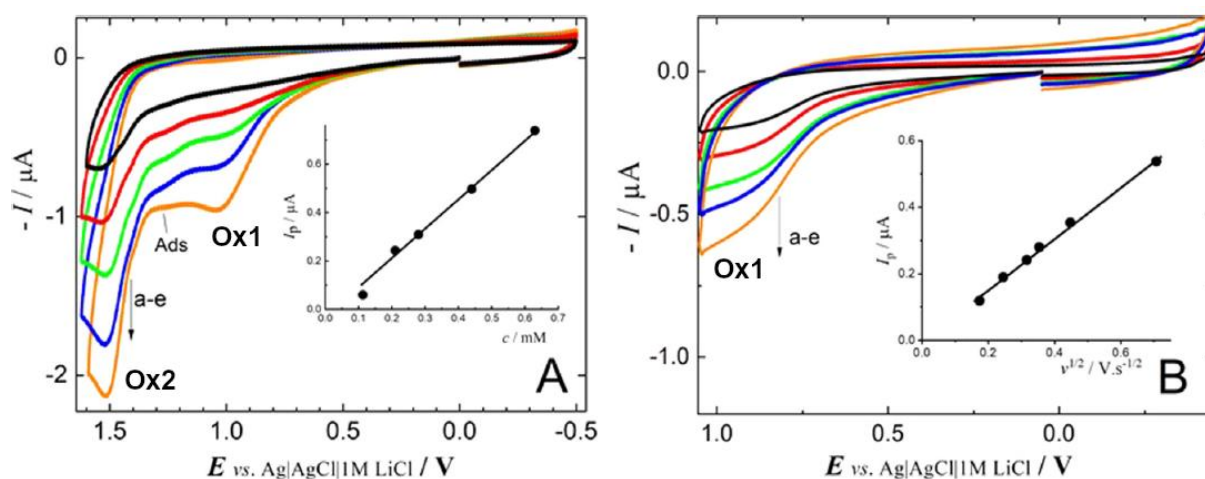


**Figure 20.** Panel A: Cyclic voltammograms of **5a** at different concentrations a) 0.11, b) 0.21, c) 0.28, d) 0.44 and e) 0.63 mM at scan rate  $0.1 \text{ V} \cdot \text{s}^{-1}$  on glassy carbon electrode. The inset of panel A represents the dependence of the faradaic peak current of the oxidation wave Ox1 on concentration. Panel B: Cyclic voltammograms of 0.28 mM **5c** at different scan rates a) 0.03, b) 0.06, c) 0.1, d) 0.125 and e)  $0.2 \text{ V} \cdot \text{s}^{-1}$ . The inset of panel B depicts the dependence of the faradaic peak current of the first oxidation wave Ox1 on the square root of scan rate. In all measurements, 0.1 M TBA PF<sub>6</sub> in acetonitrile served as a supporting electrolyte.

This behavior is a clear indication of an adsorption pre/post-wave<sup>204</sup>. Importantly, the presence of the molecular layer adsorbed at the electrode/electrolyte interface does not hamper the electron transfer processes of molecules diffusing from the bulk of the electrolyte. A detailed analysis of potential peak values of the wave Ox1 provides slopes amounting to  $\delta E_p / \delta \log v = 38 \text{ mV}$  and  $\delta E_p / \delta \log c = 29 \text{ mV}$  for compound **5a**, and  $\delta E_p / \delta \log v = 29 \text{ mV}$  and  $\delta E_p / \delta \log c = 33 \text{ mV}$  for compound **5c** (Figure 21, Supplementary material), which are consistent with the theoretical values of 29 mV per decade characteristic for ECE reaction scheme<sup>209</sup>.

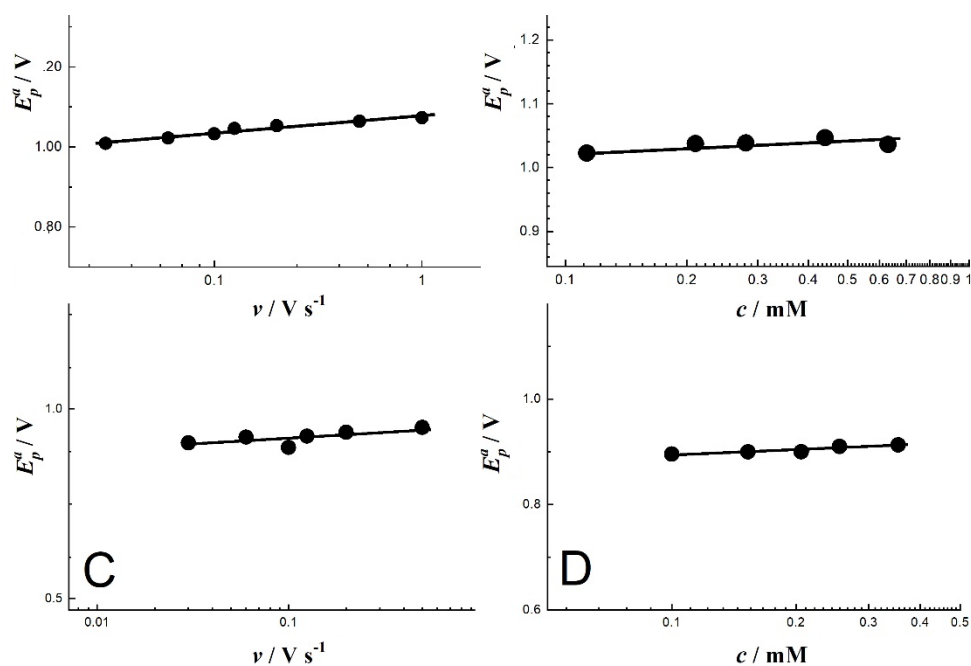


**Figure 21.** The dependence of peak potential of the first oxidation wave Ox1 on the scan rate (left) and on concentration (right) for compounds **5a** (A, B) and **5c** (C, D), respectively. In all experiments, 0.1 M TBAPF<sub>6</sub> in acetonitrile served as a supporting electrolyte.

The ECE process is followed by the nucleophilic addition of water (water traces are present in anhydrous acetonitrile, even if below 0.001%) and results in the formation of hydroxylated products **5a-P1**, **5c-P1**, which are formed at the potential of the wave Ox1. This process is analogous to what was observed for the cyanation of *N*-protected amines, which leads to cyano derivatives formed in the ortho position<sup>210,211</sup>. Concerning the oxidation process Ox2, the values calculated for  $\delta E_p / \delta \log v = 29$  mV and  $\delta E_p / \delta \log c = 29$  mV found for compound **5c** support an oxidation mechanism similar to that occurring at Ox1 (data not shown). As discussed below, compounds **5a-P2**, **5c-P2** were identified as the oxidation products at the wave Ox2, suggesting that the ECEC mechanism corresponds to the  $2e^-/2H^+$  process and nucleophilic addition of water. Peaks Ox3 and Ox4 are attributed to the oxidation of 1,10-phenanthroline moiety as corresponding features occur at similar potential values in the cyclic voltammetric response of 1,10-phenanthroline (Figure 1). The IR spectroelectrochemistry performed at the potential of the first oxidation wave shows changes in the intensity of absorption bands, and several isosbestic points are present in the spectra (Figure 22).

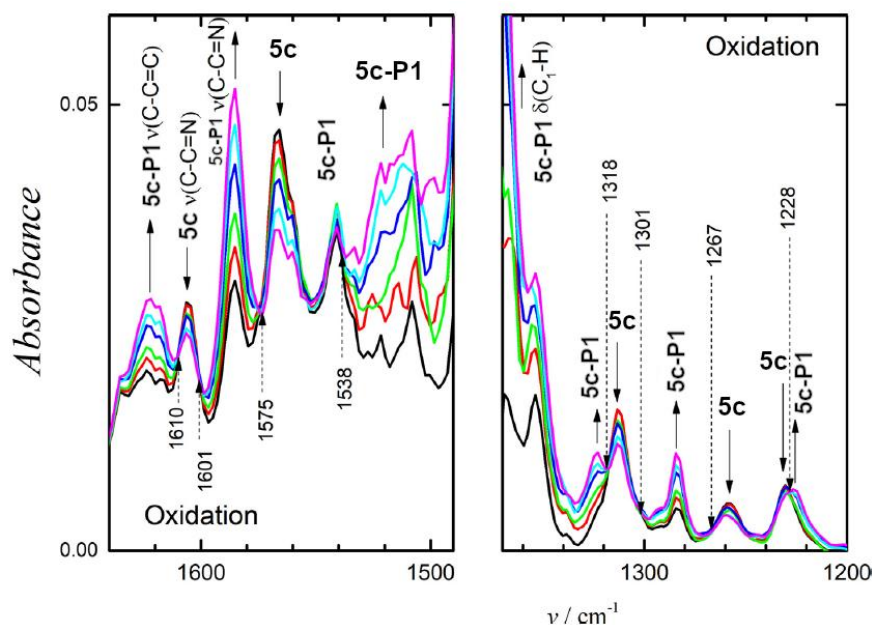


**Figure 22.** IR spectroelectrochemistry of 2.9 mM compound **5c** recorded while sweeping the electrode potential through the first oxidation wave in 0.1 M TBAPF<sub>6</sub> in acetonitrile. Wavenumbers of obtained isosbestic points are marked with dashed arrows.

Since theoretical calculations of IR spectra result in very similar IR spectra of **5c** and **5c-P1** (4-(2-hydroxypyrrolidin-1-yl)-2,9-dimethyl-7-(pyrrolidin-1-yl)-1,10-phenanthroline) as presented in Table 1 and Figure 23, the appropriate changes in the absorption bands were difficult to resolve.

**Table 1.** Calculated and experimental values of wavenumbers of compounds **5c** and **5c-P1** in cm<sup>-1</sup>.

4,7-di(pyrrolidine-1-yl)-2,9-dimethyl-1,10-phenanthroline ( <b>5c</b> )													
<b>Calc.</b>	1606	1592	1577	1543	1501	1351	1320	1279	1247	1233			
<b>Experim.</b>	1623	1606	1585	1567	1543	1354	1313	1284	1258	1230			
4-(2-hydroxypyrrolidin-1-yl)-2,9-dimethyl-7-(pyrrolidin-1-yl)-1,10-phenanthroline ( <b>5c-P1</b> )													
<b>Calc.</b>	1606	1591	1576	1542	1502	1373	1351	1333	1320	1286	1280	1241	1214
<b>Experim.</b>	1623	1606	1585	1567	1543	1367	1354	1324	1313	1293	1284	1258	1225



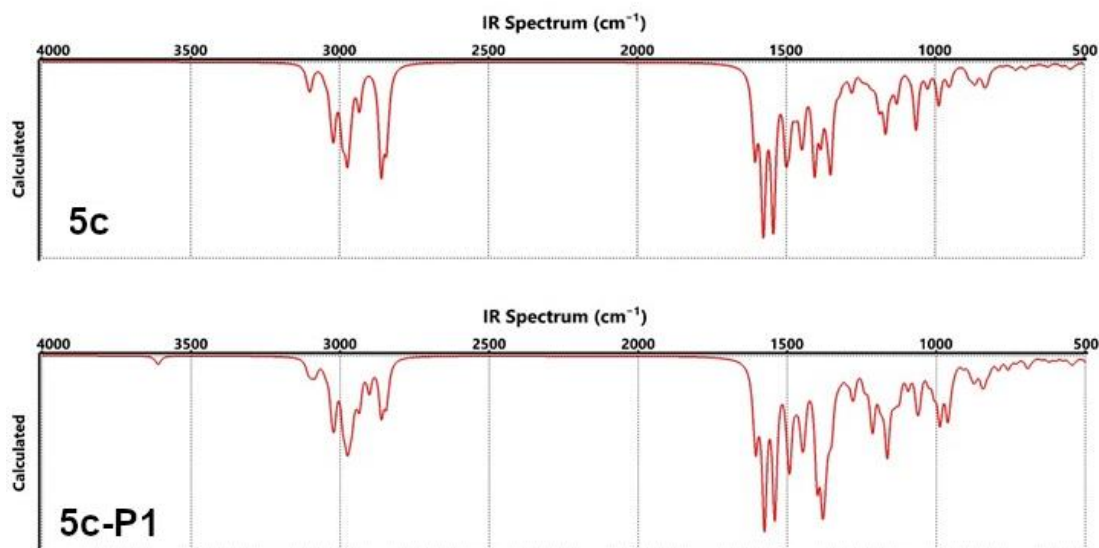


**Figure 23.** IR spectra of 4,7-di(pyrrolidine-1-yl)-2,9-dimethyl-1,10-phenanthroline (**5c**), 4-(2-hydroxypyrrolidin-1-yl)-2,9-dimethyl-7-(pyrrolidin-1-yl)-1,10-phenanthroline (**5c-P1**) calculated using the DFT employing the EDF2 functional and 6-31G\* basis set.

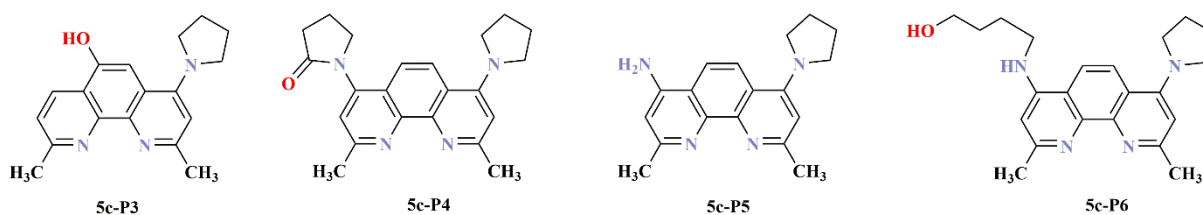
The absorption bands of **5c** at 1606, 1567, 1313, 1258, and 1230  $\text{cm}^{-1}$  decrease to the intensity of the band belonging to the oxidation product **5c-P1** (calculated as 1591, 1542, 1320, and 1241  $\text{cm}^{-1}$  for **5c-P1**). Simultaneously, the absorption bands of **5c-P1** corresponding to stronger vibrations than in molecule **5c** at 1623, 1585, and 1284  $\text{cm}^{-1}$  increase in the resulting absorption spectrum. Nevertheless, new absorption bands attributed to **5c-P1** are developed at 1516, 1324, and 1225  $\text{cm}^{-1}$  (Figure 22). Also, absorption bands of **5c-P1** at 1293 and 1284  $\text{cm}^{-1}$  increase. The formation of the hydroxylated derivative is also consistent with the increased absorption at 1367  $\text{cm}^{-1}$  (Figure 22) (calculated as 1373  $\text{cm}^{-1}$  for **5c-P1**). The expected band of O–H valence vibration was not experimentally confirmed as it was hidden in the absorption of water traces in the solvent (data not shown). Importantly, IR spectroelectrochemical measurements clearly confirmed the formation of a product **5c-P1**.

The product **5c-P1** was further identified by HPLC-MS/MS in solution after oxidative electrolysis of **5c** at  $m/z$  value 363.2186  $[\text{M} + \text{H}]^+$  with fragments at  $m/z$  : 292.1715, 277.1636 and 237.8430. Similarly, the hydroxylated derivative **5a-P1** (4-(2-hydroxypyrrolidin-1-yl)-7-(pyrrolidin-1-yl)-1,10-phenanthroline) was found as the oxidation product in solution after oxidation of compound **5a** (Scheme 59) with  $m/z$  value 335.1860 corresponding to  $[\text{M} + \text{H}]^+$  with fragments at  $m/z$  : 317.1794, 307.1487, 291.1599, 277.1452, 265.1420 and 249.1191. All other identified oxidation products are summarized in Table 2 . The formation of the open

structure **5c-P6** (4-((4-hydroxybutyl)amino)-2,9-dimethyl-7-(pyrrolidin-1-yl)-1,10-phenanthroline) (Scheme **59**) during the oxidation of **5c-P1** can be explained by the primary formation of the oxo derivative **5c-P4** (2,9-dimethyl-4-(2-oxopyrrolidin-1-yl)-7-(pyrrolidin-1-yl)-1,10-phenanthroline) and subsequent opening of the ring as described in literature<sup>212</sup>. The amino derivative **5c-P5** (2,9-dimethyl-7-(pyrrolidin-1-yl)-1,10-phenanthroline-4-amine) most likely originates from the further decomposition of **5c-P5** accompanied by the cleavage of 1-butanol. Importantly, the derivatives presented in Scheme **59** were found as minor products only upon the oxidation of **5c** at the potential of the second oxidation wave.

**Table 2.** Oxidation products of **5a** and **5c**: mass spectrometric data of the compounds depicted in Schemes **58** and **59**.

Compound	The molecular formula of MS precursor	MS precursor ion: m/z	MS <sup>2</sup> product ions: m/z
<b>5a-P1</b>	[C <sub>20</sub> H <sub>22</sub> N <sub>4</sub> O + H] <sup>+</sup>	335.1867	317.1794, 291.1599, 277.1452, 265.1420, 249.1191
<b>5c-P1</b>	[C <sub>22</sub> H <sub>26</sub> N <sub>4</sub> O + H] <sup>+</sup>	363.2178	345.2140, 292.1715, 277.1636
<b>5c-P2</b>	[C <sub>22</sub> H <sub>26</sub> N <sub>4</sub> O <sub>2</sub> + H] <sup>+</sup>	379.2112	361.2025, 320.1638, 308.1564, 292.1669
<b>5c-P3</b>	[C <sub>18</sub> H <sub>19</sub> N <sub>3</sub> O + H] <sup>+</sup>	294.1599	264.1116, 252.1141, 225.0983
<b>5c-P4</b>	[C <sub>22</sub> H <sub>24</sub> N <sub>4</sub> O + H] <sup>+</sup>	361.2018	333.1784, 319.1556, 305.1755, 292.1540, 277.1539
<b>5c-P5</b>	[C <sub>18</sub> H <sub>20</sub> N <sub>4</sub> + H] <sup>+</sup>	293.1764	263.1298, 251.1309, 237.1266, 224.1174
<b>5c-P5</b>	[C <sub>22</sub> H <sub>28</sub> N <sub>4</sub> O + Na] <sup>+</sup>	387.2092	378.1942, 361.1942, 351.1715, 326.1434
	[C <sub>22</sub> H <sub>28</sub> N <sub>4</sub> O + H] <sup>+</sup>	365.2275	not acquired



**Scheme 59.** Minor products identified in solution after the oxidation of molecule **5c**.

#### 6.2.4.2 Reduction

The reduction properties of compounds **5a** and **5c** were investigated using a glassy carbon electrode. The first reduction wave, Red1 of compound **5a**, occurs at  $-1.39$  V and is irreversible (Figure 24). The second reduction wave was found almost  $0.7$  V negatively at potential  $-2.082$  V. Similarly, compound **5c** yields two irreversible reduction waves at  $-1.54$  V and  $-2.21$  V. Both reduction processes of compound **5c**, expectedly occur at a more negative potential than for compound **5a** due to the positive inductive effect (+I) of methyl group. Similarly, the calculated energy  $E_{\text{LUMO}}$  (**5a**) =  $-1.05$  eV is lower than  $E_{\text{LUMO}}$  (**5c**) =  $-0.90$  eV. Since the LUMO orbitals are mainly localized on the 1,10-phenanthroline core (inset of Figure 24), the first electron is likely transferred to the aromatic moiety, and a radical anion is formed (Scheme 60). The comparison of these results with the cyclic voltammogram of unmodified 1,10-phenanthroline recorded under the same conditions (reduction waves obtained at  $-1.92$  V and  $-2.15$  V are represented by a dotted curve in Figure 24) indicates that the reduction of this aromatic structure is facilitated by the presence of pyrrolidine-1-yl functional groups and that the corresponding radical anion is formed at the first stage of the reaction. As confirmed by the further identification of reduction products (Scheme 60), the pyrrolidine moiety is cleaved upon the reduction step Red1 similarly as chloride in chlorinated 1,10-phenanthrolines, see chapter 6.2.2.2. In the currently described structures, the presence of a pyrrolidine-1-yl functional group causes a negative inductive effect, similar to phenyl or chlorine substituents in the reduction of substituted heterocyclic rings<sup>213</sup>. Therefore, the formation of a radical anion is followed by the cleavage of pyrrolidine, while the resulting aryl radical accepts the second electron, and the reaction is terminated by an abstraction of a proton from the solvent (Scheme 60). The proton may be taken from the water traces present in anhydrous acetonitrile (0.001% as described in the Experimental part, chapter 6.1), or the proton donor can be another molecule of the compound

**5c** as discussed below since the peak potential Red1 is shifted to positive potentials with increasing concentration of **5c** with the result of  $\delta E_p / \delta \log c = 39$  mV.

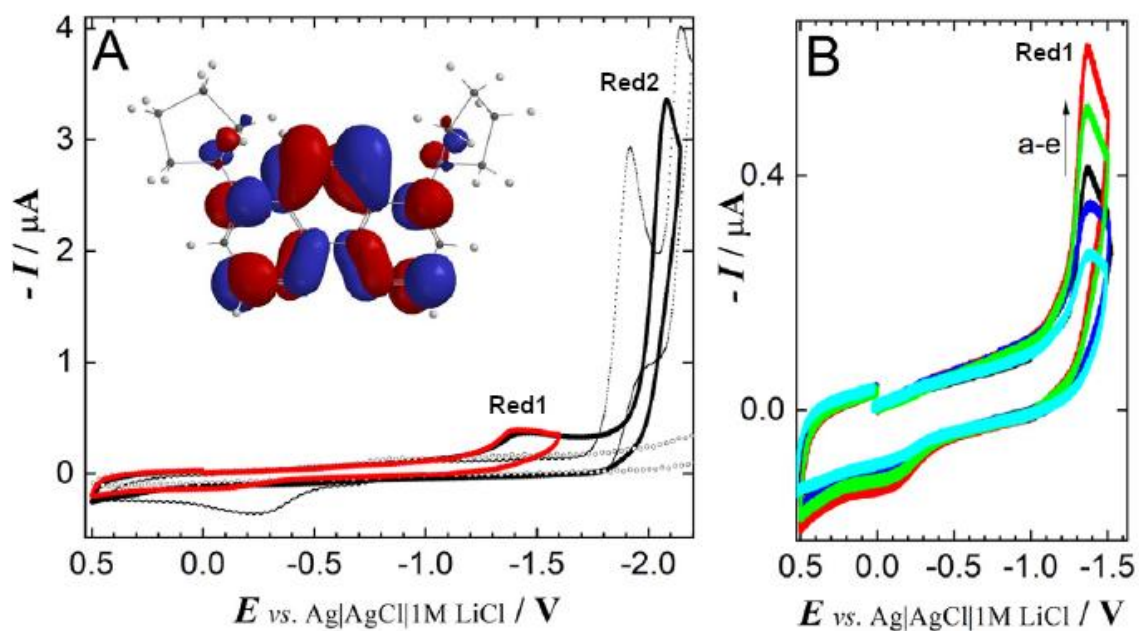
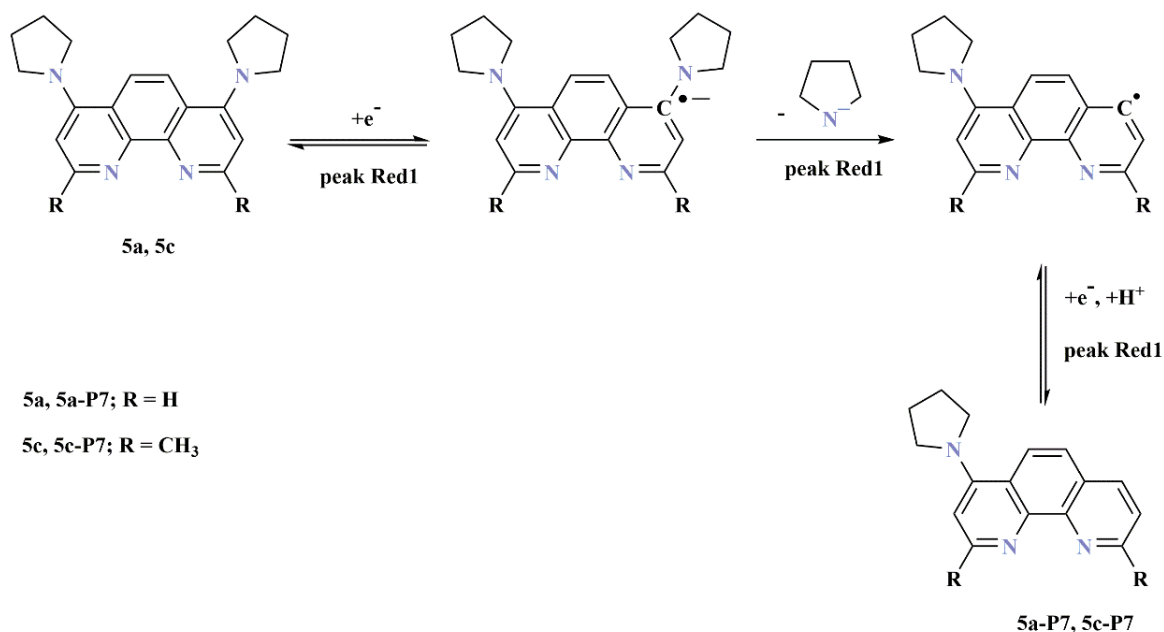


**Figure 24.** Panel A: cyclic voltammograms of 0.63 mM **1a** in 0.1 M TBAPF<sub>6</sub> /acetonitrile recorded at scan rate 0.1 V · s<sup>-1</sup> on glassy carbon electrode. The direction of polarity was changed behind the first (Red1 - red dotted curve) and second (Red2 - black solid curve) reduction waves. The dotted curve represents the cyclic voltammogram of 0.63 mM 1,10-phenanthroline acquired in the same conditions. The cyclic voltammogram acquired in the supporting electrolyte (background) is depicted by the curve of empty black circles. The inset shows the spatial distribution of LUMO calculated for the **5a** molecule. Panel B: Cyclic voltammograms of **5a** at different concentrations a) 0.11, b) 0.21, c) 0.28, d) 0.44 and e) 0.63 mM at scan rate 0.1 V · s<sup>-1</sup>. (For interpretation of the references to color in this figure legend, the reader is referred to the web version of this article.)



**Scheme 60.** Proposition of the mechanism of reduction of **5a** and **5c** at the first reduction step Red1.

Conversely, in the case of compound **5a**, the value of the peak potential is shifted negatively, and the following values were obtained:  $\delta E_p / \delta \log v = 50$  mV and  $\delta E_p / \delta \log c = 29$  mV (Figure 25).

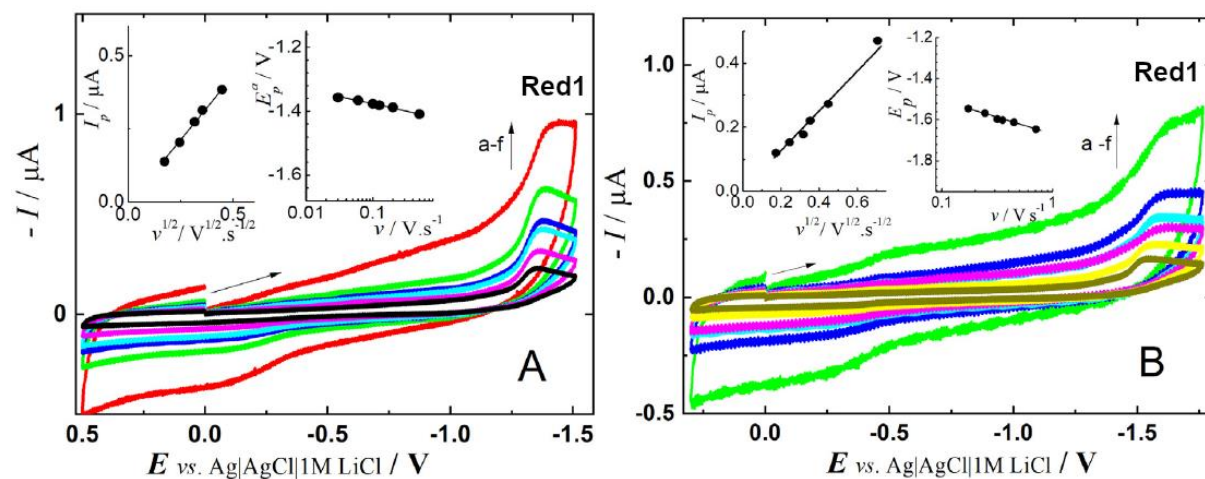


**Figure 25.** Cyclic voltammograms of 0.28 mM **5a** (Panel A) and 0.28 mM **5c** (Panel B) at different scan rates a) 0.03, b) 0.06, c) 0.1, d) 0.125, e) 0.2 and f) 0.5  $\text{V} \cdot \text{s}^{-1}$ . The insets of both panels show the dependences of the peak current of the first reduction wave Red1 on the square root of scan rate (left) and the dependences of peak potential on scan rate (right). In all experiments, 0.1 M TBAPF<sub>6</sub> in acetonitrile served as supporting electrolyte, and a glassy carbon electrode was used as working electrode.

The exhaustive reductive electrolysis was further performed to identify the reduction products using HPLC-DAD and HPLC-MS/MS techniques. The electric charge consumed at the potential of the first and second reduction waves corresponds to 1 and 4 electrons, respectively. The low ratio between the peak currents Red1 and Red2 in Figure 24 is most likely caused by the kinetic character of current Red1, and possibly a self-protonation during reduction mechanism is involved as described for several organic compounds in general, and specifically for heterocyclic nitrogen compounds (chapter 6.2.2)<sup>214</sup>. In detail, both the height of the first reduction wave and the consumed electric charge corresponding to a one-electron overall process, if calculated for the total initial amount of the compound. If half of this amount serves as a proton donor to enable the reaction, as shown in Scheme 60, the height of the first reduction wave will correspond to a half electron consumption, and therefore, two electrons would participate in the first reduction wave Red1. The cyclic voltammogram recorded after the electrolysis performed at the second wave displays two reduction waves at potentials  $-1.90$  and  $-2.20$  V attributed to 1,10-phenanthroline being present in the solution. The main reduction product of the compound **5a** was found by HPLC-MS/MS at  $m/z = 250.1343$  as  $[C_{16}H_{15}N_3 + H]^+$  and was identified as 4-(pyrrolidin-1-yl)-1,10-phenanthroline **5a-P7** (Scheme 60, Figure 26A). The MS/MS spectrum is shown in Figure 26B. This is a derivative with one remaining pyrrolidine substituent. Similarly, the corresponding derivative without one pyrrolidinyl substituent (2,9-dimethyl-4-(pyrrolidin-1-yl)-1,10-phenanthroline, **5c-P7**) was found in solution after the electrolysis of compound **5c** at the potential of the first reduction wave with  $m/z$  value of  $278.1652$  ( $[C_{18}H_{19}N_3 + H]^+$ ) (Scheme 60). This compound elutes at longer retention times than **5a-P7** because of the presence of two additional methyl group. The electrochemical reduction at the potential of the second wave Red2 leads to the cleavage of both pyrrolidine rings and the regeneration of 1,10-phenanthroline identified as  $[C_{12}H_8N_2 + H]^+$  at  $m/z = 181.0764$  (the sodium adduct is also present as  $[C_{12}H_8N_2 + Na]^+$  at  $m/z = 203.0580$ ). In the mass spectrum of the product ion of  $181.0764$ , the main fragments occur at  $m/z$  values:  $166.0547$ ,  $154.0655$ , and  $127.0546$ . The cleavage of pyrrolidine rings was also observed for compound **5c** at the second reduction wave (chromatogram in Figure 26D).

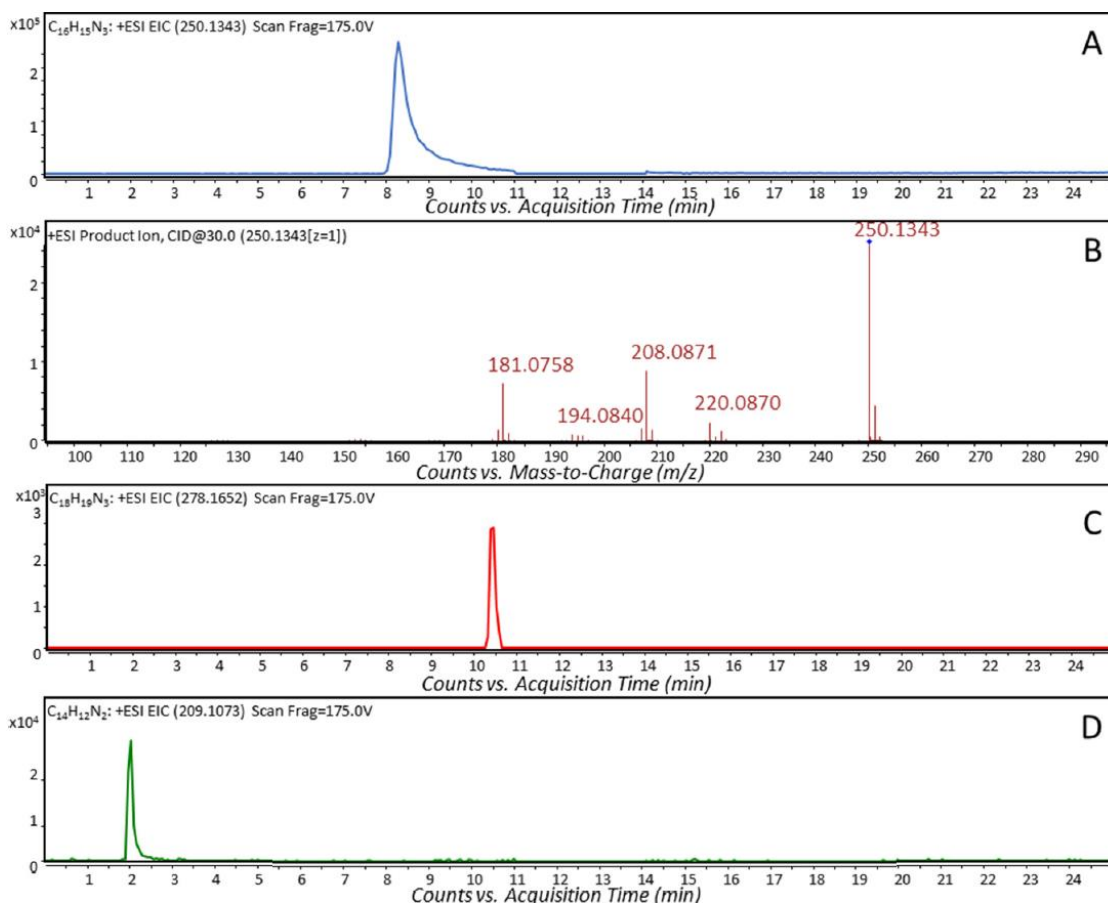


**Figure 26.** HPLC-ESI-MS/MS extracted ion chromatograms (EICs) after the reduction of A) **5a** at the potential of the first reduction wave (EIC of the exact mass of  $[\text{C}_{16}\text{H}_{15}\text{N}_3 + \text{H}]^+$ ,  $m/z$  250.1343); B) product ion mass spectrum of the is eluting at 8.8 min in the chromatogram (A) with the raw formula  $[\text{C}_{16}\text{H}_{15}\text{N}_3 + \text{H}]^+$  ( $m/z$  250.1343) acquired at 30 V in the collision cell; C) **5c** at the potential of the first reduction wave (EIC of the exact mass of  $[\text{C}_{18}\text{H}_{19}\text{N}_3 + \text{H}]^+$ ,  $m/z$  278.1652); D) **5c** at the potential of the second reduction wave (EIC of the exact mass of  $[\text{C}_{14}\text{H}_{12}\text{N}_2 + \text{H}]^+$ ,  $m/z$  209.1073).

The peaks with molecular ions  $[\text{C}_{14}\text{H}_{12}\text{N}_2 + \text{H}]^+$  at  $m/z = 209.1073$  (with the sodium adduct  $[\text{C}_{14}\text{H}_{12}\text{N}_2 + \text{Na}]^+$  at  $m/z = 231.0935$ ) are attributed to the resulting 2,9-dimethyl-1,10-phenanthroline (**phen-2CH<sub>3</sub>**). The main  $m/z$  values in the product ion mass spectrum of 209.1073 are at  $m/z$  values: 194.0817, 181.0846, and 167.0718. Chromatograms recorded by means of HPLC-DAD before, during, and after electrolysis of **5a** solution are shown in Figure 27. The obtained results agree with the findings described above, i.e., the chromatographic peak of **5a** decreased during electrolysis, while a new peak corresponding to **5a-P7** increased. Additionally, a new peak attributed to 1,10-phenanthroline appeared at the potential of the second reduction wave (Figure 4 D, E).

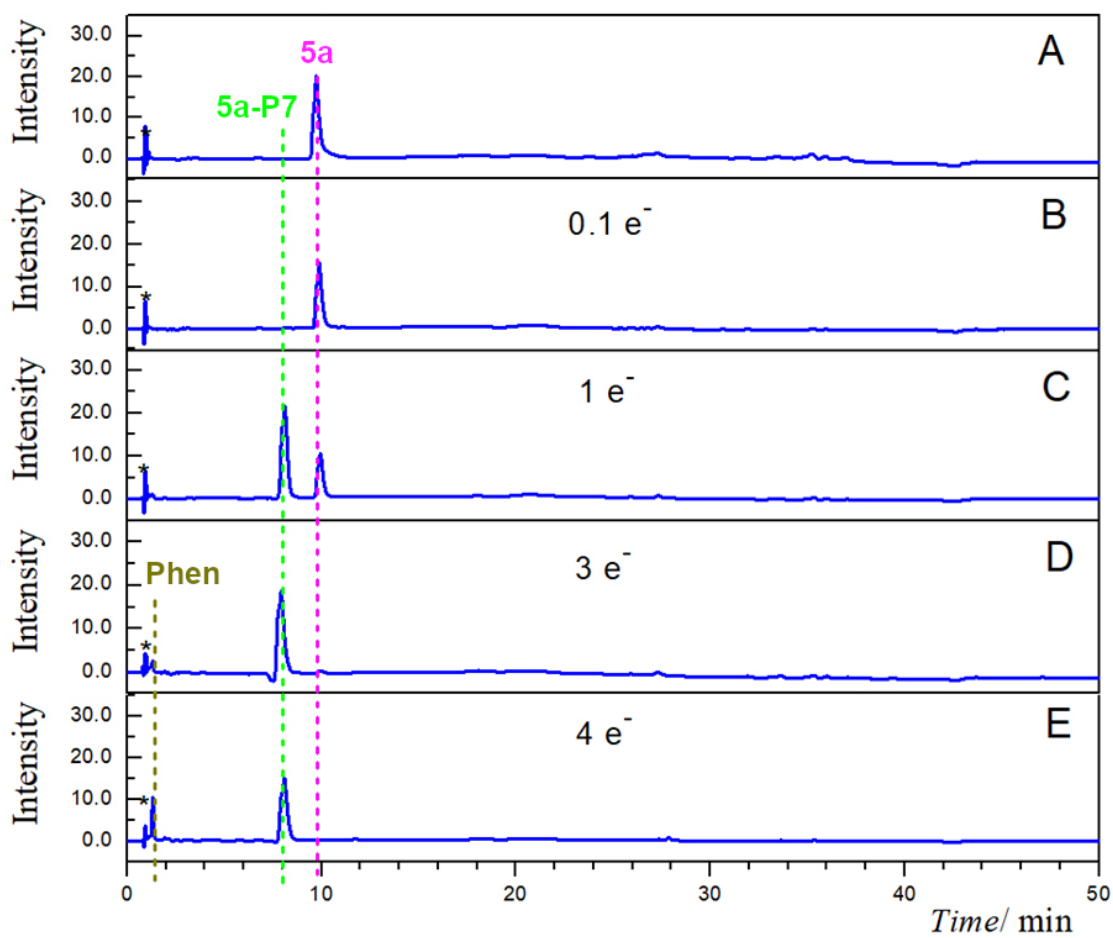


**Figure 27.** Chromatograms of solution A) before and (B,C) during reductive electrolysis of compound **5a** at the potential of the first reduction wave, and D,E) during and after electrolysis at the potential of the second reduction wave. A number of consumed electrons is inserted in every panel.

The IR-spectroelectrochemistry performed at the potential of the first reduction wave resulted in a decrease of the absorption bands related to compound **5c** at 1623, 1585, and 1284  $\text{cm}^{-1}$  (Figure 28). These changes are accompanied by an increase of the bands at 1606, 1567, 1543, 1313, and 1258  $\text{cm}^{-1}$ .



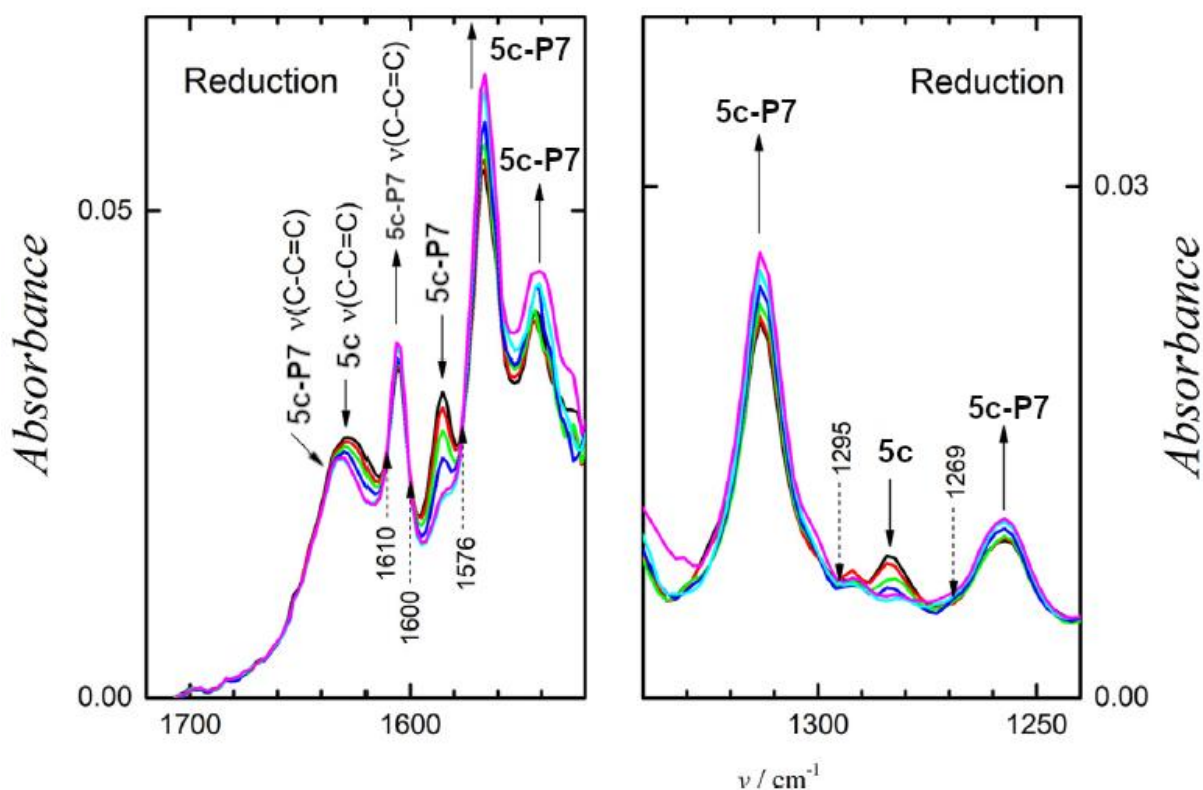


**Figure 28.** IR spectroelectrochemistry of 2.9 mM compound **5c** recorded while sweeping the electrode potential through the first reduction wave in 0.1 M TBAPF<sub>6</sub> in acetonitrile. Wavenumbers of obtained isosbestic points are marked with dashed arrows.

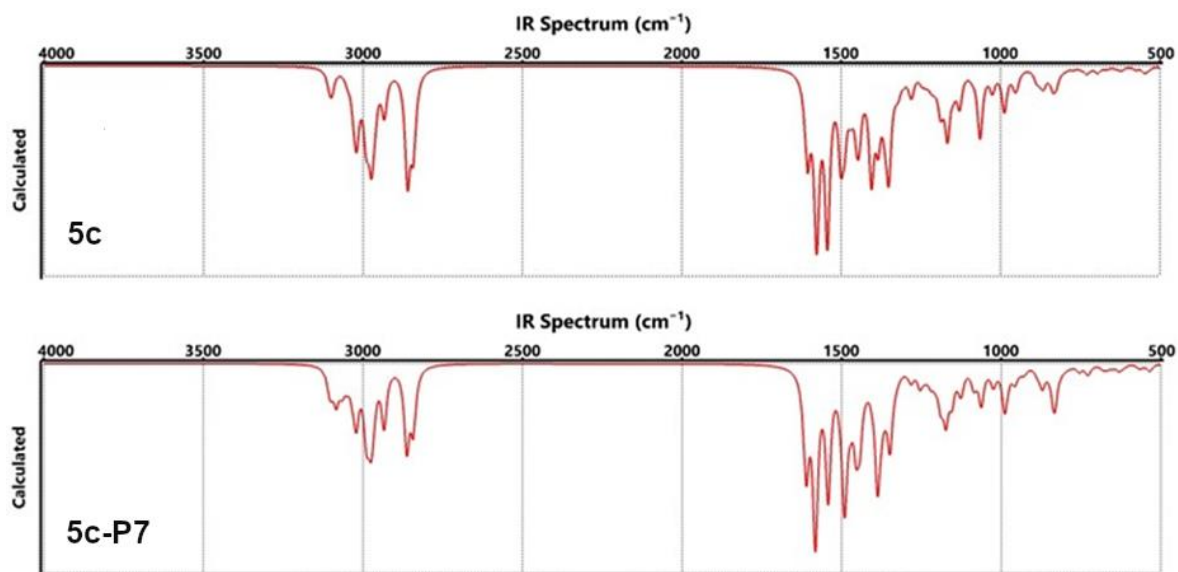
DFT calculations were performed for compound **5c** and reduction product (calculated IR spectra and corresponding wavenumbers are reported in Table 3 and Figure 29 and), which show that the vibrational bands of **5c** and **5c-P7** occur in a similar range of the spectrum (Table 3, Figure 29). This is consistent with the experimental data depicted in Figure 28, showing that the reaction mostly produces a change in the relative intensities of bands. Significantly, the absorption band of **5c** shifts from 1623 cm<sup>-1</sup> to higher wavenumbers due to the development of a new absorption band attributed to the vibrations of aromatics between carbons C5=C6-C7=C8 in the new product **5c-P7**. The calculated values for the same region for **5c-P7** are 1612 cm<sup>-1</sup> and 1608 cm<sup>-1</sup> (C=N-C=C), respectively, while the calculated value for **5c** is 1606 cm<sup>-1</sup>, as mentioned above.

**Table 3.** Calculated and experimental values of wavenumbers of compounds **5c** and **5c-P7** in  $\text{cm}^{-1}$ .

4,7-di(pyrrolidine-1-yl)-2,9-dimethyl-1,10-phenanthroline ( <b>5c</b> )										
<b>Calc.</b>	1606	1592	1577	1543	1501	1351	1320	1279	1247	1233
<b>Experim.</b>	1623	1606	1585	1567	1543	1354	1313	1284	1258	1230

2,9-dimethyl-4-(pyrrolidin-1-yl)-1,10-phenanthroline ( <b>5c-P7</b> )										
<b>Calc.</b>	1612	1608	1582	1542	1497	1349	1320	1255	1238	
<b>Experim.</b>	1632	1623	1606	1567	1543	1354	1313	1258	1230	



**Figure 29.** IR spectra of 4,7-di(pyrrolidine-1-yl)-2,9-dimethyl-1,10-phenanthroline (**5c**) and 2,9-dimethyl-4-(pyrrolidin-1-yl)-1,10-phenanthroline (**5c-P7**) calculated using the DFT employing the EDF2 functional and 6-31G\* basis set.

### 6.2.5 Electrochemical and spectroelectrochemical studies of 4,7-di(9H-carbazol-9-yl)-1,10-phenanthroline

The reduction and oxidation mechanisms of 4,7-di(9H-carbazol-9-yl)-1,10-phenanthroline were investigated in a non-aqueous environment using cyclic voltammetry (CV), controlled potential electrolysis, in-situ UV-Vis and IR spectroelectrochemistry, and HPLC-DAD and HPLC-MS/MS techniques.

The research results in this chapter have been published in our paper<sup>215</sup>.

### 6.2.5.1 Oxidation

The cyclic voltammetry of compound **5f** shows two overlapping irreversible oxidation waves at 1.78 (Ox1) and 1.88 V (Ox2) (Figure 30, Table 4).

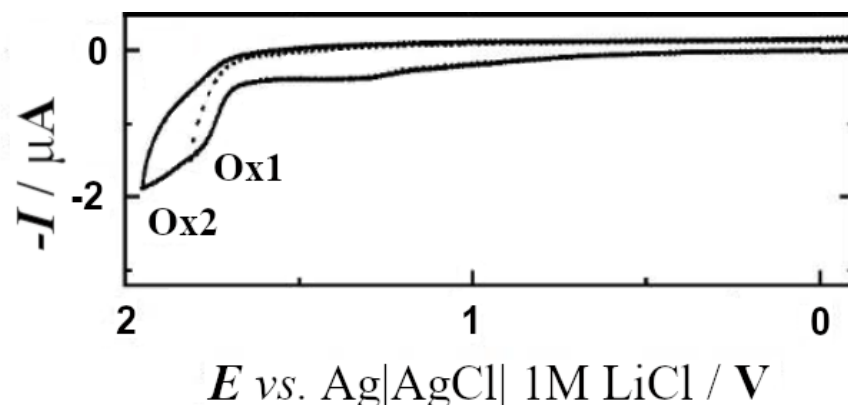


**Figure 30.** Cyclic voltammograms of 0.30 mM **5f** in 0.1 M TBAPF<sub>6</sub>/acetonitrile on glassy carbon electrode. The scan rate was  $0.1 \text{ V}\cdot\text{s}^{-1}$ .

**Table 4.** Peak potential values of compounds **5f** for oxidation ( $E_p^{\text{Ox1-3}}$ ) recorded in acetonitrile and 0.1 M TBAPF<sub>6</sub> against Ag|AgCl|1M LiCl and energies of frontier orbitals (HOMO, HOMO(-1)) calculated by DFT referenced against vacuum.

	$E_{\text{HOMO}}$ /eV	$E_{\text{HOMO}(-1)}$ /eV	$E_p^{\text{Ox1}}$ / V	$E_p^{\text{Ox2}}$ / V
<b>5f</b>	-5.6	-5.6	1.78	1.88

The linear relationship between the Faradaic peak current and the square root of scan rate (Figure 31) proves the diffusion-controlled character of the redox process. On the contrary to compounds **5j**, **5k**, **5l** (Figure 31, Figure 36 chapter 5.2.6.1), the peak potential scales linearly with the scan rate and concentration, being the slope  $\delta E_p / \delta \log v = 17 \text{ mV}$  and  $\delta E_p / \delta \log c = 18 \text{ mV}$ .

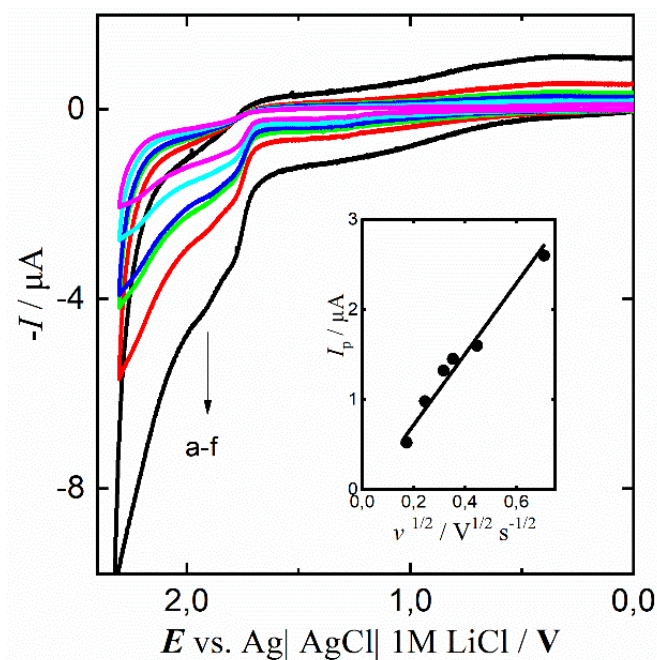


**Figure 31.** Cyclic voltammograms of 0.3 mM **5f** at different scan rates a) 0.03, b) 0.06, c) 0.1, d) 0.125, e) 0.2 and f) 0.5  $\text{V}\cdot\text{s}^{-1}$ . The insets show the dependence of the faradaic peak current of the first oxidation wave on the square root of the scan rate. The supporting electrolyte was 0.1 M TBAPF<sub>6</sub> in acetonitrile.

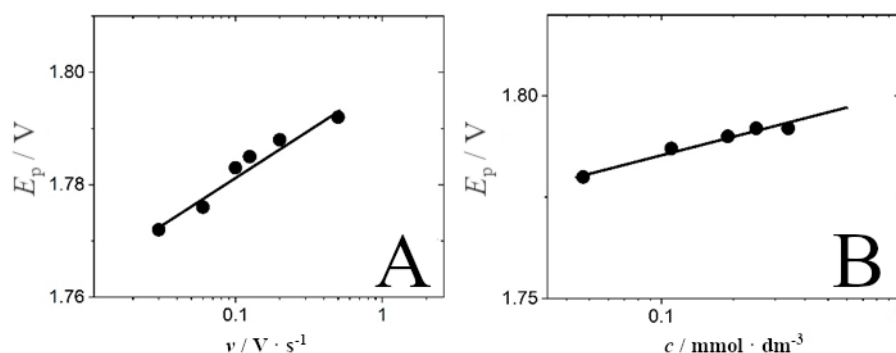
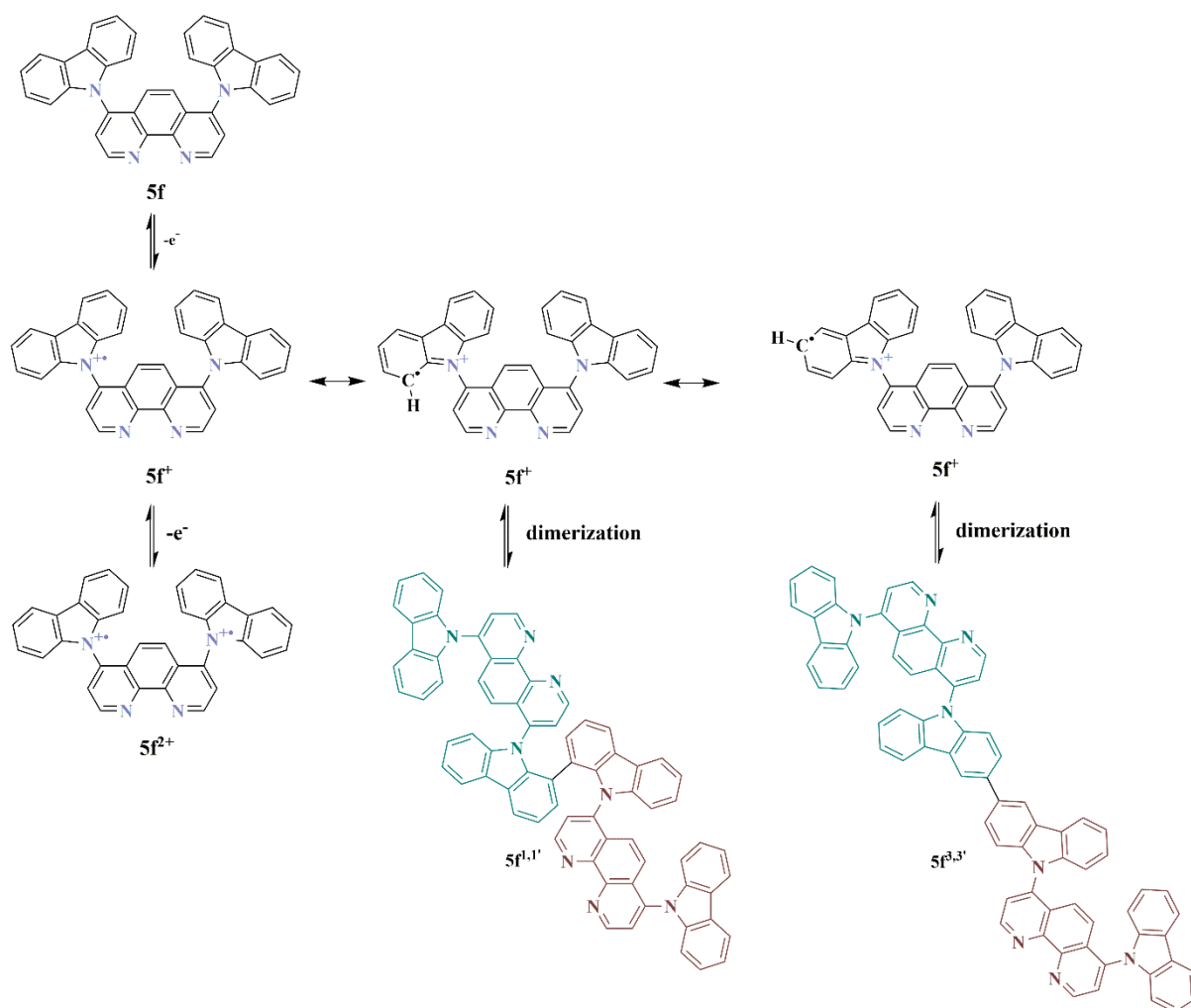


**Figure 32.** Dependence of peak potential of molecule **5f** on A) scan rate and B) concentration.

This result approaches theoretical values 19 mV/decade for the EC<sup>2</sup> reaction scheme<sup>209</sup>, implying that after the removal of the first electron, the formed radical cation undergoes a chemical reaction, most probably dimerization (Scheme 61). The formation of a dimer in the case of organic amines and carbazole derivatives was described in the literature<sup>216,217,218</sup> and the spectroelectrochemical investigation performed in this work supports this hypothesis (Scheme 61).



**Scheme 61.** Proposed oxidation mechanism of compound **5f** at the oxidation wave Ox1.

The measured absorption spectrum of **5f** (Figure 33A, black curve) shows characteristic bands at 231, 275, and 331 nm, oxidation results in the increase of absorption bands at 210, 231, 277, and 388 nm (Figure 33A, red curve, Table 5). The spectral changes are attributed to the formation of a radical cation ( $5f^+$ ) and biradical dication ( $5f^{2+}$ ) (one or two carbazole substituents oxidized) as intermediates and of the final dimeric products ( $5f^{1,1'}$ ,  $5f^{3,3'}$ ; Scheme 61). When applying potential values higher than 1.8 V (i. e., beyond the peak Ox1, Figure 30), the spectral response changes, the band at 338 nm shifts bathochromically to 410 nm, and a new band at 720 nm appear (dotted and dashed curves in Figure 33A). During the rereduction (performed at -0.2 V, Figure 33B) the bands at 410 and 720 nm disappear, and the final spectrum is similar to the original spectrum of **5f**; however, the intensities of the original bands are different.

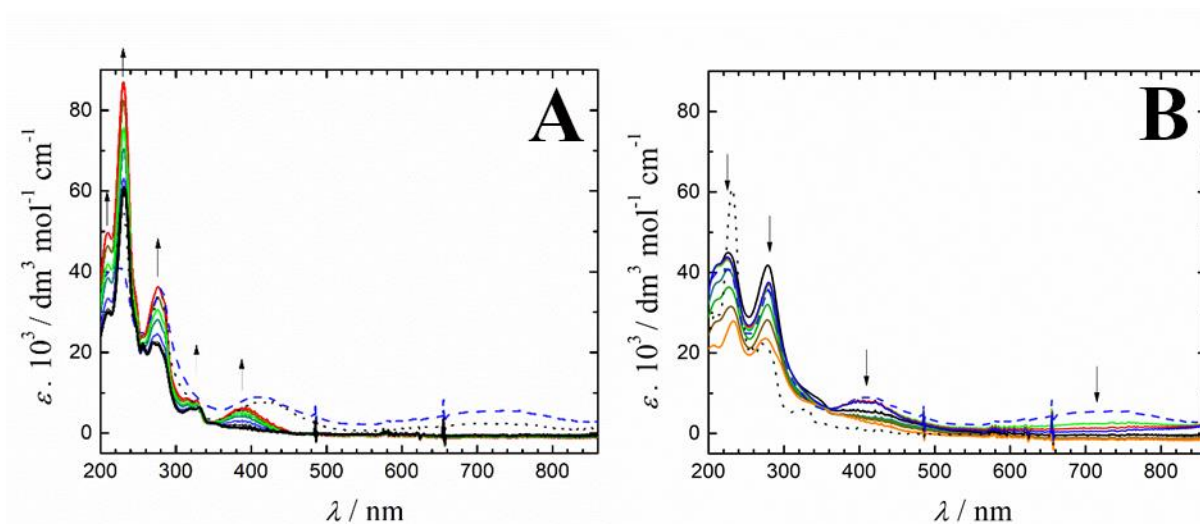


**Figure 33.** UV–Vis spectroelectrochemistry of compound **5f** at the first oxidation wave (Panel A) and the rereduction of the formed oxidation product (Panel B).

**Table 5.** Values of absorption maxima and molar extinction coefficients obtained for molecule **5f** and oxidation products.

	$\lambda_{\max} / \text{nm} (\epsilon / 10^3 \text{ M}^{-1} \text{cm}^{-1})$					
<b>5f</b>	210 (30.4)	231 (60.4)	270 (22.2)	275 (22.0)	319 (6.1)	331 (6.3)
<b>5f<sup>2+</sup></b>						
<b>5f<sup>1,1'</sup></b>	210(49.7)*	231(66.9)*	277(36.0)*	313 (8.7)*	328 (7.8)*	388 (6.1)*
<b>5f<sup>3,3'</sup></b>						

\* Spectrum belongs to a mixture of products **5f<sup>2+</sup>**, **5f<sup>1,1'</sup>**, **5f<sup>3,3'</sup>** (Scheme 61)

HPLC-MS/MS results did not show any dimer in solution after oxidative electrolysis. This can be due to the instability of dimers in the highly oxidized state. This is consistent with the cyclic voltammogram, which does not show the typical response for dimers in multiple scans (Figure 34).

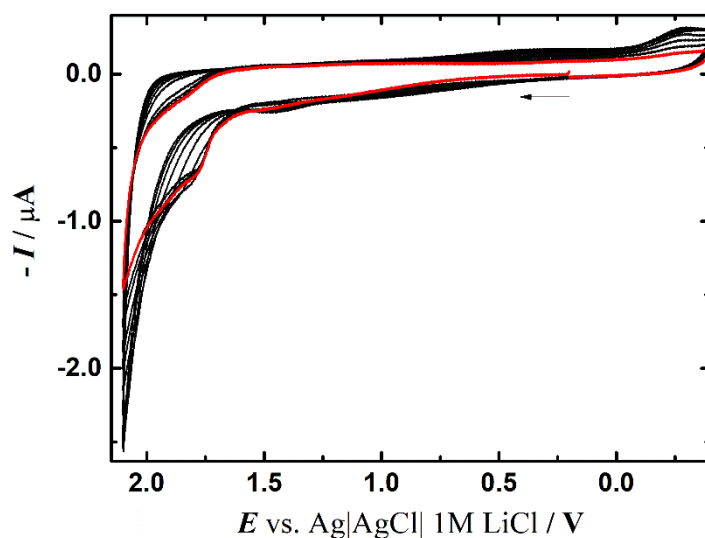


**Figure 34.** Cyclic voltammetry of 12 scans of 0.07 mM **5f** and 0.1 M TBAPF<sub>6</sub> in acetonitrile. The scan rate was 0.1 V·s<sup>-1</sup>. The red curve indicates the first scan.

### 6.2.5.2 Reduction

The reduction properties of the compounds with fused aromatic rings are substantially determined by low lying  $\pi$ -orbital system of the rings. This system can be strongly influenced when coordination with metals is established. The cyclic voltammogram obtained for the reduction of compound **5f** (Figure 35) shows five cathodic waves corresponding to the reduction of 1,10-phenanthroline moiety in the molecules.

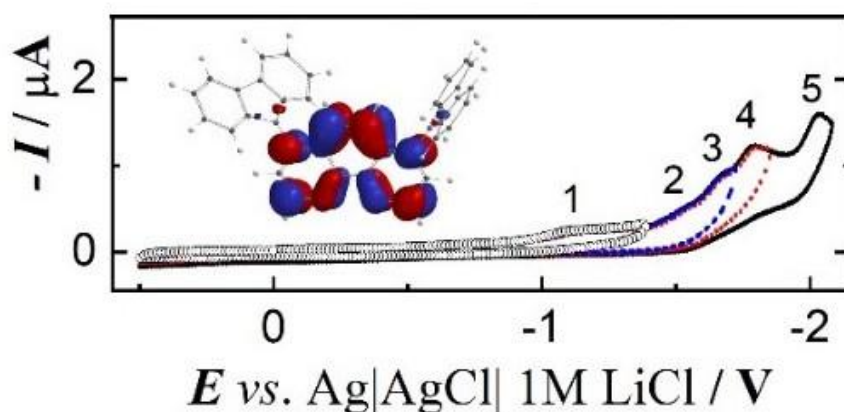


**Figure 35.** Cyclic voltammogram 0.30 mM **5f** in acetonitrile / 0.1 M TBAPF<sub>6</sub> on glassy carbon electrode. The scan rate was 0.1 V·s<sup>-1</sup>.

The reduction of 1,10-phenanthroline in the solution of 0.1 M TBAPF<sub>6</sub> in acetonitrile is shown in chapter 4.11.1. The spatial distribution of LUMO for compound **5f** is shown in Figure 36. The values of LUMO energies referenced against vacuum correlate to the obtained cathodic peak potentials and are summarized in Table 6.

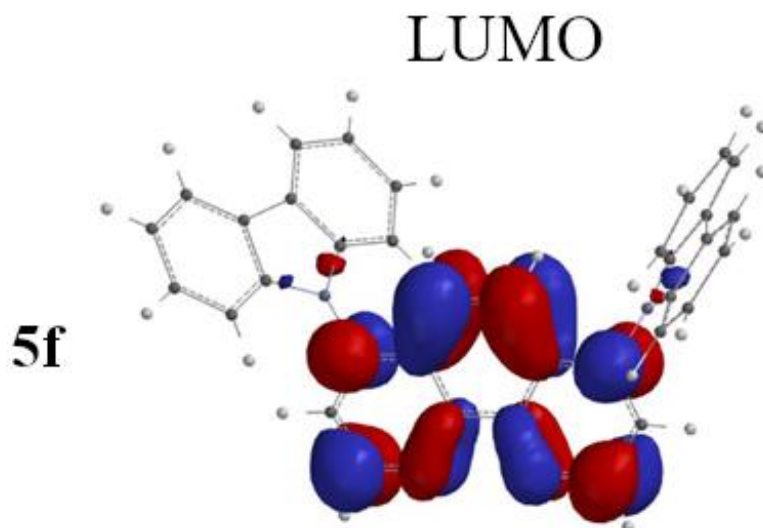


**Figure 36.** Spatial distribution of molecular orbitals LUMO calculated for molecules **5f** using the density functional theory (DFT) employing the B3LYP functional and 6-31G\* basis set with optimized geometry in a vacuum.

**Table 6.** Peak potential values of compound **5f** for reduction ( $E_p^{\text{Red1-5}}$ ) recorded in acetonitrile and 0.1 M TBAPF<sub>6</sub> against Ag|AgCl|1M LiCl and energies of frontier orbital (LUMO) calculated by DFT referenced against vacuum.

	$E_{\text{LUMO}}$	$E_p^{\text{Red1}}$	$E_p^{\text{Red2}}$	$E_p^{\text{Red3}}$	$E_p^{\text{Red4}}$	$E_p^{\text{Red5}}$
	/eV	/V	/V	/V	/V	/V
<b>5f</b>	-1.80	-1.10	-1.54	-1.67	-1.78	-2.03

All five reduction waves are irreversible. The first of them was investigated in larger detail. It is diffusion controlled as confirmed by the linear dependence of the Faradaic peak current on the square root of the scan rate (Figure 37). The dependences of the peak potential on the scan rate and compound concentration suggest an ECE mechanism (results  $\delta E_p / \delta \log \nu = 30$  mV and  $\delta E_p / \delta \log c = 26$  mV for **5f**, Figure 37).



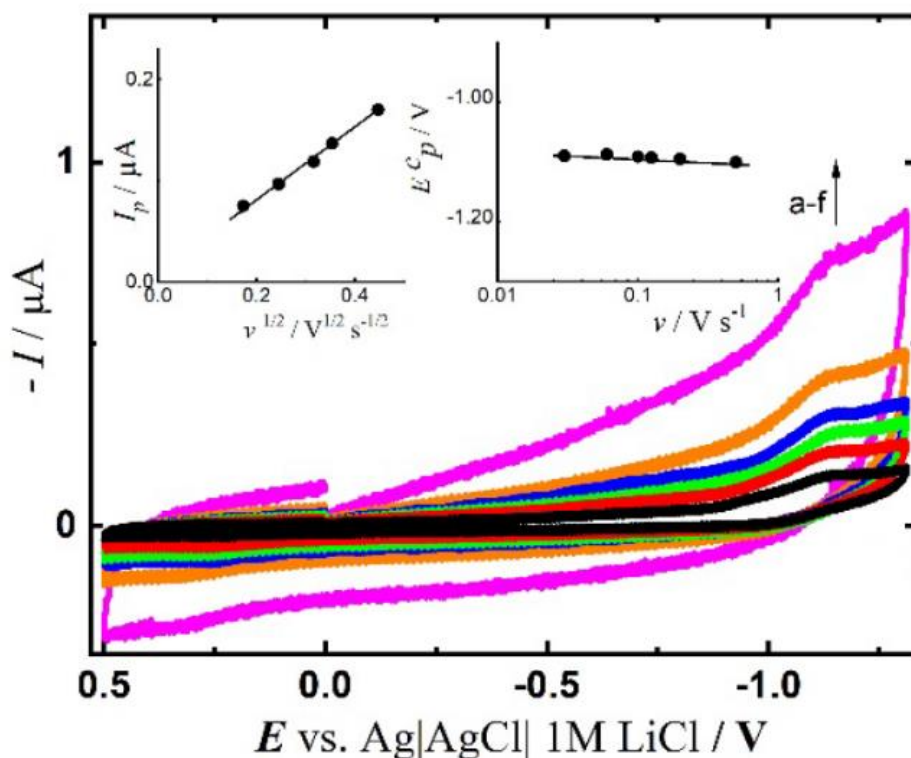


**Figure 37.** Cyclic voltammograms of 0.3 mM **5f** at different scan rates a) 0.03, b) 0.06, c) 0.1, d) 0.125, e) 0.2 and f) 0.5 V·s<sup>-1</sup>. The insets show the dependence of the faradaic peak current of the first reduction wave on the square root of scan rate and the dependence of peak potential on scan rate. Supporting electrolyte was 0.1 M TBAPF<sub>6</sub> in acetonitrile

Solutions of compounds **5f** taken before and after the exhaustive reductive electrolysis were inspected by HPLC-MS/MS. The identified products were the corresponding 4-(9*H*-carbazol-9-yl)-1,10-phenanthroline (**5f-P1**), which lost one carbazole substituent from the molecule, and 1,10-phenanthroline (**Phen**) formed after the cleavage of both substituents. The characteristic species with retention times, corresponding molecular ions, along the product ions in tandem mass spectra are reported in Table 7.

**Table 7.** Retention time, raw formula, calculated and experimental  $m/z$  for the  $[M+H]^+$  ion and main fragment ions detected in the tandem mass spectra for the solution reduction of compound **5f**.

Compound name	Retention time (min)	Raw formula	Calculated $m/z$ for $[M+H]^+$	Experimental $m/z$ for $[M+H]^+$	$\Delta$ ppm	Fragment ions ( $m/z$ )
<b>5f</b>	22.8	C <sub>36</sub> H <sub>22</sub> N <sub>4</sub>	511.1923	511.1911	-2.3	465.2232 319.1908 331.1101
<b>5f-P1</b>	16.7	C <sub>24</sub> H <sub>15</sub> N <sub>3</sub>	346.1344	346.1357	3.8	180.0686 166.0647 153.0574
<b>Phen</b>	1.3	C <sub>12</sub> H <sub>8</sub> N <sub>2</sub>	181.0766	181.0768	1.1	154.0655 127.0546

### 6.2.6 Electrochemical and spectroelectrochemical studies of selected 4,7-di(10*H*-phenothiazine-10-yl)-1,10-phenanthroline

The reduction and oxidation mechanisms of selected 4,7-di(10*H*-phenothiazine-10-yl)-1,10-phenanthroline were investigated in non-aqueous environment using cyclic voltammetry (CV), controlled potential electrolysis, in-situ UV-Vis and IR spectroelectrochemistry, and HPLC-DAD and HPLC-MS/MS techniques.

The research results in this chapter have been published in our paper<sup>215</sup>.

#### 6.2.6.1 Oxidation

The electrochemical oxidation of compounds **5j**, **5k**, and **5l** was investigated in acetonitrile by cyclic voltammetry combined with DFT calculations. The symmetric molecule **5j** exhibits four oxidation peaks, labeled Ox1, Ox2, Ox2' and Ox3 (Figure 38A) with peak potentials 1.12, 1.70, 1.78, and 1.89 V, respectively.

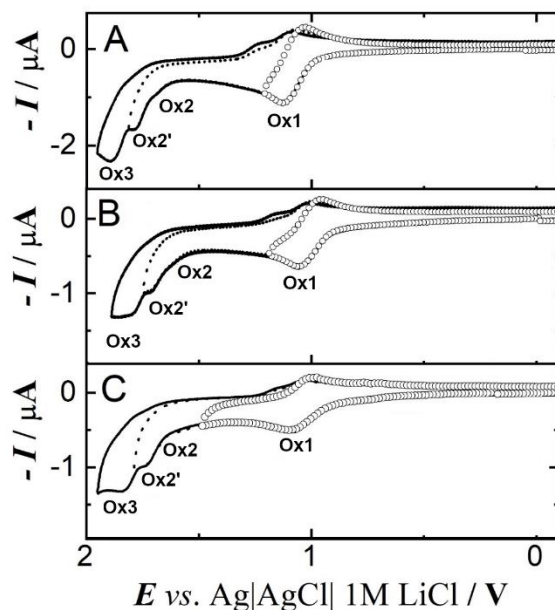


**Figure 38.** Cyclic voltammograms of A) 0.20 mM **5j**, B) 0.15 mM **5k** and C) 0.13 mM **5l** in 0.1 M TBAPF<sub>6</sub>/acetonitrile on glassy carbon electrode. The scan rate was 0.1 V·s<sup>-1</sup>.

Linear dependence of the Faradaic peak currents on the square root of scan rate (Figure 39) proves the diffusion-controlled character of redox processes.

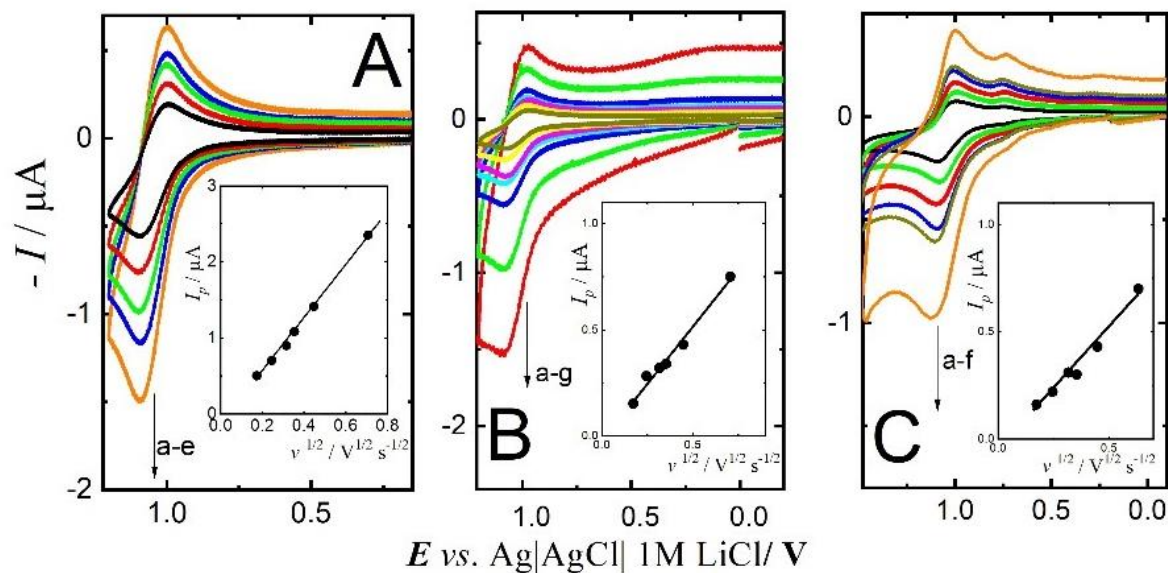


**Figure 39.** Cyclic voltammograms of A) 0.11 mM **5j**, B) 0.07 mM **5k** and C) 0.07 mM **5l** at different scan rates a) 0.03, b) 0.06, c) 0.1, d) 0.125, e) 0.2 and f) 0.5 V·s<sup>-1</sup> for Panels A, C and a) 0.03, b) 0.06, c) 0.1, d) 0.125, e) 0.2, f) 0.4 and g) 0.5 V·s<sup>-1</sup> for Panel B. The insets show the dependence of faradaic peak current of the first oxidation wave on the square root of scan rate. Supporting electrolyte was 0.1 M TBAPF<sub>6</sub> in acetonitrile.

Controlled potential coulometry performed at the potential slightly positive to the first oxidation peak (1.2 V vs. Ag|AgCl|1 M LiCl reference electrode) confirmed the consumption of two electrons per molecule in this process. The peak potential of the first oxidation process (1.12 V) does not change with neither increasing scan rate nor concentration of compound **5j** (Figure 40), as expected for a reversible transfer of electron(s). On the contrary, the experimentally observed peak-to-peak separation  $|E_p^a - E_p^c| = 88$  mV (Figure 38A, empty circles) deviates from the value expected for a reversible two-electron step (29.5 mV), implying that the observed pair of maxima is due to overlapped two one-electron processes at close standard redox potentials.

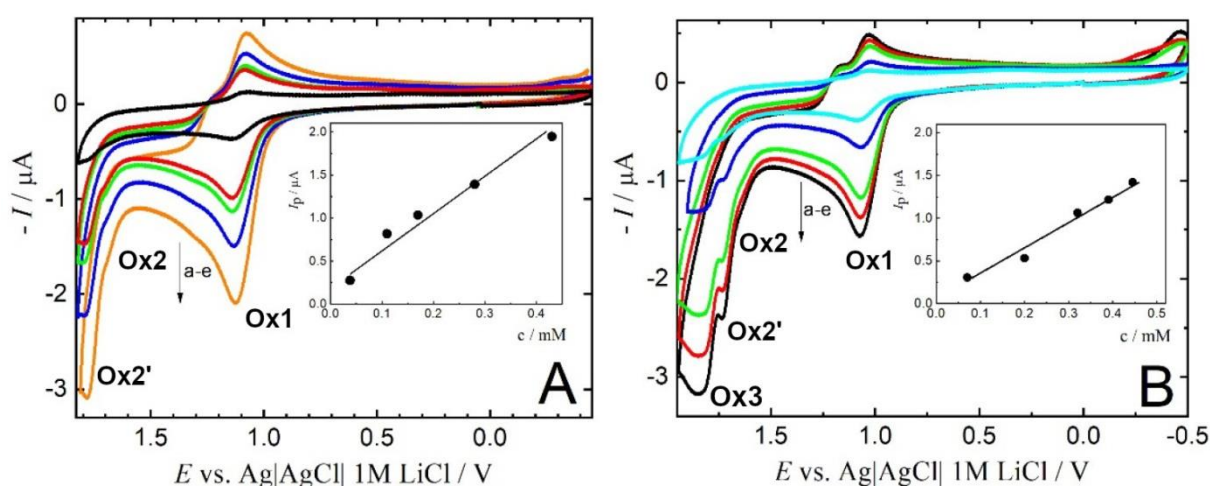
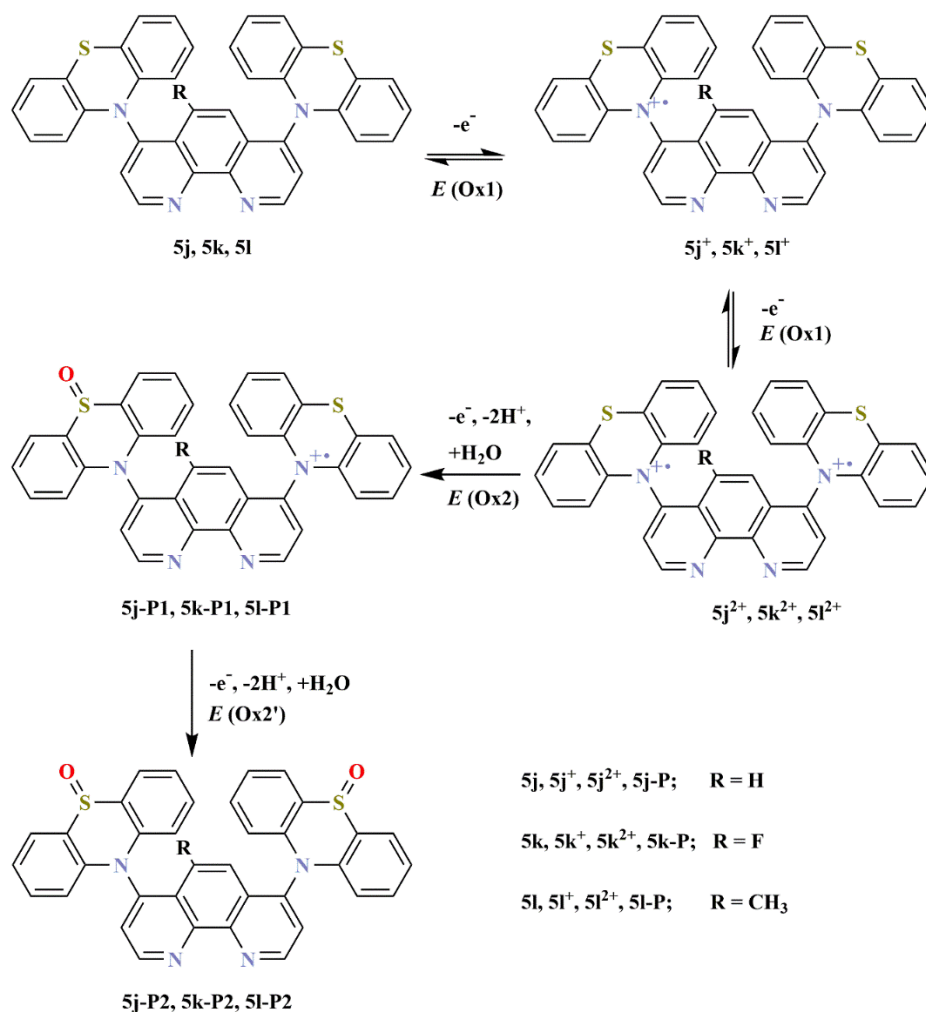


**Fig. 40.** Cyclic voltammograms of A) **5j** at different concentrations a) 0.038, b) 0.11, c) 0.17, d) 0.28, e) 0.43 mM and B) **5k** at different concentrations a) 0.07, b) 0.2, c) 0.32, d) 0.39 and e) 0.43 mM. The scan rate was 0.1 V/s.

Furthermore, the peak current corresponds rather to a twofold value in comparison to a one-electron process (ferrocene used for this comparison) and not to  $2^{3/2}$  (~2.8) times higher value expected for the simultaneous transfer of two electrons (Randles-Sevcik equation)<sup>204</sup>. Furthermore, convolution voltammetry (semi-integration of linear sweep voltammograms) was used to obtain data in the format suitable for further analysis according to literature<sup>219,220</sup> (also Experimental part, chapter 7.1). The semi-integration of anodic current and subsequent logarithmic analysis results in the  $RT/nF$  slope of 105 mV (where symbols bear their standard meaning), which according to the established procedure (explained in detail in reference<sup>204</sup>) corresponds to two one-electron processes with their standard redox potential values spaced by 62 mV. In the case of independent, electronically non-communicating centers the electron transfer from the first and second center proceeds at approximately equal potential ( $\Delta E^\circ =$

( $RT/nF \ln 4$ , i.e., 35.6 mV at 298 °C<sup>221,222,223</sup>) resulting in one-electron-like (by shape) wave in the voltammetry. When the centers electronically communicate, the voltammetric waves can be more separated. The results lead us to conclude that the  $1+1e^-$  oxidation processes occur on two almost independent phenothiazine redox centers attached to the 1,10-phenanthroline moiety in equivalent (4 and 7) positions (Scheme 62).



**Scheme 62.** Oxidation mechanism of compounds **5j**, **5k**, **5l**.

This finding is further corroborated by theoretical (DFT) calculations. They clearly demonstrate that the degenerated HOMO and HOMO(-1) are localized on phenothiazine substituents (Figure 41) and have energies  $E_{HOMO}(5j) = E_{HOMO(-1)}(5j) = -5.2$  eV, respectively. Further oxidation of phenothiazine substituents to their sulfoxide proceeds at 1.70 V (wave Ox2) and 1.78 V (wave Ox2') (Scheme 62). The oxidation wave Ox3 at 1.89 V is attributed to the oxidation of 1,10-phenanthroline moiety (the oxidation of unsubstituted 1,10-

phenanthroline has the peak potential at 1.90 V) (chapter 5.11.1 also Figure 6F chapter 6.2.2.1).

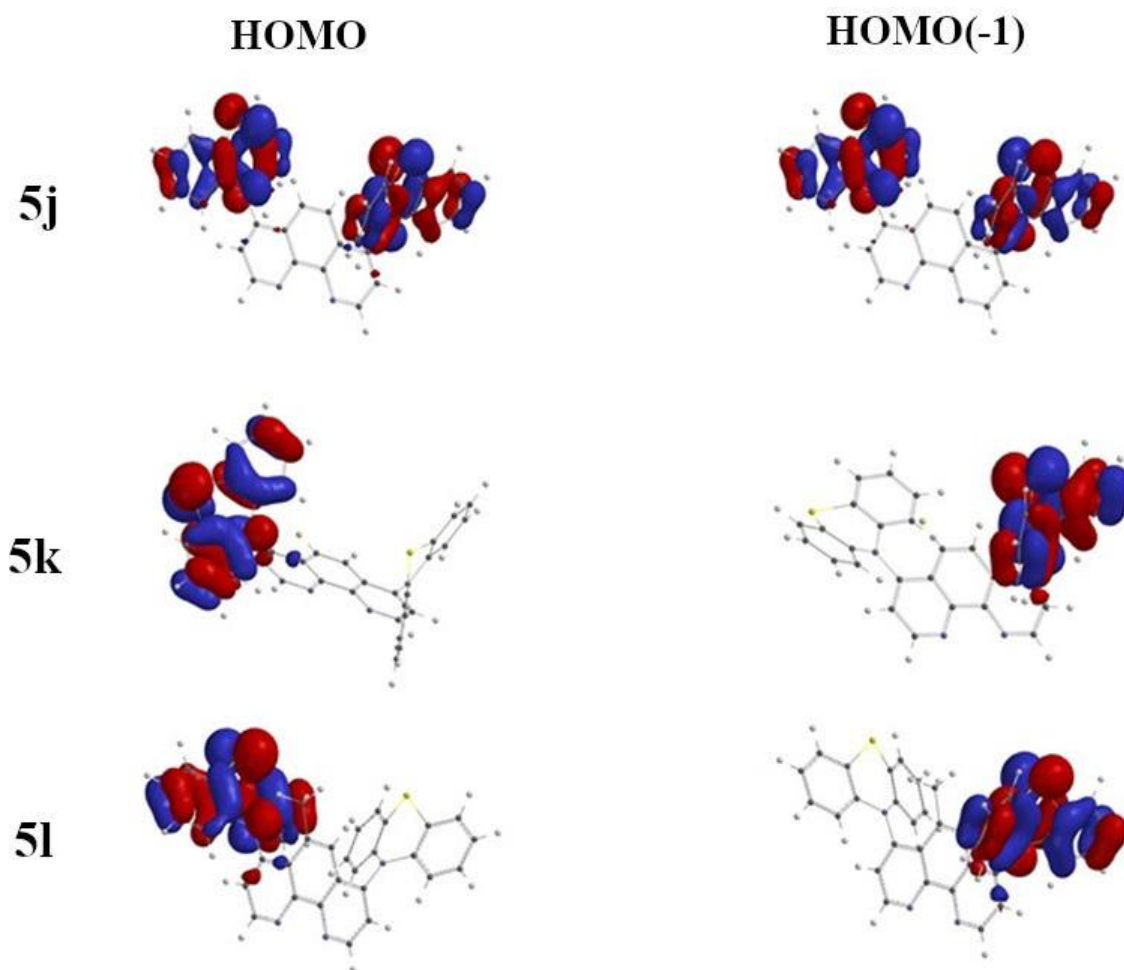


**Figure 41.** Spatial distribution of molecular orbitals HOMO, HOMO(-1) calculated for molecules **5j**, **5k**, **5l** using the density functional theory (DFT) employing the B3LYP functional and 6-31G\* basis set with optimized geometry in a vacuum.

The first oxidation process of **5k** and **5l** occurs at 1.05 and 1.09 V, respectively (Figure 38B,C). Both values are slightly negatively shifted compared to the oxidation potential of **5j**. Such shifts, being in the same direction for both **5k** and **5l**, cannot be ascribed to an electron-withdrawing or electron-donating effect of fluorine and methyl substituents on the 1,10-phenanthroline core, respectively. This confirms that the electronic communication between the 1,10-phenanthroline moiety and phenothiazine redox centers is very limited. Similarly, as observed for **5j**, the analysis of the cyclic voltammograms revealed only a little higher anodic-to-cathodic peak-to-peak separations ( $|E_p^a - E_p^c| = 82$  mV and 87 mV for **5k** and **5l** respectively) than the theoretical prediction (the discussion above). Importantly, the

reversibility of the first charge transfer process is retained upon introducing fluorine and methyl substituents (empty circles in Figure 38B,C). The peak potentials do not vary with neither scan rate nor the compound concentration. Albeit the compounds **5k** and **5l** both lack symmetry and DFT show slightly energetically separated HOMO and HOMO(-1) orbitals (Table 8), the oxidation mechanism appears to be the same as for the compound **5j**. The potential of the oxidation peaks are summarized in Table 8. The oxidation of both phenothiazines is terminated in the irreversible waves Ox2 and Ox2' at 1.63 and 1.71 V for **5k** and 1.67 and 1.75 V for **5l** (Figure 38), ultimately leading to sulfoxide derivatives (**5k-P1**, **5l-P1**; Scheme 62). HPLC-MS/MS allowed the identification of the sulfoxide (two isomers) and the di(sulfoxide) (Table 10). Oxidation of 1,10-phenanthroline core occurs at the wave Ox3 (chapter 4.11.1, also Figure 6F chapter 5.2.2.1).

**Table 8.** Peak potential values of compounds **5j**, **5k**, **5l** for oxidation ( $E_p^{\text{Ox}1-3}$ ) recorded in acetonitrile and 0.1 M TBAPF<sub>6</sub> against Ag|AgCl|1M LiCl and energies of frontier orbitals (HOMO, HOMO(-1)) calculated by DFT referenced against vacuum.

	$E_{\text{HOMO}}$ /eV	$E_{\text{HOMO(-1)}}$ /eV	$E_p^{\text{Ox1}}$ / V	$E_p^{\text{Ox2}}$ / V	$E_p^{\text{Ox2'}}$ / V	$E_p^{\text{Ox3}}$ / V
<b>5j</b>	-5.2	-5.2	1.12	1.70	1.78	1.89
<b>5k</b>	-5.0	-5.3	1.05	1.63	1.71	1.81
<b>5l</b>	-5.1	-5.2	1.09	1.67	1.75	1.84

The absorption spectrum of **5j** exhibits bands at 203, 239, 253, 269, and 325 nm (Figure 42A, blue curve). During oxidation, new absorption bands at 210, 232, 265, 275, and 510 nm of **5j<sup>2+</sup>** (red curve) appear. The change of the absorption spectra during backward reduction of electrogenerated **5j<sup>2+</sup>** confirms that the redox process is chemically reversible (Figure 42B). The new band in the visible region (at 510 nm, resulting in greenish color) obviously originates from the formation of a singly occupied orbital (SOMO) on the oxidized phenothiazine units of **5j<sup>2+</sup>**. Consequently, when applying the potential corresponding to the second oxidation step, Ox2+Ox2', the band at 510 nm and the greenish color disappears (Figure 42C).

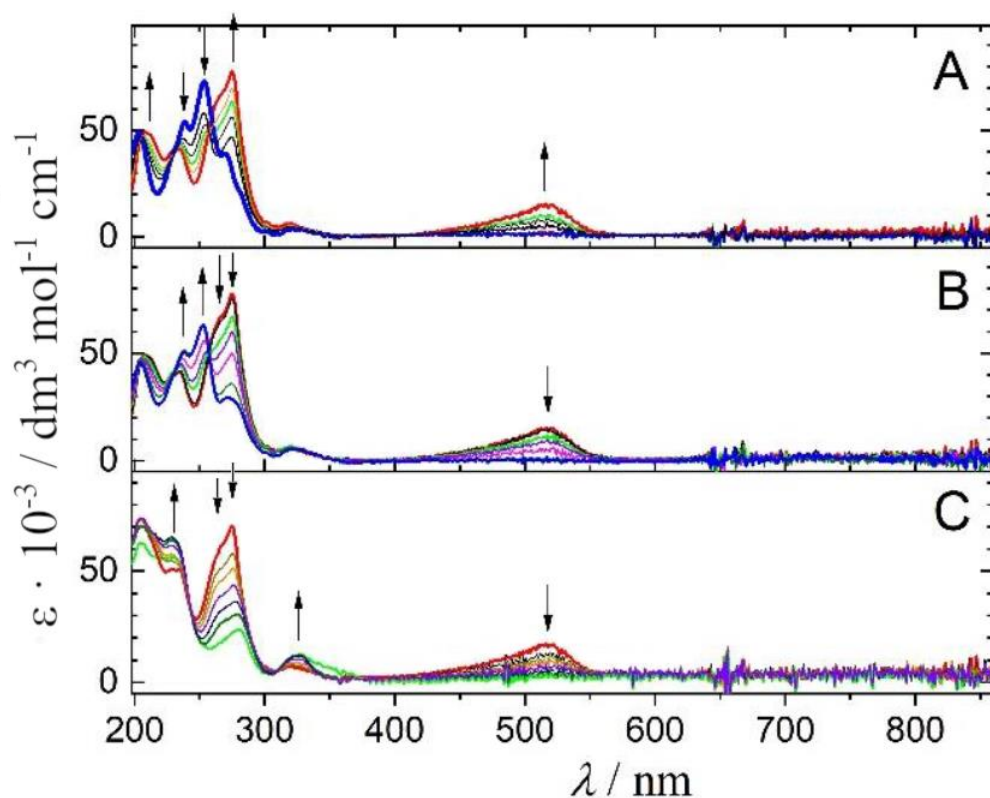


**Figure 42.** UV-Vis spectroelectrochemistry of **5j** during A) oxidation  $5j \rightarrow 5j^{2+}$  (first oxidation process Ox1, spectra registered at potentials 0.50, 0.80, 0.95, 1.00, 1.15 and 1.20 V), B) rereduction (backward reduction of generated intermediate  $5j^{2+} \rightarrow 5j$ ) and C) further oxidation  $5j^{2+} \rightarrow 5j\text{-P2}$  (second oxidation process at Ox2 + Ox2', spectra registered at potentials 1.20, 1.30, 1.40, 1.50, 1.60, 1.70 and 1.80 V).

The spectral changes during the oxidation of **5k** and **5l** in the UV, and visible region are similar as observed for **5j** (Table 9). In addition, low intense bands were detected at longer wavelengths (at 705, 790, and 886 nm) for both  $5k^{2+}$  and  $5l^{2+}$  (Figure 43). These bands (as well as the band peaking at 514 nm) are associated with the presence of SOMO on the half oxidized phenothiazine units and disappear in the second oxidation step. In comparison to compound **5j**, which does not exhibit spectroelectrochemical detectable bands above 600 nm (Figure 42), the increased intensity and, therefore detectable longwavelength bands with **5k** and **5l** are attributed to the lower symmetry of these (effect of fluoro or methyl substituents) compounds.



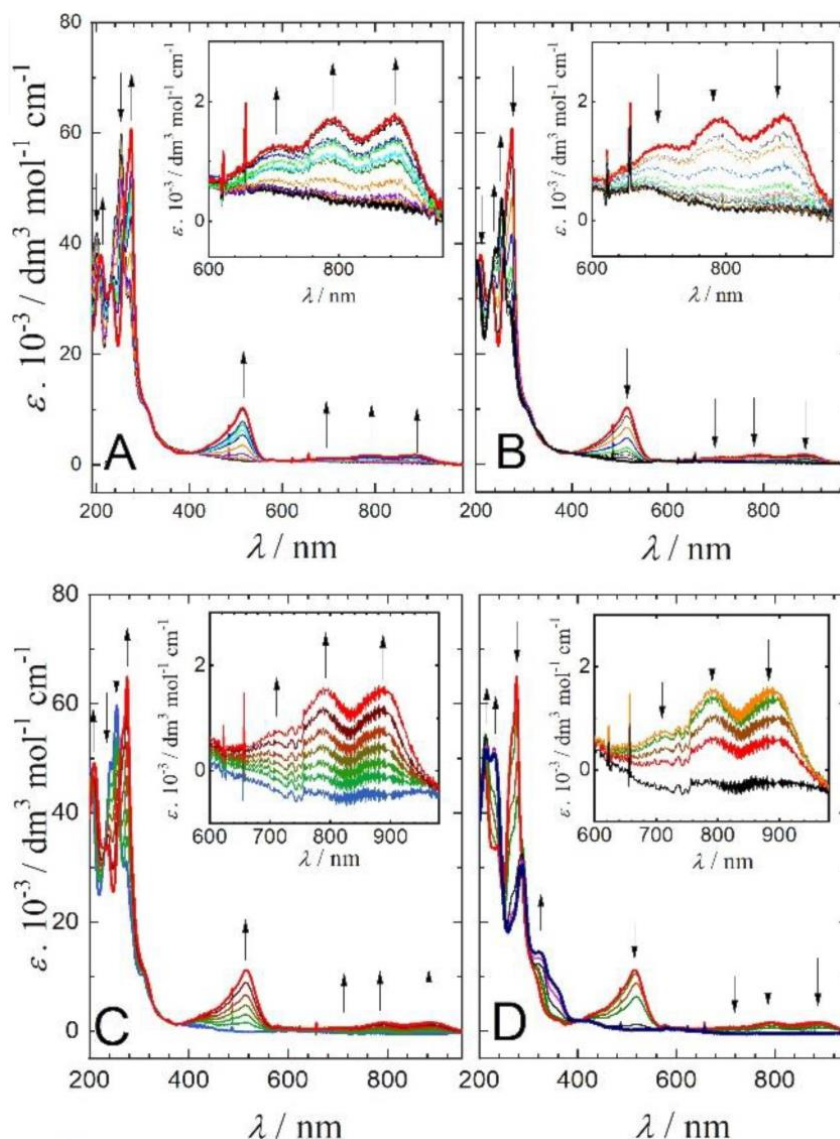


**Figure 43.** UV-Vis spectroelectrochemistry of **5k** during A) oxidation  $5k \rightarrow 5k^{2+}$  (first oxidation process Ox1, spectra registered at potentials 0.50, 0.65, 0.70, 0.75, 0.80, 0.85, 0.90, 0.95, 1.00 and 1.15 V) and B) rereduction (backward reduction of generated intermediate  $5k^{2+} \rightarrow 5k$ ). UV-Vis spectroelectrochemistry of **5l** during C) oxidation  $5l \rightarrow 5l^{2+}$  (first oxidation process Ox1, spectra registered at potentials 0.50, 0.80, 0.95, 1.00, 1.15, 1.20 and 1.25 V), D) oxidation  $5l^{2+} \rightarrow 5l\text{-P2}$  (second oxidation process at Ox2+Ox2', spectra registered at potentials 1.25, 1.40, 1.50, 1.60 and 1.75 V).

The absorption maxima and extinction coefficients of all studied compounds and their dications are summarized in Table 9. Transients of absorption spectra of the newly developed band at 514 nm at the first oxidation step of compounds **5j**, **5k**, **5l** and their subsequent reduction (Figure 44) confirms the reversibility of this electron transfer process.

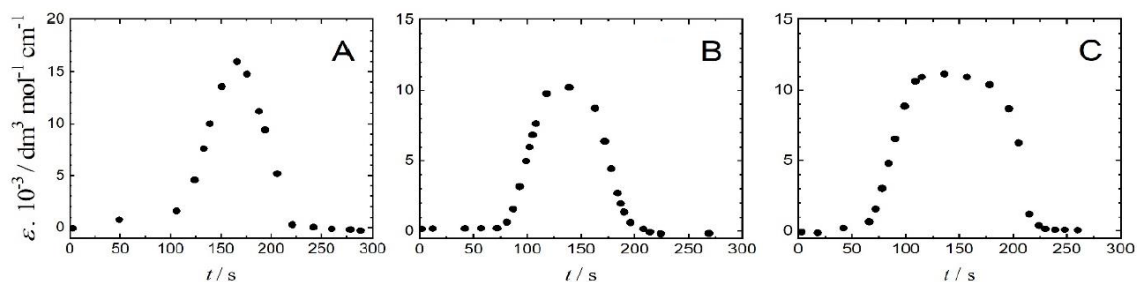


**Figure 44.** Transients of absorption spectra obtained during UV-Vis spectroelectrochemistry of compounds **5j** (A), **5k** (B), and **5l** (C) during oxidation in the first step and the subsequent rereduction.

**Table 9.** Values of absorption maxima and molar extinction coefficients obtained for **5j-5l** and their dication.

Compound	$\lambda_{\max} / \text{nm}$ ( $\epsilon / 10^3 \text{ M}^{-1} \text{ cm}^{-1}$ ) sh: shoulder	
	<b>5</b>	dication <b>5<sup>2+</sup></b>
<b>5j</b>	203 (49.1), 239 (54.1), 253 (73.1), 269 (38.9), 325 (3.7)	210 (49.1), 232 (41.2), 265sh (66.8), 275 (77.3), 321 (6.2), 541 (16.5)
<b>5k</b>	200 (41.8), 240 (44.6), 253 (59.6), 269 (31.0), 306 (9.9)	210 (37.8), 231 (32.1), 268sh (53.9), 274 (60.9), 306 (9.9), 488sh (6.4), 514 (10.2), 705 (1.2), 790 (1.7), 886 (1.7)
<b>5l</b>	202 (47.5), 241 (49.2), 254 (59.6), 274 (30.5), 366sh (10.4)	210 (49.3), 236 (33.8), 267sh (55.3), 275 (64.5), 428 (3.1), 514 (10.9), 705 (0.7), 790 (1.5), 886 (1.5)

The IR spectroelectrochemistry of **5j** and **5l** does not show significant changes in absorption spectra during the oxidation at the first oxidation wave, Ox1. The wide absorption band at  $1633 \text{ cm}^{-1}$  and other bands at  $1577$ ,  $1558$ ,  $1540$ , and  $1265 \text{ cm}^{-1}$  corresponding to vibrations of aromatic rings in molecule **5j** remained constant. Only a decrease of the absorption bands at  $1312$  and  $1241 \text{ cm}^{-1}$  is observed. In the second oxidation process in merged waves Ox2+Ox2', the appearance of the characteristic absorption band at  $1037 \text{ cm}^{-1}$  corresponding to the vibration of the S=O functional group is observed (Figure 45A). Simultaneously, the increase of other bands at  $1577$ ,  $1558$ ,  $1519$ ,  $1506$ ,  $1312$ ,  $1284$ , and  $1242 \text{ cm}^{-1}$  is observed.

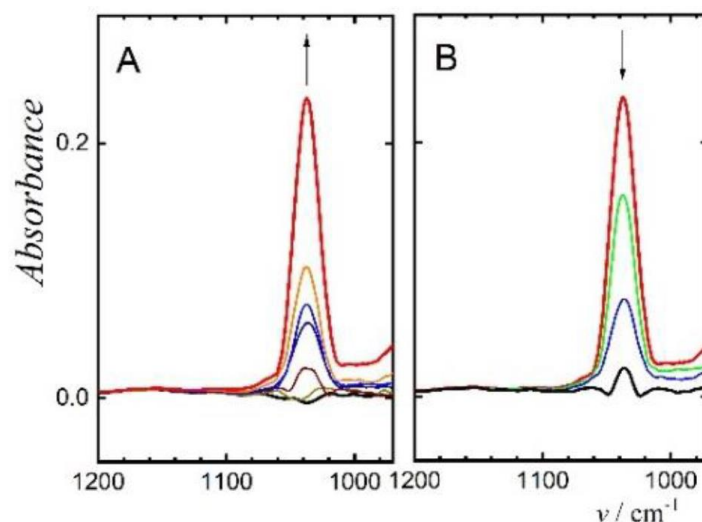


**Figure 45A.** IR spectroelectrochemistry of compound **5j** A) during oxidation at the waves Ox2+Ox2'; B) during backward reduction of **5j-P1** at 0 V.

Solutions of **5l** after electrolysis at potential 1.77 V (i.e., between the Ox2` wave and the Ox3 wave) were analyzed by HPLC-MS/MS. Both the hypothesized final products 5-methyl-4,7-bis(5-oxido-10*H*-phenothiazin-10-yl)-1,10-phenanthroline (**5l-P2**, Scheme 62) and an intermediate species 5-methyl-4-(5-oxido-10*H*-phenothiazin-10-yl)-7-(10*H*-phenothiazin-10-yl)-1,10-phenanthroline (**5l-P1**, Scheme 62) were identified in electrolyzed samples (Figure 46). The characteristic species with retention times, corresponding molecular ions, along the product ions in tandem mass spectra are reported in Table 10.

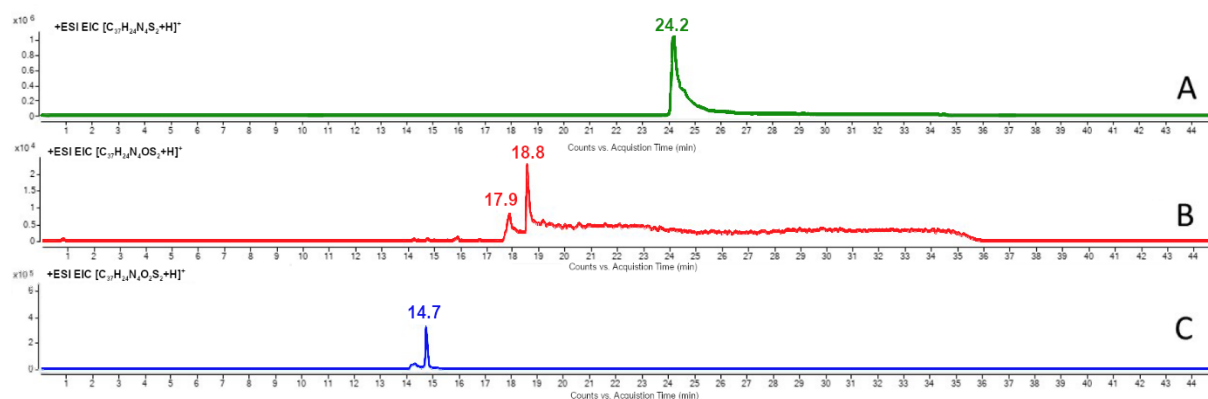


**Figure 46.** Extracted chromatograms detected in the sample after oxidation of compound **5l** related to A) compound **5l**, B) **5l-P1**, and C) **5l-P2**.

**Table 10.** Retention time, raw formula, calculated and experimental  $m/z$  for the  $[M+H]^+$  ion and main fragment ions detected in the tandem mass spectra for the solution before and after oxidation for compound **5l**.

Compound name	Retention time (min)	Raw formula	Calculated $m/z$ for $[M+H]^+$	Experimental $m/z$ for $[M+H]^+$	$\Delta$ ppm	Fragment ions ( $m/z$ )
<b>5l</b>	24.2	$C_{37}H_{24}N_4S_2$	589.1521	589.1524	0.5	390.1049
<b>5l-P1</b>	17.9 and 18.8	$C_{37}H_{24}N_4OS_2$	605.1470	605.1476	1.0	557.1772 198.0367
<b>5l-P2</b>	14.7	$C_{37}H_{24}N_4O_2S_2$	621.1419	621.1423	0.6	198.0363

### 6.2.6.2 Reduction

The reduction properties of the compounds with fused aromatic rings are substantially determined by low lying  $\pi$ -orbital system of the rings. This system can be strongly influenced when coordination with metals is established. In the case of the cyclic voltammograms obtained for the reduction of compounds **5j**, **5k**, **5l** CV show five cathodic waves corresponding to the reduction of 1,10-phenanthroline moiety in the molecules (Figure 47).

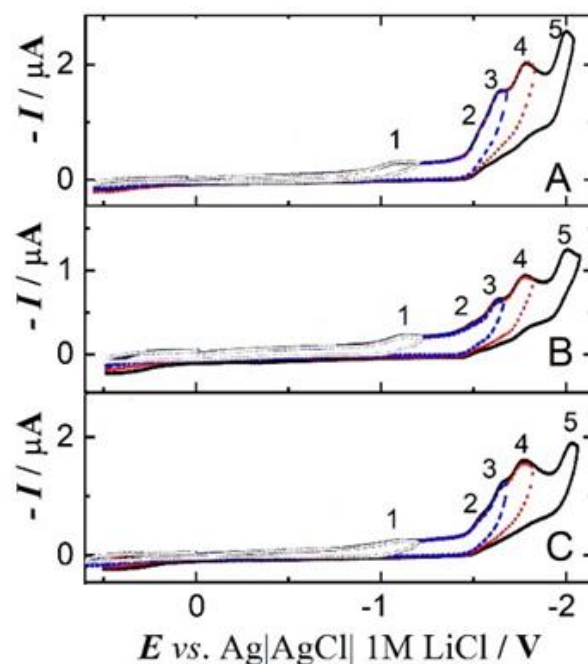


**Figure 47.** Cyclic voltammograms of A) 0.20 mM **5j**, B) 0.15 mM **5k** and C) 0.18 mM **5l** in acetonitrile / 0.1 M TBAPF<sub>6</sub> on glassy carbon electrode. The scan rate was 0.1 V·s<sup>-1</sup>.

Reduction of 1,10-phenanthroline in a solution of 0.1 M TBAPF<sub>6</sub> in acetonitrile is shown in chapter 5.11.1. The spatial distribution of LUMO of compounds **5j**, **5k**, and **5l** are shown in Figure 48. The values of LUMO energies referenced against vacuum correlate to the obtained cathodic peak potentials and are summarized in Table 11.

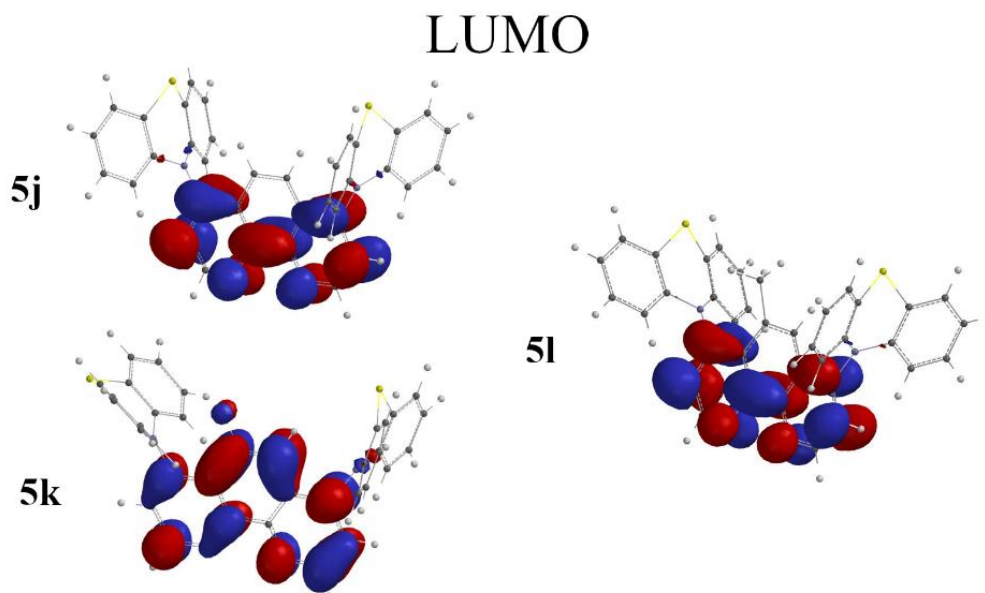


**Figure 48.** Spatial distribution of molecular orbitals LUMO calculated for molecules **5j**, **5l**, **5k** using the density functional theory (DFT) employing the B3LYP functional and 6-31G\* basis set with optimized geometry in a vacuum.

**Table 11.** Peak potential values of compounds **5j**, **5k**, **5l** for reduction ( $E_p^{\text{Red1-5}}$ ) recorded in acetonitrile and 0.1 M TBAPF<sub>6</sub> against Ag|AgCl|1M LiCl and energies of frontier orbital (LUMO) calculated by DFT referenced against vacuum.

	$E_{\text{LUMO}}$	$E_p^{\text{Red1}}$	$E_p^{\text{Red2}}$	$E_p^{\text{Red3}}$	$E_p^{\text{Red4}}$	$E_p^{\text{Red5}}$
	/eV	/V	/V	/V	/V	/V
<b>5j</b>	-1.76	-1.08	-1.54	-1.63	-1.78	-2.00
<b>5l</b>	-1.75	-1.07	-1.55	-1.66	-1.77	-2.03
<b>5k</b>	-1.95	-1.11	-1.51	-1.63	-1.77	-2.00

All five reduction waves are irreversible. The first of them was investigated in larger detail. It is diffusion controlled as confirmed by the linear dependence of the Faradaic peak current on the square root of the scan rate (Figure 49). The dependences of the peak potential on the scan rate and compound concentration suggest an ECE mechanism (results  $\delta E_p / \delta \log v$

= 24 and 32 mV and  $\delta E_p / \delta \log c = 33$  and 33 mV for **5j** and **5k**, and  $\delta E_p / \delta \log v = 29$  mV and  $\delta E_p / \delta \log c = 30$  mV for **5l**, respectively, Figure 49).

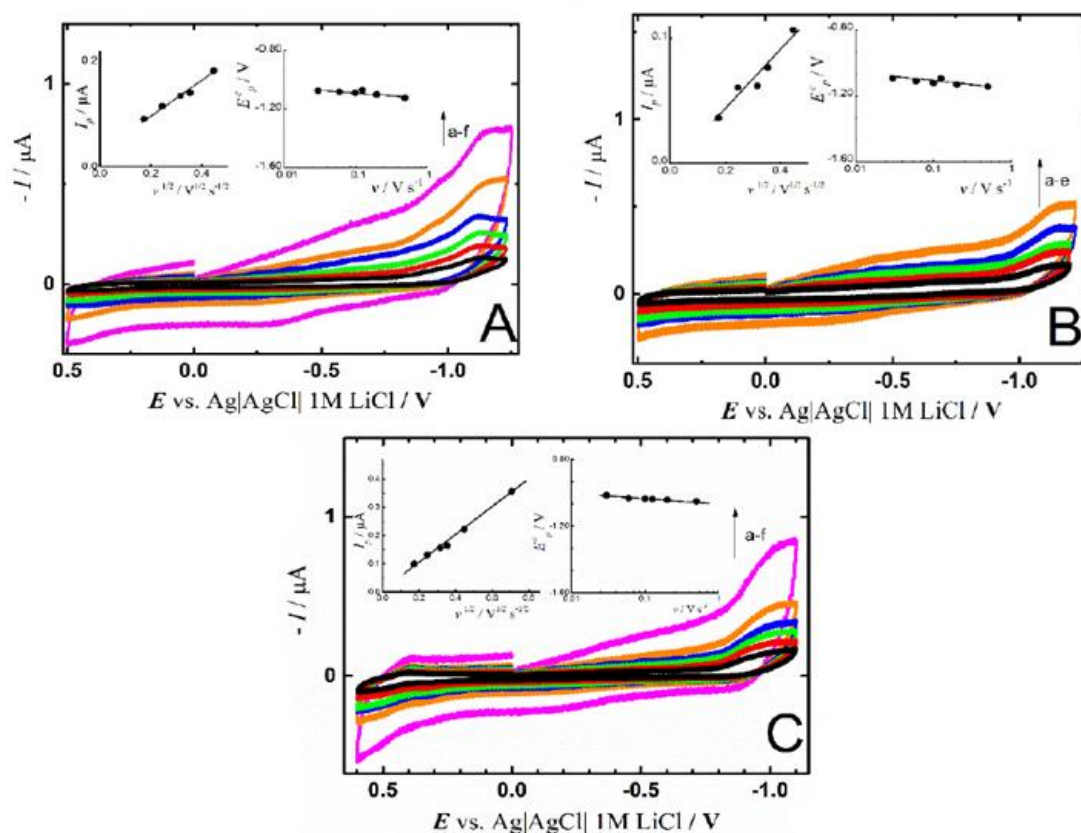


**Figure 49.** Cyclic voltammograms of A) 0.11 mM **5j**, B) 0.07 mM **5k** and C) 0.07 mM **5l** at different scan rates a) 0.03, b) 0.06, c) 0.1, d) 0.125, e) 0.2 and f) 0.5  $\text{V} \cdot \text{s}^{-1}$ . The insets show the dependence of faradaic peak current of the first reduction wave on the square root of scan rate and the dependence of peak potential on scan rate. The supporting electrolyte was 0.1 M TBAPF<sub>6</sub> in acetonitrile.

Solution of compound **5l** taken before and after the exhaustive reductive electrolysis were inspected by HPLC-MS/MS. The identified product was the corresponding species 5-methyl-4-(10*H*-phenothiazin-10-yl)-1,10-phenanthroline (**5l-P3**), which lost one phenothiazine substituent from the molecule, and 5-methyl-1,10-phenanthroline formed after the cleavage of both substituents (Figure 50). The characteristic species with retention times, corresponding molecular ions, along the product ions in tandem mass spectra are reported in Table 12.

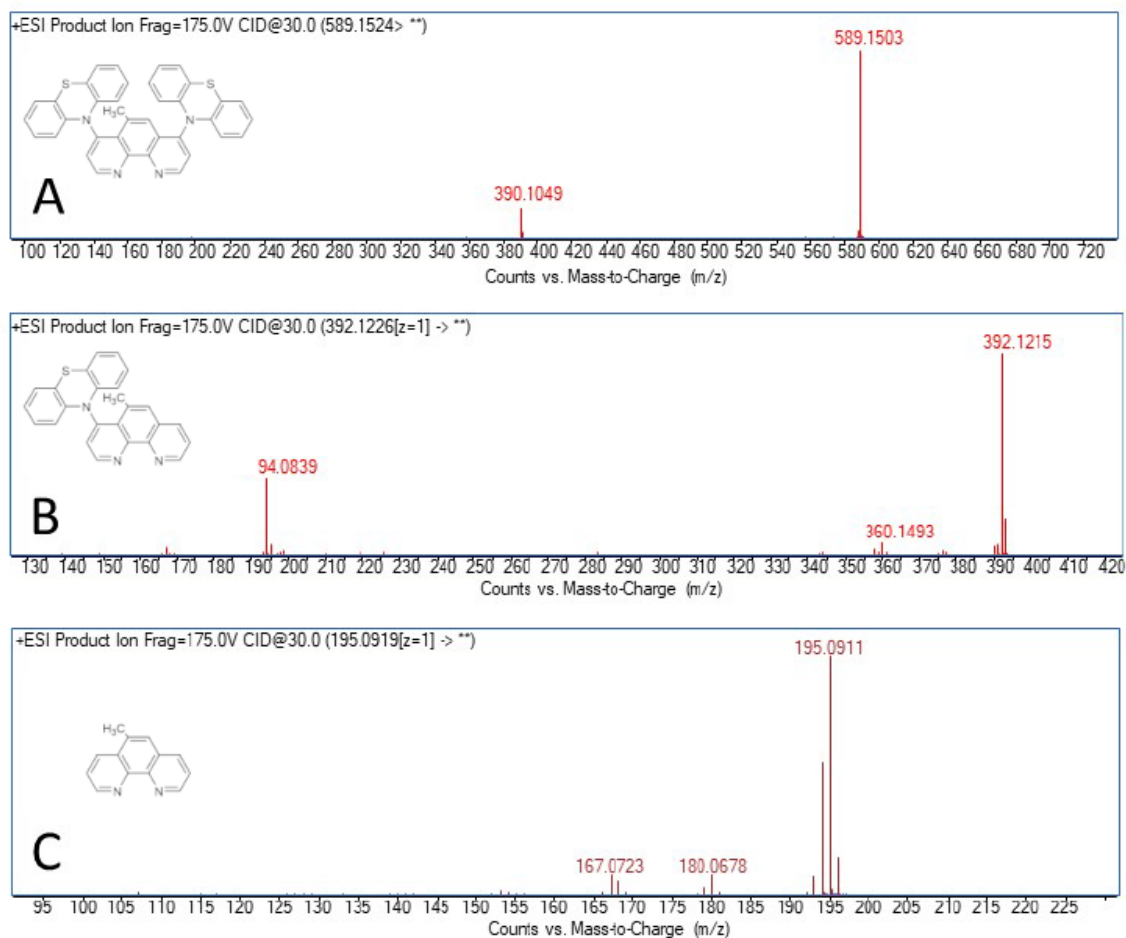


**Figure 50.** Tandem mass spectra detected in the sample after reduction of compound **5I**, related to A) compound **5I**, B) 5-methyl-4-phenothiazine-1,10-phenanthroline (**5I-P3**), C) 5-methyl-1,10-phenanthroline.

**Table 12.** Retention time, raw formula, calculated and experimental  $m/z$  for the  $[M+H]^+$  ion and main fragment ions detected in the tandem mass spectra for the solution before and after reduction of compound **5I**.

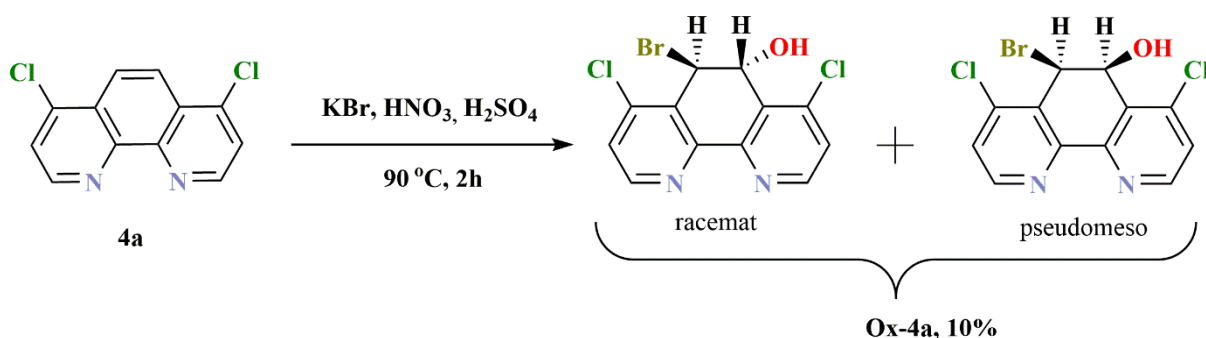
Compound name	Retention time (min)	Raw formula	Calculated $m/z$ for $[M+H]^+$	Experimental $m/z$ for $[M+H]^+$	$\Delta$ ppm	Fragment ions ( $m/z$ )
<b>5I</b>	24.2	$C_{37}H_{24}N_4S_2$	589.1521	589.1524	0.5	390.1049
<b>5I-P3</b>	18.2	$C_{25}H_{17}N_3S$	392.1221	392.1226	1.3	360.1493 194.0839
<b>5-methyl-1,10-phenanthroline</b>	2.0	$C_{37}H_{24}N_4O_2S_2$	621.1419	621.1423	0.6	195.0911 180,0678 167,0723

## 6.2.7 Oxidation and hydrolysis reactions of selected 1,10-phenanthroline

### 6.2.7.1 Oxidation of 4,7-dichloro-1,10-phenanthroline

The research start by oxidation studies of 4,7-dichloro-1,10-phenanthroline. Based on the work, C. Wang et al.<sup>224,225</sup> the oxidation reaction analogous to that presented in chapter 5.6.1 (Scheme 23) was performed.

The reaction consisted of adding 4,7-dichloro-1,10-phenanthroline and potassium bromide in sequence to an ice-cold sulfuric acid (96%). The nitric acid (70%) was then introduced into the solution. The mixture was kept in an ice-water bath for 10 min. Next, the mixture was heated and stirred at 90 °C. After 2 hours of heating, the mixture was then poured onto the ice and neutralized with 30% NaOH solution to pH 6. The product was extracted with chloroform and dried. The product has been purified in a chromatography column using eluting solvent chloroform-methanol (1:1). The product **Ox-4a** was crystallized in chloroform (Scheme 63).



**Scheme 63.** The oxidation of 4,7-dichloro-1,10-phenanthroline based on procedure of C. Wang et al.<sup>224</sup>

In this dissertation work, based on the collected literature summarized in Chapter 5.6.1, it was suggested that the obtained reaction product of **4a** can be an intermediate product of dione derivative. This dione derivative was suggested as a possible formed compound due to its comparable construction in position C5-C6 with compound **2** on Scheme 25 ( Chapter 5.6.1) in work by W. Z. Antkowiak et al.<sup>102</sup>. The formation of a racemate and a pseudomeso structure was suggested, and it is discussed in chapter 5.6.1 (Scheme 24).

Figure 51 shows the mass spectrum of the ion characterized by  $m/z$  346.9166, corresponding to the molecular ion  $[M + H]^+$ ; 368.8979 corresponding to  $[M + Na]^+$  of compound **Ox-4a**.



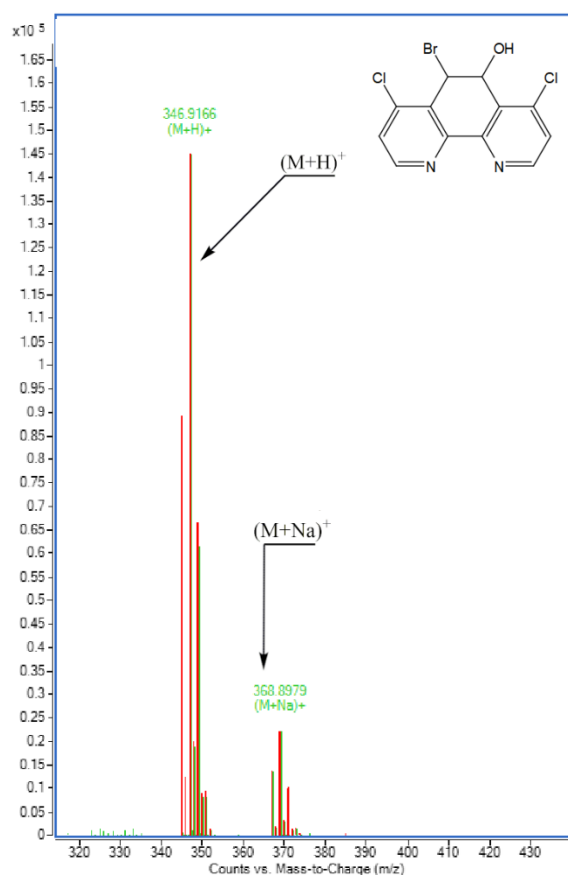


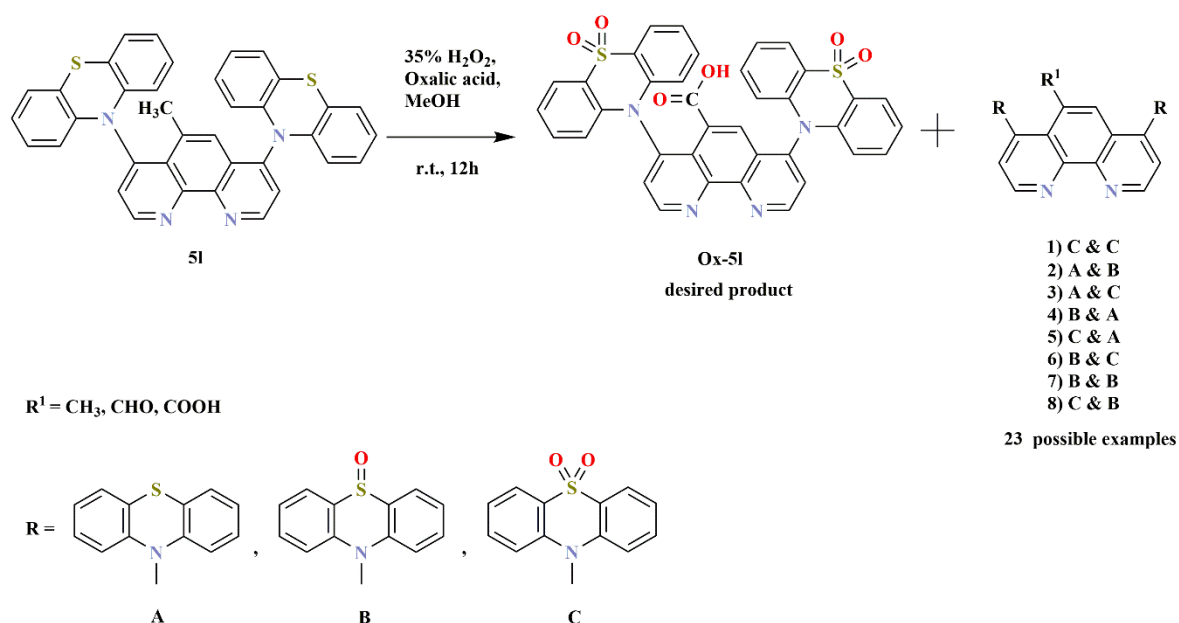
**Figure 51.** ESI-MS spectrum of **Ox-4a**.

### 6.2.7.2 Oxidation of 5-methyl-4,7-di(10*H*-phenothiazin-10-yl)-1,10-phenanthroline

Another reaction that was performed is the oxidation of 5-methyl-4,7-di(10*H*-phenothiazin-10-yl)-1,10-phenanthroline (**5I**). Based on the procedure of A. S. Touchy et al.<sup>226</sup>. The reaction did not give the desired product. The reaction mixture, in turn, contained more than one reaction product.

The reaction consisted of adding 35% hydrogen peroxide to solution of 5-methyl-4,7-di(10*H*-phenothiazin-10-yl)-1,10-phenanthroline (**5I**) in methanol. Then oxalic acid dihydrate was added to the reaction mixture, and the solution was stirred for another 12 hours at room temperature. Until TLC analysis showed, the starting material **5I** was gone. Then a 3% solution of Na<sub>2</sub>SO<sub>3</sub> was added, due to which the green color of the solution disappeared. The obtained reaction mixture did not contain the desired product (**Ox-5I**, Scheme 64). Scheme 64 shows the possible reaction by-products that may have resulted from the designed reaction on

oxidation of 5-methyl-4,7-di(10*H*-phenothiazin-10-yl)-1,10-phenanthroline. The oxidation reaction of **5I** can lead to the formation of 24 possible products. Due to the possible oxidation reaction of phenothiazine groups (R, Scheme 64), it is possible to obtain eight variations among them (they are presented in Scheme 64 in a descriptive form, e.g., A & B, where A - refers to the unoxidized substituent of phenothiazine and B- refers to the oxime substituent of phenothiazine). An additional aspect is that the methyl group oxidation reaction can also lead to obtaining a carbonyl group, giving an aldehyde or a carboxylic acid derivative. However, this finding also suggests that the steric hindrance for the methyl group could prevent its oxidation reactions. For this reason, derivatives with an unchanged methyl group are considered as expected reaction products.



**Scheme 64.** Oxidation of 5-methyl-4,7-di(10*H*-phenothiazin-10-yl)-1,10-phenanthroline (**5I**).

As a result of the research, a complex reaction mixture was obtained. Both functional groups, phenothiazine and methyl, can be separately oxidized. In addition, spatially large substituents of phenothiazine may hinder the oxidation of the methyl group located in C5 position for reasons of steric hindrance. It was found that between the phenothiazine functional groups, a molecule of solvent is incorporated, which is difficult to remove (chapter 5.2.3, Figure 16, 17). It has shown that oxidizing reagents may have problems with access to the C5-methyl group, especially when the phenothiazine substituents are further oxidized.

Transition metals were deliberately not used for the oxidation procedure as the 1,10-phenanthroline structure exhibits excellent complexing properties (section 4.6.3).

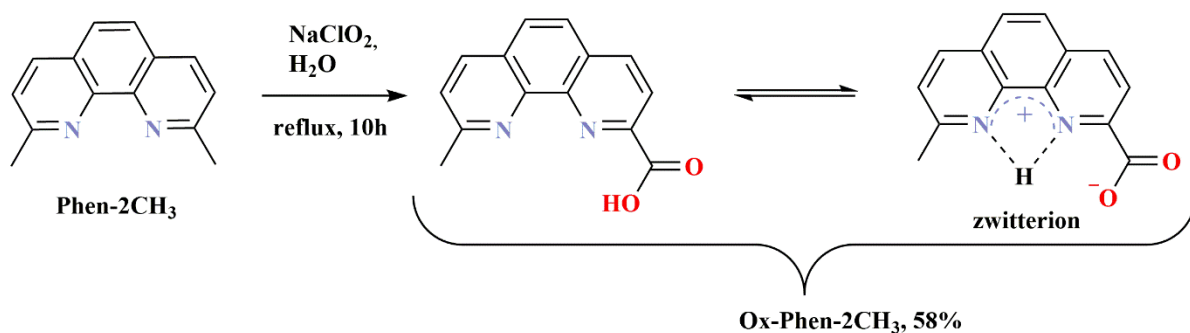
In turn, the performed oxidation reaction may be influenced by many factors, such as reaction conditions, where the change of temperature or solvent may affect the selectivity of the reaction. Therefore, further research will be devoted to the modification of the reaction conditions.

### 6.2.7.3 Oxidation of 2,9-dimethyl-1,10-phenanthroline (neocuproine)

In this chapter, the oxidation reactions of 2,9-dimethyl-1,10-phenanthroline (neocuproine, **Phen-2CH<sub>3</sub>**) were successfully performed. Two different products, were obtained through two separate oxidation reactions.

The first procedure of neocuproine oxidation was a reaction based on previously conducted studies on the oxidation of quinolinecarbaldehydes (chapter 5.4.2). The choice of this procedure was based on the low cost of its implementation and the availability of reagents. As a result of the reaction, 9-methyl-1,10-phenanthroline-2-carboxylic acid (**Ox-Phen-2CH<sub>3</sub>**, Scheme 65) was selectively synthesized. Additionally, the possible formation of zwitterion for the **Ox-Phen-2CH<sub>3</sub>** product due to the molecule's structure is shown (Scheme 65).

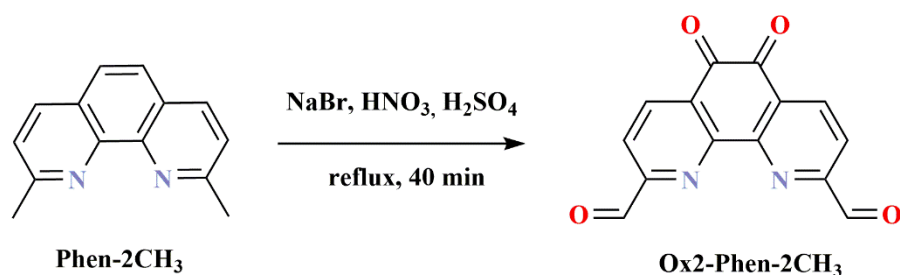
The reaction proceeds the following way: the compound 2,9-dimethyl-1,10-phenanthroline (**Phen-2CH<sub>3</sub>**) is introduced into water, then an excess of NaClO<sub>2</sub> is added, the reaction is carried out initially at room temperature, and then the suspension is heated to reflux temperature with constant stirring for 10 hours. Next, the solution was carefully acidified with 10% HCl solution until the pH was acidic (pH=2.8). Another step was the evaporation and extraction with methanol. After concentration, the crude product obtained is washed with dichloromethane, and next is purified by crystallization from water or methanol. The preparation procedure and the structure of the obtained acid are submitted to the Polish patent office.



**Scheme 65.** Preparation of 9-methyl-1,10-phenanthroline-2-carboxylic acid (**Ox-Phen-2CH<sub>3</sub>**).

In this dissertation thesis was also performed the second oxidation procedure for neocuproine based on the research by C. Hiort et al.<sup>227</sup> (Scheme 66). The reaction itself is an analogous oxidation system through sulfuric acid, nitric acid, and bromine salt, as for the oxidation of 4,7-dichloro-1,10-phenanthroline, which has already been described in this chapter. The procedure is based on the reaction developed by Yamada et al., which is discussed in chapter 5.6.1 (Scheme 19). The oxidation of neocuproine gives two carbonyl group and additional characteristic 5,6-dione unit on the 1,10-phenanthroline skeleton (**Ox2-Phen-2CH<sub>3</sub>**, Scheme 66).

This reaction consisted of dissolving 2,9-dimethyl-1,10-phenanthroline and then sodium bromide in sulfuric acid (96%). After the addition of substrates was complete, nitric acid (70%) was added to the solution. The mixture was then heated under reflux for 40 min. After cooling, it was poured onto ice and carefully neutralized to pH 7 with sodium hydroxide. After neutralization, the solution was left for 30 minutes. The separated precipitate was filtered and extracted with boiling water, and the combined aqueous phases were extracted with dichloromethane. Then the separated organic phase was rewashed with water and dried with dry magnesium sulfate. Finally, the organic phase was evaporated under reduced pressure. The results showed a complex reaction mixture. The products identified only by MS analysis suggest a structure of molecule **Ox2-Phen-2CH<sub>3</sub>**. The obtained product 5,6-dioxo-5,6-dihydro-1,10-phenanthroline-2,9-dicarbaldehyde (**Ox2-Phen-2CH<sub>3</sub>**) was crystallized from methanol (Scheme 66).



**Scheme 66.** Oxidation of 2,9-dimethyl-1,10-phenanthroline (**Phen-2CH<sub>3</sub>**). The procedure base on work C. Hiort et al.<sup>227</sup>.

The compound **Ox2-Phen-2CH<sub>3</sub>** has not been fully characterized due to its difficult isolation from a complex reaction mixture. However, it was confirmed that this molecule was obtained in the reaction by mass spectrometry analysis (Figure 52).

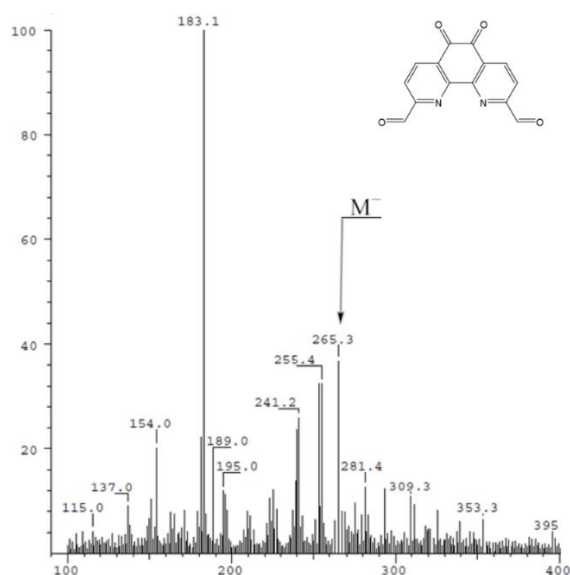
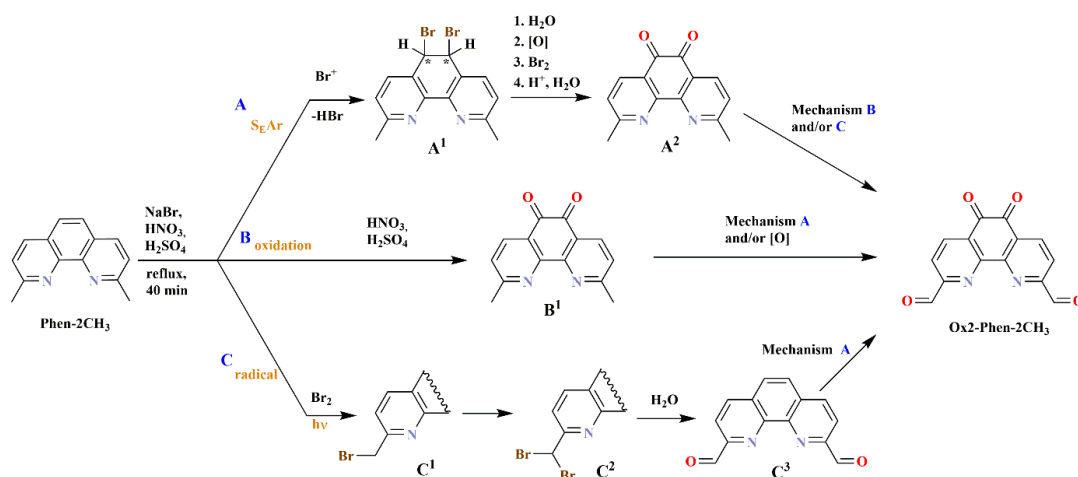


**Figure 52.** FAB-MS negative ion mass spectra of **Ox2-Phen-2CH<sub>3</sub>**.

The resulting product **Ox2-Phen-2CH<sub>3</sub>** may proceed through a number of possible mechanisms. In the case of the reaction mechanism, it is not simple, and it was not optimized in this research. Considering the literature research and the result of the MS analysis (Figure 52), in Scheme 67, three possible mechanisms leading to the obtaining of **Ox-Phen-2CH<sub>3</sub>** are presented. The first one **A** (Scheme 67, A), follows the  $S_{\text{E}}\text{Ar}$  reaction. The second mechanism **B** is the oxidation reaction through an oxidizing mixture of concentrated nitric and sulfuric acids. The third mechanism **C** is based on the bromine (generated *in situ*) radical reaction (Scheme 67, B).



**Scheme 67.** Possible reaction mechanisms for the preparation of **Ox2-Phen-2CH<sub>3</sub>**. Intermediate products were not isolated and identified (**A<sup>1-2</sup>**, **B<sup>1</sup>**, **C<sup>1-3</sup>**), square brackets were not marked for simplicity. Mechanism **A** based on S. A. Mitsov et al.<sup>99</sup>. \* - chiral carbon atoms.

In this reaction, a mixture of reagents composed inter alia of sodium bromide generates *in situ* bromine (discussed in chapter 5.6.1, Scheme 19).

In the 1,10-phenanthroline structure, positions C5 and C6 are exclusive to electrophilic substitution S<sub>E</sub>Ar. Mechanism **A** (Scheme 67, A) presents this type of transformation based on the mechanism shown by S. A Mitsov et al. (discussed in section 5.6.1 of Scheme 21).

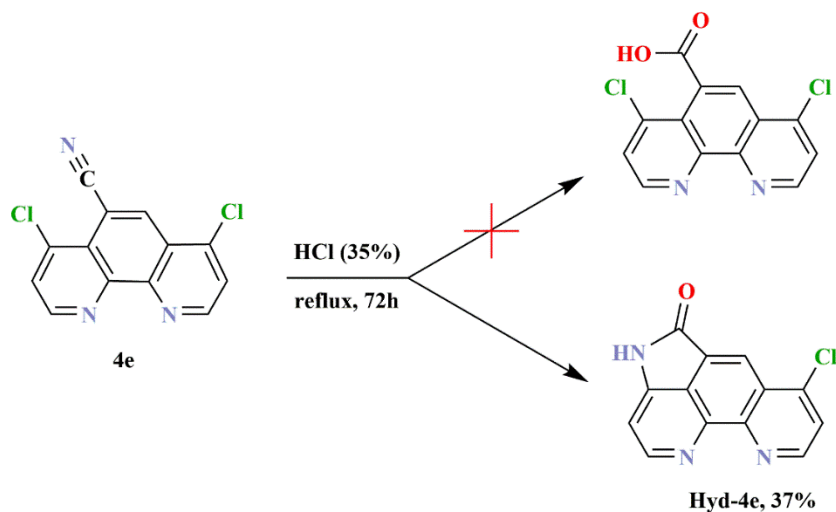
Another possible mechanism **B** (Scheme 67, B) leading to intermediate B<sup>1</sup> of the dion type was suggested based on the work of P. G. Sammes et al.<sup>96</sup> where in nitration reaction of 1,10-phenanthroline it is also possible to find 1,10-phenanthroline-5,6-dione as a by-product. However, this experimental procedure requires drastic conditions to introduce the NO<sub>2</sub> group in the C5 position through a mixture of fuming acids; nitric and sulfuric (oleum).

If the reaction is exposed to light, the mechanism **C** may occur, where bromine displaces the hydrogen from the methyl group on the radical pathway creating a C2-Br bond giving intermediate C<sup>1</sup> and subsequently intermediate C<sup>2</sup> with two C-Br bonds (Scheme 67, C). It is comparable to the toluene bromination reaction under irradiation<sup>228</sup>. Then C2Br2 fragment hydrolyzes to give a carbonyl group (Scheme 67, C); this type of reaction is well known in the literature<sup>229</sup>. In Scheme 67, a radical pathway was simplified by highlighting the reactions for one methyl group. Still, the reaction occurs for both groups, shown by the hydrolysis to the product C3, where two carbonyl groups were obtained.

#### 6.2.7.4 Hydrolysis of 4,7-dichloro-1,10-phenanthroline-5-carbonitrile

The 4,7-dichloro-1,10-phenanthrolines with a carboxylic acid group as substituent should be readily soluble in waters. These bifunctional compounds should mimic amino acids or nicotinic acid. Therefore, in order to synthesize appropriate carboxylic acids, out the hydrolysis of the CN group in 4,7-dichloro-1,10-phenanthroline-5-carbonitrile (**4e**) was carried out, using an excess of hydrochloric acid. It is shown in Scheme 68 that the reactions do not lead to the formation of the expected 4,7-dichloro-1,10-phenanthroline-5-carboxylic acid, but the unexpected product **Hyd-4e** was isolated.

The reaction was to dissolve **4e** in concentrated hydrochloric acid (35%) at room temperature. The solution was then heated at 100 °C for 72 hours, whereupon the volatiles were evaporated. The crude product was purified by Soxhlet extraction (H<sub>2</sub>O). Finally, the product was dried over P<sub>4</sub>O<sub>10</sub> to give 7-chloropyrrolo[2,3,4-de][1,10] phenanthroline-5(4*H*)-one (**Hyd-4e**, 37%).



**Scheme 68.** The hydrolysis reaction of **4e**.

An important point in the case of a hydrolysis reaction is whether the reaction medium is acidic or alkaline. This is of great importance in the case of 4,7-dichloro-1,10-phenanthroline derivatives. Chlorine atoms present in molecules in C4 and C7 positions in the alkaline environment can easier undergo a hydrolysis reaction in which one or both chlorine atoms are substituted with a hydroxyl group. The work of J. King-Underwood et al. presents reactions in an alkaline environment where the hydrolysis of the chlorine atom occurs<sup>230</sup>.

Even though the more preferred medium should be alkaline for the hydrolysis reaction, the alkaline environment activates C4-Cl positions. Unfortunately, this facilitates hydrolysis by withdrawing the product towards the dione substrate. Hence, to hydrolyze only the nitrile group, an acidic environment was used.

#### 6.2.7.5 Hydrolysis of 4,7-disubstituted-1,10-phenanthrolines

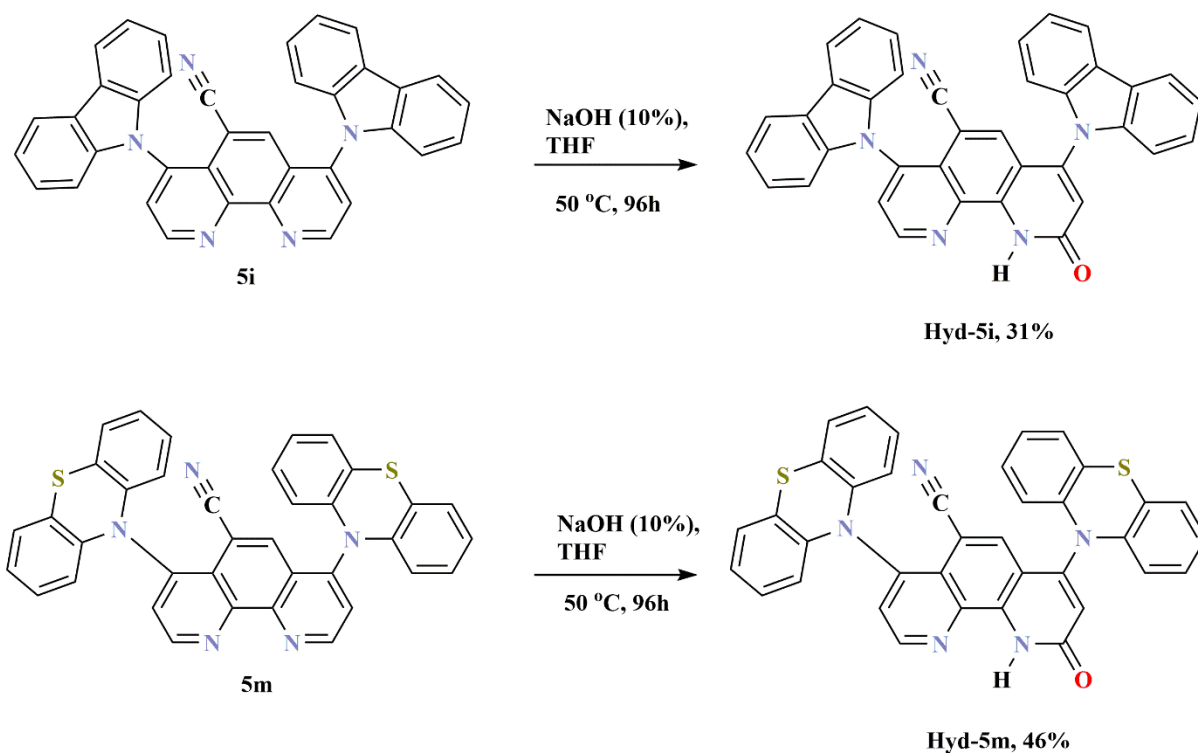
As for the previously discussed example for 4,7-dichloro-1,10-phenanthroline in 4,7-disubstituted-1,10-phenanthroline, the carboxyl group in the C5 position should significantly change the solubility in water. Still, the oxidation reactions are complicated by many side reactions, including the oxidation of substituents (chapter 5.2.7.2). For this reason, the hydrolysis reactions of selected carbonitrile derivatives were carried out, where it is possible to obtain acid derivatives by a hydrolysis reaction, avoiding the isolation of a complicated oxidation mixture.

Therefore, to synthesize appropriate carboxylic acids, the hydrolysis of the CN group using an excess of sodium hydroxide in the case of 4,7-di(9*H*-carbazol-9-yl)-1,10-phenanthroline-5-carbonitrile (**5i**) and 4,7-di(10*H*-phenothiazine-10-yl)-1,10-phenanthroline-5-carbonitrile (**5m**) under the applied conditions were carried out. The alkaline medium for the hydrolysis reaction were chosen because the substrates do not have any other groups than the carbonitrile group that could undergo a hydrolysis reaction (Scheme 69).

The hydrolysis of heterocycles **5i** and **5m** consisted of dissolving the selected compound in THF. Next, the solution of sodium hydroxide (10%) was added. Then the solution was heated at 50 °C for 96h. After this time, it was cooled to room temperature and acidified to neutral pH. After evaporation of the solvents, the crude product was purified by column chromatography using methanol/dichloromethane as the eluent to give a white powder. Finally, the powder was crystallized in a mixture of dichloromethane and hexane.

Reaction led to surprising compounds, namely 4,7-di(9*H*-carbazol-9-yl)-9-oxo-9,10-dihydro-1,10-phenanthroline-5-carbonitrile (**Hyd-5i**) and 9-oxo-4,7-di(10*H*-phenothiazin-10-yl)-9,10-dihydro-1,10-phenanthroline-5-carbonitrile (**Hyd-5m**)(Scheme 69). Both molecules were possibly obtained through a reaction of oxidative nucleophilic substitutions of hydrogen (ONSH) of the type S<sub>N</sub>ArH, with hydroxide ion as a nucleophile and in the presence of air as an oxidized reagent<sup>231,232</sup>. In both cases, nucleophile attacks were selective only at C2 rather than at the C9 position.





**Scheme 69.** The hydrolysis reaction of compounds **5i** and **5m**.

The natural atomic charges show that both heterocycles possess greater electron density on the C2 (0.040 for compound **5i** and 0.038 for compound **5m**) than on the C9 position (0.046 for compound **5i** and 0.044 for compound **5m**) (Figures 53 and 54).

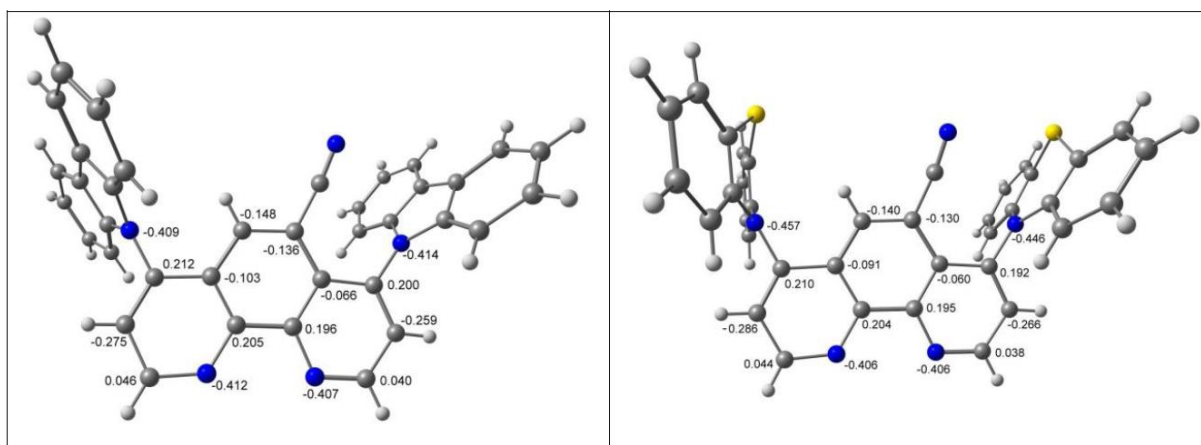


**Figure 53.** Natural atomic charges of compounds **5i** (left) and **5m** (right).

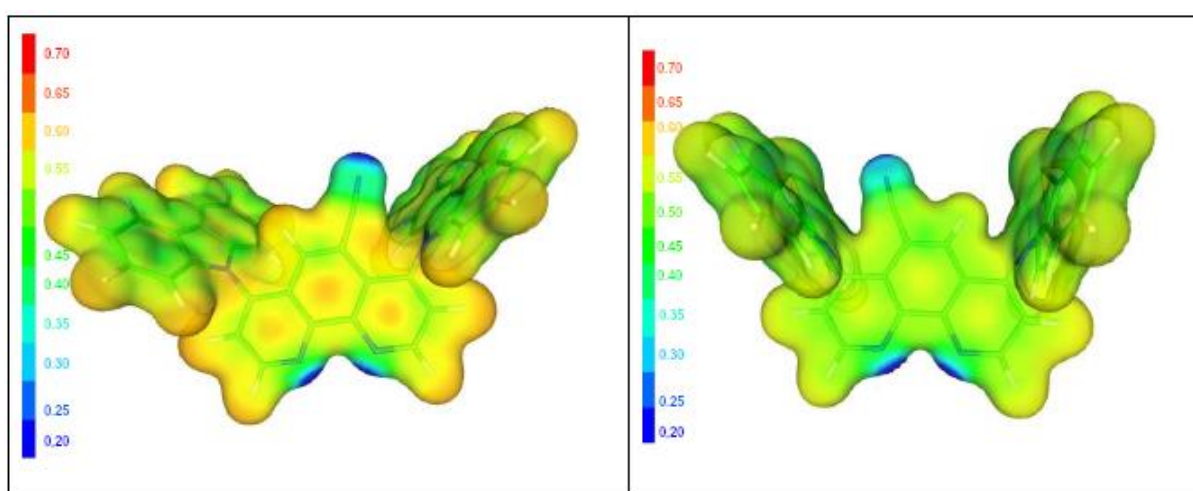


**Figure 54.** The plot of the electrostatic potential for compounds **5i** (left) and **5m** (right).

Both compounds **Hyd-5i** and **Hyd-5m** were isolated in a crystalline form, and their structures were characterized by X-ray crystallography (Figure 55, 56).

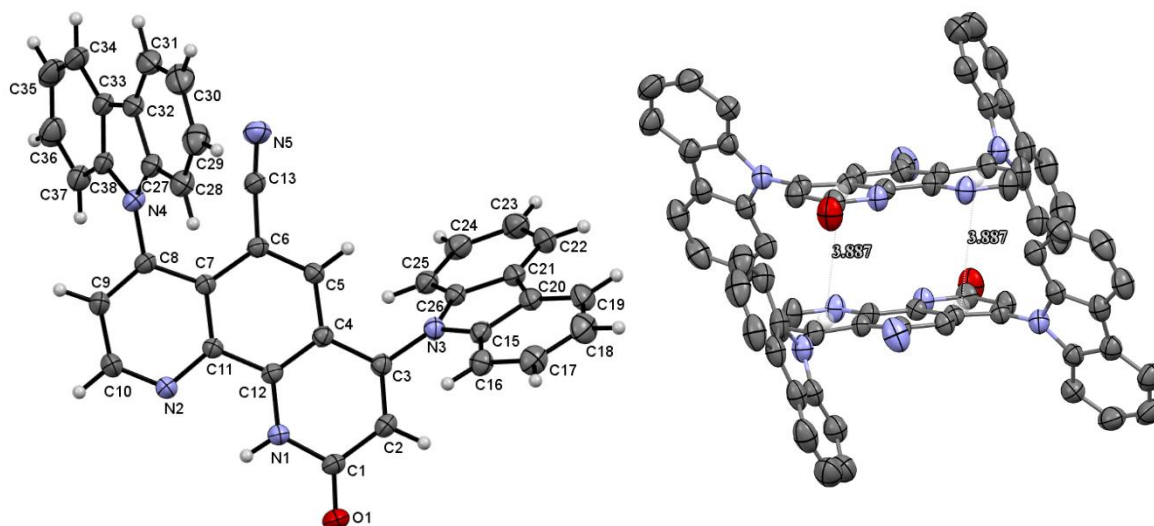


**Figure 55.** ORTEP drawing of compound **Hyd-5i** with 30% probability (left). The solvent molecules were omitted for clarity. ORTEP drawing of the  $\pi$ -stacking interactions in cell packing of compound (right).

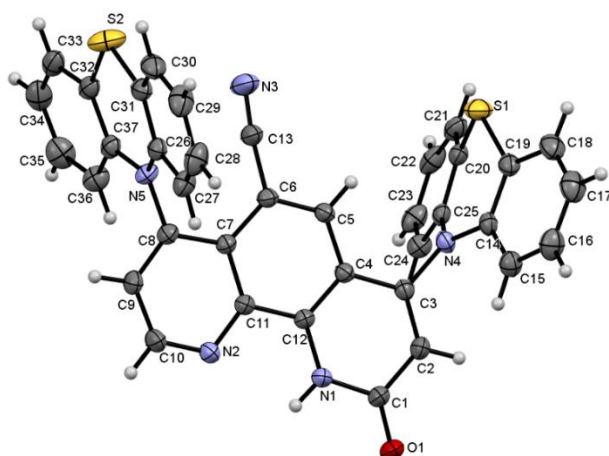


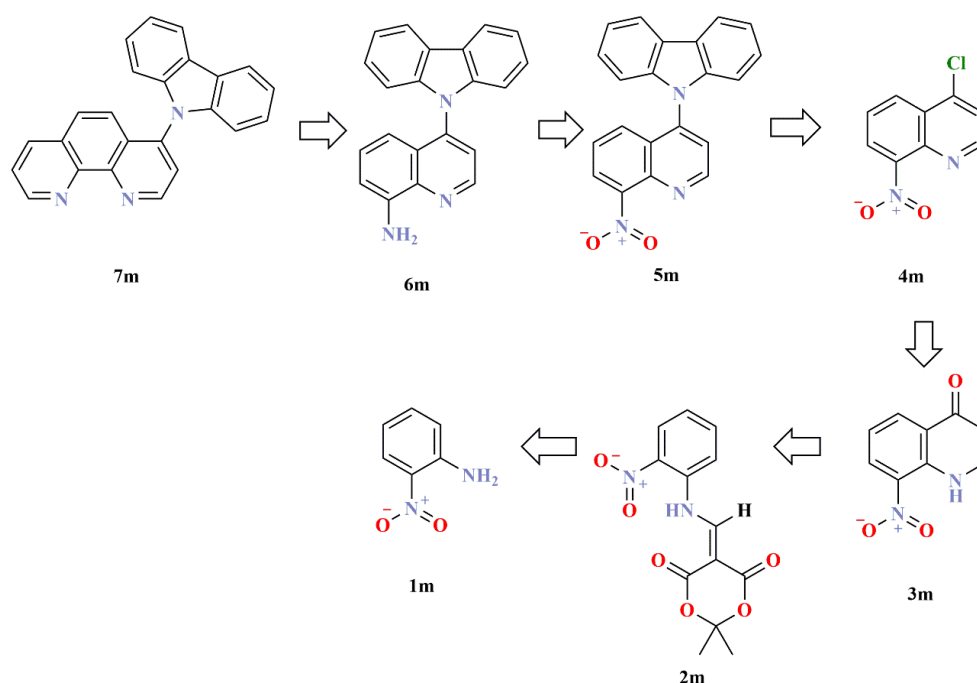
**Figure 56.** ORTEP drawings of compound **Hyd-5m** with 30% probability. Solvent molecules are omitted for clarity.

### 6.3 Symmetrical and unsymmetrical 1,10-phenanthroline derivatives

This chapter presents additional studies on the preparation of unsymmetric 1,10-phenanthroline derivatives. They were presented due to the resulting compounds' interesting properties and intermediate products, such as quinoline derivatives. The reactions were conducted to understand the limitations of the reactions and the compounds' unsymmetric

properties. In the case of products at individual stages, it was possible to obtain appropriate quality crystals, allowing for X-ray structure analysis.

The main aim of these studies was to obtain mono-substituted 1,10-phenanthrolines. For this purpose, a series of reactions were designed to get the desired product **7m** as shown in Scheme 70. The start of the reaction was based on the classical reaction using Meldrum acid reaction for 2-nitroaniline, where the products **1m-4m** were obtained and fully spectroscopically characterized (Scheme 72A). The next reaction was to obtain product **5m** by aromatic nucleophilic substitution (Scheme 70).



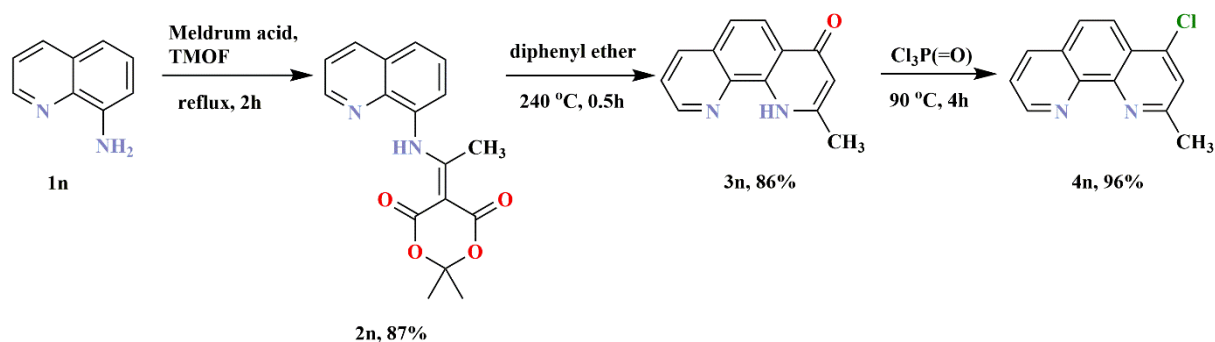
**Scheme 70.** Retrosynthetic analysis of monosubstituted 1,10-phenanthroline **7m**.

Interestingly, the reaction not only proceeded with the substitution of a chlorine atom but also as a result of the competitive reaction of VNS. This type of transformation led to a dead-end of the reaction from which further steps of the reaction could not be carried out.

This chapter presents studies devoted to the preparation of unsymmetric mono and dichloro-1,10-phenanthrolines (**4n**, **4o**, **4p**; Scheme 71, Scheme 72, and Scheme 73) derivatives, different in terms of their preparation from the previously presented results for 4,7-dichloro-1,10-phenanthroline derivatives (chapter 6.2.1). These compounds were taken over for further research in terms of their substitution with selected *N*-heterocyclic substituents.

On the other hand, further research inspired by competitive VNS reaction is presented in a separate chapter on nitro quinoline derivatives (chapter 6.5).

The first example is the preparation of 4-chloro-2-methyl-1,10-phenanthroline (**4n**). The reaction is presented separately for the reagents used. For this purpose, the 8-aminoquinoline was used as a substrate (**1n**), which was then converted using the Meldrum acid procedure (Scheme 71). During this synthesis, the products at every stage were isolated and fully characterized. For the compounds, **2n** and **3n**, crystals of appropriate quality and their X-ray structure analysis were obtained (Figure 57).



**Scheme 71.** Preparation of 4-chloro-2-methyl-1,10-phenanthroline **4n**.

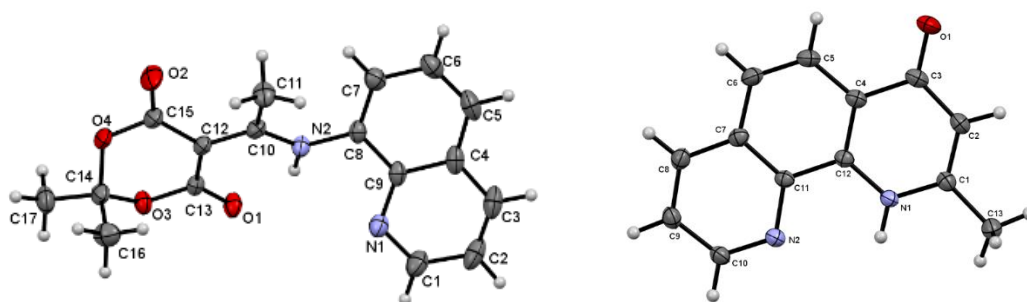


**Figure 57.** Crystallographic structures of molecules **2n** (left) and **3n** (right).

A second example for the preparation of unsymmetric 1,10-phenanthroline is a series of reactions leading to the preparation of 4,7-dichloro-2-methyl-1,10-phenanthroline (**4o**). In the first phase, a multi-stage reaction based on Meldrum acids (Scheme 72A) was performed. The products were isolated and characterized spectroscopically at each stage of the reaction. When obtaining 4-chloro-8-nitroquinoline (**4m**, also in chapter 6.5), a crystal of appropriate quality was isolated, which resulted in the X-ray structure analysis (Figure 58).

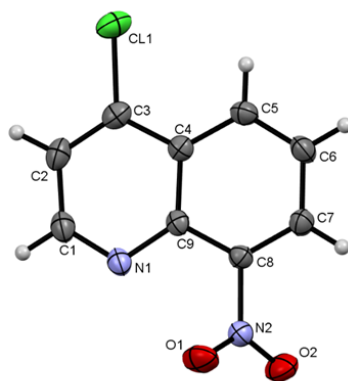
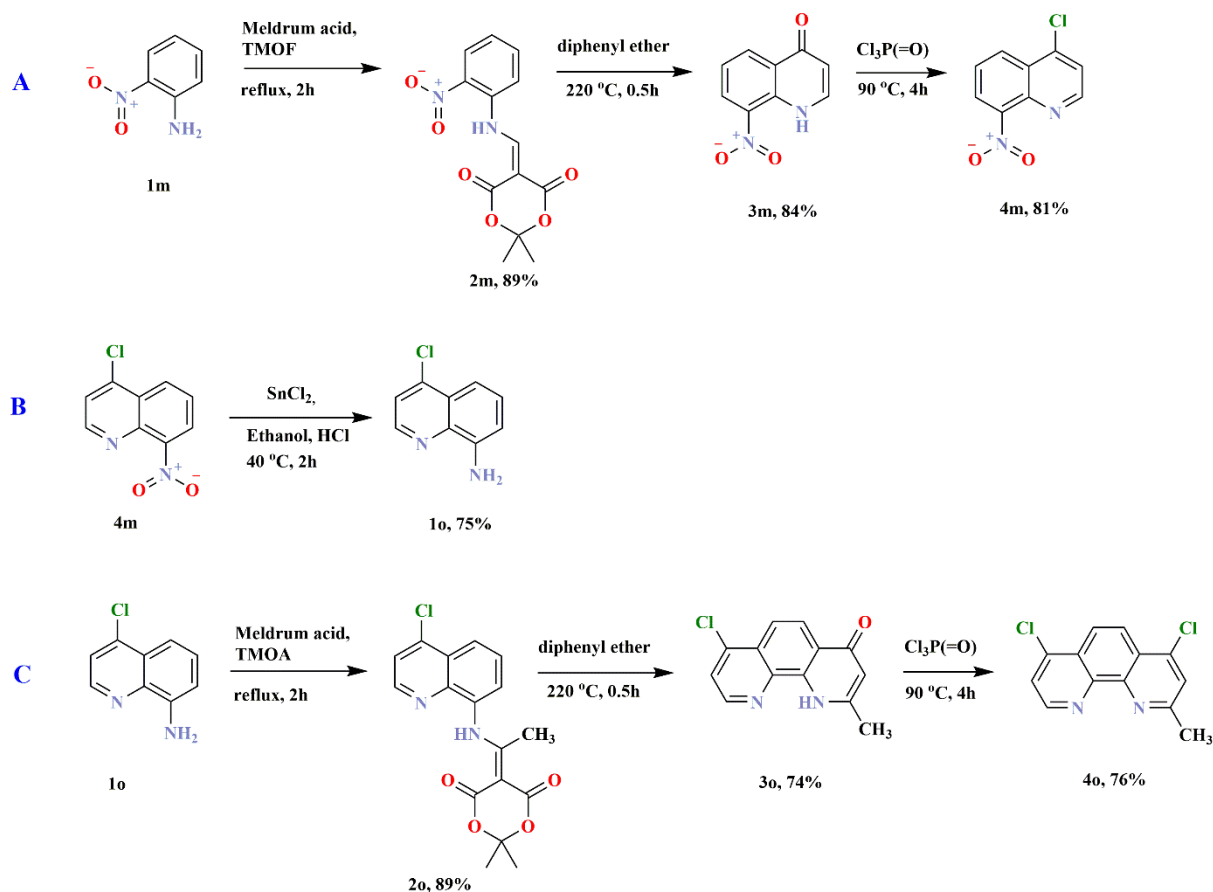


**Figure 58.** Crystallographic structures of 4-chloro-8-nitroquinoline (**4m**).

The next step to obtain the selected 1,10-phenanthroline was reducing the nitro group for 4-chloro-8-nitroquinoline (Scheme 72B). The procedure consisted of dissolving selected nitroquinoline in ethanol and hydrochloric acid solution and then introducing tin(II) chloride. Tin(II) chloride was used as a reducing agent. The reaction was carried out first at room temperature for 30 min, and the mixture was heated at 50 °C for 2h. After cooling, the mixture was alkalinized with ammonia solution and extracted into chloroform. Evaporating the solvent gave a yellow precipitate of 4-chloro-8-aminoquinoline (**1o**) (Scheme 72B).

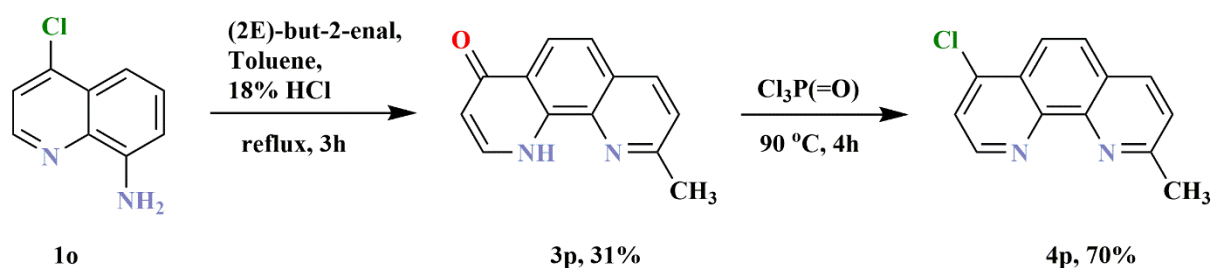
The last phase was to repeat the procedure based on synthesis with Meldrum's acids (Scheme 54). At each stage of the reaction, the products were isolated and characterized spectroscopically. By a series of reactions, 4,7-dichloro-2-methyl-1,10-phenanthroline (**4o**) was obtained.



**Scheme 72.** Three phases of obtaining 4,7-dichloro-2-methyl-1,10-phenanthroline **4o**.

A final example is a preparation of 7-chloro-2-methyl-1,10-phenanthroline (**4p**) (Scheme 73). This compound was obtained by a combination of the Skraup–Doebner–Von Miller reaction and the reaction with phosphoryl trichloride. In order to obtain the selected 1,10-phenanthroline, the previously prepared 4-chloro-8-aminoquinoline (**1o**) was used as the starting material (Scheme 73). The procedure consisted in adding to the selected amine dissolved in hydrochloric acid solution and then adding toluene and crotonaldehyde. Reactions were carried out under reflux for 3 hours. The aqueous phase was separated and neutralized with 10% sodium hydroxide solution. Next, the solution was extracted with dichloromethane, and after drying, the residue was purified by crystallization. The 9-methyl-1,10-phenanthroline-4(1*H*)-one (**3p**) was obtained by the Skraup–Doebner–Von Miller reaction and fully characterized spectroscopically (Scheme 73). As a result of carrying out the reaction in an aqueous medium, the reaction also proceeded with the chlorine atom's substitution by oxygen.

The compound so obtained was then dissolved in phosphoryl trichloride; the reaction was carried out for 4 hours at 90 °C. After this time, the excess phosphoryl trichloride was evaporated off under reduced pressure. The solution was then poured onto a mixture of ice and water. After about 15 minutes of continuous stirring, the reaction mixture was basified to a pH of 13-14 with 40% sodium hydroxide solution. The aqueous phase was extracted with methyl chloride. The crude product of 7-chloro-2-methyl-1,10-phenanthroline (**4p**) was obtained after evaporation of the organic phase. It was purified by silica gel column chromatography in methanol/dichloromethane as an eluent and then crystallized from dichloromethane alone (Scheme 73).



**Scheme 73.** Preparation of 7-chloro-2-methyl-1,10-phenanthroline (**4p**).

## 6.4 Synthesis and functionalization of selected mono and diformyl quinolines

This chapter presents research on the preparation and functionalization of carbaldehyde quinolines and their spectroscopic characteristics supported by theoretical calculations. Additionally, the reaction yields for the preparation of selected mono formyl quinolines were compared. Two sub-chapters have been distinguished. One is devoted to preparing quinolinecarbaldehyde derivatives, and the other to the method of their oxidation.

### 6.4.1 Synthesis of selected mono and diformyl quinolines in the Reimer-Tiemann, Vilsmeier-Haack, and Duff reactions

This topic is a continuation of Dr. Marcin Szala's research on the preparation of mono carbaldehydes. This research continued his work by extending the study to the Duff and

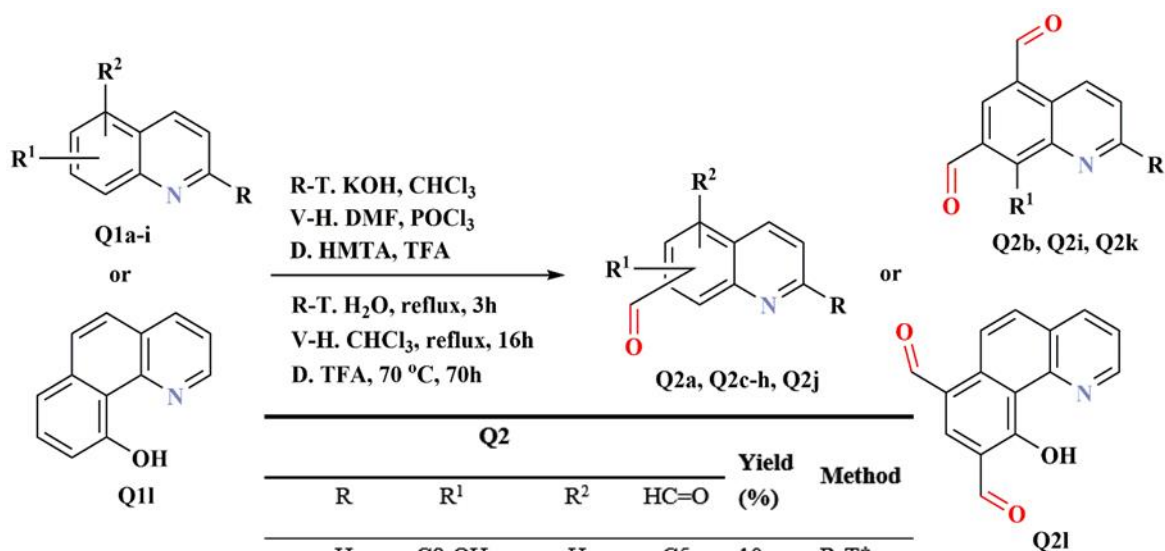


Vilsmeier-Haack reactions for selected new substrates which were used to obtain acid derivatives (presented in the next chapter 5.4.2).

Aldehydes are a class of compounds of great interest from the synthetic, theoretical, and application point of view, which can be transformed into a wide range of structural frameworks by applying various reactions (chapter 5.9). There are many different protocols for the synthesis of these compounds, including the classic Reimer-Tiemann, Vilsmeier-Haack, and Duff reactions. These reactions are known as versatile synthetic tools for formulating electron-rich aromatic compounds.

However, literature data has often inaccurately reported the position of the newly formed carbonyl group(s). Formylation via the Reimer-Tiemann reaction for 8-hydroxyquinoline can proceed to the C5 (38%) and C7 (10%) positions<sup>233</sup>. On the other hand, Gonzalez-Vera et al.<sup>234</sup> present the formylation of 2-methyl-quinoline-8-ol, leading to only 8-hydroxy-2-methylquinoline-5-carbaldehyde at 64% yield. Ding. et al. only obtained 8-hydroxy-7-quinolinecarbaldehyde, a product formylated in a different position<sup>235</sup>.

The experimental work on this topic started by carrying out the Reimer-Tiemann, Vilsmeier-Haack, and Duff reactions for selected quinoline derivatives shown in Scheme 74. The obtained reaction products were fully characterized spectroscopically. A crystallographic structure for 2-methyl-8-hydroxyquinoline-5,7-dicarbaldehyde (**Q2i**) was obtained and it is shown in Figure 59. The main aim of the research was to obtain new carboxylic acid precursors for selected quinolines and benzo[*h*]quinolines. An additional aim was to compare the reaction efficiency and the C5 / C7 position preferences on the benzene ring. In the research on quinoline derivatives, the results for 10-hydroxybenzo[*h*]quinoline derivatives were included due to the similar structure and properties to quinolines.



**Scheme 74.** Synthesis of quinolinecarbaldehyde derivatives **Q2**. \*-Compounds obtained by Dr. Marcin Szala, which are included in the table for comparison with other methods.

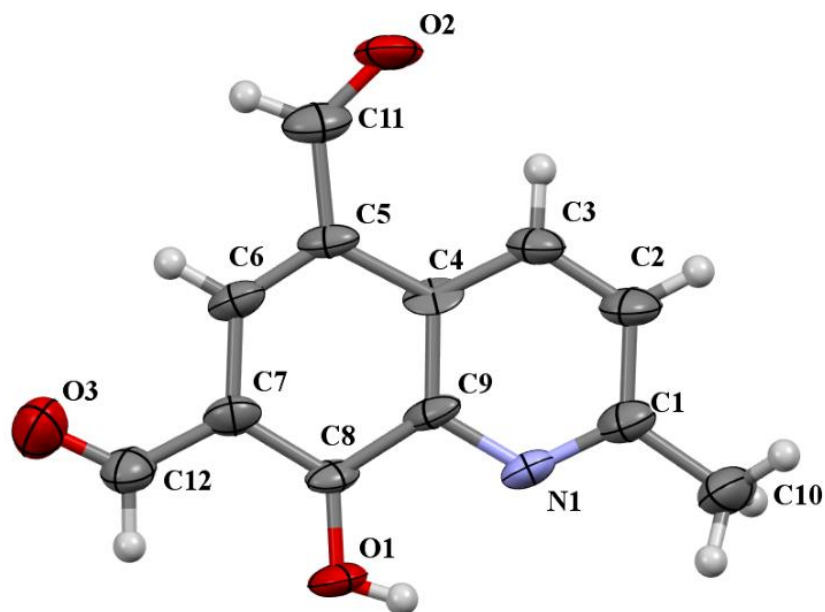
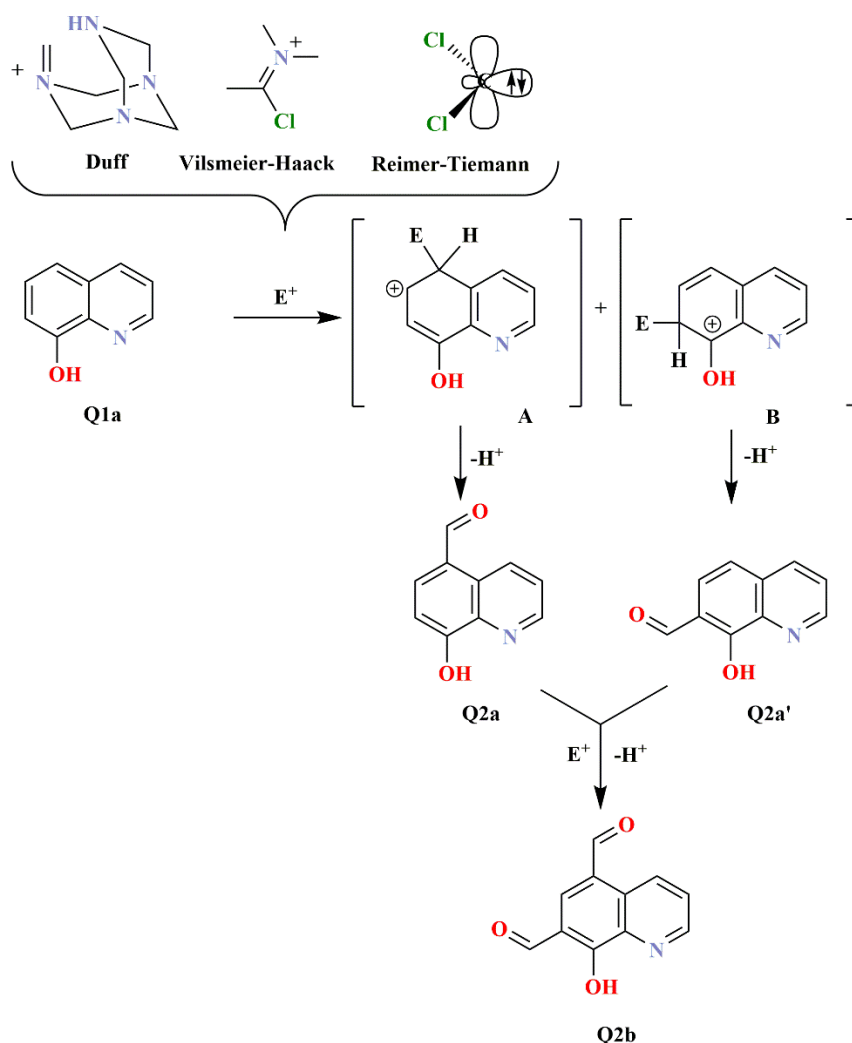


**Figure 59.** ORTEP drawing of compound **Q2i** with 50% probability. The solvent molecules were omitted for clarity.

As mentioned in chapter 5.8, in the case of groups of substituents containing a lone pair of electrons, their position affects the electron density by increasing it at the C5 and C7 positions. When considering individual electrophilic aromatic substitution mechanisms, it can be noticed the mutual similarities between the Reimer-Tiemann, Vilsmeier-Haack, and Duff reactions. However, there are significant differences in the initial electrophilic reaction. In the Reimer-Tiemann reaction, a carbene electrophile is generated *in situ*. For Vilsmeier-Haack's reaction, this is the so-called "Vilsmeier reagent," and in the case of the Duff reaction, it proceeds through initial aminoalkylations and then dehydrogenations (generated from HMTA) (Scheme 75).



**Scheme 75.** The proposition of formylation and diformylation mechanism of **Q1a**. The compound **Q2b** was obtained only by Duff reaction.

The attack by an electrophile generates a Wheland intermediate cation (or arenium ion) followed by the loss of a proton to restore the aromaticity (Scheme 75, **A** and **B**). Vilsmeier's reagent and electrophilic dichlorocarbene possess electron-withdrawing (EW) ability. One consequence of the existence of EWG groups in electrophiles is a decreased electron density in the newly generated Wheland cations, which deactivate the *N,N*-dimethylaniline (or phenol) ring for the next substitution. A dimethylamino moiety, like a hydroxyl group in the C8 position, increases the electron density at both the C5 and C7 sites, which makes double formylation leading to 8-(dimethylamino)quinoline-5,7-dicarbaldehyde (**Q2k**, yield < 1%) possible in the case of the Vilsmeier-Haack transformation (Scheme 74). In contrast, the Duff cyclic electrophile, after the generation of a Wheland cation (Scheme 75), does not deactivate the phenol ring for the next substitution, which allows the double

formylation to generate 8-hydroxy-quinoline-5,7-dicarbaldehyde (**Q2b**), 8-hydroxy-2-methylquinoline-5,7-dicarbaldehyde (**Q2i**) and 10-hydroxybenzo[*h*]quinoline-7,9-dicarbaldehyde (**Q2l**) in good yields (Scheme 74).

The absence of a methyl group in the C2 (R) position positively affects the yield of the products obtained. Comparing the performance of **Q2b** and **Q2i**, a significant increase in performance for **Q2b** can be seen. The methyl group at the C2 position for **Q2i** may be subject to further side reactions. Additionally, monoformyl products were present in all reaction mixtures for all three diformyl derivatives.

Interestingly, for the formylation of 6-hydroxyquinoline (**Q1h**) by the Duff procedure, the reaction only leads to monocarbaldehyde, where the carbonyl group is attached only to the C5 position<sup>236</sup>. The differences in reactivity between 8-hydroxyquinoline (**Q1a**), 6-hydroxyquinoline (**Q1h**), *N,N*-dimethylquinolin-6-amine (**Q1e**) and *N,N*-dimethylquinolin-8-amine (**Q1i**) could be explained by the differences in electrostatic potentials of the atoms participating in the formylation transformation. In order to compare their electrostatic potentials, theoretical calculations were performed for selected quinoline derivatives, which are presented in Figure 60.

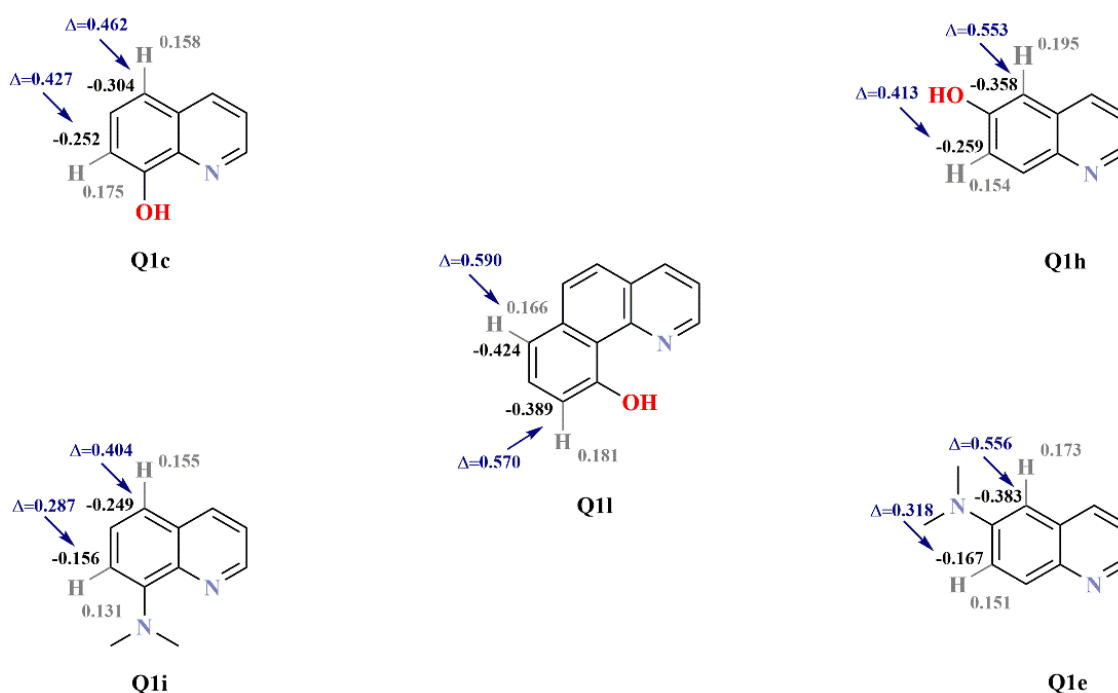


**Figure 60.** The electrostatic potentials for the selected quinolines.

A positive charge indicates a deficiency of electrons on an atom and a negative charge, an excess of electrons. The electrostatic potential for a hydrogen atom is marked in gray

(positive value) and for carbon in black (negative value). The differences in their potential are marked in blue. The higher difference in atomic charges between C5 and C7 positions shows the preference of selected monoformylations products with novel carbonyl group only in the C5 position. The difference of electrostatic potential of C5-H bond 0.556 for **Q1e** suggests the easier cleavage of H atom from C5, compared to C7-H with electrostatic potential difference 0.318 (for **Q1h**, similarly). The smaller differences in the atomic charges difference of atoms in bonds C5- and C7-H suggest the possibility of double formylation and the presence of both regioisomers with new carbonyl group in C5 and C7 positions (Figure 60). Formylation of 2-methylquinolin-8-ol (**Q1b**) and 8-hydroxyquinoline (**Q1c**) in all the presented methodologies led to complicated reaction mixtures. However, it was noticed that dialdehydes **Q2b**, **Q2i**, and **Q2l** were easy to isolate because of their low solubility in most solvents. In this case, isolation relies on filtration, followed by washing with chloroform and methanol.

Analysis of  $^1\text{H}$  NMR spectra for **Q2** molecules showed typical H-1 signals for a proton in the carbonyl groups at positions C5 and C7 (or C7 and C9 for compound **Q2l**) with chemical shifts of ca. 10.1 and 10.5 ppm, respectively. The analysis of the trends in  $^1\text{H}$  NMR chemical shifts revealed that the presence of intramolecular hydrogen bonds between neighboring carbonyl group located at C7 position and hydroxyl or dimethylamino group at C8 position increased the deshielding effect, resulting in the low-field signals. The chemical shifts in the DMSO solution were moved to the downfield (larger  $\delta$ ; 10.5 ppm), while the higher field signal (10.1 ppm) is for a carbonyl group located at the C5 position where intramolecular hydrogen bonds were absent (example shown in Figure 61). The  $^{13}\text{C}$ -NMR spectra showed an opposite effect to the  $^1\text{H}$ -NMR ones. The carbon atoms of the carbonyl groups located at the C5 and C7 positions showed distinctive signals with  $^{13}\text{C}$  chemical shifts of ca. 192 and 188 ppm, respectively. The chemical shifts were moved to downfield (larger  $\delta$ ) for a non-protonated carbonyl group at the C5 position with resonance signals at ca. 192 ppm.

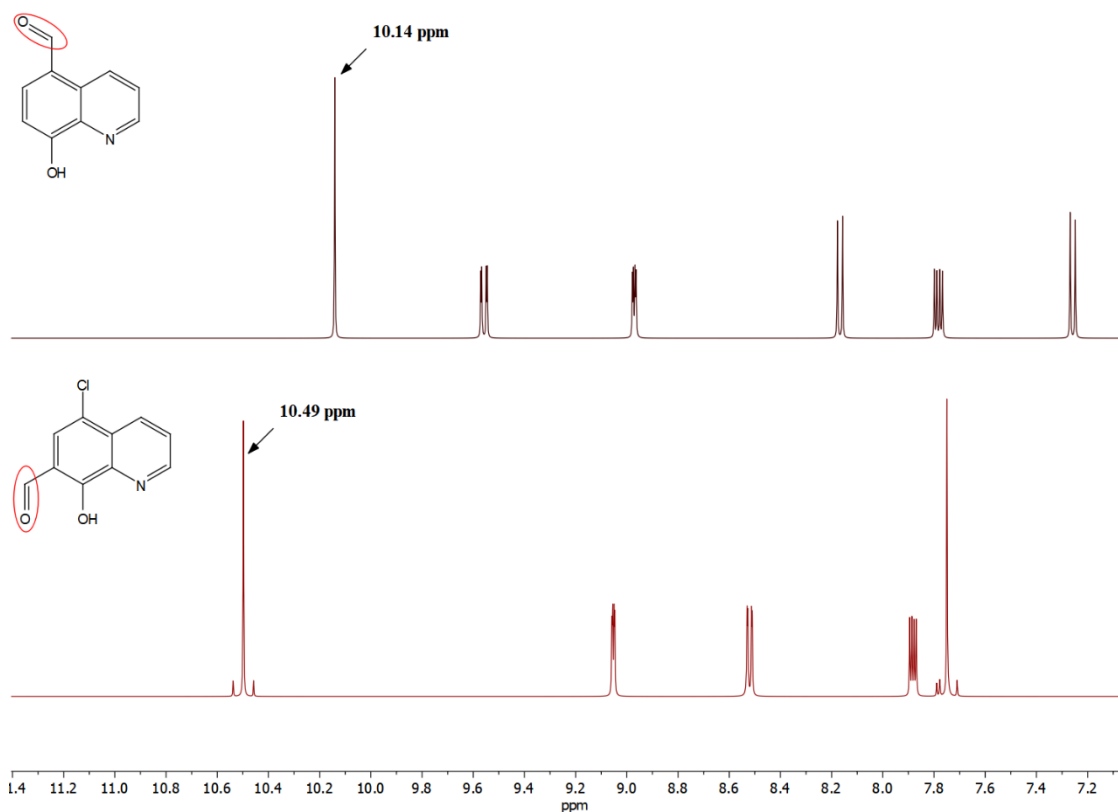


**Figure 61.** Compare <sup>1</sup>H NMR spectra (DMSO-d<sub>6</sub>) for **Q2a** and **Q2c**, aromatic range.

The IR spectra of molecule **Q2** showed distinctive carbonyl signals for the groups located at C5 and C7 (or C7 and C9 in the case of heterocycle **Q2l**) positions in the range 1663–1686  $\nu_{\text{C=O}}$ . The analysis of the trends suggests that the carbonyl group located at C5 possesses rather smaller values than that at C7. In the case of **Q2j**, two signals from both carbonyl groups located at C5 and C7 were registered (Figure 62). Comparison of the double formylated products **Q2h** and **Q2j** revealed that the presence of intramolecular and intermolecular hydrogen bonds between the carbonyls and hydroxyl groups has an impact on overlapping signals. This could explain why compound **Q2k** possesses a dimethylamino group at the C8 position instead of a hydroxyl group and has two separate signals at 1678  $\nu_{\text{C=O}}$  and 1661  $\nu_{\text{C=O}}$ .

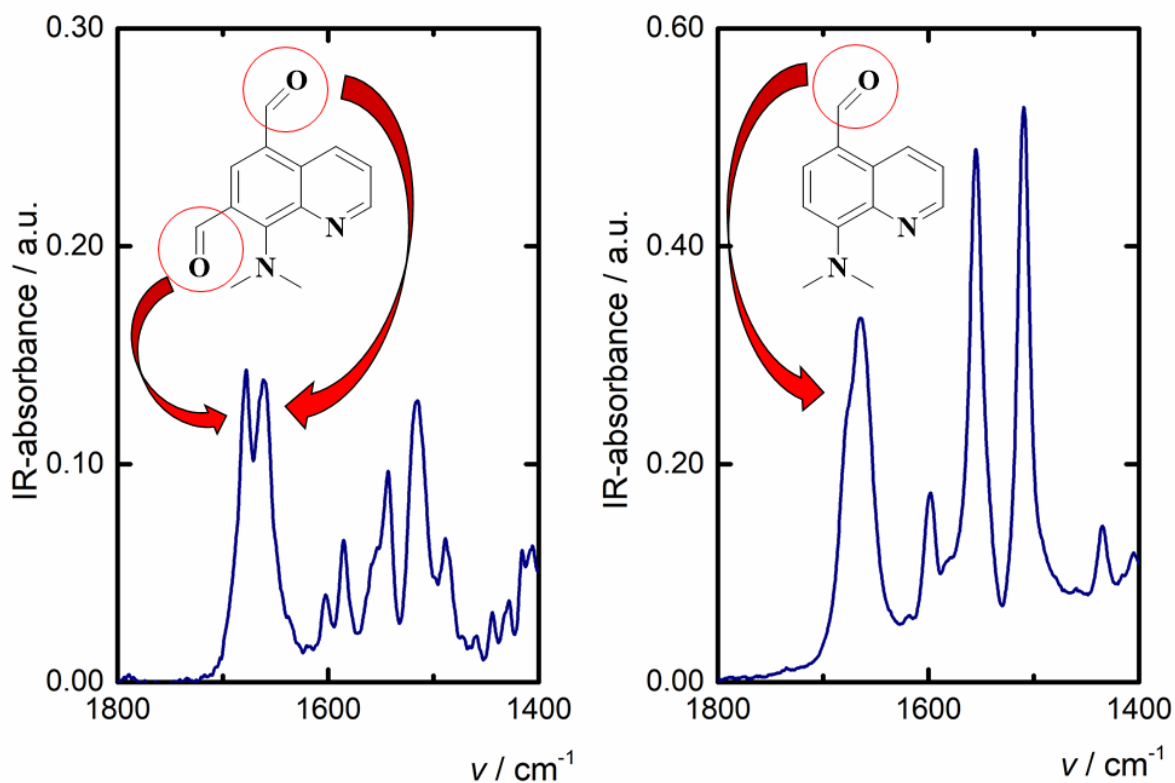


**Figure 62.** IR spectra of **Q2k** (left) and **Q2j** (right).

Comparing the reactions of Reimer Tiemann, Vilsmeier Haack, and Duff, the first two reactions take place in a basic environment, while the Duff procedure requires a strongly acidic reaction environment. A negative impact on the synthesis of quinolinecarbaldehydes **Q2** was noticed during the final stage when alkaline environment was applied in hydrolysis reactions. This is not surprising because aromatic aldehydes can disproportionate in strongly alkaline solutions according to the well-known Cannizzaro reaction mechanism, especially during the long time exposure. To avoid this possible reactivity in an alkaline environment, the reaction time was reduced to three hours for the Reimer-Tiemann protocol. The next limitation or potentially a further development for both Reimer-Tiemann and Vilsmeier-Haack reactivity could be linked to the presence of a methyl group at the R position in the quinoline skeleton. The newly formed aldehydes can be reacted under base-catalyzed condensation reactions, such as the Perkin transformation, leading to styryl type compounds.

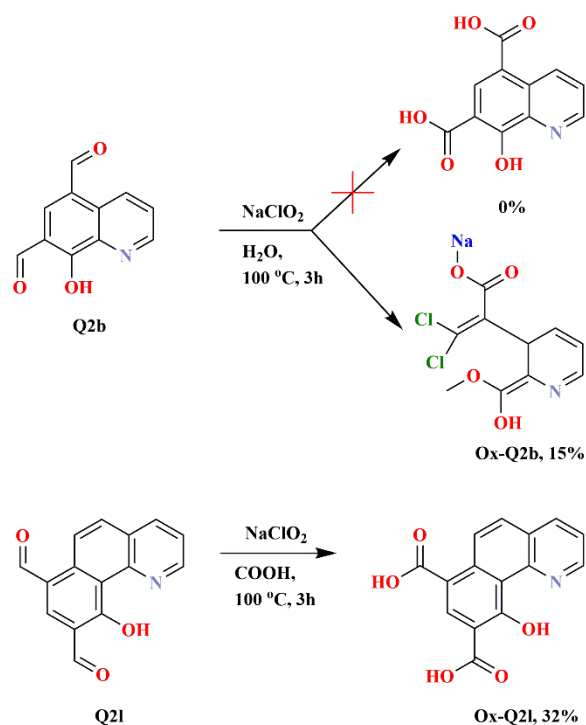
#### 6.4.2 Oxidation of selected diformyl quinolines. Hydroxy dicarboxylic acids

This thread discusses the oxidation of selected dicarbaldehydes in terms of selected hydroxy dicarboxylic acids. These studies aimed to present the methods of oxidation of *N*-heterocyclic derivatives and functionalization of dicarbaldehyde derivatives. Hydroxy



dicarboxylic acids is an intriguing topic of research and may be expected to produce more interesting results due to the carboxyl and hydroxyl groups' presence. Due to the place for donor power and excellent chelating properties related to the hydroxyl group's presence in the nitrogen atom's vicinity, the described elements are used as ligands in coordination chemistry and complexometric chemical processing<sup>237,238,239</sup>. On the other hand, the carboxyl group itself in the described acids' structure can undergo many chemical transformations and allow for further functionalization in the aqueous environment.

Chemical oxidation of the molecules 8-hydroxyquinoline-5,7-dicarbaldehyde (**Q2b**) and 10-hydroxy-benzo[*h*]quinoline-7,9-dicarbaldehyde (**Q2l**) (Scheme 76) was investigated. To test the possible limitations of the reaction, the aldehydes with different structures were chosen. The reaction was initially carried out under mild conditions at room temperature until gas evolution ceased and then at a temperature of 100 °C. The solvent used in the reaction was water for **Q2b** and formic acid for **Q2l**. The use of formic acid resulted from better solubility of the selected quinoline. Sodium chlorite was used as an oxidant in the reaction.



**Scheme 76.** Oxidation of molecules **Q2b** and **Q2l**.

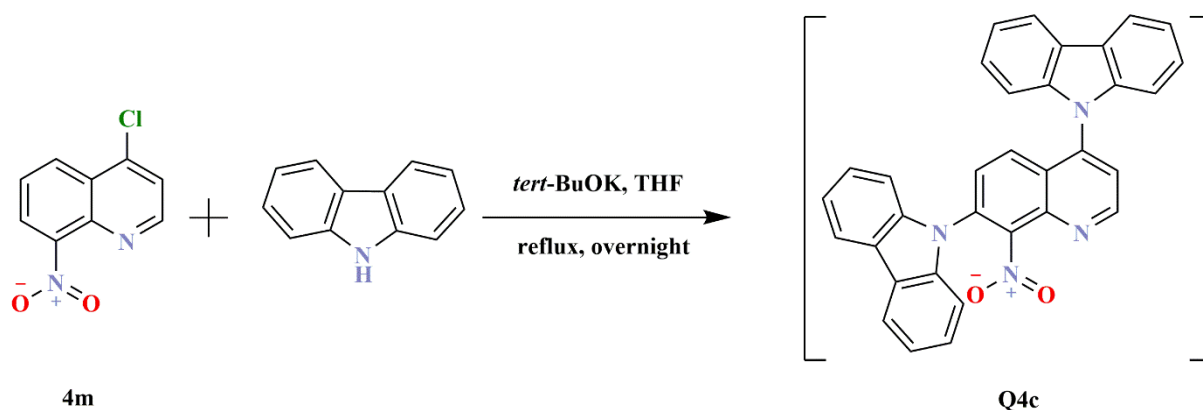
In the reaction of **Q2b** with sodium chlorite, the reaction was not towards a decent product. The reaction resulted in breaking the bond in the phenyl ring and further side reactions. This may be due to a different distribution of electron density, which influenced the compound itself's reactivity. The nitrogen atom's effect on the electron density is greater of

the phenyl ring directly attached to the pyridine ring than that of the compound, where the middle phenyl ring decomposes the electron density. The obtained products **Ox-Q2b** and **Ox-Q2l** were characterized by spectroscopy and by mass spectrometry.

The oxidation procedure has been optimized to improve the efficiency of the reaction. In the case of the sodium chlorate salt used, its use is not limited to carbonyl groups' oxidation. The great advantage of this reagent is the possibility of carrying out the reaction in an aqueous medium. This procedure was successfully used for the oxidation of 2,9-dimethyl-1,10-phenanthroline. These results are presented in a separate chapter on the oxidation of selected 1,10-phenanthroline (chapter 6.2.7).

## 6.5 VNS reaction in electron-deficient nitroquinolines

Another topic of the research was to get unsymmetric monosubstituted 1,10-phenanthroline. As a result of the series of reactions, a precursor of monosubstituted 1,10-phenanthrolines, i.e., 4-chloro-8-nitroquinoline (**4m**), was obtained. At this stage of the research, a planned series of reactions envisaged the substitution of activated chlorine for 4-chloro-8-nitroquinoline (**4m**, also in chapter 6.3, Scheme 72) by a selected amine. However, as the result of the reaction, the common substitution of activated chlorine occurs with the additional substitution of hydrogen atom (Scheme 77). The reaction mixture was very complicated. However, a product similar to 9,9'-(8-nitroquinoline-4,7-diyl)bis(9*H*-carbazole) (**Q4c**) as a result of VNS and  $S_NAr$  subsequent substitutions was identified. GC-MS's identified product is with  $t_r = 27.3$  min, (EI)  $M_+ = 508$  (100%), whose structure is similar to molecule **Q4c** and has an exact mass is 504 (Figure 60).



**Scheme 77.** The reaction between the potassium carbazol-9-ide and nitroquinolines **4m**.

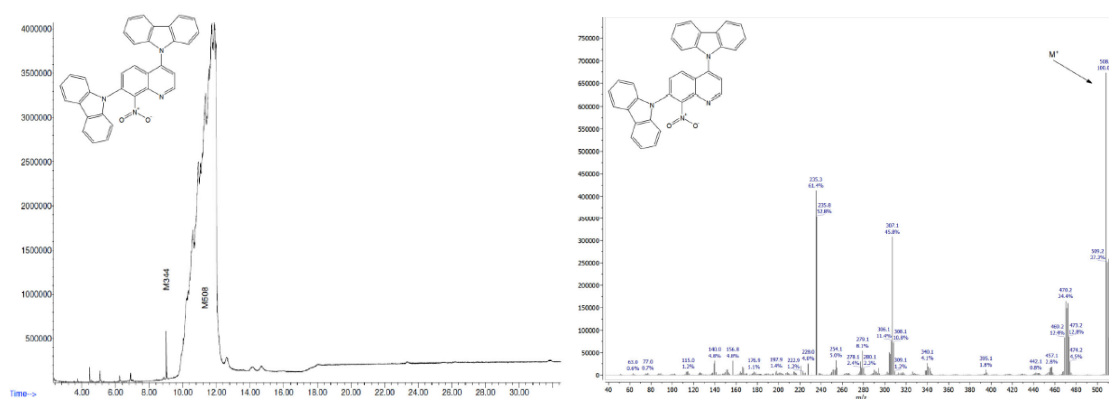


**Figure 63.** Chromatogram of the structure comparable to the molecule (left) and MS of the structure similar to molecule **Q4c** (right).

Additional studies on VNS reactions were performed in order to confirm the possible substitution of the hydrogen atom for selected nitroquinolines. The goal of performed studies was to understand this synthetic route. Only understanding the mechanism of a chemical reaction is an effective way to explore and plan more productive experiments, design new compounds or precursors for the purpose of the medicinal application, minimize the side-reactions, and increase the yield of target products. An additional advantage of research on VNS reactions is the ability to understand their mechanism deeply. Based on their mechanism, it may be possible to design reactions to exclude side reactions, which will be continued in further research.

Nitroquinoline derivatives **Q3a**, **Q3b**, and **Q3d** with the presence of hindered and non-hindered hydrogens in *ortho* and/or *para* positions were chosen in this studies.

The readily available aromatic hydrogen located in *ortho* and/or *para* position to the nitro group is the main requirement for the vicarious nucleophilic substitution from the starting material. The nitro group activates an aromatic ring to nucleophilic attack. Nucleophilic addition to carbon atoms of the nitroaromatics and heteroaromatics is a fast and reversible process<sup>120</sup>, during which negatively charged intermediates are created, i.e., the Meisenheimer complex (Scheme 78), with the stabilization of substituents via the delocalization of charge. Therefore, electron-withdrawing (EWG)-type substituents, especially the nitro group, are needed. The nucleophile's counterion, such as potassium cation, is attracted by the nitro group's negatively charged oxygen atoms (Scheme 78). The resulting adducts to restore the aromaticity have to lose hydride anions (Scheme 78). This process could be realized by

oxidation by external oxidants. N. J. Lawrence et al. suggests that the nitro group also plays a role in the oxidation processes<sup>121</sup>.

In this study, as a nucleophile, 9*H*-carbazole was chosen for the vicarious nucleophilic substitution of selected nitroquinolines. 9*H*-Carbazole has a special rigid planar structure and is a valuable building block for the synthesis of many products like drugs or innovative materials.

The commercially available 8-nitroquinoline **Q3a** and 9*H*-carbazole were initially selected to carry out the reaction to ascertain the mechanism and optimize conditions. According to previously reported data, the reaction of molecule **Q3a** was carried out with an excess (1.5 equiv.) of potassium carbazol-9-ide in THF solvent, which quickly turned red at reflux temperature. Crystalline 9-(8-nitroquinolin-7-yl)-9*H*-carbazole (**Q4a**) and (*Z*)-7-(9*H*-carbazol-9-yl)-8-(hydroxyimino)quinolin-5(8*H*)-one (**Q4b**) were isolated with low yield (Figures 64, 65 and Scheme 78).

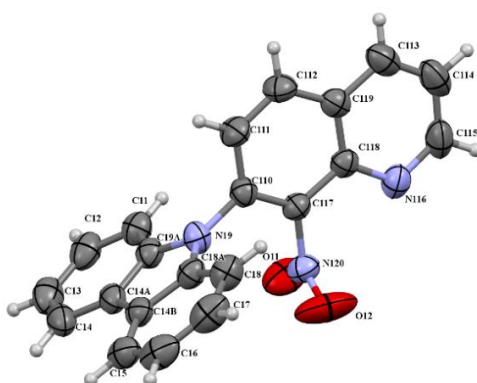


**Figure 64.** ORTEP drawings of compound **Q4a** with 30% probability.

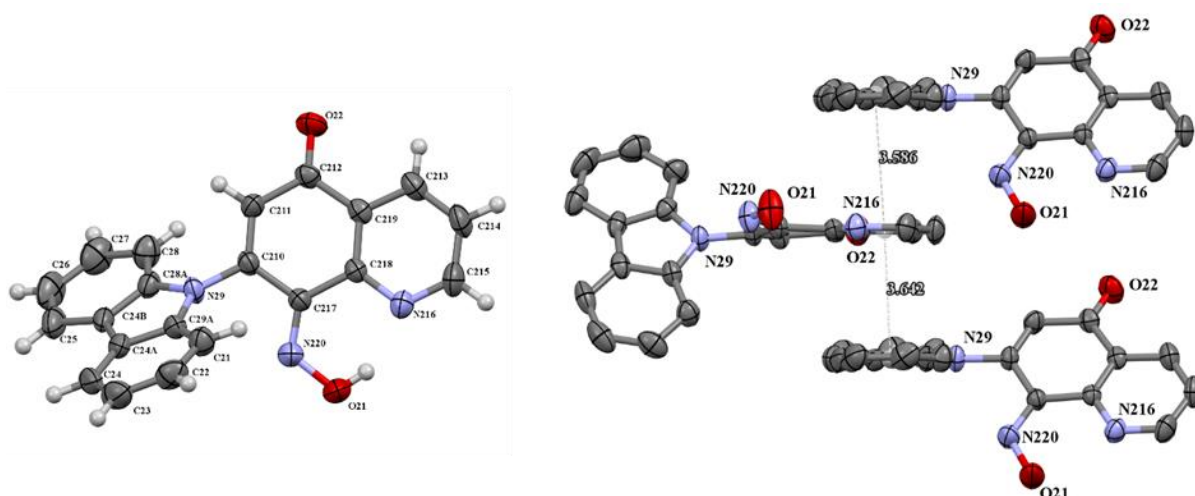
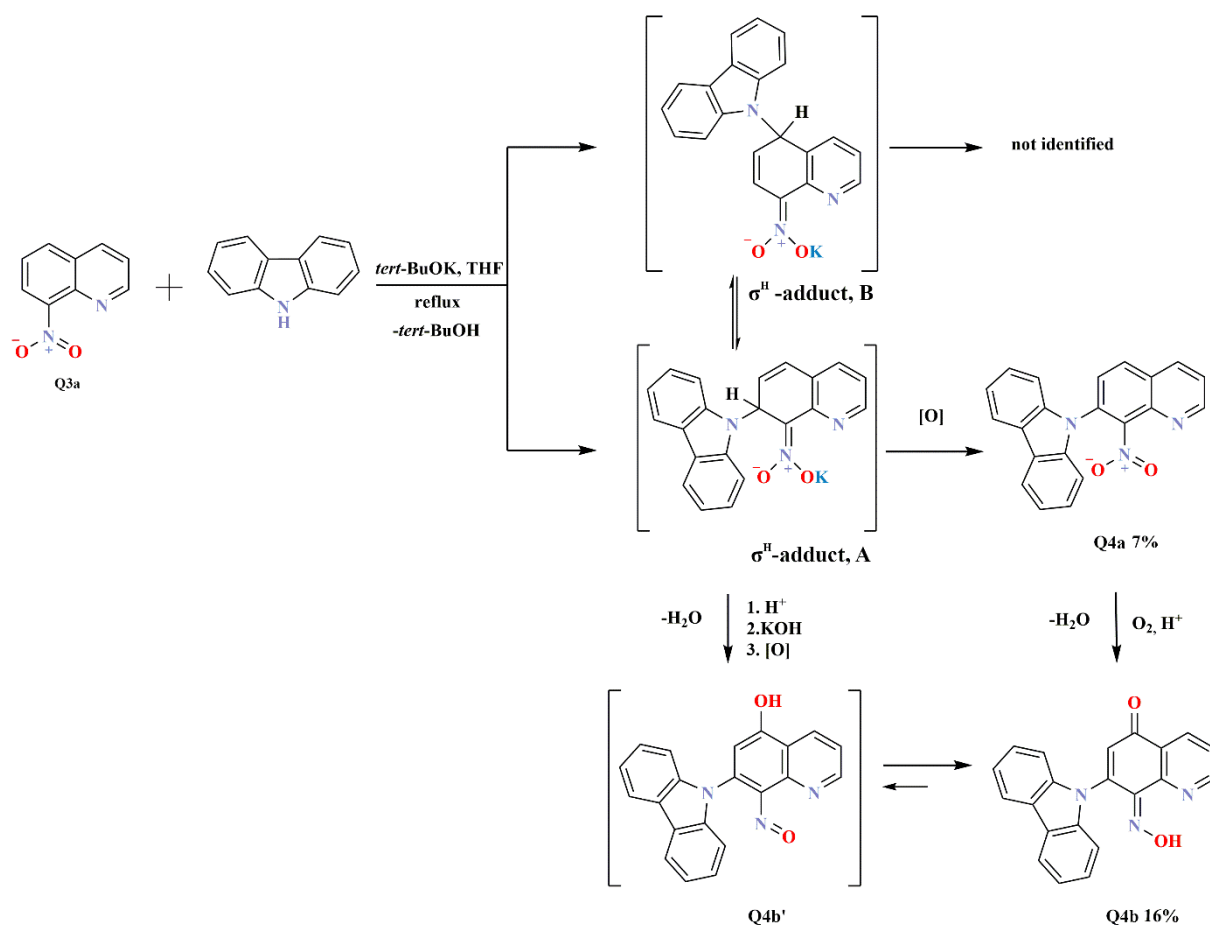


**Figure 65.** ORTEP drawings of compound **Q4b** with 30% probability (left). The  $\pi$ -stacking interactions in cell packing of compound **Q4b** (right).

At first sight, it is somewhat surprising that the vicarious nucleophilic substitution via nucleophilic displacement of aromatic hydrogen of molecule **Q4a** led to two products, both with the 9*H*-carbazolyl group located exclusively at the C7 position. The regiochemistry of this type of substitution is strongly affected by the size of the nucleophile. Because of the bulky nucleophile used, it was expected that a newly formed C-N bond would be formed rather in the C5 position than C7. This finding suggests the potassium counterion assists the interaction with the nitro group. A nucleophile's attack generates a Meisenheimer adduct ( $\sigma^H$ -adduct, **A** and **B**) followed by a loss of hydrogen to restore the aromaticity (Scheme 78). The molecule **Q4a** possesses at C7 position a newly-attached 9*H*-carbazolyl substituent in ortho location to nitro group (Scheme 78). The molecule **Q4b'** contains a hydroxyl group at C5 and nitroso substituent at the C8 position. The conversion of nitro to nitroso group is known in literature<sup>120,240</sup>.



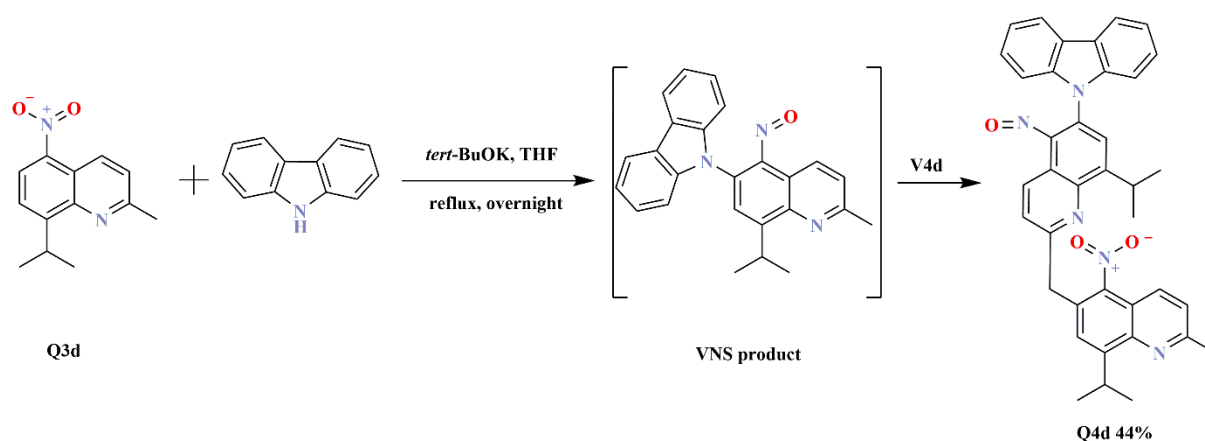
**Scheme 78.** Proposed mechanism of the reaction between the potassium carbazol-9-ide and 8-nitroquinoline **Q3a**.

The potassium carbazol-9-ide in THF was generated by potassium *tert*-butoxide and 9*H*-carbazole. The *in situ* generated *tert*-BuOH serves as a proton source (Scheme 78; step 1).

The nitro group at the C8 position in molecule **Q4a** or Meisenheimer adduct in protic media could be transformed into nitroso by protonation and the subsequent elimination of water. The origin of compound **Q4b'** requires both the transformation of the nitro group into nitroso and the presence of hydroxyl substituent (or carbonyl) at the C5 position. One explanation of the origin of the **Q4b'** could be the displacement of the potassium hydroxide from the Meisenheimer adduct in protic media (Scheme 78; step 2). The potassium hydroxide could attack Meisenheimer's nitrosophenyl ring at C5 position and form a hydroxyl group in nitroso adduct, followed by oxidation by oxygen from the air or nitro substituent to a carbonyl group (Scheme 78; step 3). E. A. Bucharova et al. showed the influence of substituents and medium on the tautomeric equilibrium between nitrosophenols and quinone oximes<sup>241</sup>. Another similar phenomenon is reported by I. R. Baxendale et al.<sup>242</sup>. A similar type of phenomenon between the nitroso adduct **Q4b'** and molecule **Q4b** was observed (Scheme 78).

The obtained compounds **Q4a**, **Q4b** based on the VNS reaction prove the VNS reaction for the derivative **Q3b** is possible as a competitive to S<sub>N</sub>Ar reaction (Scheme 77).

Another interesting example of a VNS reaction is the synthesis of 8-(iso-propyl)-2-methyl-5-nitroquinoline (**Q3d**, Scheme 79). The N-C<sub>Aryl</sub> bond formation via VNS reaction in 2-methylquinoline derivatives such as molecule **Q3d** is more complicated due to the acidic protons located on the methyl group C2 position<sup>243</sup>. Their presence in the quinoline constitution implicates a competition reaction between VNS N-C<sub>Aryl</sub> bond formation and a base attack at acidic protons located on the methyl group in C2 position. To synthesize the targeted 9-(8-isopropyl-2-methyl-5-nitrosoquinolin-6-yl)-9H-carbazole (**VNS product**; Scheme 79), a reaction was carried out where molecule **Q3d** was treated with excess (1.5 equiv.) potassium 9H-carbazol-9-ide in THF solvent at reflux temperature under the same reaction conditions as the above example. Molecule **Q3d** was chosen due to the presence of an easier diagnostic iso-propyl group. Unexpectedly a product of double VNS substitution 9-(8-isopropyl-2-((8-isopropyl-2-methyl-5-nitrosoquinolin-6-yl)methyl)-5-nitrosoquinolin-6-yl)-9H-carbazole (**Q4d**) was obtained. The formation of nitroso adduct observed was possible by the elimination of a water molecule, which is similar to the aforementioned mechanism of origin of **Q4b'** (Scheme 78). The origin of molecule **Q4d** can be explained by potassiation with potassium tert-butoxide followed by an intramolecular transfer of the 8-iso-propyl-2-methyl-5-nitroquinoline, which afforded molecule **Q4d** in 44% yield (Scheme 79). N. J. Lawrence et al. reported VNS reaction product as an intermediate react with various electrophiles<sup>121</sup>.



**Scheme 79.** The reaction between the potassium carbazol-9-ide and 8-isopropyl-2-methyl-5-nitroquinoline (**Q3d**).

These studies were performed by varying pH and solvent to examine their effect on the absorbance of molecule **Q4b** (Figure 67). Compound **Q4b** shows the ability to form a pseudoring, stabilized by an intramolecular hydrogen bond in solution, shown on  $^1\text{H-NMR}$  spectra as a signal from OH group (in  $\text{CDCl}_3$  solution 17.76 ppm, Figure 66). The phenomenon of forming a pseudo-ring, which was stabilized by an intramolecular hydrogen bond, was also observed before by M. Szala et al.<sup>244</sup>.

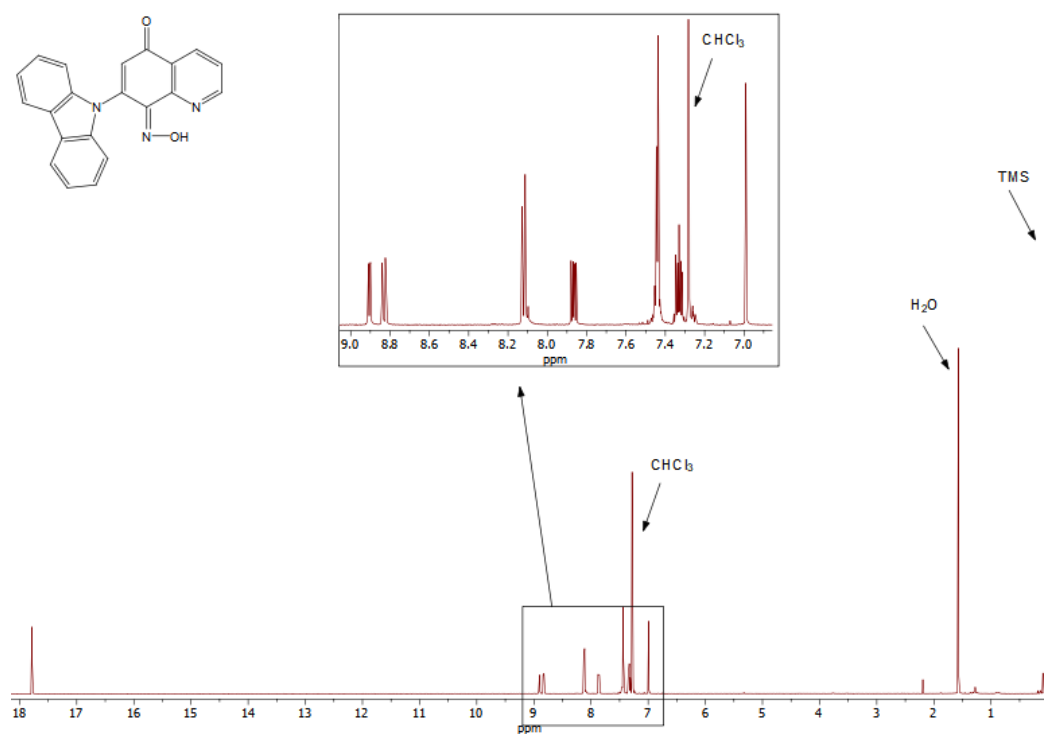


**Figure 66.**  $^1\text{H-NMR}$  ( $\text{CDCl}_3$ , 500.2 MHz) spectrum of **Q4b**.

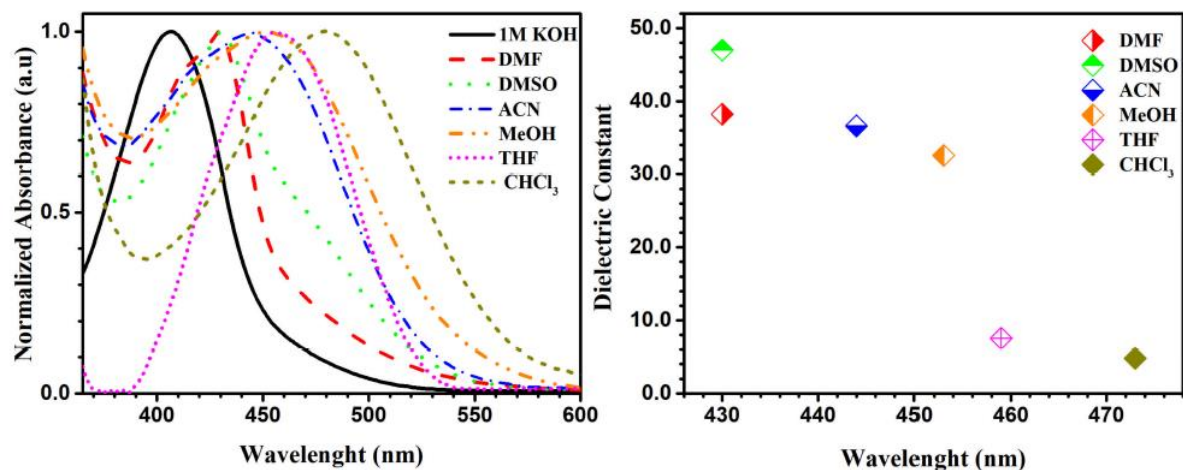


**Figure 67.** UV-Vis absorption spectra (left), the plot of the dielectric constant of solvent against wavelength of **Q4b** (right).

Additionally, the tautomerism between nitrosophenol **Q4b'** and quinine oxime **Q4b** forms presented in Scheme 78 could have an influence on absorption spectra. Figure 67 shows the graph confirming the presence of a pure anionic form of nitrosophenol **Q4b'** in 1 M KOH solution for studied molecule **Q4b** (black line). A similar tendency was observed for **Q4b** in dimethylformamide (DMF) solvent (red line). The  $\lambda_{\text{max}}$  value of compound **Q4b** in methanol in comparison with KOH and DMF solutions showed a bathochromic shift (red shift), which could be explained by the presence of hydrogen bonds between quinine oxime **Q4b** and methanol molecules (green dots). As expected, the increase of the number of hydrogen bonds between solute and more acidic  $\text{CHCl}_3$  leads to an increase in the wavelength of the absorption maxima of compound **Q4b**, which shifts bathochromically (intermittent blue line). The neutral DMSO and acetonitrile (ACN) solvents showed intermediate results. Longer wavelengths (bathochromic shift) with a decreased dielectric constant in the absorption band can be observed. Additionally, the dielectric dependence on the wavelength was presented in Figure 67.



## 7. Experimental

### 7.1 Experimental techniques and computational methods

- NMR analyzes were performed on a Bruker Avance 400 instrument (frequency 400.1 MHz for  $^1\text{H}$  NMR, 100 MHz for  $^{13}\text{C}$  NMR), Bruker Avance 500 (frequency 500.2 MHz for  $^1\text{H}$  NMR, 125 MHz for  $^{13}\text{C}$  NMR), Bruker Avance 600 (frequency 600.2 MHz for  $^1\text{H}$  NMR, 150 MHz for  $^{13}\text{C}$  NMR) and Bruker Avance 400WB; 100.65 MHz for  $^{13}\text{C}$  NMR, 40.55 MHz for  $^{15}\text{N}$ .
- The IR spectra were recorded on a Nicolet iS50 FTIR spectrometer was used for recording spectra in the IR range 4000–400  $\text{cm}^{-1}$ . FTIR spectra were recorded on a Perkin Elmer (Schwerzenbach, Switzerland) spectrophotometer in the spectral range 4000–450  $\text{cm}^{-1}$  with the samples in the form of KBr pellets. spectrometer in the range of 4000–400  $\text{cm}^{-1}$  using the KBr pellet technique,
- UV-Vis spectra were made on the Nicolet iS50 spectrometer in the range of 200–800 nm,
- HRMS measurements were made on a Synapt G2-Si mass spectrometer (Waters, New Castle, DE USA) equipped with an ESI source and quadrupole-time-of-flight mass analyser,
- The LCMS-IT-TOF analysis was performed on an Agilent 1200 Series binary LC system coupled to a micrOTOF-Q system mass spectrometer (Bruker Daltonics, Bremen, Germany).
- Elementary analysis was performed using Vario EL III apparatus (Elementar, Langensfeld, Germany).
- X-ray structure analysis was performed on an Oxford Diffraction Gemini A Ultra diffractometer for Mo K alpha and Cu K alpha radiation and a CryoJet attachment to maintain a constant sample temperature using the CrysAlisPro package,
- Melting points were determined on MPA100 OptiMelt melting point apparatus (Stanford Research Systems, Sunnyvale, CA USA) and are uncorrected.
- **Electrochemical tests:** Cyclic voltammetry was measured on a PGSTAT 12 Autolab potentiostat (Ecochemie, Utrecht, NL) in 0.1 M TBAPF<sub>6</sub> solution in acetonitrile (anhydrous, Sigma-Aldrich, the content of H<sub>2</sub>O < 0.001%, supplied under argon) or dimethylsulfoxide (DMSO, the content of H<sub>2</sub>O < 0.005%, Sigma-Aldrich). An Ag|AgCl| 1M LiCl reference electrode was separated from the examined solution by a salt bridge. The working and auxiliary electrodes were a glassy carbon electrode (diameter 0.7 mm, 0.9 mm) and a platinum wire, respectively. Values of voltammetric faradaic current were obtained by subtracting capacitance current from the total peak current<sup>204</sup>. The semi-integration of linear sweep voltammograms (convolution voltammetry) was performed in accordance with literature<sup>204,219,220</sup> and the semi-integrated currents  $I$  were obtained from the equation  $I = \pi^{-1/2} \int_0^t (I(v) / (t-v)^{1/2}) dv$ , where  $v$  is an integration variable, and  $t$  is related to the potential through the

scan rate. The logarithmic (log-plot) analysis ( $\log(I/I_{\text{lim}}-I)$  vs.  $E$ ) of semi-integrated currents were obtained according to the procedure described for the steady-state waves in order to obtain the parameters (slope) of the dependence  $E = E_{1/2} + RT/nF \ln(I/I_{\text{lim}}-I)^{204}$ . All electrochemical measurements were performed on a PGSTAT 12.

- **Quantum-mechanical calculations (DFT):** DFT calculations were performed for the selected compounds, including the optimization of the geometry of the molecules, their HOMO and LUMO orbitals, as well as energy gaps ( $E_g$ ) were determined. The Spartan '14, v.1.1.8 software (Wavefunction, Inc. USA) was used for the calculations, using the B3LYP functional with the 6-31G\* basis set. The theoretical calculations of IR spectra in vacuum were performed using the DFT employing the B3LYP, EDF2 functional and 6-31G\* basis set.

For Figure 53 and 54 (**Hyd-5i** and **Hyd-5m**) the calculations were done with the use of the density functional theory (DFT) and were carried out using the Gaussian09 program<sup>245</sup> on B3LYP/6-31g++ level<sup>246,247</sup>. Molecular geometry of the singlet ground state of the compounds was optimized in the gas phase.

- **UV-Vis and IR spectroelectrochemistry:** Measurements were carried out using an optically transparent thin-layer electrode cell<sup>248</sup>. The cell contains a three-electrode system (Ag/AgCl reference electrode) mounted in a thin layer (thickness 0.18 mm) between optical windows ( $\text{CaF}_2$ ). A  $5 \times 5 \text{ mm}^2$  of sufficiently optically transparent platinum gauze (80 mesh) was used as the working electrode, and its polarity was changed at  $5 \text{ mV} \cdot \text{s}^{-1}$  rate. Absorption spectra during the electrolysis were registered using an Agilent 8453 diode-array UV-Vis spectrometer. A Nicolet iS50 FTIR spectrometer was used for recording spectral changes in the IR 4000–1000  $\text{cm}^{-1}$  range in the same spectroelectrochemical cell with 0.09  $\text{cm}^{-1}$  spectral resolution.
- **CP-MAS in solid state NMR:** The CP MAS technique is based on a phenomenon that uses high detection sensitivity and proton polarizability (or, in fact, their high energy) to detect low-sensitivity nuclei. In this study, it was the  $^{13}\text{C}$  MAS stands for NMR techniques used in solid state measurements using the sample rotation at a magic angle of  $54^\circ 44.1'$ , relative to the magnetic field lines  $B_0$ . In practice, this means that for the  $^{13}\text{C}$  nuclei bound with protons for the CP technique, more intense signals should be observed.

## 7.2 Materials

In this work, the reagents of the following companies were used: Sigma-Aldrich, Avantor (POCH), Acros, Chempur.

**Solvents:** methylene chloride, chloroform, acetone, hexane, tetrahydrofuran, dimethylformamide, toluene, ethyl alcohol, methyl alcohol, dimethyl sulfoxide, acetonitrile, acetone, diphenyl ether.

**Specialized reagents:**

Sigma Aldrich (Poznan, Poland): Sodium hydride (dry, 95%), trimethyl orthoformate, triethyl orthoformate, triethyl orthoacetate, trimethyl orthoacetate, 1,10-phenanthroline (**Phen**), 2,9-dimethyl-1,10-phenanthroline (**Phen-2CH<sub>3</sub>**), 9*H*-carbazole, pyrrolidine, 10*H*-phenothiazine, Meldrum's acid, benzene-1,2-diamine (**1a**), 4-fluorobenzene-1,2-diamine (**1b**; to obtain **2-4b,g**), 4-chlorobenzene-1,2-diamine (**1c**), 4-methylbenzene-1,2-diamine (**1d**), 3,4-diaminobenzonitrile (**1e**), 4-bromobenzene-1,2-diamine (**1f**), 3,4-diaminobenzoic acid (**1g**), 2-nitroaniline (**1m**) and quinolin-8-amine (**1n**) were purchased from Sigma–Aldrich (Poznan, Poland), and were used without further purification.

Hexamethylenetetramine (HMTA), 8-hydroxyquinoline (**Q1a**), 5,7-dibromo-2-methylquinolin-8-ol (**Q1d**), 2-methylquinolin-8-ol (**Q1h**), and benzo[*h*]quinolin-10-ol (**Q1j**) were purchased from Sigma–Aldrich (Poznan, Poland), and were used without further purification.

5-chloroquinolin-8-ol (**Q1b**), methylquinolin-8-ol (**Q1c**), *N,N*,2-trimethylquinolin-6-amine (**Q1e**), *N,N*-dimethylquinolin-6-amine (**Q1f**), quinolin-6-ol (**Q1h**), and *N,N*-dimethylquinolin-8-amine (**Q1i**) were synthesized according to the procedures described in the literature<sup>249,250,251,252</sup>. The 8-(iso-propyl)-2-methylquinoline (**Q1k**) were synthesized according to the literature<sup>253</sup>.

Solvents were dried by usual methods (diphenyl ether, diethyl ether and THF over benzophenone ketyl, CHCl<sub>3</sub> and CH<sub>2</sub>Cl<sub>2</sub> over P<sub>4</sub>O<sub>10</sub>, hexane over sodium-potassium alloy and DMF over molecular sieves) and distilled. Chromatographic purification was carried out on silica gel 60 (0.15–0.3 mm, Macherey-Nagel GmbH & Co. KG, Düren, Germany).

2,2,2-Trifluoroacetic acid (Caution! TFA is a known nigrostriatal neurotoxin, and therefore compounds of this class should be handled using disposable gloves in a properly ventilated hood).

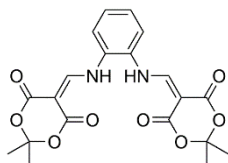
## 7.3 General Procedures for Synthesis of 4,7-dichloro-1,10-phenanthrolines

These syntheses were based on procedures described in the literature<sup>39,40</sup>. Due to the multi-stage synthesis reactions, they have been divided into three separate steps: Step A, Step B, and Step C.

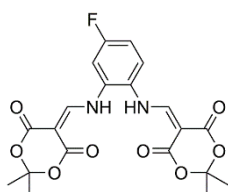
### 7.3.1 Step A

Triethyl orthoformate or trimethyl orthoformate were used in the synthesis of **2a**, **2b**, **2c**, **2d**, **2e**, and triethyl orthoacetate or trimethyl orthoacetate for **2f**, **2g**, **2h**, **2i**, **2j**, **2k**, **2l**. The orthoester (triethyl orthoformate, triethyl orthoacetate, trimethyl orthoformate or trimethyl orthoacetate, 330.0 mmol) and Meldrum's acid (1.7 g, 12.0 mmol) was brought to gentle reflux for 15 min. The resulting greenish solution was cooled to 80 °C, and the appropriate benzene-1,2-diamine **1** (5.5 mmol) was added portionwise (caution: exothermic reaction). The resulting mixture was stirring up to reflux for 2

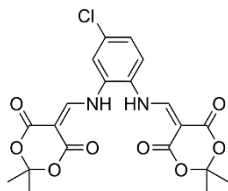
h, and left under r.t. for 16 h. Subsequently, diethyl ether or hexane was added, and the solution was cooled to  $-35\text{ }^{\circ}\text{C}$ , where a precipitate formed. The precipitate was filtered off, washed with diethyl ether (4 x 100 mL), and dried to afford a solid:



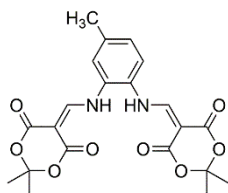
**1,2-Bis-[(2,2-dimethyl-4,6-dioxo-1,3-dioxan-5-ylidene)methyl]amino]benzene (2a)**<sup>40,254</sup>, white solid 2.0 g (4.7 mmol, 86%); m.p<sub>dec.</sub> = 207.6  $^{\circ}\text{C}$ .



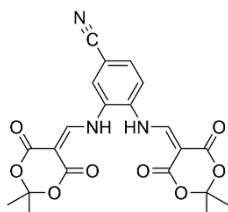
**5,5'-(((4-Fluoro-1,2-phenylene)bis(azanediyl))bis(methaneylylidene))bis(2,2-dimethyl-1,3-dioxane-4,6-dione) (2b)**; white; 2.0 g (4.6 mmol, 83%); m.p<sub>dec.</sub> = 216  $^{\circ}\text{C}$ ;  $^1\text{H-NMR}$  ( $\text{CDCl}_3$ ; 400.2 MHz)  $\delta$  = 1.73 (s, 6H, 2CH<sub>3</sub>), 1.74 (s, 6H, 2CH<sub>3</sub>), 7.06–7.12 (dt,  $^3J_{\text{H,H}}$  = 8.1 Hz,  $^4J_{\text{F,H}}$  = 2.6 Hz, 1H, aromatic), 7.20 (dd,  $^3J_{\text{F,H}}$  = 8.7 Hz,  $^4J_{\text{F,H}}$  = 2.5 Hz, 1H, aromatic), 7.38 (dd,  $^3J_{\text{F,H}}$  = 8.9 Hz,  $^3J_{\text{H,H}}$  = 5.1 Hz, aromatic), 8.38 (d,  $^3J_{\text{H,H}}$  = 13.5 Hz, 1H, vinyl), 8.52 (d,  $^3J_{\text{H,H}}$  = 13.4 Hz, 1H, vinyl), 11.15 (d,  $^3J_{\text{H,H}}$  = 13.5 Hz, 1H, NH), 11.42 (d,  $^3J_{\text{H,H}}$  = 13.3 Hz, 1H, NH);  $^{13}\text{C}\{^1\text{H}\}\text{-NMR}$  ( $\text{CDCl}_3$ ; 125.78 MHz)  $\delta$  = 27.2, 27.3, 89.6, 90.3, 105.8 (d,  $^3J_{\text{C,F}}$  = 14.3 Hz), 107.4 (d,  $^2J_{\text{C,F}}$  = 26.8 Hz), 115.0 (d,  $^2J_{\text{C,F}}$  = 22.9 Hz), 124.9 (d,  $^4J_{\text{C,F}}$  = 9.5 Hz), 126.9, 133.3 (d,  $^3J_{\text{C,F}}$  = 10.1 Hz), 161.1, 155.1 (d,  $^1J_{\text{C,F}}$  = 342.9 Hz), 162.9, 163.2, 165.4, 165.5;  $^{19}\text{F}\{^1\text{H}\}\text{-NMR}$  ( $\text{CDCl}_3$ ; 470.5 MHz)  $\delta$  = -108.94;  $^{19}\text{F-NMR}$  ( $\text{CDCl}_3$ ; 470.5 MHz)  $\delta$  = -108.94 (dd,  $^3J_{\text{F,H}}$  = 12.9 Hz,  $^3J_{\text{F,H}}$  = 7.8 Hz); UV-Vis (methanol;  $\lambda$  [nm] (log $\epsilon$ )): 329 (4.48), 292 (4.56), 212 (4.43).



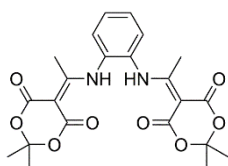
**5,5'-(((4-Chloro-1,2-phenylene)bis(azanediyl))bis(methaneylylidene))bis(2,2-dimethyl-1,3-dioxane-4,6-dione) (2c)**<sup>40</sup>; white; 2.1 g (4.6 mmol, 84%); m.p<sub>dec.</sub> = 202.7  $^{\circ}\text{C}$ ; UV-Vis (methanol;  $\lambda$  [nm] (log $\epsilon$ )): 332 (4.59), 296 (4.75), 223 (4.47), 206 (4.46).



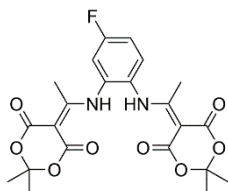
**5,5'-(((4-Methyl-1,2-phenylene)bis(azanediyl))bis(methaneylylidene))bis(2,2-dimethyl-1,3-dioxane-4,6-dione) (2d)**; white; 2.2 g (5.2 mmol, 94%)<sup>265</sup>; m.p<sub>dec.</sub> = 212 °C; UV-Vis (methanol;  $\lambda$  [nm] (log $\epsilon$ )): 330 (4.85), 296 (4.93), 221 (4.83).



**3,4-Bis(((2,2-dimethyl-4,6-dioxo-1,3-dioxan-5-ylidene)methyl)amino)benzonitrile (2e)**; beige, 1.7 g (3.8 mmol, 69%); m.p<sub>dec.</sub> = 250 °C; <sup>1</sup>H-NMR (DMSO-*d*<sub>6</sub>; 400.2 MHz)  $\delta$  = 1.68 (s, 6H, 2CH<sub>3</sub>), 1.68 (s, 6H, 2CH<sub>3</sub>), 7.81-7.84 (m, 2H, aromatic), 8.16 (dd, <sup>3</sup>*J*<sub>H,H</sub> = 4.3 Hz, <sup>4</sup>*J*<sub>H,H</sub> = 0.8 Hz, 1H, aromatic), 8.33 (d, <sup>3</sup>*J*<sub>H,H</sub> = 14.1 Hz, 1H, vinyl), 8.41 (d, <sup>3</sup>*J*<sub>H,H</sub> = 13.9 Hz, 1H, vinyl), 11.33 (d, <sup>3</sup>*J*<sub>H,H</sub> = 14.1 Hz, 1H, NH), 11.43 (d, <sup>3</sup>*J*<sub>H,H</sub> = 14.0 Hz, 1H, NH); <sup>13</sup>C{<sup>1</sup>H}-NMR (DMSO-*d*<sub>6</sub>; 125.8 MHz) = 26.5, 26.6, 88.3, 88.8, 104.1, 104.3, 110.0, 117.4, 122.7, 128.0, 132.0, 133.6, 137.5, 155.6, 157.4, 162.3, 162.5, 163.5, 163.6; UV-Vis (methanol;  $\lambda$ [nm] (log $\epsilon$ )): 342 (4.11), 296 (4.19), 219 (4.00).

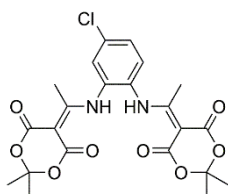


**5,5'-((1,2-Phenylenebis(azanediyl))bis(ethan-1-yl-1-ylidene))bis(2,2-dimethyl-1,3-dioxane-4,6-dione) (2f)**<sup>39,40</sup>; white; 1.2 g (2.8 mmol, 51%); m.p<sub>dec.</sub> = 189.6 °C.

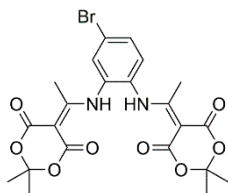


**5,5'-(((4-Fluoro-1,2-phenylene)bis(azanediyl))bis(ethan-1-yl-1-ylidene))bis(2,2-dimethyl-1,3-dioxane-4,6-dione) (2g)**; white, 0.9 g (2.0 mmol, 36%); m.p<sub>dec.</sub> = 218.0 °C; <sup>1</sup>H-NMR (CDCl<sub>3</sub>; 400.2 MHz)  $\delta$  = 1.70 (s, 6H, 2CH<sub>3</sub>), 1.71 (s, 6H, 2CH<sub>3</sub>), 2.50 (s, 3H, CH<sub>3</sub>), 2.58 (s, 3H, CH<sub>3</sub>), 7.12 (dd, <sup>3</sup>*J*<sub>H,F</sub> = 8.2 Hz, <sup>4</sup>*J*<sub>H,H</sub> = 2.3 Hz, 1H, aromatic), 7.18-7.20 (m, 1H, aromatic), 7.35 (dd, <sup>3</sup>*J*<sub>H,F</sub> = 8.7 Hz, <sup>3</sup>*J*<sub>H,H</sub> =

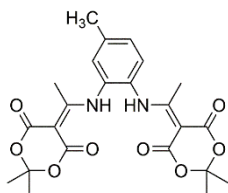
5.4 Hz, 1H, aromatic), 12.68 (s, 1H, NH), 12.85 (s, 1H, NH);  $^{13}\text{C}\{^1\text{H}\}$ -NMR ( $\text{CDCl}_3$ ; 125.8 MHz)  $\delta$  = 19.6, 19.7, 26.7, 26.7, 87.6, 88.0, 103.4, 103.5, 115.4 (d,  $^2J_{\text{C,F}} = 24.8$  Hz), 116.4 (d,  $^2J_{\text{C,F}} = 22.4$  Hz), 128.5 (d,  $^4J_{\text{C,F}} = 3.7$  Hz), 129.7 (d,  $^3J_{\text{C,F}} = 9.5$  Hz), 134.1 (d,  $^3J_{\text{C,F}} = 10.3$  Hz), 161.8 (d,  $^1J_{\text{C,F}} = 252.9$  Hz), 162.3, 162.5, 167.7, 167.6, 172.8, 173.5;  $^{19}\text{F}\{^1\text{H}\}$ -NMR ( $\text{CDCl}_3$ ; 470.5 MHz)  $\delta$  = -108.53;  $^{19}\text{F}$ -NMR ( $\text{CDCl}_3$ ; 470.5 MHz)  $\delta$  = -108.53 (dd,  $^3J_{\text{F,H}} = 13.3$  Hz,  $^4J_{\text{F,H}} = 7.7$  Hz); UV-Vis (methanol;  $\lambda$  [nm] ( $\log\epsilon$ )): 311 (4.30), 283 (4.66), 226 (4.38), 201 (4.27).



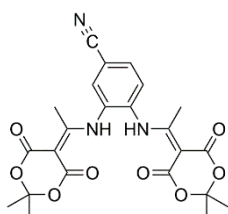
**5,5'-(((4-Chloro-1,2-phenylene)bis(azanediyl))bis(ethan-1-yl-1-ylidene))bis(2,2-dimethyl-1,3-dioxane-4,6-dione) (2h)**; white, 1.4 g (2.9 mmol, 52%); m.p.<sub>dec.</sub> = 203.8 °C;  $^1\text{H}$ -NMR ( $\text{CDCl}_3$ ; 400.2 MHz)  $\delta$  = 1.71 (s, 12H, 4CH<sub>3</sub>), 2.53 (s, 3H, CH<sub>3</sub>), 2.56 (s, 3H, CH<sub>3</sub>), 7.30 (d,  $^3J_{\text{H,H}} = 8.5$  Hz, 1H, aromatic), 7.38 (d,  $^4J_{\text{H,H}} = 1.6$  Hz, 1H, aromatic), 7.48 (dd,  $^3J_{\text{H,H}} = 8.5$  Hz,  $^4J_{\text{H,H}} = 1.8$  Hz, 1H, aromatic), 12.76 (s, 1H, NH), 12.81 (s, 1H, NH);  $^{13}\text{C}\{^1\text{H}\}$ -NMR ( $\text{CDCl}_3$ ; 100.5 MHz)  $\delta$  = 19.7, 19.7, 26.7, 87.9, 88.0, 103.5, 103.5, 128.1, 129.0, 129.5, 131.1, 133.6, 135.0, 162.3, 162.4, 167.7, 167.7, 173.0, 173.1; UV-Vis (methanol;  $\lambda$  [nm] ( $\log\epsilon$ )): 315 (4.36), 285 (4.74), 226 (4.46), 202 (4.38).



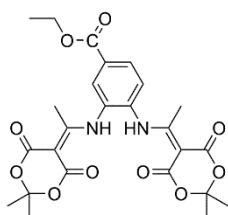
**5,5'-(((4-Bromo-1,2-phenylene)bis(azanediyl))bis(ethan-1-yl-1-ylidene))bis(2,2-dimethyl-1,3-dioxane-4,6-dione) (2i)**; white, 0.9 g (1.8 mmol, 32%); m.p.<sub>dec.</sub> = 204.6 °C;  $^1\text{H}$ -NMR ( $\text{CDCl}_3$ ; 400.2 MHz)  $\delta$  = 1.71 (s, 12H, 4CH<sub>3</sub>), 2.53 (s, 3H, CH<sub>3</sub>), 2.56 (s, 3H, CH<sub>3</sub>), 7.23 (d,  $^3J_{\text{H,H}} = 8.5$  Hz, 1H, aromatic), 7.53 (d,  $^4J_{\text{H,H}} = 1.5$  Hz, 1H, aromatic), 7.63 (dd,  $^3J_{\text{H,H}} = 8.5$  Hz,  $^4J_{\text{H,H}} = 1.7$  Hz, 1H, aromatic), 12.76 (s, 1H, NH), 12.81 (s, 1H, NH);  $^{13}\text{C}\{^1\text{H}\}$ -NMR ( $\text{CDCl}_3$ ; 125.78 MHz)  $\delta$  = 19.6, 19.7, 26.6, 87.7, 87.8, 103.4, 103.4, 122.3, 129.1, 131.0, 131.6, 132.4, 133.7, 162.2, 162.3, 167.5, 172.9; UV-Vis (methanol;  $\lambda$  [nm] ( $\log\epsilon$ )): 313 (4.29), 284 (4.65), 226 (4.38), 201 (4.37).



**5,5'-(((4-Methyl-1,2-phenylene)bis(azanediyl))bis(ethan-1-yl-1-ylidene))bis(2,2-dimethyl-1,3-dioxane-4,6-dione) (2j)**; white, 1.3 g (2.9 mmol, 52%); m.p<sub>dec.</sub> = 204.2 °C; <sup>1</sup>H-NMR (CDCl<sub>3</sub>; 400.2 MHz) δ = 1.70 (s, 12H, 4CH<sub>3</sub>), 2.45 (s, 3H, CH<sub>3</sub>), 2.51 (s, 3H, CH<sub>3</sub>), 2.52 (s, 3H, CH<sub>3</sub>), 7.17 (s, 1H, aromatic), 7.23 (d, <sup>3</sup>J<sub>H,H</sub> = 8.1 Hz, 1H, aromatic), 7.30 (d, <sup>3</sup>J<sub>H,H</sub> = 8.3 Hz, 1H, aromatic), 12.68 (s, 1H, NH), 12.71 (s, 1H, NH); <sup>13</sup>C{<sup>1</sup>H}-NMR (CDCl<sub>3</sub>; 125.78 MHz) δ = 19.6, 19.6, 21.2, 26.6, 87.1, 87.2, 103.2, 127.7, 128.5, 129.8, 130.1, 132.2, 140.1, 162.5, 162.5, 167.6, 173.2, 173.4; UV-Vis (methanol; λ [nm] (logε)): 319 (4.12), 283 (4.60), 227 (4.38), 203 (4.23).

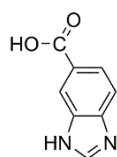


**3,4-Bis((1-(2,2-dimethyl-4,6-dioxo-1,3-dioxan-5-ylidene)ethyl)amino)benzonitrile (2k)**; white, 1.0 g (2.2 mmol, 40%); m.p<sub>dec.</sub> = 205.6 °C; <sup>1</sup>H-NMR (CDCl<sub>3</sub>; 400.2 MHz) δ = 1.72 (bs, 12H, 4CH<sub>3</sub>), 2.55 (s, 3H, CH<sub>3</sub>), 2.61 (s, 3H, CH<sub>3</sub>), 7.49 (d, <sup>3</sup>J<sub>H,H</sub> = 8.2 Hz, 1H, aromatic), 7.68 (s, 1H, aromatic), 7.78 (d, <sup>3</sup>J<sub>H,H</sub> = 8.2 Hz, 1H, aromatic), 12.87 (s, 1H, NH), 13.04 (s, 1H, NH); <sup>13</sup>C{<sup>1</sup>H}-NMR (CDCl<sub>3</sub>; 125.8 MHz) δ = 19.7, 19.9, 26.8, 26.8, 88.6, 89.0, 103.7, 103.7, 112.7, 116.7, 128.2, 131.6, 132.6, 133.1, 136.9, 162.1, 162.2, 167.7, 167.7, 172.2, 172.9; UV-Vis (methanol; λ [nm] (logε)): 324 (4.27), 289 (4.58), 224 (4.40), 204 (4.40).



**Ethyl 3,4-bis((1-(2,2-dimethyl-4,6-dioxo-1,3-dioxan-5-ylidene)ethyl)amino)benzoate (2l)**; white, 0.9 g (1.7 mmol, 31%); m.p<sub>dec.</sub> = 171.4 °C; <sup>1</sup>H-NMR (CDCl<sub>3</sub>; 400.2 MHz) δ = 1.42 (t, <sup>3</sup>J<sub>H,H</sub> = 7.0 Hz, 3H, CH<sub>3</sub>), 1.71 (s, 6H, 2CH<sub>3</sub>), 1.72 (s, 6H, 2CH<sub>3</sub>), 2.54 (s, 3H, CH<sub>3</sub>), 2.59 (s, 3H, CH<sub>3</sub>), 4.43 (q, <sup>3</sup>J<sub>H,H</sub> = 7.1 Hz, 2H, OCH<sub>2</sub>), 7.43 (d, <sup>3</sup>J<sub>H,H</sub> = 8.2 Hz, 1H, aromatic), 8.02 (s, 1H, aromatic), 8.15 (d, <sup>3</sup>J<sub>H,H</sub> = 8.1 Hz, 1H, aromatic), 12.82 (s, 1H, NH), 12.95 (s, 1H, NH); <sup>13</sup>C{<sup>1</sup>H}-NMR (CDCl<sub>3</sub>; 125.8 MHz) δ = 14.4, 19.7, 19.9, 26.7, 26.7, 62.1, 87.9, 88.3, 103.5, 103.5, 127.5, 129.2, 130.2, 131.2, 132.2, 136.3,

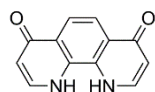
162.3, 162.4, 164.4, 167.7, 172.6, 173.3; UV-Vis (methanol;  $\lambda$  [nm] ( $\log\epsilon$ )): 321 (4.25), 287 (4.63), 225 (4.44), 204 (4.35).



**1H-benzo[d]imidazole-6-carboxylic acid**; m.p<sub>dec.</sub> = 278.0-280.0 °C; <sup>1</sup>H-NMR (DMSO-*d*<sub>6</sub>/KOD; 500.2 MHz)  $\delta$  = 7.74 (d, 3J<sub>H,H</sub> = 8.7 Hz, 1H, aromatic), 7.96 (d, 3J<sub>H,H</sub> = 8.7 Hz, 4J<sub>H,H</sub> = 1.4 Hz, 1H, aromatic), 8.23 (s, 1H, aromatic), 9.08 (s, 1H, aromatic); <sup>1</sup>H-NMR (D<sub>2</sub>O/KOD; 500.2 MHz)  $\delta$  = 7.66 (d, <sup>3</sup>J<sub>H,H</sub> = 8.5 Hz, 1H, aromatic), 7.81 (dd, <sup>3</sup>J<sub>H,H</sub> = 8.5 Hz, <sup>4</sup>J<sub>H,H</sub> = 1.5 Hz, 1H, aromatic), 8.21 (s, 1H, aromatic), 8.36 (s, 1H, aromatic); <sup>13</sup>C{<sup>1</sup>H}-NMR (DMSO-*d*<sub>6</sub>/KOD; 125.8 MHz)  $\delta$  = 116.0, 117.9, 128.4, 130.4, 132.1, 135.0, 143.1, 170.8; <sup>13</sup>C{<sup>1</sup>H}-NMR (D<sub>2</sub>O/KOD; 125.8 MHz)  $\delta$  = 115.3 (bs), 118.3 (bs), 123.8, 124.8, 144.7, 168.4; HRMS (IT TOF): m/z Calcd for C<sub>8</sub>H<sub>7</sub>N<sub>2</sub>O<sub>2</sub> [M + H]<sup>+</sup> = 163.0508, Found 163.0509.

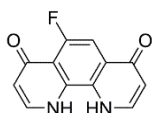
### 7.3.2 Step B

Modifications to existing procedures described in the literature<sup>39,40</sup> rely on purifications. The crude products were extracted with hexane or toluene at the Soxhlet apparatus. Into freshly distilled diphenyl ether (50 mL) at 240 °C was added compound **2** (10.0 mmol) in small portions, resulting in vigorous gas evolution. The resulting orange solution was brought to reflux for 30 min and was then allowed to cool to 70 °C. The acetone or hexane (25 mL) was added, and a dark-brown solid precipitated was filtered, washed with acetone (2 x 10 mL). The crude product was extracted with hexane or toluene at Soxhlet apparatus to yield solid as follows:

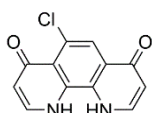


**1,10-Dihydro-1,10-phenanthroline-4,7-dione (3a)**<sup>256</sup>; brown; 1.4 g (6.8 mmol, 68%); m.p<sub>dec.</sub> > 350 °C; <sup>1</sup>H-NMR (CD<sub>3</sub>OD/KOD/D<sub>2</sub>O; 400.2 MHz)  $\delta$  = 6.62 (d, <sup>3</sup>J<sub>H,H</sub> = 5.6 Hz, 2H, aromatic), 8.08 (s, 2H, aromatic), 8.36 (d, <sup>3</sup>J<sub>H,H</sub> = 5.6 Hz, 2H, aromatic); <sup>13</sup>C{<sup>1</sup>H}-NMR (CD<sub>3</sub>OD/KOD/D<sub>2</sub>O; 100.5 MHz)  $\delta$  = 111.6, 118.8, 127.0, 148.8, 150.5, 174.7.

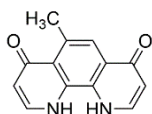




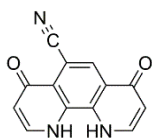
**5-Fluoro-1,10-dihydro-1,10-phenanthroline-4,7-dione (3b)**; brown; 1.8 g (7.7 mmol, 77%); m.p<sub>dec.</sub> >350.0 °C; <sup>1</sup>H-NMR (CD<sub>3</sub>OD/KOD/D<sub>2</sub>O; 400.2 MHz) δ = 6.45 (d, <sup>3</sup>J<sub>H,H</sub> = 6.5 Hz, 1H, aromatic), 6.50 (d, <sup>3</sup>J<sub>H,H</sub> = 6.2 Hz, 1H, aromatic), 7.31 (d, <sup>3</sup>J<sub>H,F</sub> = 14.1 Hz, 1H, aromatic), 8.01 (d, <sup>3</sup>J<sub>H,H</sub> = 6.4 Hz, 1H, aromatic), 8.10 (d, <sup>3</sup>J<sub>H,H</sub> = 6.1 Hz, 1H, aromatic); <sup>13</sup>C{<sup>1</sup>H}-NMR (CD<sub>3</sub>OD/KOD/D<sub>2</sub>O; 100.5 MHz) δ = 101.1 (d, <sup>2</sup>J<sub>C,F</sub> = 24.1 Hz), 113.0 (d, <sup>1</sup>J<sub>C,F</sub> = 307.7 Hz), 117.6 (d, <sup>2</sup>J<sub>C,F</sub> = 11.3 Hz), 125.0 (d, <sup>3</sup>J<sub>C,F</sub> = 9.6 Hz), 130.7, 136.4, 142.9, 143.4, 147.9, 156.4, 158.9, 175.7, 176.9; GC-MS: t<sub>r</sub> = 5.1 min, (EI) M<sup>+</sup> = 230 (< 1%); <sup>19</sup>F{<sup>1</sup>H}-NMR (CD<sub>3</sub>OD/KOD/D<sub>2</sub>O; 470.5 MHz) δ = -119.68; <sup>19</sup>F-NMR (CD<sub>3</sub>OD/KOD/D<sub>2</sub>O; 470.5 MHz) δ = -119.68 (d, <sup>3</sup>J<sub>F,H</sub> = 13.8 Hz); UV-Vis (methanol; λ [nm] (logε)): 352 (3.40), 329 (3.61), 308 (3.55), 273 (3.56), 251(3.63), 224 (3.91), 208 (3.96).



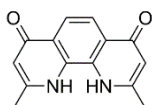
**5-Chloro-1,10-dihydro-1,10-phenanthroline-4,7-dione (3c)**<sup>40</sup>; brown; 1.5 g (6.1 mmol, 61%); m.p<sub>dec.</sub> = 272.8-273.6 °C; <sup>1</sup>H-NMR (CD<sub>3</sub>OD/KOD/D<sub>2</sub>O; 400.2 MHz) δ = 6.62 (d, <sup>3</sup>J<sub>H,H</sub> = 6.9 Hz, 1H, aromatic), 6.64 (d, <sup>3</sup>J<sub>H,H</sub> = 6.4 Hz, 1H, aromatic), 8.27 (d, <sup>3</sup>J<sub>H,H</sub> = 5.9 Hz, 1H, aromatic), 8.31 (d, <sup>3</sup>J<sub>H,H</sub> = 5.8 Hz, 1H, aromatic); <sup>13</sup>C{<sup>1</sup>H}-NMR (CD<sub>3</sub>OD/KOD/D<sub>2</sub>O; 100.5 MHz) δ = 112.0, 114.5, 120.3, 122.5, 125.4, 126.1, 144.0, 147.1, 148.6, 149.4, 169.3, 173.7, 173.8, 176.0, 176.1; GC-MS: t<sub>r</sub> = 11.5 min, (EI) M<sup>+</sup> = 246 (100%), 248 (32%), [M + H]<sup>+</sup> = 247 (8%), [M-CO]<sup>+</sup> = 218 (90%); UV-Vis (methanol; λ [nm] (logε)): 356 (3.83), 338 (4.06), 324 (4.06), 285 (3.97), 273 (4.03), 249 (4.42), 231 (4.28), 215 (4.42).



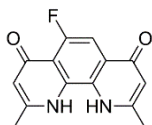
**5-Methyl-1,10-dihydro-1,10-phenanthroline-4,7-dione (3d)**; brown; 1.9 g (8.6 mmol, 86%); m.p<sub>dec.</sub> > 350.0 °C; <sup>1</sup>H-NMR (CD<sub>3</sub>OD/KOD/D<sub>2</sub>O; 500.2 MHz) δ = 2.73 (d, <sup>4</sup>J<sub>H,H</sub> = 0.8 Hz, 3H, CH<sub>3</sub>), 6.36 (d, <sup>3</sup>J<sub>H,H</sub> = 6.6 Hz, 1H, aromatic), 6.48 (d, <sup>3</sup>J<sub>H,H</sub> = 6.0 Hz, 1H, aromatic), 7.47 (d, <sup>4</sup>J<sub>H,H</sub> = 1.0 Hz, 1H, aromatic), 7.88 (d, <sup>3</sup>J<sub>H,H</sub> = 6.6 Hz, 1H, aromatic), 8.08 (d, <sup>3</sup>J<sub>H,H</sub> = 6.0 Hz, 1H, aromatic); <sup>13</sup>C{<sup>1</sup>H}-NMR(CD<sub>3</sub>OD/KOD/D<sub>2</sub>O; 125.8 MHz) δ = 24.5, 112.0, 114.0, 119.9, 124.9, 125.9, 132.6, 139.8, 141.0, 142.5, 148.0, 174.6, 180.9; GC-MS: t<sub>r</sub> = 7.0 min, (EI) [M-H]<sup>+</sup> = 225 (1%); UV-Vis (methanol; λ [nm] (logε)): 355 (3.66), 327 (3.89), 306 (3.83), 275 (3.93), 247 (4.14), 224 (4.23), 209 (4.28).



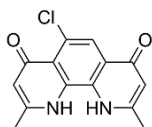
**4,7-Dioxo-1,4,7,10-tetrahydro-1,10-phenanthroline-5-carbonitrile (3e)**; beige, 1.5 g (6.4 mmol, 64%); m.p.<sub>dec.</sub> > 350 °C; <sup>1</sup>H-NMR (DMSO-*d*<sub>6</sub>/KOD/D<sub>2</sub>O; 400.2 MHz) δ = 6.37 (d, <sup>3</sup>J<sub>H,H</sub> = 6.8 Hz, 1H, aromatic), 6.41 (d, <sup>3</sup>J<sub>H,H</sub> = 6.3 Hz, 1H, aromatic), 8.02 (d, <sup>3</sup>J<sub>H,H</sub> = 6.7 Hz, 1H, aromatic), 8.16 (d, <sup>3</sup>J<sub>H,H</sub> = 6.3 Hz, 1H, aromatic), 8.26 (s, 1H, aromatic); <sup>13</sup>C{<sup>1</sup>H}-NMR (DMSO-*d*<sub>6</sub>/KOD/D<sub>2</sub>O; 125.8 MHz) δ = 101.1, 113.7, 114.2, 122.2, 123.3, 124.8, 131.2, 139.6, 142.2, 144.6, 149.7, 176.1, 176.8; UV-Vis (methanol; λ [nm] (logε)): 382 (3.27), 350 (3.50), 335 (3.44), 277 (3.39), 242 (3.78), 214 (3.81).



**2,9-Dimethyl-1,10-phenanthroline-4,7-dione (3f)**<sup>39</sup>; brown; 1.6 g (6.8 mmol, 68%); m.p.<sub>dec.</sub> = 291.8–292.5 °C; <sup>1</sup>H-NMR (CD<sub>3</sub>OD/KOD/D<sub>2</sub>O; 400.2 MHz) δ = 2.29 (s, 6H, CH<sub>3</sub>), 6.24 (s, 2H, aromatic), 7.64 (s, 2H, aromatic); <sup>13</sup>C{<sup>1</sup>H}-NMR (CD<sub>3</sub>OD/KOD/D<sub>2</sub>O; 100.5 MHz) δ = 21.8, 100.0, 110.1, 117.0, 122.9, 138.9, 155.9, 174.6.

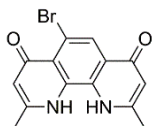


**5-fluoro-2,9-dimethyl-1,10-dihydro-1,10-phenanthroline-4,7-dione (3g)**; brown; 2.2 g (8.7 mmol, 87%); m.p.<sub>dec.</sub> = 370.2–372.8 °C; <sup>1</sup>H-NMR (CD<sub>3</sub>OD/KOD/D<sub>2</sub>O; 400.2 MHz) δ = 2.40 (bs, 6H, CH<sub>3</sub>), 6.26 (bs, 1H, aromatic), 6.35 (bs, 1H, aromatic), 7.19 (bd, <sup>3</sup>J<sub>H,F</sub> = 11.1 Hz, 1H, aromatic); <sup>13</sup>C{<sup>1</sup>H}-NMR (CD<sub>3</sub>OD/KOD/D<sub>2</sub>O; 100.5 MHz) δ = 21.4, 22.9, 100.4 (d, <sup>2</sup>J<sub>C,F</sub> = 24.2 Hz), 112.2 (d, <sup>1</sup>J<sub>C,F</sub> = 274.4 Hz), 115.5 (d, <sup>2</sup>J<sub>C,F</sub> = 11.1 Hz), 123.1 (d, <sup>3</sup>J<sub>C,F</sub> = 9.7 Hz), 135.0, 141.5 (d, <sup>4</sup>J<sub>C,F</sub> = 3.7 Hz), 154.0, 155.8, 157.8, 158.3, 175.0, 176.2, 176.2; GC-MS: t<sub>r</sub> = 10.5 min, (EI) M<sup>+</sup> = 258 (100%), [M + H-CO]<sup>+</sup> = 229 (98%); <sup>19</sup>F{<sup>1</sup>H}-NMR (CD<sub>3</sub>OD/KOD/D<sub>2</sub>O; 470.5 MHz) δ = -119.99; <sup>19</sup>F-NMR (CD<sub>3</sub>OD/KOD/D<sub>2</sub>O; 470.5 MHz) δ = -119.99 (d, <sup>3</sup>J<sub>F,H</sub> = 13.9 Hz); UV-Vis (methanol; λ [nm] (logε)): 353 (3.76), 337 (3.85), 319 (4.00), 311 (3.97), 270 (4.21), 254 (4.46), 225 (4.31), 214 (4.44).

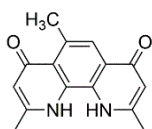


**5-chloro-2,9-dimethyl-1,10-dihydro-1,10-phenanthroline-4,7-dione (3h)**; 2.3 g (8.3 mmol, 83%); brown; m.p.<sub>dec.</sub> = 332.7–334.8 °C; <sup>1</sup>H-NMR (CD<sub>3</sub>OD/KOD/D<sub>2</sub>O; 400.2 MHz) δ = 2.46 (s, 3H, CH<sub>3</sub>), 2.49 (s, 3H, CH<sub>3</sub>), 6.40 (s, 1H, aromatic), 6.41 (s, 1H, aromatic), 7.78 (s, 1H, aromatic); <sup>13</sup>C{<sup>1</sup>H}-

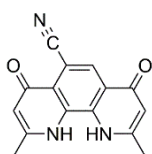
NMR (CD<sub>3</sub>OD/KOD/D<sub>2</sub>O; 100.5 MHz)  $\delta$  = 21.8, 22.6, 112.0, 114.3, 120.1, 121.1, 124.2, 126.2, 138.4, 141.6, 155.2, 156.8, 175.9, 178.1; GC-MS:  $t_r$  = 11.3 min, (EI)  $M^+$  = 273.9 (100%),  $[M-CO]^+$  = 245 (80%); UV-Vis (methanol;  $\lambda$  [nm] (log $\epsilon$ )): 357 (3.65), 340 (3.84), 327 (3.96), 316 (3.94), 280 (4.00), 254 (4.35), 230 (4.25), 216 (4.35).



**5-bromo-2,9-dimethyl-1,10-dihydro-1,10-phenanthroline-4,7-dione (3i)**; brown; 2.7 g (8.5 mmol, 85%); m.p<sub>dec.</sub> = 325.9–326.6 °C; <sup>1</sup>H-NMR (CD<sub>3</sub>OD/KOD/D<sub>2</sub>O; 400.2 MHz)  $\delta$  = 2.48 (s, 3H, CH<sub>3</sub>), 2.50 (s, 3H, CH<sub>3</sub>), 6.40 (s, 1H, aromatic), 6.43 (s, 1H, aromatic), 8.09 (s, 1H, aromatic); <sup>13</sup>C{<sup>1</sup>H}-NMR (CD<sub>3</sub>OD/KOD/D<sub>2</sub>O; 100.5 MHz)  $\delta$  = 21.6, 22.7, 112.2, 112.7, 113.9, 121.4, 124.4, 124.9, 138.9, 141.1, 154.4, 157.1, 175.8, 175.8, 178.2; GC-MS:  $t_r$  = 13.5 min, (EI)  $M^+$  = 318 (100%), 320 (96%),  $[M-CO]^+$  = 290 (63%); UV-Vis (methanol;  $\lambda$ [nm] (log $\epsilon$ )): 356 (3.87), 339 (4.08), 328 (4.17), 315 (4.13), 281 (4.19), 254 (4.55), 231 (4.46), 217 (4.53).

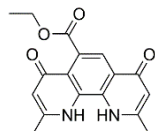


**2,5,9-Trimethyl-1,10-dihydro-1,10-phenanthroline-4,7-dione (3j)**; brown; 2.3 g (9.2 mmol, 92%); m.p<sub>dec.</sub> = 337.4–338.9 °C; <sup>1</sup>H-NMR (CD<sub>3</sub>OD/KOD/D<sub>2</sub>O; 400.2 MHz)  $\delta$  = 2.31 (s, 3H, CH<sub>3</sub>), 2.36 (s, 3H, CH<sub>3</sub>), 2.66 (s, 3H, OCH<sub>3</sub>), 6.16 (s, 1H, aromatic), 6.31 (s, 1H, aromatic), 7.28 (s, 1H, aromatic); <sup>13</sup>C{<sup>1</sup>H}-NMR (CD<sub>3</sub>OD/KOD/D<sub>2</sub>O; 100.5 MHz)  $\delta$  = 21.1, 23.5, 24.4, 111.4, 113.2, 119.3, 123.0, 123.9, 131.6, 138.2, 139.6, 152.8, 157.5, 174.2, 180.3; GC-MS:  $t_r$  = 12.1 min, (EI)  $M^+$  = 254 (100%),  $[M + H-CO]^+$  = 225 (56%); UV-Vis (methanol;  $\lambda$  [nm] (log $\epsilon$ )): 354 (3.72), 338 (3.95), 320 (4.14), 282 (4.30), 257 (4.45), 226 (4.40), 217 (4.42), 204 (4.40).



**2,9-Dimethyl-4,7-dioxo-1,4,7,10-tetrahydro-1,10-phenanthroline-5-carbonitrile (3k)**; brown; 1.6 g (6.2 mmol, 62%); m.p<sub>dec.</sub> = 390.7–392.5 °C; <sup>1</sup>H-NMR (CD<sub>3</sub>OD/KOD/D<sub>2</sub>O; 400.2 MHz)  $\delta$  = 2.45 (s, 3H, CH<sub>3</sub>), 2.46 (s, 3H, CH<sub>3</sub>), 6.45 (s, 1H, aromatic), 6.47 (s, 1H, aromatic), 8.21 (s, 1H, aromatic); <sup>13</sup>C{<sup>1</sup>H}-NMR (CD<sub>3</sub>OD/KOD/D<sub>2</sub>O; 100.5 MHz)  $\delta$  = 23.8, 100.0, 112.1, 112.2, 122.0, 122.9, 123.3,

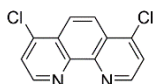
130.5, 144.5, 146.7, 159.1, 159.2, 162.1, 169.4, 173.8, 174.1; GC-MS:  $t_r = 9.4$  min, (EI)  $M_+ = 265$  (5%); UV-Vis (methanol;  $\lambda$  [nm] ( $\log \epsilon$ )): 350 (3.90), 343 (3.93), 328 (3.87), 286 (3.82), 276 (3.90), 252 (4.31), 228 (4.15), 217 (4.28).



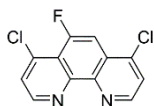
**Ethyl 2,9-dimethyl-4,7-dioxo-1,4,7,10-tetrahydro-1,10-phenanthroline-5-carboxylate (31)**; brown; 2.0 g (6.5 mmol, 65%); m.p<sub>dec.</sub> = 301.4–301.8 °C; <sup>1</sup>H-NMR (CD<sub>3</sub>OD/KOD/D<sub>2</sub>O; 400.2 MHz)  $\delta$  = 1.41 (t, 3H, H = 7.1 Hz, 3H, OCH<sub>2</sub>CH<sub>3</sub>), 2.36 (s, 3H, CH<sub>3</sub>), 2.38 (s, 3H, CH<sub>3</sub>), 4.46 (q, 3H, H = 7.0 Hz, 2H, OCH<sub>2</sub>), 6.29 (s, 1H, aromatic), 6.37 (s, 1H, aromatic), 7.79 (s, 1H, aromatic); GC-MS:  $t_r = 17.9$  min, (EI)  $M^+ = 312$  (50%); UV-Vis (methanol;  $\lambda$  [nm] ( $\log \epsilon$ )): 354 (3.58), 345 (3.81), 330 (4.04), 316 (3.99), 279 (4.03), 252 (4.44), 227 (4.26), 214 (4.36).

### 7.3.3 Step C

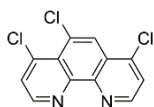
Modifications to the existing procedure described in the literature<sup>39,40</sup> rely on the evaporation of excess phosphoryl chloride under reduced pressure and the addition of CH<sub>2</sub>Cl<sub>2</sub> or CHCl<sub>3</sub> into reaction mixture after alkalinized by NaOH solution because of the very exothermic hydrolysis of residual phosphoryl chloride. Next, the crude products were purified by chromatography and crystallization from CH<sub>2</sub>Cl<sub>2</sub>. Freshly distilled phosphoryl chloride (82.0 g, 50 mL, 534.8 mmol) was mixed under argon with compounds **3** (5.0 mmol), and the resulting solutions were stirred at 90 °C for 4 h. The excess phosphoryl chloride was slowly evaporated under reduced pressure. The reaction mixture was slowly added to a well stirred mixture of ice (50 g) in water (100 mL). After stirring for 15 min. the resulting reaction mixture was carefully brought to pH 13–14 (pH 7 in the case of molecule **4g**) by adding NaOH solution (40%). The aqueous layer was extracted with CH<sub>2</sub>Cl<sub>2</sub> (4 x 10 mL). The combined organic layers were separated and dried over MgSO<sub>4</sub>. Evaporation of the brown colored solvent afforded products **4** as light tan crystals. Next, the crude products were purified by chromatography on silica gel using methanol/dichloromethane as eluent and finally crystallization from CH<sub>2</sub>Cl<sub>2</sub> to yield precipitates as follows:



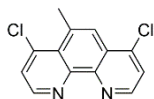
**4,7-Dichloro-1,10-phenanthroline (4a)**<sup>86,255</sup>; beige; 1.041 g (4.2 mmol, 84%); m.p.<sub>dec.</sub> = 254.8-255.0 °C; UV-Vis (methanol;  $\lambda$  [nm] (log $\epsilon$ )): 300 (3.83), 264 (4.40), 239 (4.33), 225 (4.29), 202 (4.36); IR (KBr):  $\tilde{\nu}$  = 3422, 3034, 1563, 1487, 1418, 835, 720 cm<sup>-1</sup>.



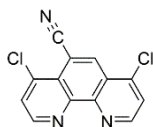
**4,7-Dichloro-5-fluoro-1,10-phenanthroline (4b)**; beige; 1.130 g (4.2 mmol, 85%); m.p.<sub>dec.</sub> = 217.8-218.0 °C; <sup>1</sup>H NMR (CDCl<sub>3</sub>; 600.2 MHz)  $\delta$  = 7.75 (d, <sup>3</sup>J<sub>H,H</sub> = 4.7 Hz, 1H, aromatic), 7.77 (d, <sup>3</sup>J<sub>H,H</sub> = 4.8 Hz, 1H, aromatic), 7.94 (d, <sup>3</sup>J<sub>H,F</sub> = 13.3 Hz, 1H, aromatic), 9.02 (dd, <sup>3</sup>J<sub>H,H</sub> = 4.8 Hz, <sup>5</sup>J<sub>H,F</sub> = 0.5 Hz, 1H, aromatic), 9.08 (d, <sup>3</sup>J<sub>H,H</sub> = 4.8 Hz, 1H, aromatic); <sup>13</sup>C{<sup>1</sup>H} NMR (CDCl<sub>3</sub>; 150.0 MHz)  $\delta$  = 106.7 (d, <sup>2</sup>J<sub>C,F</sub> = 25.9 Hz), 119.9 (d, <sup>2</sup>J<sub>C,F</sub> = 12.6 Hz), 124.4, 126.3, 126.8 (d, <sup>3</sup>J<sub>C,F</sub> = 10.8 Hz), 140.3, 142.0 (d, <sup>3</sup>J<sub>C,F</sub> = 6.2 Hz), 144.7, 148.9 (d, <sup>4</sup>J<sub>C,F</sub> = 2.3 Hz), 149.7 (d, <sup>4</sup>J<sub>C,F</sub> = 2.6 Hz), 151.0, 156.3 (d, <sup>1</sup>J<sub>C,F</sub> = 263.6 Hz); <sup>19</sup>F{<sup>1</sup>H} NMR (CDCl<sub>3</sub>; 470.5 MHz)  $\delta$  = -108.98; <sup>19</sup>F NMR (CDCl<sub>3</sub>; 470.5 MHz)  $\delta$  = -108.98 (d, <sup>3</sup>J<sub>F,H</sub> = 13.4 Hz); GC-MS: t<sub>r</sub> = 9.0 min, (EI) M<sup>+</sup> = 266.0 (100 %); Anal. Calcd for C<sub>12</sub>H<sub>5</sub>N<sub>2</sub>Cl<sub>2</sub>F: C, 53.96; H, 1.89; N, 10.49; Found: C, 53.90; H, 1.93; N, 10.45; UV-Vis (methanol;  $\lambda$  [nm] (log $\epsilon$ )): 305 (4.01), 268 (4.46), 240 (4.47), 225 (4.40), 203 (4.45); IR (KBr):  $\tilde{\nu}$  = 3422, 3035, 1626, 1571, 1546, 1410, 842, 752 cm<sup>-1</sup>.



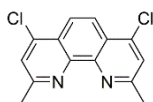
**4,5,7-Trichloro-1,10-phenanthroline (4c)**<sup>86</sup>; beige; 1.057 g (3.8 mmol, 75%); m.p.<sub>dec.</sub> = 194.6-195.0 °C; GC-MS: t<sub>r</sub> = 9.4 min, (EI) M<sup>+</sup> = 281.9 (100 %), 283.9 (95%), (M-Cl)<sup>+</sup> = 247 (46%); UV-Vis (methanol;  $\lambda$  [nm] (log $\epsilon$ )): 314 (3.82), 302 (3.87), 270 (4.32), 247 (4.31), 209 (4.30); IR (KBr):  $\tilde{\nu}$  = 3356, 3021, 2920, 2191, 1567, 1403, 833, 716 cm<sup>-1</sup>.



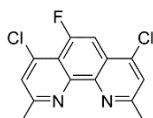
**4,7-Dichloro-5-methyl-1,10-phenanthroline (4d)**<sup>40</sup>; beige; 1.192 g (4.6 mmol, 91%); m.p.<sub>dec.</sub> = 166.8-167.0 °C; GC-MS: t<sub>r</sub> = 9.6 min, (EI) M<sup>+</sup> = 262.1 (100 %); UV-Vis (methanol;  $\lambda$  [nm] (log $\epsilon$ )): 304 (4.09), 271 (4.50), 241 (4.49), 225 (4.42), 205 (4.47); IR (KBr):  $\tilde{\nu}$  = 3454, 3089, 2933, 1685, 1550, 1432, 1400, 1085, 844, 744 cm<sup>-1</sup>.



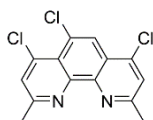
**4,7-Dichloro-1,10-phenanthroline-5-carbonitrile (4e)**; beige, 0.655 g (2.4 mmol, 48%); m.p. = 249.7-250.0 °C;  $^1\text{H}$  NMR ( $\text{CDCl}_3$ ; 400.2 MHz)  $\delta$  = 7.84 (m, 2H, aromatic), 8.88 (s, 1H, aromatic), 9.13 (d,  $^3J_{\text{H,H}} = 4.7$  Hz, 1H, aromatic), 9.19 (d,  $^3J_{\text{H,H}} = 4.7$  Hz, 1H, aromatic);  $^{13}\text{C}\{^1\text{H}\}$  NMR ( $\text{CDCl}_3$ ; 125.78 MHz)  $\delta$  = 108.1, 118.1, 124.2, 125.2, 125.3, 126.5, 135.4, 142.3, 143.6, 147.5, 148.1, 151.5, 153.4; GC-MS:  $t_{\text{r}} = 10.1$  min, (EI)  $M^+ = 273.0$  (100 %); Anal. Calcd for  $\text{C}_{13}\text{H}_5\text{N}_3\text{Cl}_2$ : C, 56.96; H, 1.84; N, 15.33; Found: C, 56.90; H, 1.94; N, 15.29; UV-Vis (methanol;  $\lambda$  [nm] (log $\epsilon$ )): 315 (3.67), 302 (3.76), 292 (3.68), 268 (4.15), 249 (4.11), 231 (4.02), 210 (4.11); IR (KBr):  $\tilde{\nu} = 3406, 3029, 2224, 1569, 1498, 1406, 1084, 846, 798$   $\text{cm}^{-1}$ .



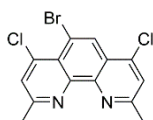
**4,7-Dichloro-2,9-dimethyl-1,10-phenanthroline (4f)**<sup>39,86,256,257</sup>; beige; 1.269 g (4.6 mmol, 92%); m.p.<sub>dec.</sub> = 201.0-201.5 °C;  $^1\text{H}$  NMR ( $\text{CDCl}_3$ ; 400.2 MHz)  $\delta$  = 2.93 (s, 6H, 2 $\text{CH}_3$ ), 7.63 (s, 2H, aromatic), 8.24 (s, 2H, aromatic);  $^{13}\text{C}\{^1\text{H}\}$  NMR ( $\text{CDCl}_3$ ; 100.5 MHz)  $\delta$  = 26.0, 122.3, 124.4, 125.1, 143.0, 146.2, 160.1; CP/MAS  $^{13}\text{C}$  NMR  $\delta$  = 25.1, 121.7, 141.3, 143.8, 159.3; CP/MAS  $^{15}\text{N}$  NMR  $\delta$  = -76.15; IR (KBr):  $\tilde{\nu} = 2963, 1637, 1568, 1522, 1402, 1385, 1363, 1026$   $\text{cm}^{-1}$ .



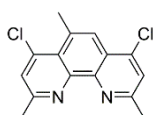
**4,7-Dichloro-5-fluoro-2,9-dimethyl-1,10-phenanthroline (4g)**<sup>257</sup>; beige; 1.367 g (4.6 mmol, 93%); m.p.<sub>dec.</sub> = 213.0-213.5 °C;  $^1\text{H}$  NMR ( $\text{CDCl}_3$ ; 400.2 MHz)  $\delta$  = 2.97 (s, 3H,  $\text{CH}_3$ ), 3.01 (s, 3H,  $\text{CH}_3$ ), 7.67 (s, 1H, aromatic), 7.68 (s, 1H, aromatic), 7.86 (d,  $^3J_{\text{H,F}} = 13.1$  Hz, 1H, aromatic);  $^{13}\text{C}\{^1\text{H}\}$  NMR( $\text{CDCl}_3$ ; 100.5 MHz)  $\delta$  = 25.3, 25.5, 105.6 (d,  $^2J_{\text{C,F}} = 26.0$  Hz), 118.0 (d,  $^3J_{\text{C,F}} = 12.5$  Hz), 125.1(d,  $^3J_{\text{C,F}} = 11.1$  Hz), 126.1 (d,  $^1J_{\text{C,F}} = 184.1$  Hz), 140.3, 142.8 (d,  $^2J_{\text{C,F}} = 68.6$  Hz), 147.0, 154.9, 157.5, 159.1, 161.3;  $^{19}\text{F}\{^1\text{H}\}$  NMR ( $\text{CDCl}_3$ ; 470.5 MHz)  $\delta$  = -110.97;  $^{19}\text{F}$  NMR ( $\text{CDCl}_3$ ; 470.5 MHz)  $\delta$  = -110.97 (d,  $^3J_{\text{F,H}} = 11.5$  Hz); GC-MS:  $t_{\text{r}} = 8.2$  min, (EI)  $M^+ = 294$  (100%), 296. (64%), ( $M-\text{Cl}$ ) $^+ = 259$  (12%); Anal. Calcd for  $\text{C}_{14}\text{H}_9\text{N}_2\text{Cl}_2\text{F}$ : C, 56.97; H, 3.07; N, 9.49; Found: C, 56.90; H, 3.19; N, 9.32; UV-Vis (methanol;  $\lambda$  [nm] (log $\epsilon$ )): 309 (3.88), 296 (3.95), 273 (4.46), 241 (4.47), 211 (4.40); IR (KBr):  $\tilde{\nu} = 3471, 3075, 1628, 1579, 1375, 1145, 858$   $\text{cm}^{-1}$ .



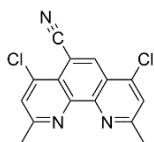
**4,5,7-Trichloro-2,9-dimethyl-1,10-phenanthroline (4h)**; beige; 1.209 g (3.9 mmol, 78%); m.p.<sub>dec.</sub> = 162.9-163.7 °C; <sup>1</sup>H NMR (CDCl<sub>3</sub>; 400.2 MHz) δ = 2.92 (s, 3H, CH<sub>3</sub>), 2.94 (s, 3H, CH<sub>3</sub>), 7.63 (s, 1H, aromatic), 7.66 (s, 1H, aromatic), 8.27 (s, 1H, aromatic); <sup>13</sup>C{<sup>1</sup>H} NMR (CDCl<sub>3</sub>; 100.5 MHz) δ = 25.3, 25.7, 122.7, 124.5, 124.6, 125.0, 128.0, 129.0, 142.1, 142.3, 144.8, 147.6, 160.2, 160.3; GC-MS: t<sub>r</sub> = 9.9 min, (EI) M<sup>+</sup> = 310 (100%), 312 (95%), (M-Cl)<sup>+</sup> = 275 (11%), (M-2Cl)<sup>+</sup> = 240 (40%); Anal. Calcd for C<sub>14</sub>H<sub>9</sub>N<sub>2</sub>Cl<sub>3</sub>: C, 53.97; H, 2.91; N, 8.99; Found: C, 53.90; H, 3.01; N, 8.87; UV-Vis (methanol; λ [nm] (logε)): 316 (4.16), 304 (4.21), 274 (4.64), 247 (4.67), 210 (4.55); IR (KBr):  $\tilde{\nu}$  = 3456, 3065, 2922, 1594, 1576, 1528, 1332, 905, 874 cm<sup>-1</sup>.



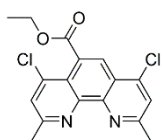
**5-Bromo-4,7-dichloro-2,9-dimethyl-1,10-phenanthroline (4i)**; beige; 1.203 g (3.4 mmol, 68%); m.p.<sub>dec.</sub> = 180.1-181.7 °C; <sup>1</sup>H NMR (CDCl<sub>3</sub>; 400.2 MHz) δ = 2.93 (s, 3H, CH<sub>3</sub>), 2.95 (s, 3H, CH<sub>3</sub>), 7.63 (s, 1H, aromatic), 7.69 (s, 1H, aromatic), 8.58 (s, 1H, aromatic); <sup>13</sup>C{<sup>1</sup>H} NMR (CDCl<sub>3</sub>; 100.5 MHz) δ = 25.2, 25.8, 116.2, 123.2, 125.0, 125.1, 127.8, 129.2, 142.1, 143.0, 145.0, 147.2, 160.0, 160.5; GC-MS: t<sub>r</sub> = 12.5 min, (EI) M<sup>+</sup> = 354 (63.7%), 356 (100%), 358 (44%), (M-Br)<sup>+</sup> = 275 (28%); Anal. Calcd for C<sub>14</sub>H<sub>9</sub>N<sub>2</sub>Cl<sub>2</sub>Br: C, 47.23; H, 2.55; N, 7.87; Found: C, 47.90; H, 2.67; N, 7.86; UV-Vis (methanol; λ [nm] (logε)): 318 (3.97), 306 (4.02), 275 (4.43), 249 (4.43), 213 (4.34); IR (KBr):  $\tilde{\nu}$  = 3452, 2923, 1588, 1438, 1117, 900, 876, 718 cm<sup>-1</sup>.



**4,7-Dichloro-2,5,9-trimethyl-1,10-phenanthroline (4j)**<sup>86,257</sup>; beige; 1.247 g (4.3 mmol, 86%); m.p. = 111.9-112.6 °C; <sup>1</sup>H NMR (CDCl<sub>3</sub>; 400.2 MHz) δ = 2.92 (s, 3H, CH<sub>3</sub>), 2.96 (s, 3H, CH<sub>3</sub>), 3.11 (s, 3H, CH<sub>3</sub>), 7.62 (bs, 2H, aromatic), 7.95 (s, 1H, aromatic); <sup>13</sup>C{<sup>1</sup>H} NMR (CDCl<sub>3</sub>; 100.5 MHz) δ = 25.2, 25.6, 26.3, 123.9, 124.5, 124.6, 125.4, 126.9, 133.8, 142.3, 143.1, 144.9, 147.2, 159.0, 159.1; CP/MAS <sup>13</sup>C NMR δ = 25.0, 27.5, 122.5, 123.5, 131.0, 139.0, 143.3, 145.3, 158.3; CP MAS <sup>15</sup>N NMR δ = -75.52; GC-MS: t<sub>r</sub> = 9.7 min, (EI) M<sup>+</sup> = 290 (100%), (M-Cl)<sup>+</sup> = 255 (12%); Anal. Calcd for C<sub>15</sub>H<sub>12</sub>N<sub>2</sub>Cl<sub>2</sub>: C, 61.88; H, 4.15; N, 9.62; Found: C, 61.89; H, 4.20; N, 9.60; UV-Vis (methanol; λ [nm] (logε)): 343 (3.57), 311 (3.73), 275 (4.30), 254 (4.34), 213 (4.24); IR (KBr):  $\tilde{\nu}$  = 3452, 2924, 1609, 1579, 1530, 1439, 1380, 1236, 902, 871, 716 cm<sup>-1</sup>.



**4,7-Dichloro-2,9-dimethyl-1,10-phenanthroline-5-carbonitrile (4k)**; beige; 0.482 g (1.6 mmol, 32%); m.p.<sub>dec.</sub> = 188.6-189.9 °C; <sup>1</sup>H NMR (CDCl<sub>3</sub>; 400.2 MHz) δ = 2.96 (s, 3H, CH<sub>3</sub>), 2.99 (s, 3H, CH<sub>3</sub>), 7.72 (s, 1H, aromatic), 7.73 (s, 1H, aromatic), 8.79 (s, 1H, aromatic); <sup>13</sup>C{<sup>1</sup>H} NMR (CDCl<sub>3</sub>; 125.78 MHz) δ = 25.6, 26.2, 106.9, 118.4, 122.6, 123.7, 125.6, 127.0, 134.3, 142.2, 143.7, 146.1, 146.8, 161.6, 163.8; GC-MS: t<sub>r</sub> = 10.5 min, (EI) M<sup>+</sup> = 301 (100%), (M-Cl)<sup>+</sup> = 266 (14%); Anal. Calcd for C<sub>15</sub>H<sub>9</sub>N<sub>3</sub>Cl<sub>2</sub>: C, 59.63; H, 3.00; N, 13.91; Found: C, 59.89; H, 3.27; N, 13.87; UV-Vis (methanol; λ [nm] (logε)): 353 (3.07), 337 (3.68), 319 (4.24), 307 (4.31), 275 (4.67), 249 (4.60), 235 (4.54), 211 (4.59); IR (KBr):  $\tilde{\nu}$  = 3471, 3406, 2223, 1587, 1443, 1357, 1338, 908, 847 cm<sup>-1</sup>.



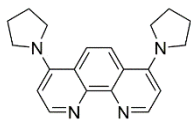
**Ethyl 4,7-dichloro-2,9-dimethyl-1,10-phenanthroline-5-carboxylate (4l)**; beige; 0.661 g (1.9 mmol, 38%); m.p. = 115.9-116.2 °C; <sup>1</sup>H NMR (CDCl<sub>3</sub>; 400.2 MHz) δ = 1.43 (t, <sup>3</sup>J<sub>H,H</sub> = 7.1 Hz, 3H, OCH<sub>2</sub>CH<sub>3</sub>), 2.93 (s, 3H, CH<sub>3</sub>), 2.94 (s, 3H, CH<sub>3</sub>), 4.49 (q, <sup>3</sup>J<sub>H,H</sub> = 7.1 Hz, 2H, OCH<sub>2</sub>), 7.65 (2s, 2H, aromatic), 8.31 (s, 1H, aromatic); <sup>13</sup>C{<sup>1</sup>H} NMR (CDCl<sub>3</sub>; 100.5 MHz) δ = 14.1, 25.5, 25.9, 62.6, 122.1, 123.5, 123.8, 124.9, 126.0, 129.3, 141.7, 143.6, 146.3, 146.6, 160.5, 161.5, 169.0; GC-MS: t<sub>r</sub> = 10.9 min, (EI) M<sup>+</sup> = 348 (45%), (M-Cl)<sup>+</sup> = 313 (21%); Anal. Calcd for C<sub>17</sub>H<sub>14</sub>N<sub>2</sub>Cl<sub>2</sub>O<sub>2</sub>: C, 58.47; H, 4.04; N, 8.02; Found: C, 58.90; H, 4.25; N, 7.98; UV-Vis (methanol; λ [nm] (logε)): 308 (3.88), 295 (3.95), 272 (4.43), 245 (4.44), 212 (4.33); IR (KBr):  $\tilde{\nu}$  = 3432, 2980, 1727, 1577, 1275, 1248, 1214, 1190, 1122, 1031 cm<sup>-1</sup>.

## 7.4 Synthesis of selected 4,7-di(pyrrolidin-1-yl)-1,10-phenanthrolines

This synthesis was done according to a literature procedure<sup>123</sup>. The modifications to this procedure involve purification. The appropriate compounds **4a**, **4c**, **4f**, **4g**, or **4j** (1.0 mmol) were mixed with pyrrolidine (1.5 g, 21.0 mmol) in a microwave vial equipped with a magnetic stir bar. The vial was sealed, placed in a microwave reactor, and heated at 130 °C for 45 min (for compound **5a**) or 2 h (for compounds **5b**, **5c**, **5d**, and **5e**). The mixture was cooled to r.t., transferred to a round bottom flask (100 mL), and evaporated under reduced pressure. The residue has been washed with saturated NaHCO<sub>3</sub> (2 - 10 mL) with stirring and then with water (2 - 10 mL). The organic residue has been dissolved with CH<sub>2</sub>Cl<sub>2</sub> (20 mL), dried over MgSO<sub>4</sub>, and evaporated under reduced pressure affording

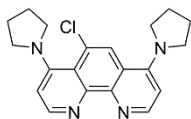


the corresponding products. Next, the crude products were purified by chromatography on silica gel using methanol/dichloromethane as eluent and finally crystallization from CH<sub>2</sub>Cl<sub>2</sub> to yield precipitates as follows:

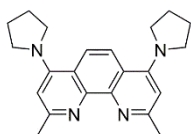


**4,7-Di(pyrrolidin-1-yl)-1,10-phenanthroline (5a)**<sup>123,258</sup>; 0.134 g (0.4 mmol, 38%); m.p.<sub>dec.</sub> = 246.8-247.7 °C; <sup>1</sup>H NMR (CDCl<sub>3</sub>; 400.2 MHz) δ = 2.03 (m, 8H, 4CH<sub>2</sub>), 3.67 (m, 8H, 4CH<sub>2</sub>), 6.69 (d, <sup>3</sup>J<sub>H,H</sub> = 5.5 Hz, 2H, aromatic), 7.93 (s, 2H, aromatic), 8.72 (d, <sup>3</sup>J<sub>H,H</sub> = 5.4 Hz, 2H, aromatic); <sup>13</sup>C{<sup>1</sup>H} NMR (CDCl<sub>3</sub>; 100.5 MHz) δ = 26.1, 52.4, 105.6, 119.5, 119.6, 148.5, 149.4, 152.9; MS-IT-TOF [M+H]<sup>+</sup> = 319 (100%), HRMS (IT TOF): m/z Calcd for C<sub>20</sub>H<sub>23</sub>N<sub>4</sub> [M+H]<sup>+</sup>: 319.1917, Found 319.1916; UV-Vis (methanol; λ [nm] (logε)): 362 (4.26), 328 (4.18), 274 (4.48), 255 (4.43), 217 (4.54); IR (ATR):  $\tilde{\nu}$  = 2952, 2935, 2860, 1662, 1615, 1552, 1434, 1349, 791, 729 cm<sup>-1</sup>.

The data differ with literature values, in the additional signal 7.93 (s, 2H, aromatic) in the proton spectrum. In the case of the cited literature, the authors did not include this signal in the characteristics.

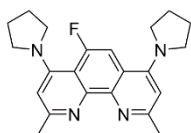


**5-Chloro-4,7-di(pyrrolidin-1-yl)-1,10-phenanthroline (5b)**; 0.148 g (0.4 mmol, 42%); m.p. = 151.0-151.6 °C; <sup>1</sup>H NMR (CDCl<sub>3</sub>; 400.2 MHz) δ = 1.99 (m, 4H, 2CH<sub>2</sub>), 2.07 (m, 4H, 2CH<sub>2</sub>), 3.53 (m, 4H, 2CH<sub>2</sub>), 3.70 (m, 4H, 2CH<sub>2</sub>), 6.67 (d, <sup>3</sup>J<sub>H,H</sub> = 5.8 Hz, 1H, aromatic), 6.90 (d, <sup>3</sup>J<sub>H,H</sub> = 5.6 Hz, 1H, aromatic), 7.92 (s, 1H, aromatic), 8.73 (d, <sup>3</sup>J<sub>H,H</sub> = 5.7 Hz, 1H, aromatic), 8.74 (d, <sup>3</sup>J<sub>H,H</sub> = 5.7 Hz, 1H, aromatic); <sup>13</sup>C{<sup>1</sup>H} NMR (CDCl<sub>3</sub>; 100.5 MHz) δ = 25.1, 26.1, 52.1, 52.4, 105.9, 107.9, 117.7, 118.5, 122.4, 124.1, 145.2, 147.7, 148.2, 148.9, 152.7, 153.9; MS-IT-TOF [M+H]<sup>+</sup> = 353 (100%), HRMS (IT TOF): m/z Calcd for C<sub>20</sub>H<sub>22</sub>ClN<sub>4</sub> [M+H]<sup>+</sup>: 353.1527, Found 353.1526; UV-Vis (methanol; λ [nm] (logε)): 372 (3.98), 333 (3.88), 281 (4.22), 262 (4.19), 220 (4.65); IR (ATR):  $\tilde{\nu}$  = 2956, 2870, 1572, 1514, 1445, 1350, 803 cm<sup>-1</sup>.

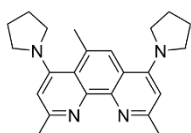


**2,9-Dimethyl-4,7-di(pyrrolidin-1-yl)-1,10-phenanthroline (5c)**; 0.166 g (0.5 mmol, 48%); m.p. = 165.8-166.0 °C; <sup>1</sup>H NMR (CDCl<sub>3</sub>; 500.18 MHz) δ = 2.04 (m, 8H, 4CH<sub>2</sub>), 2.77 (s, 6H, 2CH<sub>3</sub>), 3.68 (m,

8H, 4CH<sub>2</sub>), 6.61 (s, 2H, aromatic), 7.90 (s, 2H, aromatic); <sup>13</sup>C{<sup>1</sup>H} NMR (CDCl<sub>3</sub>; 100.5 MHz) δ = 25.8, 26.0, 52.4, 105.7, 118.2, 119.0, 146.3, 158.4, 157.5; CP/MAS <sup>13</sup>C NMR δ = 26.0, 51.8, 104.7, 117.5, 147.3, 149.6, 154.6; CP/MAS <sup>15</sup>N NMR δ = -291.94, -62.66; MS-IT-TOF [M+H]<sup>+</sup> = 347 (100%), HRMS (IT TOF): m/z Calcd for C<sub>22</sub>H<sub>27</sub>N<sub>4</sub> [M+H]<sup>+</sup>: 347.2230, Found 347.2229; UV-Vis (methanol; λ [nm] (logε)): 387 (3.80), 358 (4.10), 322 (4.04), 273 (4.34), 245 (4.26), 214 (4.35); IR (ATR):  $\tilde{\nu}$  = 2954, 2866, 1539, 1423, 1349, 1078, 802 cm<sup>-1</sup>.



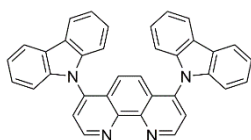
**5-Fluoro-2,9-dimethyl-4,7-di(pyrrolidin-1-yl)-1,10-phenanthroline (5d)**; 0.186 g (0.5 mmol, 51%); m.p. = 100.9-101.0 °C; <sup>1</sup>H NMR (CDCl<sub>3</sub>; 500.18 MHz) δ = 1.96 (m, 4H, 2CH<sub>2</sub>), 2.01 (m, 4H, 2CH<sub>2</sub>), 2.74 (s, 3H, CH<sub>3</sub>), 2.76 (s, 3H, CH<sub>3</sub>), 3.47 (m, 4H, 2CH<sub>2</sub>), 3.61 (m, 4H, 2CH<sub>2</sub>), 6.58 (s, 1H, aromatic), 6.65 (s, 1H, aromatic), 7.45 (d, <sup>3</sup>J<sub>H,F</sub> = 15.5 Hz, 1H, aromatic); <sup>13</sup>C{<sup>1</sup>H} NMR (CDCl<sub>3</sub>; 100.5 MHz) δ = 25.6, 25.6, 25.8, 25.9, 25.9, 51.7, 51.8, 52.0, 102.9 (d, <sup>1</sup>J<sub>C,F</sub> = 27.1 Hz), 106.1, 109.9 (d, <sup>2</sup>J<sub>C,F</sub> = 16.2 Hz), 117.6 (d, <sup>2</sup>J<sub>C,F</sub> = 10.6 Hz), 144.5, 148.7 (d, <sup>3</sup>J<sub>C,F</sub> = 4.1 Hz), 152.1 (d, J = 1.0 Hz), 152.3, 152.9 (d, <sup>3</sup>J<sub>C,F</sub> = 4.3 Hz), 154.8, 157.1 (d, <sup>4</sup>J<sub>C,F</sub> = 1.6 Hz), 158.7; <sup>19</sup>F NMR (CDCl<sub>3</sub>; 470.5 MHz) δ = -112.29 (d, <sup>3</sup>J<sub>F,H</sub> = 15.5 Hz); <sup>19</sup>F{<sup>1</sup>H} NMR (CDCl<sub>3</sub>; 470.5 MHz) δ = -112.29; MS-IT-TOF [M+H]<sup>+</sup> = 365 (100%), HRMS (IT TOF): m/z Calcd for C<sub>22</sub>H<sub>26</sub>FN<sub>4</sub> [M+H]<sup>+</sup>: 365.2136, Found 365.2135; UV-Vis (methanol; λ [nm] (logε)): 407 (3.91), 359 (4.30), 325 (4.26), 281 (4.56), 256 (4.46), 221 (4.73); IR (ATR):  $\tilde{\nu}$  = 2957, 2866, 1564, 1431, 1352, 1090, 820 cm<sup>-1</sup>; CCDC 1479401.



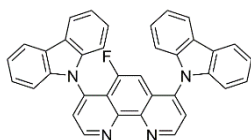
**2,5,9-Trimethyl-4,7-di(pyrrolidin-1-yl)-1,10-phenanthroline (5e)**; 0.140 g (0.4 mmol, 39%); m.p. = 101.7-102.0 °C; <sup>1</sup>H NMR (CDCl<sub>3</sub>; 400.2 MHz) δ = 1.97 (m, 4H, 2CH<sub>2</sub>), 2.03 (m, 4H, 2CH<sub>2</sub>), 2.68 (s, 3H, CH<sub>3</sub>), 2.76 (s, 3H, CH<sub>3</sub>), 2.77 (s, 3H, CH<sub>3</sub>), 3.35 (m, 4H, 2CH<sub>2</sub>), 3.68 (m, 4H, 2CH<sub>2</sub>), 6.61 (s, 1H, aromatic), 6.85 (s, 1H, aromatic), 7.63 (s, 1H, aromatic); <sup>13</sup>C{<sup>1</sup>H} NMR (CDCl<sub>3</sub>; 100.5 MHz) δ = 21.4, 24.4, 25.6, 25.7, 26.0, 52.0, 52.3, 105.8, 109.3, 117.9, 120.8, 122.4, 127.4, 145.1, 146.7, 153.2, 155.4, 156.7, 157.5; MS-IT-TOF [M+H]<sup>+</sup> = 361 (100%), HRMS (IT TOF): m/z Calcd for C<sub>23</sub>H<sub>29</sub>N<sub>4</sub> [M+H]<sup>+</sup>: 361.2386, Found 361.2385; UV-Vis (methanol; λ [nm] (logε)): 361 (4.17), 325 (4.15), 285 (4.44), 260 (4.36), 216 (4.54); IR (ATR):  $\tilde{\nu}$  = 2962, 2846, 1541, 1424, 1349, 1077, 801 cm<sup>-1</sup>.

## 7.5 Synthesis of 4,7-di(9H-carbazol-9-yl)-1,10-phenanthrolines derivatives

These were based on the procedure described in the literature<sup>259</sup>. To a suspension of NaH (0.1 g, 3.94 mmol) in THF (50 mL) 9H-carbazole (0.5 g, 3.01 mmol) was added and stirred until the evolution of H<sub>2</sub> ceased. Reagents were stirred under reflux for 30 min. under argon. Compounds **4a**, **4b**, **4d**, or **4e** (1.50 mmol) was then added to the reaction mixture, which was refluxed overnight. After evaporation of the solvent to give a solid, water (20 mL) and chloroform (100 mL) were added. The organic layer was separated, and the aqueous layer was extracted four times with chloroform. The combined organic layers were dried over MgSO<sub>4</sub>. After solvent evaporating, the crude product was purified by column chromatography on silica gel using methanol/dichloromethane as eluent to afford a white powder, and finally crystallization from a mixture of CH<sub>2</sub>Cl<sub>2</sub> and hexane to yield solids as follows:

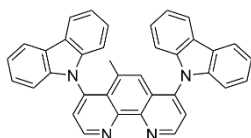


**4,7-Di(9H-carbazol-9-yl)-1,10-phenanthroline**<sup>259</sup> (**5f**) white 0.658 g (1.29 mmol, 86%); m.p.<sub>dec.</sub> = 275.1-280.0 °C; <sup>1</sup>H NMR (CDCl<sub>3</sub>; 500.2 MHz) δ = 7.06 (d, <sup>3</sup>J<sub>H,H</sub> = 7.9 Hz, 4H, aromatic), 7.28-7.36 (m, 10H, aromatic), 7.85 (d, <sup>3</sup>J<sub>H,H</sub> = 4.7 Hz, 2H, aromatic), 8.15 (d, <sup>3</sup>J<sub>H,H</sub> = 7.2 Hz, 4H, aromatic), 9.49 (d, <sup>3</sup>J<sub>H,H</sub> = 4.7 Hz, 2H, aromatic); <sup>13</sup>C{<sup>1</sup>H} NMR (CDCl<sub>3</sub>; 125.78 MHz) δ = 110.1, 120.7, 121.0, 123.0, 124.1, 126.5, 126.7, 141.3, 143.5, 148.8, 151.6; CP/MAS <sup>13</sup>C NMR δ = 109.4, 120.2, 122.0, 123.6, 124.8, 127.4, 139.4, 141.2, 147.5, 149.2, 150.3; CP/MAS <sup>15</sup>N NMR δ = -250.68, -73.05; UV-Vis (methanol; λ [nm] (logε)): 353 (3.10), 332 (3.54), 319 (3.54), 277 (4.03), 268 (4.06), 247 (4.16), 230 (4.50), 210 (4.18); IR (ATR):  $\tilde{\nu}$  = 3062, 2371, 1448, 1222, 750, 725 cm<sup>-1</sup>.



**4,7-Di(9H-carbazol-9-yl)-5-fluoro-1,10-phenanthroline** (**5g**) 0.428 g (0.81 mmol, 54%); m.p.<sub>dec.</sub> = 184.3-185.0 °C; <sup>1</sup>H NMR (CDCl<sub>3</sub>; 400.2 MHz) δ = 7.03 (d, <sup>3</sup>J<sub>H,F</sub> = 12.6 Hz, 1H, aromatic), 7.09 (dd, <sup>3</sup>J<sub>H,H</sub> = 7.7 Hz, <sup>3</sup>J<sub>H,H</sub> = 5.2 Hz, 4H, aromatic), 7.30-7.43 (m, 8H, aromatic), 7.91 (dd, <sup>3</sup>J<sub>H,H</sub> = 9.9 Hz, <sup>3</sup>J<sub>H,H</sub> = 4.7 Hz, 2H, aromatic), 8.18 (t, <sup>3</sup>J<sub>H,H</sub> = 8.4 Hz, 4H, aromatic), 9.47 (d, <sup>3</sup>J<sub>H,H</sub> = 4.4 Hz, 1H, aromatic), 9.54 (d, <sup>3</sup>J<sub>H,H</sub> = 4.6 Hz, 1H, aromatic); <sup>13</sup>C{<sup>1</sup>H} NMR (CDCl<sub>3</sub>; 100.5 MHz) δ = 106.5 (d, <sup>1</sup>J<sub>C,F</sub> = 24.7 Hz), 109.4, 110.0, 119.6, 120.7, 120.8 (d, <sup>4</sup>J<sub>C,F</sub> = 1.0 Hz), 121.0, 121.2, 121.4, 123.6, 124.1

(d,  $^2J_{C,F} = 17.7$  Hz), 125.1, 125.5, 126.56 (d,  $^3J_{C,F} = 4.8$  Hz), 126.58 (d,  $^2J_{C,F} = 23.6$  Hz), 141.1, 141.6, 141.7 (d,  $^4J_{C,F} = 1.9$  Hz), 143.2 (d,  $^3J_{C,F} = 6.0$  Hz), 146.1, 150.0 (d,  $^4J_{C,F} = 2.5$  Hz), 150.9, 152.6, 154.2, 156.8;  $^{19}\text{F}$  NMR ( $\text{CDCl}_3$ ; 470.5 MHz)  $\delta = -112.43$  (d,  $^3J_{F,H} = 10.6$  Hz);  $^{19}\text{F}\{^1\text{H}\}$  NMR ( $\text{CDCl}_3$ ; 470.5 MHz)  $\delta = -112.43$ ; MS-IT-TOF  $[\text{M}+\text{H}]^+ = 529$  (100%), HRMS (IT TOF):  $m/z$  Calcd for  $\text{C}_{36}\text{H}_{22}\text{FN}_4$   $[\text{M}+\text{H}]^+$ : 529.1828, Found 529.1823. UV-Vis (methanol;  $\lambda$  [nm] ( $\log\epsilon$ )): 367 (3.14), 329 (3.37), 318 (3.37), 278 (3.88), 256 (3.88), 230 (4.33), 209 (4.08); IR (ATR):  $\tilde{\nu} = 3045, 3023, 2361, 1445, 1224, 744, 720$   $\text{cm}^{-1}$ .



**4,7-Di(9H-carbazol-9-yl)-5-methyl-1,10-phenanthroline (5h)** white 0.702 g (1.34 mmol, 89%); m.p.<sub>dec.</sub> >350 °C;  $^1\text{H}$  NMR ( $\text{CDCl}_3$ ; 500.2 MHz)  $\delta = 1.60$  (d,  $^4J_{H,H} = 0.8$  Hz, 3H,  $\text{CH}_3$ ), 6.93 (d,  $^3J_{H,H} = 8.1$  Hz, 2H, aromatic), 7.10 (d,  $^3J_{H,H} = 8.1$  Hz, 2H, aromatic), 7.22 (d,  $^4J_{H,H} = 1.0$  Hz, 1H, aromatic), 7.29-7.40 (m, 8H, aromatic), 7.68 (d,  $^3J_{H,H} = 4.6$  Hz, 1H, aromatic), 7.80 (d,  $^3J_{H,H} = 4.7$  Hz, 1H, aromatic), 8.16 (d,  $^3J_{H,H} = 7.7$  Hz, 2H, aromatic), 8.18 (d,  $^3J_{H,H} = 8.1$  Hz, 2H, aromatic), 9.43 (dd,  $^3J_{H,H} = 6.9$  Hz,  $^3J_{H,H} = 4.7$  Hz, 2H, aromatic);  $^{13}\text{C}\{^1\text{H}\}$  NMR ( $\text{CDCl}_3$ ; 100.5 MHz)  $\delta = 21.1, 109.7, 110.1, 120.70, 120.73, 120.8, 121.0, 123.1, 123.7, 124.0, 124.5, 125.6, 126.2, 126.5, 126.8, 128.2, 133.6, 141.4, 142.2, 142.4, 143.4, 148.0, 149.7, 150.9, 151.2$ ; CP/MAS  $^{13}\text{C}$  NMR  $\delta = 23.4, 111.3, 116.6, 120.7, 123.3, 126.7, 128.2, 133.7, 136.6, 142.0, 147.4, 148.5, 150.3$ ; CP/MAS  $^{15}\text{N}$  NMR  $\delta = -254.60, -249.48, -78.17, -54.38$ ; MS-IT-TOF  $[\text{M}+\text{H}]^+ = 525$  (30%), HRMS (IT TOF):  $m/z$  Calcd for  $\text{C}_{37}\text{H}_{25}\text{N}_4$   $[\text{M}+\text{H}]^+$ : 525.2001, Found 525.2091; UV-Vis (methanol;  $\lambda$  [nm] ( $\log\epsilon$ )): 355 (3.32), 333 (3.83), 319 (3.76), 277 (4.28), 256 (4.25), 245 (4.41), 232 (4.72), 210 (4.38); IR (ATR):  $\tilde{\nu} = 3046, 2363, 1449, 1230, 747, 723$   $\text{cm}^{-1}$ .

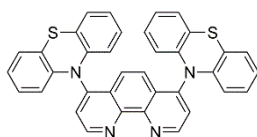


**4,7-Di(9H-carbazol-9-yl)-1,10-phenanthroline-5-carbonitrile (5i)** brown 0.690 g (1.29 mmol, 86%); m.p.<sub>dec.</sub> = 145-147 °C;  $^1\text{H}$  NMR ( $\text{CDCl}_3$ ; 400.2 MHz)  $\delta = 6.93$  (d,  $^3J_{H,H} = 7.4$  Hz, 2H, aromatic), 7.07 (d,  $^3J_{H,H} = 7.3$  Hz, 2H, aromatic), 7.31-7.43 (m, 8H, aromatic), 7.88 (d,  $^3J_{H,H} = 4.6$  Hz, 1H, aromatic), 7.93 (d,  $^3J_{H,H} = 4.7$  Hz, 1H, aromatic), 8.05 (s, 1H, aromatic), 8.18 (d,  $^3J_{H,H} = 7.3$  Hz, 4H, aromatic), 9.55 (d,  $^3J_{H,H} = 4.6$  Hz, 1H, aromatic), 9.60 (d,  $^3J_{H,H} = 4.7$  Hz, 1H, aromatic);  $^{13}\text{C}\{^1\text{H}\}$  NMR ( $\text{CDCl}_3$ ; 100.5 MHz)  $\delta = 107.1, 109.2, 109.6, 115.7, 121.0, 121.1, 121.3, 121.7, 123.8, 124.4, 124.5, 125.2, 125.6, 125.8, 126.6, 126.9, 134.4, 141.2, 142.3, 143.1, 144.5, 148.8, 149.6, 153.1, 154.7$ ; MS-IT-TOF  $[\text{M}+\text{H}]^+ = 536$  (100%), HRMS (IT TOF):  $m/z$  Calcd for  $\text{C}_{37}\text{H}_{22}\text{N}_5$   $[\text{M}+\text{H}]^+$ : 536.1875, Found

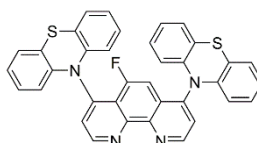
536.1876; UV-Vis (methanol;  $\lambda$  [nm] ( $\log\epsilon$ )): 368 (3.28), 323 (3.77), 292 (4.23), 286 (4.22), 257 (4.33), 232 (4.73); IR (ATR):  $\tilde{\nu}$  = 3050, 2925, 2224, 1450, 1226, 752, 726  $\text{cm}^{-1}$ .

## 7.6 Synthesis of 4,7-di(10*H*-phenothiazin-10-yl)-1,10-phenanthrolines derivatives

To the suspension of NaH (1.1 g, 48.1 mmol) in THF (50 mL) 10*H*-phenothiazine (8.0 g, 40.0 mmol) was added and stirred until evolution of H<sub>2</sub> ceased. Reagents were stirred under reflux for 30 min. under argon. Then compounds **4a**, **4b**, **4d** or **4e** (20.0 mmol) were added to the reaction mixture in one portion. After heating under reflux for 24 h, the solvent was evaporated and a mixture composed of CH<sub>2</sub>Cl<sub>2</sub> (20 mL) and water (20 mL) was added. The organic layer was separated and the aqueous layer was extracted four times with chloroform (4 x 20 mL). The combined organic layers were dried over MgSO<sub>4</sub>, and the crude product was purified by crystallization from mixture of THF (CH<sub>2</sub>Cl<sub>2</sub>) and hexane to yield solid as follows:

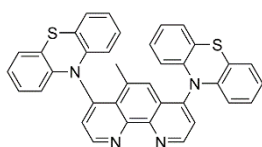


**4,7-di(10*H*-phenothiazin-10-yl)-1,10-phenanthroline (5j)** greenish 10.791 g (18.8 mmol, 94%); m.p.<sub>dec.</sub> = 149.4-150.0 °C; <sup>1</sup>H NMR (CDCl<sub>3</sub>; 500.2 MHz)  $\delta$  = 6.10 (dd, <sup>3</sup>J<sub>H,H</sub> = 8.2 Hz, <sup>4</sup>J<sub>H,H</sub> = 1.1 Hz, 4H, aromatic), 6.76 (dt, <sup>3</sup>J<sub>H,H</sub> = 7.8 Hz, <sup>4</sup>J<sub>H,H</sub> = 1.6 Hz, 4H, aromatic), 6.82 (td, <sup>3</sup>J<sub>H,H</sub> = 7.5 Hz, <sup>4</sup>J<sub>H,H</sub> = 1.2 Hz, 4H, aromatic), 7.07 (dd, <sup>3</sup>J<sub>H,H</sub> = 7.6 Hz, <sup>4</sup>J<sub>H,H</sub> = 1.5 Hz, 4H, aromatic), 7.88 (d, <sup>3</sup>J<sub>H,H</sub> = 4.7 Hz, 2H, aromatic), 8.15 (s, 2H, aromatic), 9.50 (d, <sup>3</sup>J<sub>H,H</sub> = 4.7 Hz, 2H, aromatic); <sup>13</sup>C{<sup>1</sup>H} NMR (CDCl<sub>3</sub>; 125.78 MHz)  $\delta$  = 116.0, 121.1, 123.4, 123.5, 127.1, 127.3, 128.5, 142.9, 146.5, 149.5, 152.0; MS-IT-TOF [M+H]<sup>+</sup> = 575 (100%), HRMS (IT TOF): m/z Calcd for C<sub>36</sub>H<sub>23</sub>N<sub>4</sub>S<sub>2</sub> [M+H]<sup>+</sup>: 575.1364, Found 575.1358. UV-Vis (methanol;  $\lambda$  [nm] ( $\log\epsilon$ )): 302 (3.56), 270 (4.09), 251 (4.33), 237 (4.21), 228 (4.15), 208 (4.14); IR (ATR):  $\tilde{\nu}$  = 3055, 2984, 1460, 1305, 1234, 748, 734, 632  $\text{cm}^{-1}$ .

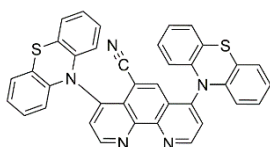


**5-fluoro-4,7-di(10*H*-phenothiazin-10-yl)-1,10-phenanthroline (5k)** brown 11.366 g (19.2 mmol, 96%); m.p.<sub>dec.</sub> = 186.1-187.0 °C; <sup>1</sup>H NMR (CDCl<sub>3</sub>; 500.2 MHz)  $\delta$  = 5.84 (d, <sup>3</sup>J<sub>H,H</sub> = 8.2 Hz, <sup>4</sup>J<sub>H,H</sub> = 0.8 Hz, 2H, aromatic), 6.17 (d, <sup>3</sup>J<sub>H,H</sub> = 8.1 Hz, <sup>4</sup>J<sub>H,H</sub> = 1.2 Hz, 2H, aromatic), 6.69 (td, <sup>3</sup>J<sub>H,H</sub> = 7.4 Hz, <sup>4</sup>J<sub>H,H</sub> = 1.6 Hz, 2H, aromatic), 6.75 (td, <sup>3</sup>J<sub>H,H</sub> = 7.5 Hz, <sup>4</sup>J<sub>H,H</sub> = 1.3 Hz, 2H, aromatic), 6.80 (td, <sup>3</sup>J<sub>H,H</sub> = 7.4

Hz,  $^4J_{\text{H,H}} = 1.7$  Hz, 2H, aromatic), 6.85 (td,  $^3J_{\text{H,H}} = 7.4$  Hz,  $^4J_{\text{H,H}} = 1.3$  Hz, 2H, aromatic), 6.98 (dd,  $^3J_{\text{H,H}} = 7.6$  Hz,  $^4J_{\text{H,H}} = 1.5$  Hz, 2H, aromatic), 7.08 (dd,  $^3J_{\text{H,H}} = 7.5$  Hz,  $^4J_{\text{H,H}} = 1.6$  Hz, 2H, aromatic), 7.82 (d,  $^3J_{\text{H,H}} = 4.6$  Hz, 1H, aromatic), 7.87 (d,  $^3J_{\text{H,F}} = 12.5$  Hz, 1H, aromatic), 7.92 (d,  $^3J_{\text{H,H}} = 4.6$  Hz, 1H, aromatic), 9.47 (d,  $^3J_{\text{H,H}} = 4.6$  Hz, 1H, aromatic), 9.52 (d,  $^3J_{\text{H,H}} = 4.6$  Hz, 1H, aromatic);  $^{13}\text{C}\{^1\text{H}\}$  NMR ( $\text{CDCl}_3$ ; 125.78 MHz)  $\delta = 106.5$  (d,  $^3J_{\text{C,F}} = 24.7$  Hz), 115.4 (d,  $^1J_{\text{C,F}} = 108.4$  Hz), 119.8, 121.4, 122.4 (d,  $^4J_{\text{C,F}} = 13.5$  Hz), 123.3 (d,  $^2J_{\text{C,F}} = 91.9$  Hz), 127.0 (d,  $^4J_{\text{C,F}} = 14.5$  Hz), 127.3 (d,  $^3J_{\text{C,F}} = 16.0$  Hz), 128.2, 128.4 (d,  $^2J_{\text{C,F}} = 66.8$  Hz), 142.8 (d,  $^5J_{\text{C,F}} = 11.9$  Hz), 144.3, 145.7 (d,  $^5J_{\text{C,F}} = 5.3$  Hz), 147.3, 150.6, 151.1, 153.9, 154.7, 156.8;  $^{19}\text{F}$  NMR ( $\text{CDCl}_3$ ; 470.5 MHz)  $\delta = -113.33$  (d,  $^3J_{\text{F,H}} = 11.9$  Hz);  $^{19}\text{F}\{^1\text{H}\}$  NMR ( $\text{CDCl}_3$ ; 470.5 MHz)  $\delta = -113.33$ ; MS-IT-TOF  $[\text{M}+\text{Na}]^+ = 615$  (30%), HRMS (IT TOF):  $m/z$  Calcd for  $\text{C}_{20}\text{H}_{23}\text{N}_4$   $[\text{M}+\text{Na}]^+$ : 615.1089, Found 615.1083. UV-Vis (methanol;  $\lambda$  [nm] ( $\log\epsilon$ )): 307 (3.56), 271 (4.04), 250 (4.33), 239 (4.23), 227 (4.14), 210 (4.19); IR (ATR):  $\tilde{\nu} = 3057$ , 2962, 2360, 1459, 1312, 1235, 739, 643  $\text{cm}^{-1}$ .



**5-methyl-4,7-di(10H-phenothiazin-10-yl)-1,10-phenanthroline (5l)** purple 9.878 g (16.8 mmol, 84%); m.p.<sub>dec.</sub> >350 °C;  $^1\text{H}$  NMR ( $\text{CDCl}_3$ ; 500.2 MHz)  $\delta = 2.91$  (s, 3H,  $\text{CH}_3$ ), 5.80 (d,  $^3J_{\text{H,H}} = 8.0$  Hz, 2H, aromatic), 6.11 (d,  $^3J_{\text{H,H}} = 7.9$  Hz, 2H, aromatic), 6.65-6.85 (m, 8H, aromatic), 6.96 (d,  $^3J_{\text{H,H}} = 7.3$  Hz, 2H, aromatic), 7.07 (d,  $^3J_{\text{H,H}} = 7.4$  Hz, 2H, aromatic), 7.70 (d,  $^3J_{\text{H,H}} = 4.5$  Hz, 1H, aromatic), 7.83 (d,  $^3J_{\text{H,H}} = 4.5$  Hz, 1H, aromatic), 7.92 (s, 1H, aromatic), 9.45 (dd,  $^3J_{\text{H,H}} = 8.4$  Hz,  $^3J_{\text{H,H}} = 4.6$  Hz, 2H, aromatic);  $^{13}\text{C}\{^1\text{H}\}$  NMR( $\text{CDCl}_3$ ; 100.5 MHz)  $\delta = 23.6$ , 115.6, 116.0, 119.0, 120.9, 123.0, 123.3, 124.2, 126.8, 127.06, 127.1, 127.2, 127.8, 129.0, 129.4, 134.5, 142.6, 142.8, 145.4, 146.4, 148.6, 151.0, 151.3, 151.7; CP/MAS  $^{13}\text{C}$  NMR  $\delta = 25.9$ , 116.8, 123.4, 124.6, 127.2, 135.3, 141.5, 144.8, 147.1, 149.0, 152.6, 153.5, 155.6; CP/MAS  $^{15}\text{N}$  NMR  $\delta = -273.57$ ,  $-62.21$ ,  $-51.07$ ; MS-IT-TOF  $[\text{M}+\text{H}]^+ = 589$  (100%), HRMS (IT TOF):  $m/z$  Calcd for  $\text{C}_{37}\text{H}_{25}\text{N}_4\text{S}_2$   $[\text{M}+\text{H}]^+$ : 589.15207, Found 589.15059; UV-Vis (methanol;  $\lambda$  [nm] ( $\log\epsilon$ )): 332 (3.28), 307 (3.79), 273 (4.29), 255 (4.58), 242 (4.48); IR (ATR):  $\tilde{\nu} = 3059$ , 2960, 1461, 1307, 1241, 736, 631  $\text{cm}^{-1}$ .



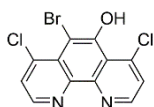
**4,7-di(10H-phenothiazin-10-yl)-1,10-phenanthroline-5-carbonitrile (5m)** brown 9.943 g (16.6 mmol, 83%); m.p.<sub>dec.</sub> = 270-275 °C;  $^1\text{H}$  NMR ( $\text{CDCl}_3$ ; 500.2 MHz)  $\delta = 5.67$  (d,  $^3J_{\text{H,H}} = 8.2$  Hz, 2H, aromatic), 6.10 (d,  $^3J_{\text{H,H}} = 8.1$  Hz, 2H, aromatic), 6.67 (t,  $^3J_{\text{H,H}} = 7.8$  Hz, 2H, aromatic), 6.77 (t,  $^3J_{\text{H,H}} = 7.4$  Hz, 2H, aromatic), 6.82 (t,  $^3J_{\text{H,H}} = 7.8$  Hz, 2H, aromatic), 6.90 (t,  $^3J_{\text{H,H}} = 7.2$  Hz, 2H, aromatic),

6.98 (d,  $^3J_{\text{H,H}} = 7.6$  Hz, 2H, aromatic), 7.13 (d,  $^3J_{\text{H,H}} = 7.6$  Hz, 2H, aromatic), 7.89 (d,  $^3J_{\text{H,H}} = 4.6$  Hz, 1H, aromatic), 8.01 (d,  $^3J_{\text{H,H}} = 4.6$  Hz, 1H, aromatic), 8.76 (s, 1H, aromatic), 9.58 (d,  $^3J_{\text{H,H}} = 4.6$  Hz, 1H, aromatic), 9.65 (d,  $^3J_{\text{H,H}} = 4.6$  Hz, 1H, aromatic);  $^{13}\text{C}\{^1\text{H}\}$  NMR( $\text{CDCl}_3$ ; 125.78 MHz)  $\delta = 107.5$ , 115.1, 115.9, 117.6, 119.6, 121.7, 123.4, 124.1, 126.9, 127.1, 127.3, 127.7, 128.6, 129.2, 135.0, 142.1, 142.8, 146.4, 147.4, 149.8, 150.7, 154.3, 155.1; MS-IT-TOF  $[\text{M}+\text{H}]^+ = 600$  (100%), HRMS (IT TOF):  $m/z$  Calcd for  $\text{C}_{37}\text{H}_{22}\text{N}_5\text{S}_2$   $[\text{M}+\text{H}]^+$ : 600.1317, Found 600.1323; UV-Vis (methanol;  $\lambda$  [nm] ( $\log\epsilon$ )): 332 (3.59), 313 (3.79), 298 (3.87), 272 (4.18), 249 (4.47), 206 (4.35); IR (ATR):  $\tilde{\nu} = 3053$ , 2926, 2215, 1466, 1313, 1239, 742, 633  $\text{cm}^{-1}$ .

## 7.7 Oxidation and hydrolysis reaction of selected 1,10-phenanthroline products

### 7.7.1 Oxidation of 4,7-dichloro-1,10-phenanthroline

The sulfuric acid (96%, 19 mL) was cooled with ice-water bath and the temperature was maintained at 0 - 5 °C. Next, a mixture of 4,7-dichloro-1,10-phenanthroline (1.0 g, 4.0 mmol) and potassium bromide (6.2 g, 52.1 mmol) was slowly added in several small portions. Then concentrated  $\text{HNO}_3$  (70%, 9.5 mL) was then introduced into the solution. The mixture was kept in ice-water bath for 10 min and an oil-water separator was connected to the flask. The mixture was heated to 90 °C for 2 h. After cooling, the crude product was poured onto ice, then neutralized with NaOH to pH = 6. Next, the crude products were purified by chromatography using  $\text{CHCl}_3$  : MeOH (1 : 1). The resulting mixture was dissolved in  $\text{CHCl}_3$ .

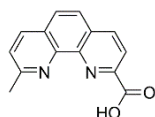


**6-bromo-4,7-dichloro-5,6-dihydro-1,10-phenanthrolin-5-ol (Ox-4a)** 0.138 g (0.4 mmol, 10%);  $m.p._{\text{dec.}} = 220\text{-}220.5$  °C;  $^1\text{H}$  NMR ( $\text{CDCl}_3$ ; 400.2 MHz)  $\delta = 5.69$  (d,  $^3J_{\text{H,H}} = 2.6$  Hz, 1H), 5.76 (d,  $^3J_{\text{H,H}} = 2.5$  Hz, 1H), 7.31 (d,  $^3J_{\text{H,H}} = 5.2$  Hz, 1H, aromatic), 7.38 (d,  $^3J_{\text{H,H}} = 5.2$  Hz, 1H, aromatic), 8.45 (d,  $^3J_{\text{H,H}} = 5.2$  Hz, 1H, aromatic), 8.51 (d,  $^3J_{\text{H,H}} = 5.2$  Hz, 1H, aromatic);  $^{13}\text{C}\{^1\text{H}\}$  NMR( $\text{CDCl}_3$ ; 125.78 MHz)  $\delta = 42.8$ , 68.0, 125.6, 125.9, 130.1, 130.2, 145.3, 145.7, 150.3, 150.5, 150.6, 150.9; HRMS (ESI TOF):  $m/z$  Calcd for  $\text{C}_{12}\text{H}_7\text{BrCl}_2\text{N}_2\text{O}$   $[\text{M}+\text{H}]^+$ : 346.9132, Found 346.9166;  $m/z$  Calcd for  $\text{C}_{12}\text{H}_6\text{BrCl}_2\text{N}_2\text{NaO}$   $[\text{M}+\text{Na}]^+$ : 368.8942, Found 368.8979; UV-Vis (ACN;  $\lambda$  [nm] ( $\log\epsilon$ )): 333 (2.71), 296 (3.63), 263 (3.71), 212 (4.23).

## 7.7.2 Procedures for Oxidation of 2,9-dimethyl-1,10-phenanthroline

### 7.7.2.1 First oxidation procedure of 2,9-dimethyl-1,10-phenanthroline

The 2,9-Dimethyl-1,10-phenanthroline (1.0 g, 4.8 mmol) was added to a solution of NaClO<sub>2</sub> (5.0 g, 55.3 mmol) in 50 mL of water at room temperature. Then the temperature was increased to 90 °C. After carrying out the reaction for 6 hours at this temperature, the resulting solution was acidified very slowly to pH 2.8 by adding HCl solution (10%). The water was then evaporated under reduced pressure, and the crude product was extracted with MeOH and purified by Soxhlet extraction (MeOH). After the concentration of MeOH, the product was washed with CH<sub>2</sub>Cl<sub>2</sub> and finally dried over P<sub>4</sub>O<sub>10</sub>.

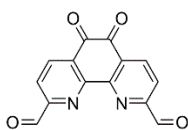


**9-methyl-1,10-phenanthroline-2-carboxylic acid (Ox-Phen-2CH<sub>3</sub>)** 0.66 g (2.78 mmol, 58%); m.p. > 300 °C ; <sup>1</sup>H NMR (D<sub>2</sub>O/KOD; 400.2 MHz) δ = 2.46 (s, 3H, CH<sub>3</sub>), 6.99 (bs, 2H, arom), 7.02 (d, <sup>3</sup>J<sub>H,H</sub> = 8.2 Hz, 1H, aromatic), 7.50 (d, <sup>3</sup>J<sub>H,H</sub> = 8.2 Hz, 1H, aromatic), 7.68-7.76 (m, 2H, aromatic), 8.41 (bs, 1H, OH); <sup>13</sup>C{<sup>1</sup>H} NMR (D<sub>2</sub>O; 100.5 MHz) δ = 23.3, 122.2, 123.7, 124.6, 125.9, 126.8, 128.5, 136.8, 137.0, 142.0, 142.6, 151.2, 158.2, 172.4; HRMS (ESI TOF): m/z Calcd for C<sub>14</sub>H<sub>11</sub>N<sub>2</sub>O<sub>2</sub> (M – H)<sup>–</sup> = 237.0664, Found 237.0662; UV-Vis (methanol; λ [nm] (logε)): 314 (3.06), 275 (3.95), 230 (4.10); IR (KBr):  $\tilde{\nu}$  = 1628, 1393, 1007, 972, 835 cm<sup>–1</sup>.

### 7.7.2.2 Second oxidation procedure of 2,9-dimethyl-1,10-phenanthroline

The 2,9-dimethyl-1,10-Phenanthroline (5.00 g, mmol) was dissolved in portions during stirring in 30 mL of concentrated sulfuric acid (96%). Then, sodium bromide (2.50 g, mmol) was added, followed by 15 mL of 70% nitric acid. The mixture was heated to boiling and then kept refluxing for 40 min. After being cooled to room temperature, the mixture was poured onto 400 g of ice, carefully neutralized to pH 7 with NaOH, and allowed to stand for 30 min. The mixture was filtered, and the solids were extracted with 100 mL of boiling water. The insoluble material was removed from the cooled extract by filtration, and the combined aqueous solutions were extracted with dichloromethane (5 x 100 mL). The organic phase was washed with 50 mL of water, dried over MgSO<sub>4</sub>, and evaporated under reduced pressure. The crystalline residue was recrystallized from methanol. The complex reaction mixture was obtained. The products identified only by MS suggest a structure of molecule **Ox2-Phen-2CH<sub>3</sub>**,

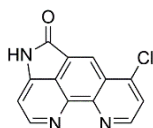




### 5,6-dioxo-5,6-dihydro-1,10-phenanthroline-2,9-dicarbaldehyde (Ox2-Phen-2CH<sub>3</sub>)

#### 7.7.3 Hydrolysis of 4,7-dichloro-1,10-phenanthroline-5-carbonitrile

Compound **4e** (1.0 g, 3.7 mmol) was dissolved in concentrated hydrochloric acid (35%) (23 mL) at r.t. After stirring for 72 h at 100 °C, the volatiles were evaporated. The crude product was purified by extraction at Soxhlet apparatus (H<sub>2</sub>O) and finally was dried over P<sub>4</sub>O<sub>10</sub> to yield a precipitate of 7-chloropyrrolo [2,3,4-*de*][1,10]phenanthroline-5(4H)-one (**Ox-4e**, 0.3 g, 1.4 mmol, 37%).

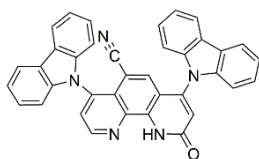


**7-Chloropyrrolo[2,3,4-*de*][1,10]phenanthroline-5(4H)-one (Ox-4e)** 0.358 g (1.4 mmol, 37%). beige; m.p.<sub>dec.</sub> = 310-330 °C; <sup>1</sup>H NMR (D<sub>2</sub>O/KOD; 500.2 MHz) δ = 6.47 (d, <sup>3</sup>J<sub>H,H</sub> = 6.9 Hz, 1H, aromatic), 6.61 (d, <sup>3</sup>J<sub>H,H</sub> = 5.9 Hz, 1H, aromatic), 7.69 (s, 1H, aromatic), 8.05 (d, <sup>3</sup>J<sub>H,H</sub> = 6.9 Hz, 1H, aromatic), 8.28 (d, <sup>3</sup>J<sub>H,H</sub> = 5.9 Hz, 1H, aromatic); <sup>1</sup>H NMR (D<sub>2</sub>O/D<sub>2</sub>SO<sub>4</sub>; 400.2 MHz) δ = 7.29 (d, <sup>3</sup>J<sub>H,H</sub> = 6.8 Hz, 1H, aromatic), 7.42 (d, <sup>3</sup>J<sub>H,H</sub> = 6.8 Hz, 1H, aromatic), 8.28 (s, 1H, aromatic), 8.78 (d, <sup>3</sup>J<sub>H,H</sub> = 6.8 Hz, 1H, aromatic), 8.87 (d, <sup>3</sup>J<sub>H,H</sub> = 6.8 Hz, 1H, aromatic); <sup>13</sup>C{<sup>1</sup>H} NMR (D<sub>2</sub>O/KOD; 125.8 MHz) δ = 111.5, 111.6, 114.8, 120.7, 125.1, 132.5, 138.1, 139.2, 140.7, 149.3, 173.8, 178.0, 179.7; MS-IT-TOF (M-H)<sup>-</sup> = 254 (80%), (M+H)<sup>+</sup> = 256 (30%), HRMS (IT TOF): m/z Calcd for C<sub>13</sub>H<sub>7</sub>N<sub>3</sub>ClO (M+H)<sup>+</sup>: 256.0278, Found 256.0279; UV-Vis (methanol; λ [nm] (logε)): 348 (3.28), 334 (3.27), 278 (3.31), 245 (3.64), 221 (3.36); IR (KBr):  $\tilde{\nu}$  = 3086, 1560, 1522, 1402, 1385, 1363, 1026 cm<sup>-1</sup>.

#### 7.7.4 Hydrolysis of 4,7-disubstituted-9-oxo-9,10-dihydro-1,10-phenanthroline-5-carbonitrile

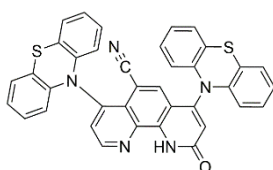
Compounds **5i** or **5m** (3.5 mmol) dissolved in a mixture composed of THF and 10% sodium hydroxide (55 mL) were stirred for 4 days at 50 °C. The cooled solution was acidified to neutral pH with concentrated hydrochloric acid. After solvent evaporation, the crude product was purified by column chromatography on silica gel using methanol/dichloromethane as eluent to afford a

white powder, and finally crystallization from the mixture of CH<sub>2</sub>Cl<sub>2</sub> and hexane to yield solids as follows:



**4,7-di(9H-carbazol-9-yl)-9-oxo-9,10-dihydro-1,10-phenanthroline-5-carbonitrile (Hyd-5i)**

yellowish 0.606 g (1.1 mmol, 31%); m.p.<sub>dec.</sub> 195-200 °C; <sup>1</sup>H NMR (CDCl<sub>3</sub>; 400.2 MHz) δ = 6.90 (d, <sup>3</sup>J<sub>H,H</sub> = 7.3 Hz, 2H, aromatic), 7.14 (s, 1H, aromatic), 7.21 (d, <sup>3</sup>J<sub>H,H</sub> = 8.0 Hz, 2H, aromatic), 7.29-7.45 (m, 8H, aromatic), 7.65 (s, 1H, aromatic), 7.83 (d, <sup>3</sup>J<sub>H,H</sub> = 4.3 Hz, 1H, aromatic), 8.16-8.17 (m, 4H, aromatic), 9.27 (d, <sup>3</sup>J<sub>H,H</sub> = 4.3 Hz, 1H, aromatic), 11.24 (bs, 1H, NH); <sup>13</sup>C{<sup>1</sup>H} NMR (CDCl<sub>3</sub>; 100.5 MHz) δ = 100.8, 109.1, 110.0, 115.5, 115.7, 121.0, 121.2, 121.5, 121.7, 124.2, 124.4, 124.5, 126.3, 126.7, 126.8, 126.9, 133.5, 139.0, 140.1, 140.5, 142.2, 143.6, 146.5, 151.8, 161.7; MS-IT-TOF [M+H]<sup>+</sup> = 552.1830 (100%), [M-H]<sup>-</sup> = 550.1668 (100%), HRMS (IT TOF): m/z Calcd for C<sub>37</sub>H<sub>22</sub>N<sub>5</sub>O [M+H]<sup>+</sup>: 552.1824, Found 552.1830; UV-Vis (methanol; λ [nm] (logε)): 374 (3.46), 355 (3.57), 329 (3.82), 316 (3.76), 292 (4.27), 287 (4.25), 282 (4.27), 247 (4.31), 231 (4.62), 210 (4.33); IR (ATR):  $\tilde{\nu}$  = 3051, 2360, 2218, 1675, 1446, 1226, 747, 723 cm<sup>-1</sup>; CCDC 191090.



**9-oxo-4,7-di(10H-phenothiazin-10-yl)-9,10-dihydro-1,10-phenanthroline-5-carbonitrile (Hyd-5m)**

yellowish 0.984 g (1.6 mmol, 46%); m.p.<sub>dec.</sub> 220-230 °C; <sup>1</sup>H NMR (CDCl<sub>3</sub>; 400.2 MHz) δ = 5.63 (d, <sup>3</sup>J<sub>H,H</sub> = 8.2 Hz, 2H, aromatic), 6.63-6.58 (m, 2H, aromatic), 6.66 (dd, <sup>3</sup>J<sub>H,H</sub> = 7.8 Hz, <sup>4</sup>J<sub>H,H</sub> = 0.9 Hz, 2H, aromatic), 6.77 (t, <sup>3</sup>J<sub>H,H</sub> = 7.5 Hz, 2H, aromatic), 6.90-7.00 (m, 6H, aromatic), 7.12-7.18 (m, 2H, aromatic), 7.25 (s, 1H, aromatic), 7.84 (d, <sup>3</sup>J<sub>H,H</sub> = 4.5 Hz, 1H, aromatic), 8.45 (s, 1H, aromatic), 9.27 (d, <sup>3</sup>J<sub>H,H</sub> = 4.6 Hz, 1H, aromatic), 11.11 (bs, 1H, NH); <sup>13</sup>C{<sup>1</sup>H} NMR (CDCl<sub>3</sub>; 100.5 MHz) δ = 101.0, 115.1, 116.2, 116.7, 117.5, 119.8, 122.6, 123.5, 124.5, 127.0, 127.2, 127.5, 127.9, 128.5, 129.7, 129.8, 134.1, 139.6, 141.0, 141.9, 142.1, 146.9, 149.2, 153.0, 161.7; MS-IT-TOF [M+H]<sup>+</sup> = 616.1271 (100%), [M-H]<sup>-</sup> = 614.1110 (100%), HRMS (IT TOF): m/z Calcd for C<sub>37</sub>H<sub>20</sub>N<sub>5</sub>OS [M-H]<sup>-</sup>: 614.1109, Found 614.1110; UV-Vis (methanol; λ [nm] (logε)): 339 (3.94), 295 (4.52), 284 (4.38), 273 (4.18), 251 (4.79), 205 (4.59); IR (ATR):  $\tilde{\nu}$  = 3059, 2974, 2360, 2216, 1673, 1461, 1312, 743, 648 cm<sup>-1</sup>; CCDC 1919692.

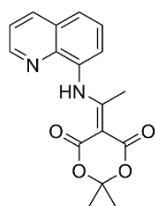
## 7.8 Symmetrical and unsymmetrical quinoline and 1,10-phenanthroline derivatives

### 7.8.1 General Procedures for Synthesis 4-chloro-2-methyl-1,10-phenanthroline

These syntheses were based on procedures described in the literature<sup>39,40</sup>. Due to the multi-stage synthesis reactions, they have been divided into 3 separate steps: Step A, Step B and Step C.

#### 7.8.1.1 Step A

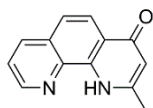
Ortho ester (Trimethyl orthoacetate, TMOA) (72.0 g, 600.0 mmol) and Meldrum's acid (11.5 g, 80.0 mmol) was brought to a gentle reflux for 30 min. The resulting greenish solution was cooled to 80 °C and quinolin-8-amine (**1n**, 8.6 g, 60.0 mmol) was added portion wise (exothermic reaction). The resulting mixture was stirring up to reflux for 2 h, and left under r.t. for 16 h. Subsequently, hexane was added and the solution was cooled to -35 °C where a precipitate formed. The precipitate was filtered off, washed with diethyl ether (4 x 100 mL) and dried to afford a solid:



**2,2-Dimethyl-5-(1-(quinolin-8-ylamino)ethylidene)-1,3-dioxane-4,6-dione (2n)**; 16.3 g (52.2 mmol, 87%); m.p. = 167-170 °C; <sup>1</sup>H NMR (CDCl<sub>3</sub>; 400.2 MHz) δ = 1.76 (s, 6H, 2CH<sub>3</sub>), 2.64 (s, 3H, CH<sub>3</sub>), 7.49 (dd, <sup>3</sup>J<sub>H,H</sub> = 8.3 Hz, <sup>4</sup>J<sub>H,H</sub> = 4.2 Hz, 1H, aromatic), 7.56-7.59 (m, 2H, aromatic), 7.82 (p, <sup>3</sup>J<sub>H,H</sub> = 3.5 Hz, 1H, aromatic), 8.21 (dd, <sup>3</sup>J<sub>H,H</sub> = 8.3 Hz, <sup>4</sup>J<sub>H,H</sub> = 1.5 Hz, 1H, aromatic), 8.95 (dd, <sup>3</sup>J<sub>H,H</sub> = 4.2 Hz, <sup>4</sup>J<sub>H,H</sub> = 1.5 Hz, 1H, aromatic), 13.49 (s, 1H, NH); <sup>13</sup>C{<sup>1</sup>H} NMR(CDCl<sub>3</sub>; 100.6 MHz) δ = 20.7, 26.8, 86.9, 102.8, 122.4, 125.4, 126.0, 127.8, 129.1, 133.9, 136.3, 142.9, 151.1, 163.2, 167.4, 173.3; UV-Vis (methanol; λ [nm] (logε)): 328 (4.43), 314 (4.48), 301 (4.49), 293 (4.51), 262 (4.14), 229 (4.79), 204 (4.79); IR (KBr):  $\tilde{\nu}$  = 2992, 2938, 1708, 1655, 1597, 1356, 1295, 1204, 802 cm<sup>-1</sup>; CCDC 1953940.

#### 7.8.1.2 Step B

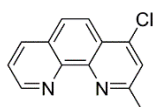
Into freshly distilled diphenyl ether (50 mL) at 220 °C was added **2n** (3.1 g, 10.0 mmol) in small portions, resulting in vigorous gas evolution. The resulting orange solution was brought to reflux for 30 min, and was then allowed to cool to 50 °C. The hexane (25 mL) was added and a brown solid precipitated was filtered, washed with hexane (2 x 10 mL). The crude product was purified by crystallization from chloroform/hexane mixture to yield solid as follows:



**2-Methyl-1,10-phenanthroline-4(1H)-one (3n)** 1.8 g (8.6 mmol, 86%); m.p. = 204-205 °C; <sup>1</sup>H NMR (DMSO-*d*<sub>6</sub>; 500.2 MHz) δ = 2.50 (s, 3H, CH<sub>3</sub>), 6.17 (d, <sup>4</sup>J<sub>H,H</sub> = 0.6 Hz, 1H, aromatic), 7.71 (d, <sup>3</sup>J<sub>H,H</sub> = 8.8 Hz, 1H, aromatic), 7.76 (dd, <sup>3</sup>J<sub>H,H</sub> = 8.2 Hz, <sup>4</sup>J<sub>H,H</sub> = 4.3 Hz, 1H, aromatic), 8.12 (d, <sup>3</sup>J<sub>H,H</sub> = 8.8 Hz, 1H, aromatic), 8.46 (dd, <sup>3</sup>J<sub>H,H</sub> = 8.2 Hz, <sup>4</sup>J<sub>H,H</sub> = 1.6 Hz, 1H, aromatic), 9.01 (dd, <sup>3</sup>J<sub>H,H</sub> = 4.1 Hz, <sup>4</sup>J<sub>H,H</sub> = 1.6 Hz, 1H, aromatic), 12.03 (s, 1H, NH); <sup>13</sup>C{<sup>1</sup>H} NMR (DMSO-*d*<sub>6</sub>; 125.8 MHz) δ = 19.6, 111.8, 121.6, 122.4, 123.1, 123.8, 128.8, 136.6, 137.3, 138.8, 149.2, 149.6, 176.4; GC-MS: t<sub>r</sub> = 9.5 min, (EI) M<sup>+</sup> = 210 (82%); UV-Vis (methanol; λ [nm] (log $\epsilon$ )): 343 (3.38), 317 (3.75), 280 (4.07), 261 (4.25), 238 (4.26), 207 (4.31); IR (KBr):  $\tilde{\nu}$  = 3342, 3250, 2931, 1621, 1548, 1522, 1407, 1371, 843, 836, 738 cm<sup>-1</sup>; CCDC 1954745.

### 7.8.1.3 Step C

Into freshly distilled phosphoryl trichloride (82.0 g, 50 mL, 534.8 mmol) under argon was mixed with **3n** (1.0 g, 5.0 mmol) and the resulting solution was stirred at 90 °C for 4 h. The excess of phosphoryl trichloride was slowly evaporated, under reduced pressure. The reaction mixture was slowly added to a well stirred mixture of ice (50 g) in water (100 mL). After stirring for 15 min. the resulting reaction mixture was carefully brought to pH 13 - 14 by adding NaOH solution (40%). The aqueous layer was extracted with CH<sub>2</sub>Cl<sub>2</sub> (4 x 10 mL). The combined organic layers were separated and dried over MgSO<sub>4</sub>. Evaporation of the brown colored solvent afforded **4n** as light tan crystals. Next, the crude products were purified by chromatography on silica gel using methanol/dichloromethane as eluent and finally crystallization from CH<sub>2</sub>Cl<sub>2</sub> to yield precipitates as follows:



**4-Chloro-2-methyl-1,10-phenanthroline (4n)** 1.1 g (4.8 mmol, 96%); m.p. = 117-118 °C; <sup>1</sup>H NMR (CDCl<sub>3</sub>; 400.2 MHz) δ = 2.93 (s, 3H, CH<sub>3</sub>), 7.62 (s, 1H, aromatic), 7.67 (dd, <sup>3</sup>J<sub>H,H</sub> = 8.1 Hz, <sup>4</sup>J<sub>H,H</sub> = 4.4 Hz, 1H, aromatic), 7.83 (d, <sup>3</sup>J<sub>H,H</sub> = 9.1 Hz, 1H, aromatic), 8.22 (d, <sup>3</sup>J<sub>H,H</sub> = 9.1 Hz, 1H, aromatic), 8.29 (dd, <sup>3</sup>J<sub>H,H</sub> = 8.1 Hz, <sup>4</sup>J<sub>H,H</sub> = 1.5 Hz, 1H, aromatic), 9.25 (dd, <sup>3</sup>J<sub>H,H</sub> = 4.3 Hz, <sup>4</sup>J<sub>H,H</sub> = 1.6 Hz, 1H, aromatic); <sup>1</sup>H NMR (DMSO-*d*<sub>6</sub>; 400.2 MHz) δ = 2.76 (s, 3H, CH<sub>3</sub>), 7.79 (dd, <sup>3</sup>J<sub>H,H</sub> = 8.1 Hz, <sup>4</sup>J<sub>H,H</sub> = 4.3 Hz, 1H, aromatic), 7.86 (s, 1H, aromatic), 8.04 (d, <sup>3</sup>J<sub>H,H</sub> = 9.1 Hz, 1H, aromatic), 8.13 (d, <sup>3</sup>J<sub>H,H</sub> = 9.0 Hz, 1H, aromatic), 8.50 (dd, <sup>3</sup>J<sub>H,H</sub> = 8.1 Hz, <sup>4</sup>J<sub>H,H</sub> = 1.5 Hz, 1H, aromatic), 9.11 (dd, <sup>3</sup>J<sub>H,H</sub> = 4.2 Hz, <sup>4</sup>J<sub>H,H</sub> = 1.5 Hz, 1H, aromatic); <sup>13</sup>C{<sup>1</sup>H} NMR (CDCl<sub>3</sub>; 125.8 MHz) δ = 25.7, 122.5, 123.5, 124.1, 125.0, 126.5, 129.0, 136.8, 142.8, 145.2, 146.6, 150.6, 159.8; GC-MS: t<sub>r</sub> = 8.5 min, (EI) M<sup>+</sup> = 228

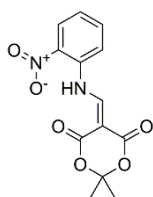
(100%), (M-Cl)<sup>+</sup> = 192 (28%); UV-Vis (methanol;  $\lambda$  [nm] (log $\epsilon$ )): 328 (3.08), 313 (3.21), 297 (3.89), 279 (4.29), 267 (4.55), 234 (4.61), 204 (4.45); IR (KBr):  $\tilde{\nu}$  = 3428, 1586, 1552, 1487, 1375, 832, 726 cm<sup>-1</sup>.

## 7.8.2 General Procedures for Synthesis of 4-chloro-8-nitroquinoline

These syntheses were based on procedures described in the literature<sup>39,40</sup>. Due to the multi-stage synthesis reactions, they have been divided into 3 separate steps: Step A, Step B and Step C.

### 7.8.2.1 Step A

Trimethyl orthoformate (TMOF, 406.2 g, 500 mL, 3.83 mol) and Meldrum's acid (21.6 g, 150.0 mmol) was brought to a gentle reflux for 30 min. The resulting greenish solution was cooled to 80 °C and 2-nitroaniline (**1m**, 15.0 g, 108.7 mmol) was added portion wise (exothermic reaction). The resulting mixture was stirring up to reflux for 2 h, and left under r.t. for 16 h. Subsequently, hexane was added and the solution was cooled to -35 °C where a precipitate formed. The precipitate was filtered off, washed with diethyl ether (4 x 100 mL) and dried to afford a solid:



**2,2-Dimethyl-5-(((2-nitrophenyl)amino)methylene)-1,3-dioxane-4,6-dione (2m)** 28.2 g (96.6 mmol, 89%); m.p. = 175-178 °C; <sup>1</sup>H NMR (CDCl<sub>3</sub>; 400.2 MHz)  $\delta$  = 1.77 (s, 6H, 2CH<sub>3</sub>), 7.41 (d, <sup>3</sup>J<sub>H,H</sub> = 7.8 Hz, 1H, aromatic), 7.66 (d, <sup>3</sup>J<sub>H,H</sub> = 8.3 Hz, 1H, aromatic), 7.79 (t, <sup>3</sup>J<sub>H,H</sub> = 7.7 Hz, 1H, aromatic), 8.32 (d, <sup>3</sup>J<sub>H,H</sub> = 7.6 Hz, 1H, aromatic), 8.75 (d, <sup>3</sup>J<sub>H,H</sub> = 13.6 Hz, 1H, vinyl), 13.02 (d, <sup>3</sup>J<sub>H,H</sub> = 13.6 Hz, 1H, NH); <sup>13</sup>C{<sup>1</sup>H} NMR(CDCl<sub>3</sub>; 100.6 MHz)  $\delta$  = 27.3, 91.4, 105.5, 118.0, 125.9, 127.0, 134.4, 136.1, 138.1, 151.2, 163.3, 164.2; UV-Vis (methanol;  $\lambda$  [nm] (log $\epsilon$ )): 357 (4.59), 308 (4.68), 274 (4.49), 256 (4.40), 216 (4.67); IR (KBr):  $\tilde{\nu}$  = 3161, 3094, 3004, 1733, 1686, 1604, 1518, 1343, 1265, 1201, 933, 741 cm<sup>-1</sup>.

### 7.8.2.2 Step B

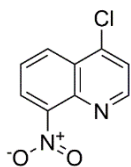
Into freshly distilled diphenyl ether (50 mL) at 220 °C was added **2m** (2.92 g, 10.0 mmol) in small portions, resulting in vigorous gas evolution. The resulting orange solution was brought to reflux for 30 min, and was then allowed to cool to 50 °C. The hexane (25 mL) was added and a brown solid precipitated was filtered, washed with hexane (2 x 10 mL). The crude product was purified by crystallization from chloroform/hexane mixture to yield solid as follows:



**8-Nitro-4(1H)-quinolinone (3m)**<sup>260</sup> 1.6 g (8.4 mmol, 84%); m.p. = 192-194 °C; <sup>1</sup>H NMR (DMSO-*d*<sub>6</sub>; 500.2 MHz)  $\delta$  = 6.24 (d, <sup>3</sup>*J*<sub>H,H</sub> = 7.5 Hz, 1H, aromatic), 7.50 (d, <sup>3</sup>*J*<sub>H,H</sub> = 8.0 Hz, 1H, aromatic), 7.97 (d, <sup>3</sup>*J*<sub>H,H</sub> = 7.5 Hz, 1H, aromatic), 8.56 (d, <sup>3</sup>*J*<sub>H,H</sub> = 7.9 Hz, 1H, aromatic), 8.63 (d, <sup>3</sup>*J*<sub>H,H</sub> = 7.9 Hz, 1H, aromatic), 11.86 (s, 1H, NH); <sup>1</sup>H NMR (CDCl<sub>3</sub>; 400.2 MHz)  $\delta$  = 6.23 (dd, <sup>3</sup>*J*<sub>H,H</sub> = 7.6 Hz, <sup>4</sup>*J*<sub>H,H</sub> = 1.8 Hz, 1H, aromatic), 7.97 (dd, <sup>3</sup>*J*<sub>H,H</sub> = 7.6 Hz, 1H, aromatic), 8.54-8.57 (m, 1H, aromatic), 8.58-8.64 (m, 1H, aromatic), 11.86 (bs, 1H, NH); <sup>13</sup>C{<sup>1</sup>H} NMR(CDCl<sub>3</sub>; 100.6 MHz)  $\delta$  = 112.5, 122.2, 128.5, 130.3, 134.9, 135.5, 138.4, 177.1; <sup>13</sup>C{<sup>1</sup>H} NMR(DMSO-*d*<sub>6</sub>; 125.8 MHz)  $\delta$  = 110.5, 121.8, 127.7, 129.7, 133.5, 134.1, 136.5, 141.2, 175.6; UV-Vis (methanol;  $\lambda$  [nm] (log $\epsilon$ )): 382 (4.07), 256 (4.30), 220 (4.51), 207 (4.54); IR (KBr):  $\tilde{\nu}$  = 3331, 3234, 1643, 1605, 1564, 1490, 1314, 1291, 1245, 1188, 1068, 745 cm<sup>-1</sup>.

### 7.8.2.3 Step C

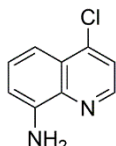
Into freshly distilled phosphoryl trichloride (82.0 g, 50 mL, 534.8 mmol) under argon was mixed with **3m** (0.9 g, 5.0 mmol) and the resulting solution was stirred at 90 °C for 4 h. The excess of phosphoryl trichloride was slowly evaporated, under reduced pressure. The reaction mixture was slowly added to a well stirred mixture of ice (50 g) in water (100 mL). After stirring for 15 min. the resulting reaction mixture was carefully brought to pH 13 - 14 by adding NaOH solution (40%). The aqueous layer was extracted with CH<sub>2</sub>Cl<sub>2</sub> (4 x 10 mL). The combined organic layers was separated and dried over MgSO<sub>4</sub>. Evaporation of the brown colored solvent afforded **4m** as light tan crystals. Next, the crude products were purified by chromatography on silica gel using methanol/dichloromethane as eluent and finally crystallization from dichloromethane to yield precipitates as follows:



**4-Chloro-8-nitroquinoline (4m)**<sup>261</sup>; 0.8 g (4.0 mmol, 81%); m.p. = 120-125 °C; <sup>1</sup>H NMR (DMSO-*d*<sub>6</sub>; 400.2 MHz)  $\delta$  = 7.93 (dd, <sup>3</sup>*J*<sub>H,H</sub> = 8.1 Hz, <sup>3</sup>*J*<sub>H,H</sub> = 7.9 Hz, 1H, aromatic), 7.98 (d, <sup>3</sup>*J*<sub>H,H</sub> = 4.7 Hz, 1H, aromatic), 8.39 (dd, <sup>3</sup>*J*<sub>H,H</sub> = 7.5 Hz, <sup>4</sup>*J*<sub>H,H</sub> = 0.8 Hz, 1H, aromatic), 8.48 (dd, <sup>3</sup>*J*<sub>H,H</sub> = 8.5 Hz, <sup>4</sup>*J*<sub>H,H</sub> = 0.9 Hz, 1H, aromatic), 8.98 (d, <sup>3</sup>*J*<sub>H,H</sub> = 4.7 Hz, 1H, aromatic); <sup>13</sup>C{<sup>1</sup>H} NMR (DMSO-*d*<sub>6</sub>; 100.6 MHz)  $\delta$  = 123.4, 124.1, 126.3, 127.40, 127.42, 139.3, 141.9, 148.2, 152.5; GC-MS:  $t_r$  = 7.228 min, (EI) M<sup>+</sup> = 208 (100%), (M-NO<sub>2</sub>)<sup>+</sup> = 162 (33%); UV-Vis (methanol;  $\lambda$  [nm] (log $\epsilon$ )): 316 (4.23), 302 (4.30), 283 (4.47), 216 (5.02); IR (KBr):  $\tilde{\nu}$  = 3047, 1958, 1847, 1535, 1484, 1358, 880, 865, 750, 717 cm<sup>-1</sup>; CCDC 1967406.

### 7.8.3 Preparation of 4-chloro-8-aminoquinoline

Stannous chloride crystal (10 equiv.) was added to a stirred solution of nitroquinoline **4m** (10.4 g, 50.1 mmol) and hydrochloric acid (5 mL) in ethanol (20 mL). After stirred 0.5 h at rt, the reaction mixture was heated to 40-50 °C for 2 h. After cooling to rt, the mixture was basified with aqueous ammonia and extracted with chloroform (3 x 15 mL). The combined extract was dried over magnesium sulfate and evaporated to afford a yellow solid, which was purified by crystallization from chloroform/hexane mixture to yield precipitates as follows:



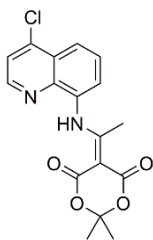
**4-Chloroquinolin-8-amine (1o)**<sup>262</sup>; 6.7 g (37.6 mmol, 75%); m.p. = 90-95 °C; <sup>1</sup>H NMR (CDCl<sub>3</sub>; 400.2 MHz)  $\delta$  = 4.94 (bs, 2H, NH<sub>2</sub>), 6.95 (d, <sup>3</sup>J<sub>H,H</sub> = 7.5 Hz, 1H, aromatic), 7.40 (t, <sup>3</sup>J<sub>H,H</sub> = 8.0 Hz, 1H, aromatic), 7.44 (d, <sup>3</sup>J<sub>H,H</sub> = 4.6 Hz, 1H, aromatic), 7.51 (dd, <sup>3</sup>J<sub>H,H</sub> = 8.4 Hz, <sup>4</sup>J<sub>H,H</sub> = 0.6 Hz, 1H, aromatic), 8.59 (d, <sup>3</sup>J<sub>H,H</sub> = 4.6 Hz, 1H, aromatic); <sup>13</sup>C{<sup>1</sup>H} NMR (CDCl<sub>3</sub>; 100.6 MHz)  $\delta$  = 110.9, 112.1, 121.5, 127.2, 128.5, 139.0, 142.6, 144.3, 146.4; GC-MS: t<sub>r</sub> = 6.305 min, (EI) M<sup>+</sup> = 178 (100%); UV-Vis (methanol;  $\lambda$  [nm] (log $\epsilon$ )): 363 (3.80), 340 (3.84), 291 (3.45), 253 (4.71), 207 (4.76); IR (KBr):  $\tilde{\nu}$  = 3426, 3285, 1620, 1501, 1358, 808, 743 cm<sup>-1</sup>.

### 7.8.4 General Procedures for Synthesis of 4,7-dichloro-2-methyl-1,10-phenanthroline

These syntheses were based on procedures described in the literature<sup>39,40</sup>. Due to the multi-stage synthesis reactions, they have been divided into 3 separate steps: Step A, Step B and Step C.

#### 7.8.4.1 Step A

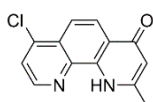
Ortho ester (TMOA) (72.0 g, 600.0 mmol) and Meldrum's acid (11.5 g, 80.0 mmol) was brought to a gentle reflux for 30 min. The resulting greenish solution was cooled to 80 °C and 5-chloro-quinolin-8-amine (**1o**) (10.7 g, 60.0 mmol) was added portion wise (exothermic reaction). The resulting mixture was stirring up to reflux for 2 h, and left under r.t. for 16 h. Subsequently, hexane was added and the solution was cooled to -35 °C where a precipitate formed. The precipitate was filtered off, washed with diethyl ether (4 x 100 mL) and dried to afford a solid:



**5-(1-((4-Chloroquinolin-8-yl)amino)ethylidene)-2,2-dimethyl-1,3-dioxane-4,6-dione (2o)**; 18.5 g (53.4 mmol, 89%); m.p.<sub>dec.</sub> = 190-195 °C; <sup>1</sup>H NMR (CDCl<sub>3</sub>; 400.2 MHz) δ = 1.78 (s, 6H, 2CH<sub>3</sub>), 2.68 (s, 3H, CH<sub>3</sub>), 7.60 (d, <sup>3</sup>J<sub>H,H</sub> = 4.7 Hz, 1H, aromatic), 7.67-7.74 (m, 2H, aromatic), 8.20 (dd, <sup>3</sup>J<sub>H,H</sub> = 7.2 Hz, <sup>4</sup>J<sub>H,H</sub> = 2.5 Hz, 1H, aromatic), 8.83 (d, <sup>3</sup>J<sub>H,H</sub> = 4.7 Hz, 1H, aromatic), 13.53 (s, 1H, NH); <sup>13</sup>C{<sup>1</sup>H} NMR(CDCl<sub>3</sub>; 100.6 MHz) δ = 20.5, 26.7, 87.1, 102.7, 122.5, 123.8, 126.0, 126.9, 127.2, 134.0, 142.9, 143.5, 150.3, 163.0, 167.2, 172.9; UV-Vis (methanol; λ [nm] (logε)): 319 (4.36), 308 (4.34), 295 (4.33), 226 (4.68), 210 (4.69); IR (KBr):  $\tilde{\nu}$  = 2991, 2982, 2940, 1713, 1665, 1584, 1315, 1289, 1204, 672 cm<sup>-1</sup>.

#### 7.8.4.2 Step B

Into freshly distilled diphenyl ether (50 mL) at 220 °C was added **2o** (3.5 g, 10.0 mmol) in small portions, resulting in vigorous gas evolution. The resulting orange solution was brought to reflux for 30 min, and was then allowed to cool to 50 °C. The hexane (25 mL) was added and a brown solid precipitated was filtered, washed with hexane (2 x 10 mL). The crude product was purified by crystallization from chloroform/hexane mixture to yield solid as follows:



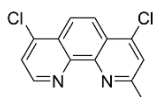
**7-Chloro-2-methyl-1,10-phenanthroline-4(1H)-one (3o)**; 1.8 g (7.4 mmol, 74%); m.p. = 250-255 °C; <sup>1</sup>H NMR (DMSO-*d*<sub>6</sub>/KOD; 400.2 MHz) δ = 2.50 (s, 3H, CH<sub>3</sub>), 6.28 (s, 1H, aromatic), 7.87 (d, <sup>3</sup>J<sub>H,H</sub> = 9.0 Hz, 1H, aromatic), 7.91 (d, <sup>3</sup>J<sub>H,H</sub> = 4.8 Hz, 1H, aromatic), 8.28 (d, <sup>3</sup>J<sub>H,H</sub> = 9.0 Hz, 1H, aromatic), 8.92 (d, <sup>3</sup>J<sub>H,H</sub> = 4.8 Hz, 1H, aromatic); <sup>13</sup>C{<sup>1</sup>H} NMR(DMSO-*d*<sub>6</sub>/KOD; 125.8 MHz) δ = 21.8, 112.0, 115.9, 123.5, 124.1, 124.9, 126.7, 140.9, 141.8, 142.9, 149.0, 153.8, 176.0; UV-Vis (methanol; λ [nm] (logε)): 348 (3.57), 325 (3.89), 277 (4.41), 260 (4.28), 241 (4.42), 211 (4.38); IR (KBr):  $\tilde{\nu}$  = 3427, 3370, 1627, 1563, 1551, 1517, 1416, 842, 819 cm<sup>-1</sup>.

#### 7.8.4.3 Step C

Into freshly distilled phosphoryl trichloride (82.0 g, 50 mL, 534.8 mmol) under argon was mixed with **3o** (1.2 g, 5.0 mmol) and the resulting solution was stirred at 90 °C for 4 h. The excess of phosphoryl trichloride was slowly evaporated, under reduced pressure. The reaction mixture was slowly added to a well stirred mixture of ice (50 g) in water (100 mL). After stirring for 15 min. the



resulting reaction mixture was carefully brought to pH 13 - 14 by adding NaOH solution (40%). The aqueous layer was extracted with CH<sub>2</sub>Cl<sub>2</sub> (4 x 10 mL). The combined organic layers were separated and dried over MgSO<sub>4</sub>. Evaporation of the brown colored solvent afforded **4o** as light tan crystals. Next, the crude products were purified by chromatography on silica gel using methanol/dichloromethane as eluent and finally crystallization from CH<sub>2</sub>Cl<sub>2</sub> to yield precipitates as follows:

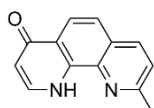


**4,7-Dichloro-2-methyl-1,10-phenanthroline (4o)**; 0.9 g (3.8 mmol, 76%); m.p. = 180-185 °C; <sup>1</sup>H NMR (CDCl<sub>3</sub>; 400.2 MHz) δ = 2.94 (s, 3H, CH<sub>3</sub>), 7.65 (s, 1H, aromatic), 7.73 (d, <sup>3</sup>J<sub>H,H</sub> = 4.8 Hz, 1H, aromatic), 8.26 (d, <sup>3</sup>J<sub>H,H</sub> = 9.4 Hz, 1H, aromatic), 8.30 (d, <sup>3</sup>J<sub>H,H</sub> = 9.4 Hz, 1H, aromatic), 9.10 (d, <sup>3</sup>J<sub>H,H</sub> = 4.8 Hz, 1H, aromatic); <sup>1</sup>H NMR (DMSO-*d*<sub>6</sub>; 500.2 MHz) δ = 2.78 (s, 3H, CH<sub>3</sub>), 7.93 (s, 1H, aromatic), 8.00 (d, *J* = 4.8 Hz, 1H, aromatic), 8.22 (d, <sup>3</sup>J<sub>H,H</sub> = 9.3 Hz, 1H, aromatic), 8.25 (d, <sup>3</sup>J<sub>H,H</sub> = 9.3 Hz, 1H, aromatic), 9.05 (d, <sup>3</sup>J<sub>H,H</sub> = 4.8 Hz, 1H, aromatic); <sup>13</sup>C{<sup>1</sup>H} NMR (CDCl<sub>3</sub>; 125.8 MHz) δ = 25.7, 122.1, 123.3, 123.6, 124.4, 125.0, 127.0, 142.8, 143.0, 146.4, 146.6, 150.2, 160.2; GC-MS: t<sub>r</sub> = 8.5 min, (EI) M<sup>+</sup> = 262 (100%), (M-Cl)<sup>+</sup> = 227 (25%); UV-Vis (methanol; λ [nm] (logε)): 332 (3.00), 303 (3.92), 292 (3.97), 268 (4.53), 239 (4.47), 209 (4.43); IR (KBr):  $\tilde{\nu}$  = 3398, 3047, 2980, 1577, 1542, 1485, 1274, 843, 820, 806, 727 cm<sup>-1</sup>.

## 7.8.5 General Procedures for Synthesis of 7-chloro-2-methyl-1,10-phenanthrolines

### 7.8.5.1 Preparation of 9-Methyl-1,10-phenanthrolin-4(1H)-one

Toluene (30 mL) and (2*E*)-but-2-enal (1.3 mL, 15.5 mmol) were added to a solution of 4-chloroquinolin-8-amine (**1o**) (2.0 g, 11.2 mmol) in aqueous 6 M HCl (200 mL), and were heated under reflux for 3 h. The mixture was allowed to cool to room temperature. The aqueous layer was separated and neutralized with aqueous solution of NaOH (10%). After extraction with CH<sub>2</sub>Cl<sub>2</sub> (3 x 50 mL), the organic layer was separated and dried over MgSO<sub>4</sub>, then was filtered and evaporated. The residue was purified by chromatography and crystallization.

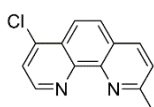


**9-Methyl-1,10-phenanthrolin-4(1H)-one (3p)**<sup>263</sup> 2.1 g (10.0 mmol, 89%); m.p. = 190-191 °C; <sup>1</sup>H NMR (CDCl<sub>3</sub>; 400.2 MHz) δ = 2.76 (s, 3H, CH<sub>3</sub>), 6.52 (d, <sup>3</sup>J<sub>H,H</sub> = 7.3 Hz, 1H, aromatic), 7.46 (d, <sup>3</sup>J<sub>H,H</sub> = 8.3 Hz, 1H, aromatic), 7.57 (d, <sup>3</sup>J<sub>H,H</sub> = 8.8 Hz, 1H, aromatic), 7.84 (d, <sup>3</sup>J<sub>H,H</sub> = 7.1 Hz, 1H, aromatic),

8.11 (d,  $^3J_{\text{H,H}} = 8.3$  Hz, 1H, aromatic), 8.29 (d,  $^3J_{\text{H,H}} = 8.8$  Hz, 1H, aromatic), 10.65 (bs, 1H, NH);  $^{13}\text{C}\{^1\text{H}\}$  NMR( $\text{CDCl}_3$ ; 100.6 MHz)  $\delta = 25.1, 113.0, 121.9, 122.1, 124.4, 124.7, 127.1, 136.3, 136.7, 138.3, 158.3, 178.5$ ; GC-MS:  $t_{\text{r}} = 9.0$  min, (EI)  $\text{M}^+ = 210$  (68%),  $(\text{M}-\text{CO})^+ = 182$  (100%); UV-Vis (methanol;  $\lambda$  [nm] ( $\log \epsilon$ )): 321 (3.81), 310 (3.80), 282 (4.06), 261 (4.15), 236 (4.20), 218 (4.17); IR (KBr):  $\tilde{\nu} = 2925, 1629, 1601, 1564, 1523, 1493, 808$   $\text{cm}^{-1}$ .

### 7.8.5.2 Preparation of 7-chloro-2-methyl-1,10-phenanthrolines

Into freshly distilled phosphoryl chloride (82.0 g, 50 mL, 534.8 mmol) under argon was mixed with **3p** (2.1 g, 10.0 mmol) and the resulting solution was stirred at 90 °C for 4 h. The excess of phosphoryl chloride was slowly evaporated, under reduced pressure. The reaction mixture was slowly added to a well stirred mixture of ice (50 g) in water (100 mL). After stirring for 15 min. the resulting reaction mixture was carefully brought to pH 13-14 by adding NaOH solution (40%). The aqueous layer was extracted with  $\text{CH}_2\text{Cl}_2$  (4x10 mL). The combined organic layers was separated and dried over  $\text{MgSO}_4$ . Evaporation of the brown colored solvent afforded **4p**. Next, the crude products were purified by chromatography on silica gel using methanol/dichloromethane as eluent and finally crystallization from  $\text{CH}_2\text{Cl}_2$  to yield precipitates as follows:

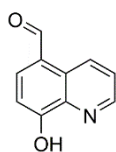


**7-Chloro-2-methyl-1,10-phenanthroline (4p)**<sup>263</sup>; 1.0 g (5.0 mmol, 50%); m.p. = 100.0-100.3 °C;  $^1\text{H}$  NMR ( $\text{CDCl}_3$ ; 400.2 MHz)  $\delta = 2.96$  (s, 3H,  $\text{CH}_3$ ), 7.55 (d,  $^3J_{\text{H,H}} = 8.2$  Hz, 1H, aromatic), 7.70 (d,  $^3J_{\text{H,H}} = 4.8$  Hz, 1H, aromatic), 7.86 (d,  $^3J_{\text{H,H}} = 9.0$  Hz, 1H, aromatic), 8.16 (d,  $^3J_{\text{H,H}} = 8.4$  Hz, 1H, aromatic), 8.19 (d,  $^3J_{\text{H,H}} = 9.2$  Hz, 1H, aromatic), 9.07 (d,  $^3J_{\text{H,H}} = 4.8$  Hz, 1H, aromatic)  $^1\text{H}$  NMR ( $\text{DMSO}-d_6$ ; 400.2 MHz)  $\delta = 3.02$  (s, 3H), 8.14 (d,  $^3J_{\text{H,H}} = 8.0$ , 1H, aromatic), 8.21 (d,  $^3J_{\text{H,H}} = 4.6$ , 1H, aromatic), 8.29 (d,  $^3J_{\text{H,H}} = 3.4$ , 2H, aromatic), 9.02 (d,  $^3J_{\text{H,H}} = 8.1$ , 1H, aromatic), 9.11 (d,  $^3J_{\text{H,H}} = 4.7$ , 1H, aromatic);  $^{13}\text{C}\{^1\text{H}\}$  NMR( $\text{CDCl}_3$ ; 100.6 MHz)  $\delta = 25.9, 121.1, 123.1, 124.3, 126.8, 126.9, 127.6, 136.3, 142.7, 145.4, 147.1, 149.7, 160.2$ ;  $^{13}\text{C}\{^1\text{H}\}$  NMR( $\text{DMSO}-d_6$ ; 100.6 MHz)  $\delta = 22.1, 122.5, 125.3, 126.8, 126.9, 127.3, 127.8, 137.6, 140.3, 142.7, 143.2, 149.7, 159.2$ ; GC-MS:  $t_{\text{r}} = 8.048$  min, (EI)  $\text{M}^+ = 228$  (100%),  $(\text{M}-\text{Cl})^+ = 193$  (5%); UV-Vis (methanol;  $\lambda$  [nm] ( $\log \epsilon$ )): 268 (3.96), 234 (4.02), 205 (3.86); IR (KBr):  $\tilde{\nu} = 3014, 2053, 1646, 1627, 1581, 1224, 857$   $\text{cm}^{-1}$ .

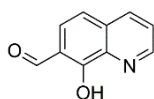
## 7.9 Synthesis of selected Quinolinecarbaldehydes

### 7.9.1 Synthesis of selected Quinolinecarbaldehydes based on Reimer-Tiemann reaction

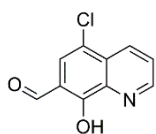
Potassium hydroxide (14.0 g, 250.0 mmol) in water (15 mL) was added into the solution of **Q1a**, **Q1b** or **Q1c** (34.5 mmol) in ethanol (20 mL) and the resulting reaction mixture was brought to a gentle reflux. Next chloroform (8.3 ml, 103.5 mmol) was subsequently gently dropped within an hour. The resulting red mixture was refluxed for another 3 h, and then was cool down to room temperature. The obtained suspension was acidified by an aqueous solution of hydrochloric acid (1%) to pH ca. 7, and then volatiles were evaporated under reduced pressure. The resulting solid was dried over P<sub>4</sub>O<sub>10</sub> and extracted at Soxhlet apparatus (chloroform). From the resulting solution the volatiles were evaporated under reduced pressure, and finally the crude product was purified on a silica gel chromatography with chloroform/methanol (3:1) as eluent, and purified by crystallization from chloroform/hexane to yield precipitates as follows:



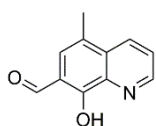
**8-Hydroxyquinoline-5-carbaldehyde (Q2a)**<sup>251</sup>; beige 0.6 g (3.5 mmol, 10.1%); m.p. = 171.3-171.8 °C; <sup>1</sup>H NMR (DMSO-*d*<sub>6</sub>; 400.2 MHz) δ = 7.26 (d, <sup>3</sup>J<sub>H,H</sub> = 8.0 Hz, 1H, aromatic), 7.78 (dd, <sup>3</sup>J<sub>H,H</sub> = 8.6 Hz, <sup>4</sup>J<sub>H,H</sub> = 4.1 Hz, 1H, aromatic), 8.17 (d, <sup>3</sup>J<sub>H,H</sub> = 8.1 Hz, 1H, aromatic), 8.97 (dd, <sup>3</sup>J<sub>H,H</sub> = 4.1 Hz, <sup>4</sup>J<sub>H,H</sub> = 1.6 Hz, 1H, aromatic), 9.56 (dd, <sup>3</sup>J<sub>H,H</sub> = 8.6 Hz, <sup>4</sup>J<sub>H,H</sub> = 1.6 Hz, 1H, aromatic), 10.14 (s, 1H, HC=O); <sup>13</sup>C{<sup>1</sup>H} NMR (DMSO-*d*<sub>6</sub>; 100.6 MHz) δ = 110.8, 122.4, 124.6, 126.8, 133.0, 138.0, 140.2, 149.0, 159.6, 192.2; GC-MS: t<sub>r</sub> = 6.024 min, (EI) m/z (rel. int.) M<sup>+</sup> = 173 (100%); (M-HCO)<sup>+</sup> = 144 (17%); UV-Vis (methanol; λ [nm] (logε)): 395 (3.04), 322 (3.89), 263 (3.96), 239 (4.40), 210 (4.13); IR (KBr):  $\tilde{\nu}$  = 3177, 2845, 1663, 1474 cm<sup>-1</sup>.



**8-Hydroxyquinoline-7-carbaldehyde (Q2a')**<sup>235</sup>; <sup>1</sup>H NMR (DMSO-*d*<sub>6</sub>; 400.2 MHz) δ = 7.24 (d, <sup>3</sup>J<sub>H,H</sub> = 7.9 Hz, 1H, aromatic), 7.57 (dd, <sup>3</sup>J<sub>H,H</sub> = 8.1 Hz, <sup>4</sup>J<sub>H,H</sub> = 4.3 Hz, 1H, aromatic), 7.99 (d, <sup>3</sup>J<sub>H,H</sub> = 8.0 Hz, 1H, aromatic), 8.78 (dd, <sup>3</sup>J<sub>H,H</sub> = 4.4 Hz, <sup>4</sup>J<sub>H,H</sub> = 1.5 Hz, 1H, aromatic), 9.07 (dd, <sup>3</sup>J<sub>H,H</sub> = 8.0 Hz, <sup>4</sup>J<sub>H,H</sub> = 1.6 Hz, 1H, aromatic), 10.41 (s, 1H, HC=O); GC-MS: t<sub>r</sub> = 6.360 min, (EI) m/z (rel. int.) M<sup>+</sup> = 173 (12%); (M-CO+H)<sup>+</sup> = 146 (100%).



**5-Chloro-8-hydroxyquinoline-7-carbaldehyde (Q2c)**<sup>264</sup>; yellow 0.5 g (2.5 mmol, 7.2%); m.p. = 170.0-170.6 °C; <sup>1</sup>H NMR (CDCl<sub>3</sub>; 500.2 MHz) δ = 7.71 (dd, <sup>3</sup>J<sub>H,H</sub> = 8.5 Hz, <sup>4</sup>J<sub>H,H</sub> = 4.2 Hz, 1H, aromatic), 7.86 (s, 1H, aromatic), 8.56 (dd, <sup>3</sup>J<sub>H,H</sub> = 8.5 Hz, <sup>4</sup>J<sub>H,H</sub> = 1.5 Hz, 1H, aromatic), 8.97 (dd, <sup>3</sup>J<sub>H,H</sub> = 4.2 Hz, <sup>4</sup>J<sub>H,H</sub> = 1.5 Hz, 1H, aromatic), 10.39 (s, 1H, HC=O); <sup>1</sup>H NMR (DMSO-*d*<sub>6</sub>; 500.2 MHz) δ = 7.74 (s, 1H, aromatic), 7.88 (dd, <sup>3</sup>J<sub>H,H</sub> = 8.5 Hz, <sup>4</sup>J<sub>H,H</sub> = 4.2 Hz, 1H, aromatic), 8.51 (dd, <sup>3</sup>J<sub>H,H</sub> = 8.5 Hz, <sup>4</sup>J<sub>H,H</sub> = 1.4 Hz, 1H, aromatic), 9.05 (dd, <sup>3</sup>J<sub>H,H</sub> = 4.2 Hz, <sup>4</sup>J<sub>H,H</sub> = 1.4 Hz, 1H, aromatic), 10.49 (s, 1H, HC=O); <sup>13</sup>C{<sup>1</sup>H} NMR (DMSO-*d*<sub>6</sub>; 125.78 MHz) δ = 118.7, 119.8, 122.7, 125.7, 129.3, 133.1, 140.2, 149.9, 158.4, 188.0; <sup>13</sup>C{<sup>1</sup>H} NMR (CDCl<sub>3</sub>; 125.78 MHz) δ = 117.8, 121.8, 124.7, 125.4, 130.2, 133.7, 139.9, 149.9, 157.6, 190.6; GC-MS: t<sub>r</sub> = 6.917 min.; (EI) m/z (rel. int.) M<sup>+</sup> = 207 (15%); (M-CO)<sup>+</sup> = 179 (100%); UV-Vis (metanol; λ [nm] (logε)): 429 (2.86), 350 (3.27), 286 (3.65), 267 (4.03), 248 (3.83), 207 (4.09); IR (KBr):  $\tilde{\nu}$  = 3344, 2859, 1667, 1425 cm<sup>-1</sup>.

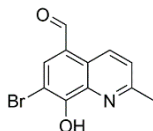


**5-Methyl-8-hydroxyquinoline-7-carbaldehyde (Q2d)**<sup>252</sup>; greenish 0.5 g; (2.8 mmol, 8.0%); m.p. = 172.7-173.5 °C; <sup>1</sup>H NMR (CDCl<sub>3</sub>; 400.2 MHz) δ = 2.56 (s, 3H, CH<sub>3</sub>), 7.53 (s, 1H, aromatic), 7.58 (dd, <sup>3</sup>J<sub>H,H</sub> = 8.2 Hz, <sup>4</sup>J<sub>H,H</sub> = 3.5 Hz, 1H, aromatic), 8.26 (d, <sup>3</sup>J<sub>H,H</sub> = 8.3 Hz, 1H, aromatic), 8.90 (d, <sup>3</sup>J<sub>H,H</sub> = 2.7 Hz, 1H, aromatic), 10.36 (s, 1H, HC=O); <sup>13</sup>C{<sup>1</sup>H} NMR (CDCl<sub>3</sub>; 100.6 MHz) δ = 17.9, 117.2, 124.3, 124.7, 124.9, 131.8, 133.0, 139.5, 148.9, 157.4, 192.3; GC-MS: t<sub>r</sub> = 7.186 min.; (EI) m/z (rel. int.) M<sup>+</sup> = 187 (19%); (M-CO)<sup>+</sup> = 159 (100%); UV-Vis (metanol; λ [nm] (logε)): 452 (2.88), 426 (3.04), 358 (3.51), 291 (3.88), 270 (4.37), 246 (4.05), 207 (4.35); IR (KBr):  $\tilde{\nu}$  = 3063, 2852, 1686, 1426 cm<sup>-1</sup>.

### 7.9.1.1 Synthesis of 7-bromo-8-hydroxy-2-methylquinoline-5-carbaldehyde through on carbene insertion reaction

Potassium hydroxide (40.0 g; 714.3 mmol) in water (15 mL) was added into the solution of Q1d (5.6 g; 18.0 mmol) in ethanol (20 mL). The resulting solution was irradiated (75W) and stirred under reflux. Next, chloroform (30 ml; 372.0 mmol) was gently dropped for an hour. The resulting red mixture was refluxed for another 16 h, and then was cool down to room temperature. Subsequently the obtained suspension was acidified by an aqueous solution of hydrochloric acid (1%) to pH ca. 7, and then volatiles were evaporated under reduced pressure. The resulting solid was dried over P<sub>4</sub>O<sub>10</sub> and extracted at Soxhlet apparatus with chloroform. From the resulting solution the volatiles were

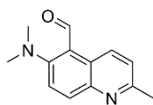
evaporated under reduced pressure, and finally the crude product was purified on a silica gel chromatography with chloroform/methanol (3:1) as eluent, and purified by crystallization from chloroform/hexane to yield precipitates as follows:



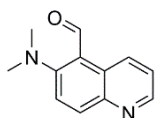
**7-Bromo-8-hydroxy-2-methylquinoline-5-carbaldehyde (Q2e)**<sup>264</sup>; < 1%; <sup>1</sup>H NMR (DMSO-*d*<sub>6</sub>; 400.2 MHz)  $\delta$  = 2.77 (s, 3H, CH<sub>3</sub>), 7.73 (d, <sup>3</sup>J<sub>H,H</sub> = 8.7 Hz, 1H, aromatic), 8.32 (s, 1H, aromatic), 9.45 (d, <sup>3</sup>J<sub>H,H</sub> = 8.7 Hz, 1H, aromatic), 10.05 (s, 1H, HC=O); GC-MS: *t*<sub>r</sub> = 7.617 min.; (EI) *m/z* (rel. int.) M<sup>+</sup> = 267 (15%); (M-CO+H)<sup>+</sup> = 238 (20%).

## 7.9.2 Synthesis of selected Quinolinecarbaldehydes based on Vilsmeier Haack reaction

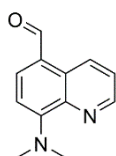
To the solution of dry chloroform (6.5 mL) and dry DMF (0.8 mL, 10.4 mmol) phosphorus trichloride (3.2 mL, 34.3 mmol) was added at 0 °C and the mixture was stirred for an hour. Next **Q1e**, **Q1f**, **Q1i** (8.0 mmol), respectively was added, and the resulting reaction mixture was brought to a gentle reflux for 16 h. The reaction was quenched by the addition of crushed ice, and was neutralized by aqueous solution of Na<sub>2</sub>CO<sub>3</sub> (10%) to pH 6 - 7 and then the layers were separated. The aqueous layer was extracted by chloroform (3 x 30 mL), collected, and was dried over anhydrous MgSO<sub>4</sub>. After filtration, the solvent was evaporated on a rotary evaporator and the obtained residue was purified by column chromatography on silica gel with chloroform/THF/hexane (2:1:1) as eluent.



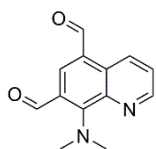
**6-(Dimethylamino)-2-methylquinoline-5-carbaldehyde (Q2f)** yellow 0.7 g (3.1 mmol, 38.6%); m.p. = 75.2-75.8 °C; <sup>1</sup>H NMR (DMSO-*d*<sub>6</sub>; 400.2 MHz)  $\delta$  = 2.58 (s, 3H, CH<sub>3</sub>), 3.11 (s, 6H, 2NCH<sub>3</sub>), 7.43 (d, <sup>3</sup>J<sub>H,H</sub> = 8.8 Hz, 1H, aromatic), 7.64 (d, <sup>3</sup>J<sub>H,H</sub> = 9.4 Hz, 1H, aromatic), 7.98 (d, <sup>3</sup>J<sub>H,H</sub> = 9.4 Hz, 1H, aromatic), 9.18 (d, <sup>3</sup>J<sub>H,H</sub> = 8.8 Hz, 1H, aromatic), 10.20 (s, 1H, HC=O); <sup>13</sup>C{<sup>1</sup>H} NMR (DMSO-*d*<sub>6</sub>; 100.6 MHz)  $\delta$  = 24.2, 45.7, 114.8, 121.9, 124.1, 125.2, 131.4, 135.2, 142.4, 155.6, 157.1, 190.4; GC-MS: *t*<sub>r</sub> = 7.683 min, (EI) *m/z* (rel. int.) M<sup>+</sup> = 214 (85%); (M-HCO)<sup>+</sup> = 185 (55%); UV-Vis (methanol;  $\lambda$  [nm] (log $\epsilon$ )): 416 (3.55), 365 (3.12), 304 (3.60), 289 (3.68), 260 (4.35), 214 (4.21); IR (KBr):  $\tilde{\nu}$  = 3386, 2878, 1671, 1498 cm<sup>-1</sup>.



**6-(Dimethylamino)quinoline-5-carbaldehyde (Q2g)** yellow 1.2 g (5.9 mmol, 73.8%); m.p. = 56.1-56.8 °C;  $^1\text{H}$  NMR (DMSO- $d_6$ ; 400.2 MHz)  $\delta$  = 3.16 (s, 6H, 2NCH $_3$ ), 7.54 (dd,  $^3J_{\text{H,H}}$  = 8.7 Hz,  $^4J_{\text{H,H}}$  = 4.2 Hz, 1H, aromatic), 7.70 (d,  $^3J_{\text{H,H}}$  = 9.5 Hz, 1H, aromatic), 8.05 (d,  $^3J_{\text{H,H}}$  = 9.4 Hz, 1H, aromatic), 8.69 (dd,  $^3J_{\text{H,H}}$  = 4.2 Hz,  $^4J_{\text{H,H}}$  = 1.6 Hz, 1H, aromatic), 9.30 (dd,  $^3J_{\text{H,H}}$  = 8.7 Hz,  $^4J_{\text{H,H}}$  = 1.5 Hz, 1H, aromatic), 10.19 (s, 1H, HC=O);  $^{13}\text{C}\{^1\text{H}\}$  NMR (DMSO- $d_6$ ; 125.8 MHz)  $\delta$  = 45.5, 113.4, 122.7, 123.6, 127.5, 132.0, 134.7, 141.6, 146.6, 157.5, 190.0; GC-MS:  $t_r$  = 7.259 min, (EI)  $m/z$  (rel. int.)  $\text{M}^+$  = 200 (76%); (M-HCO) $^+$  = 171 (20%); UV-Vis (methanol;  $\lambda$  [nm] (log $\epsilon$ )): 423 (3.61), 373 (3.18), 307 (3.60), 268 (4.33), 222 (4.17), 204 (3.96); IR (KBr):  $\tilde{\nu}$  = 3421, 2895, 1636, 1458  $\text{cm}^{-1}$ .



**8-(Dimethylamino)quinoline-5-carbaldehyde (Q2j)** yellow 0.01 g (0.05 mmol, 0.6%); m.p. = 100.8-101.0 °C;  $^1\text{H}$  NMR (CDCl $_3$ ; 400.2 MHz)  $\delta$  = 3.36 (s, 6H, 2NCH $_3$ ), 6.97 (d,  $^3J_{\text{H,H}}$  = 8.2 Hz, 1H, aromatic), 7.53 (dd,  $^3J_{\text{H,H}}$  = 8.6 Hz,  $^4J_{\text{H,H}}$  = 4.1 Hz, 1H, aromatic), 7.84 (d,  $^3J_{\text{H,H}}$  = 8.3 Hz, 1H, aromatic), 8.87 (dd,  $^3J_{\text{H,H}}$  = 4.0 Hz,  $^4J_{\text{H,H}}$  = 1.7 Hz, 1H, aromatic), 9.72 (dd,  $^3J_{\text{H,H}}$  = 8.6 Hz,  $^4J_{\text{H,H}}$  = 1.7 Hz, 1H, aromatic), 10.06 (s, 1H, HC=O);  $^{13}\text{C}\{^1\text{H}\}$  NMR (CDCl $_3$ ; 125.8 MHz)  $\delta$  = 44.1, 111.2, 122.2, 123.3, 128.3, 133.9, 139.5, 141.0, 146.9, 155.0, 191.3; GC-MS:  $t_r$  = 7.156 min, (EI)  $m/z$  (rel. int.)  $\text{M}^+$  = 200.1 (24%), (M-Me) $^+$  = 185.1 (100%), (M-HCO) $^+$  = 171.1 (38%); UV-Vis (methanol;  $\lambda$  [nm] (log $\epsilon$ )): 390 (4.07), 289 (3.91), 263 (4.20), 234 (3.99), 206 (4.36); IR (KBr):  $\tilde{\nu}$  = 2840, 1665, 1555, 1509, 1352, 1251, 1080, 760  $\text{cm}^{-1}$ .

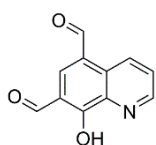


**8-(Dimethylamino)quinoline-5,7-dicarbaldehyde (Q2k)** yellow 0.006 g (0.002 mmol, 0.3%); m.p. = 100.0-100.1 °C;  $^1\text{H}$  NMR (CDCl $_3$ ; 400.2 MHz)  $\delta$  = 3.61 (s, 6H, 2NCH $_3$ ), 7.57 (dd,  $^3J_{\text{H,H}}$  = 8.6 Hz,  $^4J_{\text{H,H}}$  = 4.1 Hz, 1H, aromatic), 8.26 (s, 1H, aromatic), 8.88 (d,  $^3J_{\text{H,H}}$  = 4.1 Hz,  $^4J_{\text{H,H}}$  = 1.7 Hz, 1H, aromatic), 9.70 (dd,  $^3J_{\text{H,H}}$  = 8.6 Hz,  $^4J_{\text{H,H}}$  = 1.7 Hz, 1H, aromatic), 10.06 (s, 1H, HC=O), 10.17 (s, 1H, HC=O);  $^{13}\text{C}\{^1\text{H}\}$  NMR (CDCl $_3$ ; 125.8 MHz)  $\delta$  = 48.3, 122.1, 122.6, 124.7, 130.2, 134.0, 141.9, 144.4, 147.5, 157.0, 188.5, 191.3; GC-MS:  $t_r$  = 7.952 min, (EI)  $m/z$  (rel. int.)  $\text{M}^+$  = 227.9 (100%), (M-Me) $^+$  = 213.0 (3%), (M+2H-CO) $^+$  = 202 (10%); LCMS-IT-TOF:  $m/z$  (rel. int.) (M+H) $^+$  = 229 (100%), (M+H-CO) $^+$  = 201 (100%); HRMS (IT-TOF):  $m/z$  Calcd for C $_{13}$ H $_{13}$ N $_2$ O $_2$  (M+H) $^+$  = 229.0977, Found 229.0970;

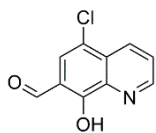
UV-Vis (methanol;  $\lambda$  [nm] ( $\log \epsilon$ )): 400 (4.33), 355 (4.04), 287 (4.38), 234 (4.33), 210 (4.33); IR (KBr):  $\tilde{\nu} = 2872, 1678, 1661, 1515, 1381, 1265, 1103, 765 \text{ cm}^{-1}$ .

### 7.9.3 Synthesis of selected Quinolinecarbaldehydes based on the Duff reaction

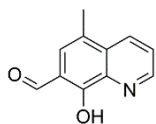
These were based on a procedure described in the literature<sup>265</sup>. To a solution of **Q1a**, **Q1b**, **Q1c**, **Q1g**, **Q1h** or **Q1i** (5.0 mmol) in a minimum amount of TFA (7–8 mL) hexamethylenetetramine (1.4 g, 10.0 mmol) was gently added under an argon atmosphere. The solution was stirred at 70 °C for 70 h and then at 100 °C for another 4 h. Subsequently, the obtained suspension was acidified by an aqueous solution of hydrochloric acid (10%, ~10 mL) and the reaction mixture was kept at 100 °C for 1 h. The whole suspension was cooled down to r.t. Next, the obtained reaction mixture was alkalinized by aqueous solution of NaOH (10%), and the resulting precipitate was collected in a Buchner funnel, followed by washing with water (3 × 50 mL) and dried to afford a solid. Next, the crude product was purified by chromatography to yield 2d precipitates as follows, or the crude product was extracted with CH<sub>2</sub>Cl<sub>2</sub> at Soxhlet apparatus to yield 2i solid as follows:



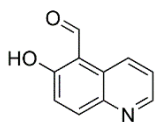
**8-Hydroxyquinoline-5,7-dicarbaldehyde (Q2b)**<sup>160</sup>; green 0.84 g (4.0 mmol, 80%); m.p. > 360 °C; <sup>1</sup>H-NMR (400 MHz, DMSO-d<sub>6</sub>)  $\delta = 8.04$  (dd, <sup>3</sup>J<sub>H,H</sub> = 8.6, <sup>4</sup>J<sub>H,H</sub> = 4.8, 1H, aromatic), 8.39 (s, 1H), 8.97 (dd, <sup>3</sup>J<sub>H,H</sub> = 4.7, <sup>4</sup>J<sub>H,H</sub> = 1.5, 1H, aromatic), 9.83 (dd, <sup>3</sup>J<sub>H,H</sub> = 8.6, <sup>4</sup>J<sub>H,H</sub> = 1.5, 1H, aromatic), 10.03 (s, 1H, HC=O), 10.46 (s, 1H, HC=O), <sup>13</sup>C{<sup>1</sup>H}- (100.6 MHz, DMSO-d<sub>6</sub>)  $\delta = 116.85, 119.13, 126.75, 130.36, 138.05, 138.33, 139.17, 145.21, 166.76, 188.06, 191.73$ . IR (KBr):  $\tilde{\nu} = 2901, 1673, 1666, 1555, 1512, 1341, 1236 \text{ cm}^{-1}$ .



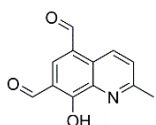
**5-Chloro-8-hydroxyquinoline-7-carbaldehyde (Q2c)**<sup>264</sup> yellow 0.7 g (3.5 mmol, 70%).



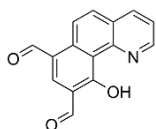
**5-Methyl-8-hydroxyquinoline-7-carbaldehyde (Q2d)**<sup>252</sup> greenish 0.7 g (3.7 mmol, 75.0%).



**6-Hydroxyquinoline-5-carbaldehyde (Q2h)**<sup>266</sup> beige 0.6 g (3.5 mmol, 28.1%); m.p. = 138.6–138.9 °C; <sup>1</sup>H-NMR (CDCl<sub>3</sub>; 400.2 MHz) δ = 7.39 (d, <sup>3</sup>J<sub>H,H</sub> = 9.3 Hz, 1H, aromatic), 7.53 (dd, <sup>3</sup>J<sub>H,H</sub> = 8.6 Hz, <sup>4</sup>J<sub>H,H</sub> = 4.2 Hz, 1H, aromatic), 8.26 (d, <sup>3</sup>J<sub>H,H</sub> = 9.3 Hz, 1H, aromatic), 8.67 (d, <sup>3</sup>J<sub>H,H</sub> = 8.6 Hz, 1H, aromatic), 8.85 (d, <sup>3</sup>J<sub>H,H</sub> = 3.1 Hz, 1H, aromatic), 10.76 (s, 1H, HC=O), 13.06 (s, 1H, OH); <sup>13</sup>C{<sup>1</sup>H}-NMR (CDCl<sub>3</sub>; 100.6 MHz) δ = 110.7, 123.1, 123.5, 127.0, 128.2, 140.7, 143.4, 148.7, 164.9, 192.4; GC-MS: t<sub>r</sub> = 6.168 min, (EI) m/z (rel. int.) M<sup>+</sup> = 173 (100%); (M – HCO)<sup>+</sup> = 144 (20%); UV-Vis (methanol; λ [nm] (logε)): 400 (2.46), 346 (3.16), 300 (3.43), 290 (3.37), 226 (4.04), 203 (0.98); IR (KBr):  $\tilde{\nu}$  = 3050, 2733, 1632, 1480 cm<sup>-1</sup>.



**8-Hydroxy-2-methylquinoline-5,7-dicarbaldehyde (Q2i)** red 0.2 g (0.7 mmol, 14.9%); m.p. > 360 °C; <sup>1</sup>H-NMR (DMSO-*d*<sub>6</sub>; 400.2 MHz) δ = 2.85 (s, 3H, CH<sub>3</sub>), 7.92 (d, <sup>3</sup>J<sub>H,H</sub> = 8.7 Hz, 1H, aromatic), 8.29 (s, 1H, aromatic), 9.71 (d, <sup>3</sup>J<sub>H,H</sub> = 8.7 Hz, 1H, aromatic), 9.95 (s, 1H, HC=O), 10.42 (s, 1H, HC=O); <sup>13</sup>C{<sup>1</sup>H}-NMR (DMSO-*d*<sub>6</sub>; 125.8 MHz) δ = 21.6, 115.6, 119.5, 128.0, 128.6, 137.8, 138.5, 139.0, 155.7, 167.2, 188.2, 191.5; LCMS-IT-TOF: m/z (rel. int.) (M – H)<sup>-</sup> = 214 (100%), M<sup>-</sup> = 215 (10%); (M – HCO)<sup>-</sup> = 186 (10%); (M – 2HCO)<sup>-</sup> = 157 (<1%); HRMS (IT-TOF): m/z Calcd for C<sub>12</sub>H<sub>8</sub>NO<sub>3</sub> (M – H)<sup>-</sup> = 214.0504, Found 214.0496; UV-Vis (methanol; λ [nm] (logε)): 359 (3.65), 282 (3.91), 237 (3.59); IR (KBr):  $\tilde{\nu}$  = 3423, 2965, 2847, 2835, 1657, 1458 cm<sup>-1</sup>; CCDC 1890715.



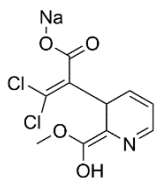
**10-hydroxybenzo[h]quinoline-7,9-dicarbaldehyde (Q2l)** red 0.9 g (3.5 mmol, 70.6%); m.p.<sub>dec.</sub> > 360 °C; <sup>1</sup>H-NMR (DMSO-*d*<sub>6</sub>/KOD/D<sub>2</sub>O; 400.2 MHz) δ = 7.51 (dd, <sup>3</sup>J<sub>H,H</sub> = 8.0 Hz, <sup>4</sup>J<sub>H,H</sub> = 4.2 Hz, 1H, aromatic), 7.96 (d, <sup>3</sup>J<sub>H,H</sub> = 9.0 Hz, 1H, aromatic), 8.10 (s, 1H, aromatic), 8.26 (dd, <sup>3</sup>J<sub>H,H</sub> = 8.1 Hz, <sup>4</sup>J<sub>H,H</sub> = 2.0 Hz, 1H, aromatic), 8.89 (dd, <sup>3</sup>J<sub>H,H</sub> = 4.2 Hz, <sup>4</sup>J<sub>H,H</sub> = 2.0 Hz, 1H, aromatic), 9.20 (d, <sup>3</sup>J<sub>H,H</sub> = 9.0 Hz, 1H, aromatic), 9.65 (s, 1H, HC=O), 10.08 (s, 1H, HC=O); <sup>13</sup>C{<sup>1</sup>H}-NMR (DMSO-*d*<sub>6</sub>/KOD/D<sub>2</sub>O; 125.8 MHz) δ = 115.1, 122.2, 123.8, 124.8, 126.1, 126.9, 132.3, 137.4, 140.0, 144.6, 148.1, 151.1, 182.0, 192.6, 192.7; HRMS (ESI): m/z Calcd for C<sub>15</sub>H<sub>9</sub>NO<sub>3</sub> M<sup>-</sup> = 251.05826, Found 251.07750; UV-



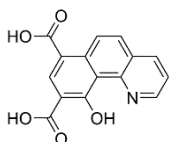
Vis (methanol;  $\lambda$  [nm] ( $\log \epsilon$ )): 453 (2.41), 405 (3.22), 364 (3.38), 329 (3.46), 315 (3.48), 274 (3.96), 260 (4.03), 241 (4.02), 223 (4.01), 211 (4.04); IR (KBr):  $\tilde{\nu}$  = 3424, 3062, 2877, 1673, 1483  $\text{cm}^{-1}$ .

## 7.10 Oxidation of selected dicarbaldehydes

To a solution of the appropriate hydroxy dicarbaldehyde (**Q2b** or **Q2l**) (1.0 mmol) in water (25 mL) (formic acid for **Q2l**) was slowly added a solution of  $\text{NaClO}_2$  (5.00 g, 55.6 mmol) in water (25 mL). The reaction was stirred at room temperature for 3 h and then at 90 °C for another 3 h. The reaction mixture was then concentrated, and the resulting suspension was cooled. The resulting precipitate was filtered off, washed with cold water (3 x 50 mL), and air-dried. The product thus obtained was further purified by crystallization from ethanol to obtain:



**Sodium (E)-3,3-dichloro-2-(2-(hydroxy(methoxy)methylene)-2,3-dihydropyridin-3-yl)acrylate (Ox-Q2b)** 0,04 g (0,15 mmol, 15.0%);  $^1\text{H}$  NMR (400.2 MHz,  $\text{DMSO-}d_6$ )  $\delta$  = 3.59 (s, 3H), 7.76 (dd,  $^3J_{\text{H,H}}$  = 4.8, 7.8 Hz, 1H), 8.43 (dd,  $^3J_{\text{H,H}}$  = 1.7,  $^4J_{\text{H,H}}$  = 7.9 Hz, 1H), 9.02 (dd,  $^3J_{\text{H,H}}$  = 1.7,  $^4J_{\text{H,H}}$  = 4.8 Hz, 1H).  $^{13}\text{C}\{^1\text{H}\}$  NMR ( $\text{DMSO-}d_6$ ; 100.6 MHz)  $\delta$  = 54.02, 86.56, 90.31, 125.80, 126.89, 134.74, 158.31, 165.55, 168.75, 186.75; HRMS (ESI TOF):  $m/z$  Calcd for  $\text{C}_{10}\text{H}_8\text{Cl}_2\text{NNaO}_4$  ( $\text{M}$ ) $^+$  = 298.9728, Found 299.9632.



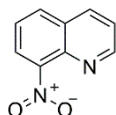
**10-Hydroxybenzo[h]quinoline-7,9-dicarboxylic acid (Ox-Q2l)** yellowish, 0,09 g (0,32 mmol, 32.4%);  $m.p.$ <sub>dec.</sub> = 235-245 °C;  $^1\text{H}$  NMR ( $\text{DMSO-}d_6$ ; 400.2 MHz; 60 °C)  $\delta$  = 8,13 (dd or t,  $^3J_{\text{H,H}}$  = 7.0 Hz, 1H, aromatic), 8.24 (d,  $^3J_{\text{H,H}}$  = 9.5 Hz, 1H, aromatic), 8.94 (s, 1H, aromatic), 9,07 (d,  $^3J_{\text{H,H}}$  = 8,0 Hz, 1H, aromatic), 9,24 (d,  $^3J_{\text{H,H}}$  = 5,4 Hz, 1H, aromatic), 9,36 (d,  $^3J_{\text{H,H}}$  = 9,4 Hz, 1H, aromatic), 16,21 (s, 1H, OH);  $^{13}\text{C}\{^1\text{H}\}$  NMR ( $\text{DMSO-}d_6$ ; 100.6 MHz; 60 °C)  $\delta$  = 112,2, 113,2, 113,4 122,2, 126,1, 127,6, 128,1, 137,5, 138,3, 141,3, 142,1, 143,1 167,5, 167,8, 172,6; HRMS (ESI TOF):  $m/z$  Calcd for  $\text{C}_{15}\text{H}_9\text{NO}_5\text{Na}$  ( $\text{M}+\text{Na}$ ) $^+$  = 306.0378, Found 306.0388; UV-Vis (methanol;  $\lambda$  [nm] ( $\log \epsilon$ )): 322 (3,96), 308 (4,03), 255 (4,49), 232 (4,84), 220 (4,85); IR (KBr):  $\tilde{\nu}$  = 2928, 1718, 1678, 1514, 1464, 1245, 846  $\text{cm}^{-1}$ .

## 7.11 Synthesis of selected nitroquinolines; VNS reaction

### 7.11.1 Synthesis of nitroquinolines

#### 7.11.1.1 Synthesis of 8-nitroquinoline

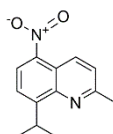
Toluene (50 mL) and acrolein (2.1 mL, 1.8 g, 31.4 mmol) were added to a solution of 2-nitroaniline **1m** (2.2 g, 15.7 mmol) in aqueous 6 M HCl (200 mL) and were heated under reflux for 16 h. The mixture was allowed to cool to room temperature. The aqueous layer was separated and neutralized with aqueous solution of K<sub>2</sub>CO<sub>3</sub>. After extraction with CH<sub>2</sub>Cl<sub>2</sub> (3 x 50 mL), the organic layer was separated and dried over MgSO<sub>4</sub>, and then was filtered and evaporated to afford yellowish crystals:



**8-Nitroquinoline (Q3a)**<sup>267</sup> 2.6 g (14.8 mmol, 94%); mp = 90.1–91.3 °C; <sup>1</sup>H-NMR (CDCl<sub>3</sub>; 400.2 MHz) δ = 7.57 (dd, <sup>3</sup>J<sub>H,H</sub> = 8.4 Hz, <sup>3</sup>J<sub>H,H</sub> = 4.2 Hz, 1H, aromatic), 7.63 (t, <sup>3</sup>J<sub>H,H</sub> = 7.9 Hz, 1H, aromatic), 8.05 (2d, <sup>3</sup>J<sub>H,H</sub> = 7.9 Hz, 2H, aromatic), 8.28 (d, <sup>3</sup>J<sub>H,H</sub> = 8.4 Hz, <sup>4</sup>J<sub>H,H</sub> = 1.4 Hz, 1H, aromatic), 9.08 (dd, <sup>3</sup>J<sub>H,H</sub> = 4.1 Hz, <sup>3</sup>J<sub>H,H</sub> = 1.4 Hz, 1H, aromatic); <sup>13</sup>C{<sup>1</sup>H}-NMR(CDCl<sub>3</sub>; 100.6 MHz) δ = 122.8, 123.8, 125.3, 129.1, 132.1, 136.2, 139.6, 147.5, 152.7.

#### 7.11.1.2 Synthesis of 8-(iso-Propyl)-2-methyl-5-nitroquinoline

8-(iso-Propyl)-2-methylquinoline **Q1k** (7.5 mmol) was dissolved in a mixture of concentrated H<sub>2</sub>SO<sub>4</sub> and HNO<sub>3</sub> (4.5 and 10.5 mL, respectively) at 5 °C. After stirring for 1 h at room temperature, no evolution of gas was observed, so the reaction mixture was heated up to 70 °C and stirred overnight. After this time, the reaction mixture was poured down to a beaker containing 25 g of ice and 25 mL of water and the precipitated solid was filtered off, washed with 10 mL of cold water, and dried on air, giving:

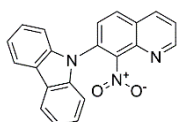


**8-(iso-Propyl)-2-methyl-5-nitroquinoline (Q3d)** beige solid. 1.3 g (5.7 mmol, 76%); mp = 59.1–60.3 °C; <sup>1</sup>H-NMR (CDCl<sub>3</sub>; 500.2 MHz) δ = 1.38 (d, <sup>3</sup>J<sub>H,H</sub> = 6.9 Hz, 6H, CH(CH<sub>3</sub>)<sub>2</sub>), 2.79 (s, 3H, CH<sub>3</sub>), 4.47 (septet, <sup>3</sup>J<sub>H,H</sub> = 6.9 Hz, 1H, CH), 7.50 (d, <sup>3</sup>J<sub>H,H</sub> = 8.9 Hz, 1H, aromatic), 7.64 (d, <sup>3</sup>J<sub>H,H</sub> = 8.1 Hz, 1H, aromatic), 8.28 (d, <sup>3</sup>J<sub>H,H</sub> = 8.1 Hz, 1H, aromatic), 8.92 (d, <sup>3</sup>J<sub>H,H</sub> = 8.9 Hz, 1H, aromatic); <sup>13</sup>C{<sup>1</sup>H}-NMR(CDCl<sub>3</sub>; 125.8 MHz) δ = 23.3, 25.4, 27.9, 119.4, 123.5, 123.8, 124.4, 132.2, 143.5, 145.3, 155.3,

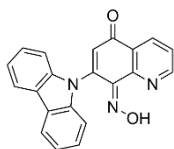
159.0; UV-Vis (methanol;  $\lambda$  (nm) (log( $\epsilon$ )): 321 (4.06), 225 (4.67), 202 (4.55); IR (KBr):  $\tilde{\nu}$  = 2963, 1960, 1895, 1606, 1517, 1449, 1342, 803  $\text{cm}^{-1}$ ; Anal. Calcd for  $\text{C}_{13}\text{H}_{14}\text{N}_2\text{O}_2$ : C, 67.81; H, 6.13; N, 12.17; O, 13.90 Found: C, 67.94; H, 6.19; N, 12.01.

### 7.11.2 VNS reaction

These were based on the procedure described in the literature<sup>268</sup>. To the suspension of *tert*-BuOK (1.0 g, 9.0 mmol) in THF (50 mL), 9*H*-carbazole (1.1 g, 6.6 mmol) was added and reagents were stirred under reflux for 30 min under argon. 8-Nitroquinolines **Q3a**, **Q3d** (4.52 mmol), respectively was then added to the reaction mixture, which was refluxed overnight. After the evaporation of the solvent to give a solid, water (20 mL) and dichloromethane (100 mL) were added. The organic layer was separated and the aqueous layer was extracted with dichloromethane (4 x 50 mL). The combined organic layers were dried over  $\text{MgSO}_4$ . After solvent evaporating, the crude product was purified by column chromatography on silica gel using methanol/dichloromethane as eluent to afford a crude solid, and finally crystallization from a mixture of dichloromethane and hexane to yield solids as follows:

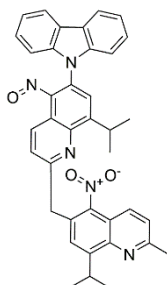


**9-(8-Nitroquinolin-7-yl)-9*H*-carbazole (Q4a)** 0.11 g (0.3 mmol, 7%); mp = 160-163  $^{\circ}\text{C}$ ;  $^1\text{H}$  NMR ( $\text{CDCl}_3$ , 500.2 MHz)  $\delta$  = 7.20 (dt,  $^3J_{\text{H,H}}$  = 8.1 Hz,  $^4J_{\text{H,H}}$  = 0.9 Hz, 2H, aromatic), 7.32 (ddd,  $^3J_{\text{H,H}}$  = 8.1 Hz,  $^4J_{\text{H,H}}$  = 7.2 Hz,  $^4J_{\text{H,H}}$  = 1.0 Hz, 2H, aromatic), 7.40 (ddd,  $^3J_{\text{H,H}}$  = 8.3 Hz,  $^4J_{\text{H,H}}$  = 7.2 Hz,  $^4J_{\text{H,H}}$  = 1.3 Hz, 2H, aromatic), 7.60 (d,  $^3J_{\text{H,H}}$  = 8.7 Hz, 1H, aromatic), 7.69 (dd,  $^3J_{\text{H,H}}$  = 8.4 Hz,  $^4J_{\text{H,H}}$  = 4.3 Hz, 1H, aromatic), 8.12 (ddd,  $^3J_{\text{H,H}}$  = 7.8 Hz,  $^4J_{\text{H,H}}$  = 1.3 Hz,  $^4J_{\text{H,H}}$  = 0.8 Hz, 2H, aromatic), 8.16 (d,  $^3J_{\text{H,H}}$  = 8.7 Hz, 1H, aromatic), 8.39 (dd,  $^3J_{\text{H,H}}$  = 8.4 Hz,  $^4J_{\text{H,H}}$  = 1.7 Hz, 1H, aromatic), 9.14 (dd,  $^3J_{\text{H,H}}$  = 4.3 Hz,  $^4J_{\text{H,H}}$  = 1.7 Hz, 1H, aromatic);  $^{13}\text{C}\{^1\text{H}\}$  NMR ( $\text{CDCl}_3$ ; 125.8 MHz)  $\delta$  = 110.2, 120.6, 121.2, 123.6, 124.3, 126.6, 127.8, 128.8, 130.5, 131.3, 136.1, 140.5, 141.5, 148.0, 153.3; HRMS (IT-TOF):  $m/z$  Calcd for  $\text{C}_{21}\text{H}_{14}\text{N}_3\text{O}_2$  ( $\text{M} + \text{H}$ ) $^+$  = 340.1086, Found 340.1094; UV-Vis (methanol;  $\lambda$  [nm] (log $\epsilon$ )): 329 (3.74), 315 (3.74), 287 (4.21), 225 (4.88), 206 (4.69); IR (KBr):  $\tilde{\nu}$  = 3060, 2925, 1731, 1541, 1450, 1225, 757  $\text{cm}^{-1}$ ; CCDC 2048038.



**(Z)-7-(9*H*-Carbazol-9-yl)-8-(hydroxyimino)quinolin-5(8*H*)-one (Q4b)** 0.24 g (0.7 mmol, 16%); mp<sub>dec.</sub> = 210-211  $^{\circ}\text{C}$ ;  $^1\text{H}$  NMR ( $\text{CDCl}_3$ , 500.2 MHz)  $\delta$  = 6.97 (s, 1H, aromatic), 7.31 (ddd,  $^3J_{\text{H,H}}$  = 8.0 Hz,  $^4J_{\text{H,H}}$  = 4.7 Hz,  $^4J_{\text{H,H}}$  = 3.4 Hz, 2H, aromatic), 7.42 (dd,  $^3J_{\text{H,H}}$  = 3.6 Hz,  $^4J_{\text{H,H}}$  = 1.0 Hz, 4H, aromatic), 7.84 (dd,  $^3J_{\text{H,H}}$  = 8.0,  $^4J_{\text{H,H}}$  = 4.9, 1H, aromatic), 8.10 (dt,  $^3J_{\text{H,H}}$  = 7.8,  $^4J_{\text{H,H}}$  = 1.0, 2H,

aromatic), 8.81 (dd,  $^3J_{\text{H,H}}=8.0$ ,  $^4J_{\text{H,H}}=1.8$  Hz, 1H, aromatic), 8.88 (dd,  $^3J_{\text{H,H}}=4.9$  Hz,  $^4J_{\text{H,H}}=1.8$  Hz, 1H, aromatic), 17.76 (s, 1H, OH);  $^1\text{H}$  NMR (DMSO- $d_6$ , 500.2 MHz)  $\delta = 7.03$  (s, 1H, aromatic), 7.29 (dd,  $^3J_{\text{H,H}}=7.4$  Hz, 2H, aromatic), 7.43 (dd,  $^3J_{\text{H,H}}=7.3$  Hz, 2H, aromatic), 7.56 (d,  $^3J_{\text{H,H}}=8.2$  Hz, 2H, aromatic), 8.03 (dd,  $^3J_{\text{H,H}}=8.0$  Hz,  $^4J_{\text{H,H}}=4.9$  Hz, 1H, aromatic), 8.21 (d,  $^3J_{\text{H,H}}=7.7$  Hz, 2H, aromatic), 8.74 (dd,  $^3J_{\text{H,H}}=8.0$  Hz,  $^4J_{\text{H,H}}=1.5$  Hz, 1H, aromatic), 9.07 (dd,  $^3J_{\text{H,H}}=4.9$  Hz,  $^4J_{\text{H,H}}=1.5$  Hz, 1H, aromatic), 17.41 (s, 1H, OH);  $^1\text{H}$  NMR (DMSO- $d_6$ /KOD, 500.2 MHz)  $\delta = 7.19$ -7.33 (m,  $^3J_{\text{H,H}}=7.0$  Hz,  $^4J_{\text{H,H}}=0.8$  Hz, 4H, aromatic), 7.40 (t,  $^3J_{\text{H,H}}=7.4$  Hz, 2H, aromatic), 7.55 (dd,  $^3J_{\text{H,H}}=7.9$  Hz,  $^4J_{\text{H,H}}=4.4$  Hz, 1H, aromatic), 8.23 (d,  $^3J_{\text{H,H}}=7.6$  Hz, 2H, aromatic), 8.66 (dd,  $^3J_{\text{H,H}}=8.1$  Hz,  $^4J_{\text{H,H}}=2.0$  Hz, 1H, aromatic), 8.94 (bs, 1H, aromatic);  $^{13}\text{C}\{^1\text{H}\}$  NMR (CDCl<sub>3</sub>; 125.8 MHz)  $\delta = 111.2$ , 120.5, 121.2, 124.6, 126.0, 126.3, 126.4, 126.7, 136.7, 140.2, 141.3, 147.6, 148.1, 150.2, 182.4; MS (IT-TOF):  $m/z$  (rel. int.) (M + H)<sup>+</sup> = 340.1091 (100%); (M - H<sub>2</sub>O)<sup>+</sup> = 322.0984 (23%); (M + Na)<sup>+</sup> = 362.0913 (9%); HRMS (IT-TOF):  $m/z$  Calcd for C<sub>21</sub>H<sub>14</sub>N<sub>3</sub>O<sub>2</sub> (M + H)<sup>+</sup> = 340.1086, Found 340.1091; UV-Vis (1M KOH;  $\lambda$  [nm] (log $\epsilon$ )): 406(4.22), 330 (3.83), 318 (3.86), 287 (4.10), 276 (4.13), 234 (4.63); (DMF;  $\lambda$  [nm] (log $\epsilon$ )): 430 (3.56), 330 (4.13), 317 (4.18); (DMSO;  $\lambda$  [nm] (log $\epsilon$ )): 430 (3.00), 331 (3.77), 320 (3.81), 290 (4.03); (ACN;  $\lambda$  [nm] (log $\epsilon$ )): 444 (2.64), 330 (3.63), 317 (3.71), 289 (3.78), 228 (4.10); (methanol;  $\lambda$  [nm] (log $\epsilon$ )): 453 (3.22), 328 (4.13), 317 (4.17), 287 (4.37), 228 (4.69); (THF;  $\lambda$  (nm) (log $\epsilon$ )): 459 (3.18), 330 (4.11), 318 (4.15), 288 (4.34), 239 (4.55); (CDCl<sub>3</sub>;  $\lambda$  [nm] (log $\epsilon$ )): 478 (3.35), 329 (4.23), 318 (4.24), 289 (4.42); IR (KBr):  $\tilde{\nu} = 3045$ , 2927, 1649, 1601, 1447, 1298, 750, 719 cm<sup>-1</sup>; CCDC 2048039.



**9-(8-isoPropyl-2-((8-isopropyl-2-methyl-5-nitroquinolin-6-yl)methyl)-5-nitrosoquinolin-6-yl)-9H-carbazole (Q4d)** 0.61 g (1.0 mmol, 44%); mp = 290.1–291.3 °C;  $^1\text{H}$ -NMR (CDCl<sub>3</sub>, 500.2 MHz)  $\delta = 1.48$  (d,  $^3J_{\text{H,H}}=6.8$  Hz, 6H, CH(CH<sub>3</sub>)<sub>2</sub>), 1.56 (d,  $^3J_{\text{H,H}}=7.0$  Hz, 6H, CH(CH<sub>3</sub>)<sub>2</sub>), 2.80 (s, 3H, CH<sub>3</sub>), 4.24 (septet,  $^3J_{\text{H,H}}=6.8$  Hz, 1H, CH), 4.47 (septet,  $^3J_{\text{H,H}}=6.8$  Hz, 1H, CH), 7.26 (s, 2H, aromatic), 7.36 (dt,  $^3J_{\text{H,H}}=7.1$  Hz,  $^4J_{\text{H,H}}=0.7$  Hz, 2H, aromatic), 7.41–7.47 (m, 3H, aromatic), 7.80 (s, 1H, aromatic), 8.17 (d,  $^3J_{\text{H,H}}=7.8$  Hz, 2H, aromatic), 8.50 (s, 2H, aromatic), 8.54 (s, 1H, aromatic), 8.77 (d,  $^3J_{\text{H,H}}=8.1$  Hz, 1H, aromatic);  $^{13}\text{C}\{^1\text{H}\}$ -NMR (CDCl<sub>3</sub>; 125.8 MHz)  $\delta = 23.1$ , 23.3, 25.6, 27.9, 28.6, 109.6, 115.3, 115.6, 116.6, 120.6, 120.7, 121.1, 121.3, 122.2, 124.1, 126.5, 126.6, 129.4, 132.1, 132.4, 140.9, 143.6, 144.9, 148.49, 148.54, 149.4, 154.1, 156.4, 160.2, 160.6; MS (ES-TOF):  $m/z$  (rel. int.) M<sup>+</sup> = 606.2502 (100%), (9-(8-isopropyl-2-methyl-5-nitrosoquinolin-6-yl)-9H-carbazole “VNS product” Scheme 79, chapter 6.5) Calcd for C<sub>25</sub>H<sub>21</sub>N<sub>3</sub>O (M - 2H)<sup>+</sup> = 377.2294 (20%); HRMS (AP-TOF):  $m/z$  Calcd. for C<sub>38</sub>H<sub>32</sub>N<sub>5</sub>O<sub>3</sub> M<sup>+</sup> = 606.2505, Found 606.2505; UV-Vis (methanol;  $\lambda$  (nm) (log $\epsilon$ )): 381 (4.46), 327 (4.17), 287 (4.57), 230 (4.86); IR (KBr):  $\tilde{\nu} = 2962$ , 1600, 1529, 1452, 1316, 1228, 750 cm<sup>-1</sup>.

## 8. Conclusions

Presented doctoral thesis was devoted to study the oxidation and reduction processes for 1,10-phenanthroline derivatives and their analogs. As a result of the work, 87 compounds (57 new ones) were synthesized, nine molecules were determined by single-crystal X-ray diffraction measurements. Part of the research includes detailed electrochemical studies, which were carried out for eleven selected 1,10-phenanthroline derivatives during the stay of 9 months at Jaroslav Heyrovský Institute of Physical Chemistry in Prague in Czech Republic under the supervision of Dr. Romana Sokolova.

In the case of research on 1,10-phenanthroline derivatives, their synthesis and functionalization were carried out in order to obtain new compounds. The obtained compounds were fully characterized by the spectroscopic techniques, elementary analysis and melting points measurements. This work has been divided into two parts focusing on the preparation of selected 1,10-phenanthroline derivatives and electrochemical studies of the compounds that were obtained:

1. The eleven 4,7-dichloro-1,10-phenanthroline derivatives were obtained based on synthesis with the use of Meldrum acid. These compounds were prepared using various substituents at the C5 position (i.e., H, F, Cl, CH<sub>3</sub>, CN) and the C2 and C9 positions (i.e., H, CH<sub>3</sub>) on the 1,10-phenanthroline backbone. The procedure of their preparation has been optimized in terms of improving the yield of individual reaction steps. Limitations in the separate stages of the reaction were analyzed, and it was proposed modifications to improve their preparation. Mass spectral analysis for the prepared 4,7-dichloro-1,10-phenanthroline showed fragmentation with an initial loss of chloride followed by the loss of the second chloride except for 5-bromo-4,7-dichloro-1,10-phenanthroline (**4i**), which was the first to eliminate bromide.

2. Substitution reactions were performed for eight selected 4,7-dichloro-1,10-phenanthroline derivatives with selected amines such as pyrrolidine, 9*H*-carbazole, and 10*H*-phenothiazine. The yield of the reaction depended mainly on the selected amine and substituents at the C2, C5, and C9 positions on the substrates. The highest yields for compounds with substituted amines are for 5-fluoro-4,7-di(10*H*-phenothiazin-10-yl)-1,10-phenanthroline (**5k**, 96%), 4,7-di(9*H*-carbazol-9-yl)-5-methyl-1,10-phenanthroline (**5h**, 89%) and 5-fluoro-2,9-dimethyl-4,7-di(pyrrolidin-1-yl)-1,10-phenanthroline (**5d**, 51%). As a result of the substitution reaction, 12 products were obtained, 9 of which are new. 5-Fluoro-2,9-

dimethyl-4,7-di(pyrrolidin-1-yl)-1,10-phenanthroline (**5d**) was determined by single-crystal X-ray diffraction measurements.

As a result of the next stage of research, comprehensive electrochemical studies were conducted, which allow to propose the mechanisms of oxidation and reduction processes supported by DFT calculations. In view of the above:

1. For five selected 4,7-dichloro-1,10-phenanthrolines, electrochemical studies were carried out to determine their oxidation and reduction potentials.

The oxidation of the studied molecules leads to the formation of an unstable dimer through a radical cation. IR spectroelectrochemistry did not show any changes in the intensity of vibrations belonging to water traces but successfully lead to the suggestion of the dimer structure, which was then confirmed by theoretical calculations.

Their reduction mechanism involves the cleavage of one or two chlorides from the molecule depending on the applied potential. This cleavage proceeds by a stepwise mechanism; the first step is forming a radical anion, and afterward, chloride is cleaved. The resulting radical accept one electron and forms an aryl anion. A reaction with a proton terminates the reaction; traces of water were confirmed as the source of protons under the used experimental conditions. The proposed pathways were confirmed by chromatographic and mass spectrometric characterization of solutions before, during and after exhaustive electrolysis.

2. The electrochemical behavior of two selected 4,7-di(pyrrolidin-1-yl)-1,10-phenanthrolines (**5a**, **5c**) was investigated.

The oxidation of these compounds leads to the formation of one dominant and several minor hydroxylated derivatives, increasing thus their solubility in water and possibly their bioavailability. The identified products of oxidation of 2,9-dimethyl-4,7-di(pyrrolidin-1-yl)-1,10-phenanthroline (**5c**) were (4-(2-hydroxypyrrolidin-1-yl)-2,9-dimethyl-7-(pyrrolidin-1-yl)-1,10-phenanthroline) (**5c-P1**) and 4-(2-hydroxypyrrolidin-1-yl)-2,9-dimethyl-7-(pyrrolidin-1-yl)-1,10-phenanthroline-5-ol (**5c-P2**) which were confirmed by mass spectrometry. The obtained oxidation products of compounds **5c** and 4,7-di(pyrrolidin-1-yl)-1,10-phenanthroline (**5a**) allow to propose their oxidation mechanism.

For their reduction mechanism, the first step is followed by cleavage of one pyrrolidine moiety from the molecular assembly, while the other pyrrolidine moiety is detached upon the second reduction step. The identified products of reduction of 4,7-di(pyrrolidin-1-yl)-1,10-phenanthroline (**5a**) were 4-(pyrrolidin-1-yl)-1,10-phenanthroline

(**5a-P7**), which lost one pyrrolidine substituent from the molecule, and 1,10-phenanthroline (**phen**) formed after the cleavage of both substituents were confirmed by mass spectrometry. The obtained reduction products of compounds **5a** and 2,9-dimethyl-4,7-di(pyrrolidin-1-yl)-1,10-phenanthroline (**5c**) allow to propose their oxidation mechanism.

3. The 4,7-di(9*H*-cabrazol-9-yl)-1,10-phenanthroline (**5f**) was also studied in terms of the processes of its reduction and oxidation.

The oxidation of compound **5f** leads to the formation of radical cation, biradical dication (one or two carbazole substituents oxidized) as intermediates, and the final dimeric products. The reduction leads to the cleavage of one carbazole moiety from the molecular assembly, while the other carbazole moiety is detached upon the second reduction step. The two identified products the 4-(9*H*-carbazol-9-yl)-1,10-phenanthroline (**5f-P1**), which lost one 9*H*-carbazole substituent from the molecule, and 1,10-phenanthroline (**phen**) formed after the cleavage of both 9*H*-carbazoles were confirmed by mass spectrometry. These products allowed me to propose a reduction mechanism.

4. The reduction and oxidation mechanisms were also proposed for selected 4,7-di(10*H*-phenothiazin-10-yl)-1,10-phenanthroline derivatives.

The oxidation proceeds in two subsequent one-electron steps, hence the overall by the four electrons. Two oxidation products 5-methyl-4,7-bis(5-oxido-10*H*-phenothiazin-10-yl)-1,10-phenanthroline (**5l-P2**) and an intermediate species 5-methyl-4-(5-oxido-10*H*-phenothiazin-10-yl)-7-(10*H*-phenothiazin-10-yl)-1,10-phenanthroline (**5l-P1**) were identified by mass spectrometry. These products allowed me to proposed an oxidation mechanism.

For the reduction processes as a result of the research, a mechanism was suggested where the reduction leads to the cleavage of one 10*H*-phenothiazine moiety from the molecular assembly, while the other 10*H*-phenothiazine moiety is eliminated upon the second reduction step (analogous to the 4,7-di(9*H*-cabrazol-9-yl)-1,10-phenanthroline). Two reduction products, 5-methyl-4-phenothiazine-1,10-phenanthroline (**5l-P3**) and 5-methyl-1,10-phenanthroline, were identified by mass spectrometry which confirms the proposed mechanism.

As part of this doctoral thesis the results of research on the oxidation and hydrolysis of selected 1,10-phenanthroline derivatives were presented.

For oxidation reaction, a procedure that was successfully used to oxidize 2,9-dimethyl-1,10-phenanthroline (**Phen-2CH<sub>3</sub>**) was developed to obtain selectively 9-methyl-1,10-phenanthroline-2-carboxylic acid (**Ox-Phen-2CH<sub>3</sub>**).

The result of the hydrolysis reaction of nitrile group for selected 4,7-dichloro-1,10-phenanthroline-5-carbonitrile (**4e**) was presented. This reaction did not lead to the expected product 4,7-dichloro-1,10-phenanthroline-5-carboxylic acid but to non-obvious cyclization of the product to give 7-chloropyrrolo[2,3,4-de][1,10]phenanthroline-5(4*H*)-one (**Hyd-4e**).

In turn, for the compounds 4,7-di(9*H*-carbazol-9-yl)-1,10-phenanthroline-5-carbonitrile (**5i**) and 4,7-di(10*H*-phenothiazine-10-yl)-1,10-phenanthroline-5-carbonitrile (**5m**) the hydrolysis reaction was also not as expected. Both products 4,7-di(9*H*-carbazol-9-yl)-9-oxo-9,10-dihydro-1,10-phenanthroline-5-carbonitrile (**Hyd-5i**) and 9-oxo-4,7-di(10*H*-phenothiazin-10-yl)-9,10-dihydro-1,10-phenanthroline-5-carbonitrile (**Hyd-5m**) were possibly obtained through a reaction of oxidative nucleophilic substitutions of hydrogen (ONSH) of the type  $S_NArH$ , with hydroxide ion as a nucleophile and in the presence of air as an oxidized reagent.

The next part of the research was the preparation of unsymmetric 1,10-phenanthroline derivatives. The reactions were carried out based on reaction using Meldrum acids and a Skraup-Doebner-Von Miller reaction. As a result of the study, new unsymmetric mono and dichloro-1,10-phenanthrolines were obtained.

Another topic of this PhD thesis was to get unsymmetric monosubstituted 1,10-phenanthroline. As a result of the series of reactions, a precursor of monosubstituted 1,10-phenanthrolines, i.e., 4-chloro-8-nitroquinoline (**4m**), was obtained. At this stage of the research, a series of reactions provide the substitution of activated chlorine for 4-chloro-8-nitroquinoline (**4m**) by a selected amine were designed. However, a competitive reaction turned out to be a limitation in the synthesis. The direct nucleophilic displacement of an aromatic hydrogen reaction proceeds together with expected aromatic nucleophilic substitution of halogen  $S_NAr$ . The product 9,9'-(8-nitroquinoline-4,7-diyl)bis(9*H*-carbazole) (**Q4c**) as a result of VNS and  $S_NAr$  subsequent substitutions was identify. The studies on VNS reactions were performed to confirm the possible substitution of the hydrogen atom of selected nitroquinoline. The conducted research confirmed that the 8-nitroquinoline (**Q3a**) was transformed through the VNS reaction and demonstrated the possibility of obtaining the product via two different substitutions (hydrogen and chloride) for 4-chloro-8-nitroquinoline (**4m**) molecule. It turned out that the VNS reaction proceeds rapidly with a visible color change of the reaction solution, which is corresponding with the literature.



Additionally, for 8-nitroquinoline (**Q3a**), the unexpected product of the VNS reaction was received (9-(8-nitroquinolin-7-yl)-9*H*-carbazole). The oxidation product ((*Z*)-7-(9*H*-carbazol-9-yl)-8-(hydroxyimino)quinolin-5(8*H*)-one) was also isolated. For both products of this reaction, single crystal x-ray diffraction measurements were carried out. The product of double VNS substitution of 8-(iso-propyl)-2-methyl-5-nitroquinoline (**Q3d**) was confirmed.

During this PhD, auxiliary syntheses on 1,10-phenanthroline analogs was conducted. These studies were devoted to preparing and functionalizing mono and dicarbaldehydes quinoline and benzo[*h*]quinoline derivatives. This research allows to learn about the complexity of their oxidation processes and develop an oxidation procedure that was used in the oxidation of 2,9-dimethyl-1,10-phenanthroline (**Ox-Phen-2CH<sub>3</sub>**). The compounds were obtained based on the Reimer-Tiemann, Vilsmeier-Haack, and the Duff reactions.

The theoretical calculations for their precursors such as 8-hydroxyquinoline (**Q1a**), 6-hydroxyquinoline (**Q1h**), *N,N*-dimethylquinolin-6-amine (**Q1e**) and *N,N*-dimethylquinolin-8-amine (**Q1i**) were carried out to explain the differences in reactivity. The formylation reaction for these compounds may depend on the electrostatic potential of the atoms participating in this transformation. The higher difference in atomic charges between C5 and C7 positions shows the preference of monoforylation products with new carbonyl group only in the C5 position. In turn, the smaller differences in the atomic charges difference of atoms in bonds C5-H and C7-H suggest the possibility of double formylation and the presence of both regioisomers with carbonyl groups in C5 and C7 positions. In the case of **Q2k** on IR spectrum two signals from both carbonyl groups located at C5 and C7 were detected. Comparison of the double formylated products **Q2i** and **Q2k** revealed that the presence of intramolecular and intermolecular hydrogen bonds between the carbonyl groups and hydroxyl groups has the impact on overlapping signals.

In the case of their functionalization, the oxidation reactions for two selected compounds, i.e., 8-hydroxyquinoline-5,7-dicarbaldehyde (**Q2b**) and 10-hydroxybenzo[*h*]quinoline-7,9-dicarbaldehyde (**Q2l**) were performed. As a result of the reaction to the path of the oxidation procedure which was developed, two oxidation products were obtained. For the quinoline derivative, the oxidation procedure led to an unexpected product. The reaction proceeded by cleavage of the phenyl ring bond and other side reactions. In turn, for the benzo[*h*]quinoline derivative, the oxidation reaction successfully leads to the preparation of 10-hydroxybenzo[*h*]quinoline-7,9-dicarboxylic acid (**Ox-Q2l**).

## 8.1 Other research achievements

During doctoral studies, research topics unrelated to the topic of the doctoral dissertation were discussed. The first research topic was the preparation and purification of graphene oxide and its modified derivatives. As a result of this research, two patents were developed:

The first patent was devoted to graphene oxide modified by 5-amino-1,10-phenanthroline, which has been tested for their use, especially for the sorption of metal ions, which are water pollutants.

The second patent concerned a method for purification of graphene oxide, proposing the use of continuous extraction in the Soxhlet apparatus using hydrochloric or hydrobromic acid.

Another unrelated research topic was the spectroelectrochemical detection of reaction intermediates and the reduction and oxidation mechanism of azoquinoline dye 2-methyl-5-[(*E*)-phenyldiazenyl]quinolin-8-ol. As a result of the research, the reduction and oxidation mechanisms for selected dyes were presented.

## 9. Summary

One of the most important scientific achievements is designing and carrying out oxidation reactions for commercially available 2,9-dimethyl-1,10-phenanthroline. This reaction selectively yields 9-methyl-1,10-phenanthroline-2-carboxylic acid. The procedure and the obtained reaction product were submitted as national patent application. The obtained carboxylic acid can be used as a ligand in complexation reactions that will be carried out in an aqueous medium.

Another significant achievement is the performance of electrochemical studies for selected 4,7-dichloro-1,10-phenanthroline, thanks to which selective elimination of chlorine atoms was showed. Electrochemical knowledge of the routes for the reductive dechlorination of one or two chloro substituents may help predict experiments in a reduction-based synthesis. These studies show an exciting possibility of obtaining monochloro derivatives of 1,10-phenanthrolines in a much shorter process than the series of reactions in classical organic synthesis, which were proposed. The selective elimination of chlorine atoms to obtain monochloro derivatives of 1,10-phenanthroline opens up new possibilities for electrosynthesis.

In the case of electrochemical research, an important achievement is also the determination of oxidation and reduction mechanisms for such groups of compounds as 4,7-di(pyrrolidin-1-yl)-1,10-phenanthroline, 4,7-di(9*H*-carbazol-9-yl)-1,10-phenanthroline and 4,7-di(10*H*-phenothiazine-10-yl)-1,10-phenanthroline derivatives. Understanding the reaction mechanism, in addition to the cognitive importance, is also important in the conscious control of the reaction in order to obtain or avoid the expected product.

## 10. Main achievements

Obtaining a pro-quality scholarship 2018/2019, 2019/2020, 2020/2021.

Obtaining the rector's scholarship in 2020/2021.

Completing internships at the Heyrovsky Institute, where I stayed for a total of 9 months. For 3 months under the project "Chemia I Staże", under the Erasmus project twice for 3 months.

I received a scholarship to travel to a foreign conference from the PROM 2019 project.

I have published a total of eight publications, where I am a co-author, in six of them I am the first author, for one in a special conference issue I am the corresponding author. As part of my achievements, I am also a co-author of 3 national patents and 2 patent applications.

I received a distinction in the 11th edition of the "Student-Wynalazca" Competition in 2021. For national patent "Tlenek grafenu modyfikowany 5-amino-1,10-fenantroliną".

Participation in the International Warsaw Invention Show in 25-27.10.2021. For national patent "Tlenek grafenu modyfikowany 5-amino-1,10-fenantroliną".

On September 15, 2021 based on data from the Web of Science database:

Hirsch index = 3

Citations = 13

ORCID: 0000-0001-5689-9105

## 11. Scientific achievements and scientific internships

### 11.1 Publications

1. R. Sokolová, Š. Ramešová, I. Degano, M. Hromadová, M. Szala, **J. Wantulok**, J. E. Nycz, M. Valášek, Application of Spectroelectrochemistry in Elucidation of Electrochemical Mechanism of Azoquinoline Dye 2-Methyl-5-[(*E*)-phenyldiazenyl]quinolin-8-ol, *Electrochimica Acta*; **2018**, 270, 509–516. DOI: 10.1016/j.electacta.2018.03.096

- J.E. Nycz, **J. Wantulok**, R. Sokolova, L. Pajchel, M. Stankevic, M. Szala, J.G. Małecki, D. Swoboda, Synthesis and electrochemical and spectroscopic characterization of 4,7-diamino-1,10-phenanthrolines and their precursors, *Molecules*, **2019**, 24, 4102 DOI: 10.3390/molecules24224102
- J. Wantulok**, I. Degano, M. Gal, J.E. Nycz, R. Sokolova, IR spectroelectrochemistry as efficient technique for elucidation of reduction mechanism of chlorine substituted 1,10-phenanthrolines, *J. Electroanal. Chem.* **2020**, 859, 113888 DOI: 10.1016/j.jelechem.2020.113888
- J. Wantulok**, M. Szala, A. Quinto, J.E. Nycz, S. Giannarelli, R. Sokolova, M. Książek, J. Kusz, Synthesis, Electrochemical and Spectroscopic Characterization of Selected Quinolinecarbaldehydes and Their Schiff Base Derivatives, *Molecules*, **2020**, 25, 2053 DOI: 10.3390/molecules25092053
- J. Wantulok**, R. Sokolova, I. Degano, V. Kolivoska, J. E. Nycz, The effects of 4,7-di(pyrrolidin-1-yl) substituents on the reduction and oxidation mechanisms of 1,10-phenanthrolines: new perspectives in tailoring of phenanthroline derivatives, *Electrochimica Acta*, **2021**, 137674 DOI: 10.1016/j.electacta.2020.137674
- J. Wantulok**, D. Swoboda, J. E. Nycz, M. Książek, J. Kusz, J. G. Małecki, V. Kubíček, Direct Amination of Nitroquinoline Derivatives via Nucleophilic Displacement of Aromatic Hydrogen, *Molecules*, **2021**, 26, 1857 DOI: 10.3390/molecules26071857
- J. Wantulok**, R. Sokolova, I. Degano, V. Kolivoska, J. E. Nycz, J. Fiedler, Spectroelectrochemical properties of 1,10-phenanthroline substituted by phenothiazine and carbazole redox-active units, *ChemElectroChem*, **2021**, 8, 2935-2943 DOI: 10.1002/celec.202100835

## 11.2 Patents

- B. Feist, J. Nycz, E. Schab-Balcerzak, R. Sitko, M. Szala, K. Kocot, **J. Wantulok**, J. Kuczera, B. Ośmiałowski, I. Grela, K. Mroczynska, Tlenek grafenu modyfikowany 5-amino-1,10-fenantroliną, 06.05.2019, P. 232998
- K. Kocot, B. Feist, R. Sitko, J. Nycz, M. Szala, **J. Wantulok**, K. Byrdy; Sposób oczyszczania tlenku grafenu; 24.01.2020, P. 235061
- J. Nycz, **J. Wantulok**; Hydroksydialdehydy pochodne 8-hydroksychinoliny lub jej analogu benzo[*h*]chinolino-10-olu oraz sposób ich otrzymywania” 11.12.2020, P. 237226

## 11.3 Proceedings

- J. Wantulok**, R. Sokolová, J. Nycz, I. Degano, Oxidation and reduction of selected 1,10-phenanthrolines.” In: Modern electrochemical methods XXXIX. [Sborník přednášek mezinárodní odborné konference XXXIX. Moderní elektrochemické metody]. Srsenová L. – Best servis Ústí n. L., 2019 - (Navrátil, T.; Fojta, M.; Schwarzová, K.) Jetřichovice (CZ), May 20-24, 2019, p. 240-243. ISBN 978-80-905221-7-6.

## 11.4 Patent applications

1. B. Feist, J. Nycz, E. Schab-Balcerzak, R. Sitko, M. Szala, K. Kocot, **J. Wantulok**, J. Kuczera, B. Ośmiałowski, I. Grela, K. Mroczyńska, Tlenek grafenu modyfikowany 5-amino-1,10-fenantroliną, P.420628
2. K. Kocot, B. Feist, R. Sitko, J. Nycz, M. Szala, **J. Wantulok**, K. Byrdy, Sposób oczyszczania tlenu grafenu; zgłoszono, P. 422466
3. J. Nycz, **J. Wantulok**, Hydroksydialdehydy pochodne 8-hydroksychinoliny lub jej analogu benzo[h]chinolino-10-olu oraz sposób ich otrzymania, P. 428704
4. J. Nycz, **J. Wantulok**, Rozpuszczalny w wodzie kwas 9-metylo-1,10-fenantrolino-2-karboksyowy oraz sposób jego otrzymania, P.435020
5. **J. Wantulok**, J. Nycz, J. Małecki, E. Schab-Balcerzak, A. Słodek, G. Szafraniec-Gorol, Fotoluminescencyjny kwas 10-hydroksybenzo[h]chinolino-7,9-dikarboksyowy oraz sposób jego otrzymania, P.436093

## 11.5 Participation in national and international conferences

### 11.5.1 National conferences

1. Katowicach 29.06.2015. **J. Wantulok**, K. Czyż, J. E. Nycz; poster pt. „Synteza perowskitów domieszkowanych związkami organicznymi” I Forum Remediacji, Rewitalizacji i Zielonej Energii.
2. Katowice 13.05.2016. **J. Wantulok**, K. Byrdy, T. Paździorek, M. Szala, J. E. Nycz; poster pt. „Opracowanie barwnych reakcji chemicznych w celu oznaczenia wybranych katynonów metodami spektroskopowymi” X Seminarium Naukowe „Aktualne Problemy Chemii Analitycznej”
3. Lublin 17.12.2016. **J. Wantulok**, M. Szala, M. Stankiewicz, J. E. Nycz; poster pt. „Synteza nowych pochodnych 4,7-dipirolidyno-1,10-fenantrolin” Zjazd Zimowy Sekcji Studenckiej PTChem 2016
4. Katowice 12.05.2017. **J. Wantulok**, J. E. Nycz; poster pt. „Synteza pochodnych 4,7-dichloro oraz 4,7-dipirolidyno-1,10-fenantrolin” XI Seminarium Naukowe „Aktualne problemy Chemii Analitycznej”
5. Katowice 11.05.2018 **J. Wantulok**, M. Szala, T. Paździorek, D. Swoboda, J. E. Nycz; poster pt. „Synteza i identyfikacja pochodnych aldehydowych chinoliny” XII Seminarium Naukowe „Aktualne problemy Chemii Analitycznej”
6. Katowice 11.05.2018 D. Swoboda, A. Płuciennik, **J. Wantulok**, poster pt. „Aktywowane światłem właściwości bakteriobójcze kopolimerów zawierających analogi błękitu metylenowego” XII Seminarium Naukowe „Aktualne problemy Chemii Analitycznej”
7. Chorzów 14.09.2018 **J. Wantulok**, M. Szala, D. Swoboda, J. E. Nycz poster pt. „Formylowanie pochodnych chinoliny z wykorzystaniem reakcji Duffa” Pomiędzy Naukami 2018

8. Katowice 17.05.2019 M. Szala, D. Swoboda, **J. Wantulok**, J. E. Nycz, poster pt. „Regioselektywne deuterowanie 2-metylo-8-hydroksychinoliny”, XIII Seminarium Naukowe „Aktualne problemy Chemii Analitycznej”

### 11.5.2 International conferences

1. Ustroń 28.05.2015. **Jakub Wantulok**, Marcin Szala, Karolina Czyż, Jacek E. Nycz; poster Wpływ domieszekorganicznych na wybrane właściwości perowskitów” II Międzynarodowe Forum Zielonej Energii i Czystej Wody.

2. Ustroń 28.05.2015. K. Byrdy, **J. Wantulok**, K. Czyż, M. Szala, J. E. Nycz; Modyfikacja tlenu grafenu za pomocą wybranych pochodnych 1,10-fenantroliny; II Międzynarodowe Forum Budownictwa Ekologicznego, Zielonej Energii i Czystej Wody.

3. Szczyrk 24-26.05.2017. **Jakub Wantulok**, Krzysztof Byrdy, Tadeusz Paździorek, Jacek E. Nycz; poster “Identification of instability products of the cathinone derivatives”,

4. Szczyrk 19-22.06.2018. **Jakub Wantulok**, Daniel Swoboda, Tadeusz Paździorek, Jacek E. Nycz; poster pt. “Synthesis and identification of derivatives of 4,7-dichloro-1,10-phenanthroline”,

5. Jetrichovice 20-24.05.2019. **J. Wantulok**, R. Sokolova, J. Nycz, I. Degano; wystąpienie ustne, prezentacja pt. „Oxidation and reduction of selected 1,10-phenanthrolines”, XXXIX Modern electrochemical methods

6. Chorzów 19-20.09.2019. **J. Wantulok**, D. Swoboda, N. Wiese, S. Balcerowska, J. G. Małecki, J. E. Nycz, poster pt. „Synthesis and identification of tribenzoylhydrazine as a potential radical precursor”, Science Beyond Disciplines 2019

7. Seville 8-11.09.2019. D. Swoboda, **J. Wantulok**, J. Nycz, M. Wainwright, J. E. Nycz, poster pt. „Synthesis of novel phenothiazinium photosensitisers”, International Symposium on Dyes & Pigments, Modern Colorants; The Synthesis and Applications of  $\pi$ -Systems.

### 11.6 Scientific internships

1. **Project CIS – Chemia i Staże**; Academy of Sciences of the Czech Republic J. Heyrovský Institute of Physical Chemistry, v.v.i.; **09-11.2017**, Czech Republic
2. **Erasmus plus**; Academy of Sciences of the Czech Republic J. Heyrovský Institute of Physical Chemistry, v.v.i. **06-08.2018**, Czech Republic
3. **Erasmus plus**; Academy of Sciences of the Czech Republic J. Heyrovský Institute of Physical Chemistry, v.v.i. **06-08.2019**, Czech Republic

## 12. Literature

---

- <sup>1</sup> K. Itaya, H. Akahoshi, S. Toshima, Polymer-modified electrodes. 2. spectroelectrochemical properties of a ligand (bathophenanthroline disulfonic acid) bound to poly-electrolytes on electrodes and the use of the modified electrodes for an electrochromic display device, *J. Electrochem. Soc.*, **1982**, 129, 762 DOI: 10.1149/1.2123967
- <sup>2</sup> A. Switlicka-Olszewska, T. Klemens, B. Machura, E. Schab-Balcerzak, K. Laba, M. Lapkowski, M. Grucela, J. E. Nycz, M. Szala, M. Kania, Rhenium(I) complexes with phenanthrolines bearing electron withdrawing Cl and electron donating CH<sub>3</sub> substituents - synthesis, photophysical, thermal and electrochemical properties with electroluminescence ability, *RSC Advances*, **2016**, 6, 112908-112918 DOI: 10.1039/C6RA23935H
- <sup>3</sup> A.V. Müller, L. D. Ramos, K. P. M. Frin, K.T. de Oliveira, A. S. Polo, A high efficiency ruthenium(ii) tris-heteroleptic dye containing 4,7-dicarbazole-1,10-phenanthroline for nanocrystalline solar cells, *RSC Adv.*, **2016**, 6, 46487-46494 DOI: 10.1039/C6RA08666G
- <sup>4</sup> L. D. Ramos, R. N. Sampaio, F. F. de Assis, K. T. de Oliveira, P. Homem-de-Mello, A. O. T. Patrocínio, K. P. M. Frin, Contrasting photophysical properties of rhenium(i) tricarbonyl complexes having carbazole groups attached to the polypyridine ligand, *Dalton Trans.*, **2016**, 45, 11688-11698 DOI: 10.1039/C6DT01112H
- <sup>5</sup> Collin, G.; Höke, H. Quinoline and Isoquinoline. In *Ullmann's Encyclopedia of Industrial Chemistry*; Wiley-VCH: Weinheim, Germany, 2003.
- <sup>6</sup> A. Chugh, A. Kumar, A. Verma, S. Kumar, P. Kumar, A review of antimalarial activity of two or three nitrogen atoms containing heterocyclic compounds, *Med. Chem. Res.*, **2020**, 29, 1723-1750 DOI: 10.1007/s00044-020-02604-6
- <sup>7</sup> N. B. Patel, H. R. Patel, Synthesis and Antibacterial and Antifungal Studies of Novel Nitrogen Containing Heterocycles from 5-Ethylpyridin-2-ethanol, *Indian J Pharm Sci.*, **2010**, 72, 613-620 DOI: 10.4103/0250-474X.78531
- <sup>8</sup> M. Ge Zayada, A. A. -H. Abdel-Rahman, F. El-Essawy, Synthesis and Antibacterial Activities of Different Five-Membered Heterocyclic Rings Incorporated with Pyridothienopyrimidine, *ACS. Omega*, **2020**, 5, 6163-6168 DOI: 10.1021/acsomega.0c00188
- <sup>9</sup> M. Yamaguchi, K. Kamei, T. Koga, M. Akima, T. Kuroki, N. Ohi, Novel antiasthmatic agents with dual activities of thromboxane A<sub>2</sub> synthetase inhibition and bronchodilation. 1. 2-[2-(1-Imidazolyl)alkyl]-1(2H)-phthalazinones, *J. Med. Chem.*, **1993**, 36, 4052-4060 DOI: 10.1021/jm00077a008
- <sup>10</sup> A. Cristina, D. Leonte, L. Vlase, L. C. Bencze, S. Imre, G. Marc, B. Apan, C. Mogosan, V. Zaharia, Heterocycles 48. Synthesis, Characterization and Biological Evaluation of Imidazo[2,1-b][1,3,4]Thiadiazole Derivatives as Anti-Inflammatory Agents, *Molecules*, **2018**, 23, 2425 DOI: 10.3390/molecules23102425
- <sup>11</sup> A. S. Denisova, M. B. Degtyareva, E. M. Dem'yanchuk, A. A. Simanova, Synthesis of Bifunctional Ligands Based on Azaheterocycles and Fragments of 12-Crown-4, *Russian Journal of Organic Chemistry*, **2005**, 41, 1690-1693 DOI: 10.1007/s11178-006-0020-1
- <sup>12</sup> K. Wang, P. Jing, M. Yang, P. Ma, J. Qin, X. Huang, L. Ma, R. Li, Metal-free nitrogen -doped carbon nanosheets: a catalyst for the direct synthesis of imines under mild conditions, *Green Chem.*, **2019**, 21, 2448-2461 DOI: 10.1039/C9GC00908F
- <sup>13</sup> A. Kai, H. Daido, K. Yoshida, H. Tsukada, Y. Takahashi, M. Nomura, N. Kawahara, H. Katsuta, T. Wakita, MITSUI CHEMICALS, INC., Amide derivative and pesticide containing such compound, **2006**, WO2006/137376
- <sup>14</sup> P. Daw, A. Sinha, S. M. Wahidur Rahaman, S. Dinda, J. K. Bera, Bifunctional Water Activation for Catalytic Hydration of Organonitriles, *Organometallics*, **2012**, 31, 3790-3797 DOI: 10.1021/om300297y

- 
- <sup>15</sup> C. Costentin, M. Robert, J. -M. Saveant, Successive Removal of Chloride Ions from Organic Polychloride Pollutants. Mechanisms of Reductive Electrochemical Elimination in Aliphatic Gem-Polychlorides, *r*,*s*-Polychloroalkenes, and *r*,*s*-Polychloroalkanes in Mildly Protic Medium, *J. Am. Chem. Soc.*, **2003**, 125, 10729–10739 DOI: 10.1021/ja036141t
- <sup>16</sup> A. A. Pevery, T. L. Dresbach, K. N. Knut, T. F. Koss, M. K. Longmire, D. G. Peters, Electrochemical reduction of 2,4-dichloro-1-(4-chloro-2-methoxyphenoxy)benzene (methyl triclosan) at glassy carbon cathodes in dimethylformamide, *J. Electroanal. Chem.*, **2014**, 731, 1-5 DOI: 10.1016/j.jelechem.2014.07.032
- <sup>17</sup> D. Sadowsky, K. McNeill, C. J. Cramer, Dehalogenation of Aromatics by Nucleophilic Aromatic Substitution, *Environ. Sci. Technol.* **2014**, 48, 18, 10904–10911 DOI: 10.1021/es5028822
- <sup>18</sup> M. L. Buil, M. A. Esteruelas, S. Niembro, M. Olivan, L. Orzechowski, C. Pelayo, A. Vallribera, Dehalogenation and Hydrogenation of Aromatic Compounds Catalyzed by Nanoparticles Generated from Rhodium Bis(imino)pyridine Complexes, *Organometallics*, **2010**, 29, 19, 4375–4383 DOI: 10.1021/om1003072
- <sup>19</sup> S. Sekiguchi, T. Horie, T. Suzuki, Aromatic nucleophilic substitution reactions of 1-dialkylamino-2,4-dinitronaphthalene with primary or secondary amines in organic solvents: facile amine–amine exchange, *J. Chem. Soc., Chem. Commun.*, **1988**, 698-700 DOI: 10.1039/C39880000698
- <sup>20</sup> C. Xia, Y. Wu, S. Layek, J. Fiordeliso, Bicarbazole containing compounds for OLEDs, **2011**, US2011/260138
- <sup>21</sup> M. -Y. Hu, Q. He, S. -J. Fan, Z. -C. Wang, L. -Y. Liu, Y. -J. Mu, Q. Peng, S. -F. Zhu, Ligands with 1,10-phenanthroline scaffold for highly regioselective iron-catalyzed alkene hydrosilylation, *Nat. Commun.*, **2018**, 9, 221 DOI: 10.1038/s41467-017-02472-6
- <sup>22</sup> IUPAC Compendium of Chemical Terminology - the Gold Book heterocyclic compounds, **2009**, [http:// goldbook.iupac.org/H02798.html](http://goldbook.iupac.org/H02798.html) (accessed on **6.04.2020**).
- <sup>23</sup> Ullmann's Encyclopedia of Industrial Chemistry, Wiley, **2007**
- <sup>24</sup> J. A. Joule, K. Mills, *Heterocyclic Chemistry*, Wiley-Blackwell, **2010**
- <sup>25</sup> M. K. Cyranski, Energetic Aspects of Cyclic Pi-Electron Delocalization: Evaluation of the Methods of Estimating Aromatic Stabilization Energies, *Chem Rev.*, **2005**, 105, 3773 DOI: 10.1021/cr0300845
- <sup>26</sup> S. Badoglu, S. Yurdakul, A quantum chemical investigation on methylated pyridines, *Struct. Chem.*, **2010**, 21, 1103–1109 DOI: 10.1007/s11224-010-9651-5
- <sup>27</sup> R.T. Sanderson, *Encyclopædia Britannica*, Nitrogen, *Encyclopædia Britannica*, **2019**, <https://www.britannica.com/science/nitrogen> (accessed on **27.04.2020**)
- <sup>28</sup> Z. H. Skraup, G. Vortmann, Uber Derivate des dipyridyls, *Monatsh. Chem.*, **1882**, 3, 570-602 DOI: 10.1007/BF01516825
- <sup>29</sup> A. Kaufmann, R. Radosevic, Uber das p-Phenanthrolin, *Ber.*, **1909**, 42, 2612-2622 DOI: 10.1002/cber.190904202173
- <sup>30</sup> A. A. Schilt, *Analytical Applications of 1,10-Phenanthroline and Related Compounds: International Series of Monographs in Analytical Chemistry*, Elsevier (Illinois, USA), **2013**
- <sup>31</sup> F. Blau, Uber neue organische Metallverbindungen, *Monatsh. Chem.*, **1898**, 19, 647-689 DOI: 10.1007/BF01517438
- <sup>32</sup> S. A. Yamashkin, E. A. Oreshkina, Traditional and modern approaches to the synthesis of quinoline systems by the Skraup and Doebner-Miller methods. (Review), *Chem. Heterocycl. Compd.*, **2006**, 42, 701-718 DOI: 10.1007/s10593-006-0150-y
- <sup>33</sup> P. Belser, S. Bernhard, U. Guerig, Synthesis of mono- and dialkylsubstituted 1,10-phenanthrolines, *Tetrahedron*, **1996**, 52, 2937- 2944 DOI: 10.1016/0040-4020(95)01118-8
- <sup>34</sup> D. Pomeranc, V. Heitz, J.-C. Chambron J.-P. Octahedral Fe(II) and Ru(II) Complexes Based on a New Bis 1,10-Phenanthroline Ligand That Imposes a Well Defined Axis, *J. Am. Chem. Soc.*, **2001**, 123, 12215-12221 DOI: 10.1021/ja011250y
- <sup>35</sup> H. Saggadi, D. Luart, N. Thiebault, I. Polaert, L. Estel, C. Len, Quinoline and phenanthroline preparation starting from glycerol via improved microwave-assisted modified Skraup reaction, *RSC Adv.*, **2014**, 4, 21456–21464 DOI: 10.1039/c4ra00758a



- 
- <sup>36</sup> K. Panda, I. Siddiqui, P. K. Mahata, H. Ila, H. Junjappa, Heteroannulation of 3-Bis(methylthio)acrolein with Aromatic Amines - A Convenient Highly Regioselective Synthesis of 2-(Methylthio)quinolines and their Benzo/Hetero Fused Analogs - A Modified Skraup Quinoline Synthesis, *Synlett.*, **2004**, 3, 449–450 DOI: 10.1055/s-2004-815400
- <sup>37</sup> K. J. Shaffer, D. C. Parr, M. Wenzel, G. J. Rowlands, P. G. Plieger, The Proton Sponge Effect: Substitution of Quino[7,8-h]quinoline and the First Structurally Characterised Derivatives, *Eur. J. Org. Chem.*, **2012**, 35, 6967–6975 DOI: 10.1002/ejoc.201201131
- <sup>38</sup> B. Boganyi, J. Kaman, A concise synthesis of indoloquinoline skeletons applying two consecutive Pd-catalyzed reactions, *Tetrahedron*, **2013**, 69, 9512–9519 DOI: 10.1016/j.tet.2013.08.019
- <sup>39</sup> A. F. Larsen, T. Ulven, Efficient synthesis of 4,7-diamino substituted 1,10-phenanthroline-2,9-dicarboxamides. *Org. Lett.*, **2011**, 13, 3546–3548 DOI: 10.1021/ol201321z
- <sup>40</sup> G. I. Graf, D. Hastreiter, L. E. da Silva, R. A. Rebelo, A. G. Montalban, A. McKillop, The synthesis of aromatic diazatriacycles from phenylenediamine-bis(methylene Meldrum's acid) derivatives, *Tetrahedron*, **2002**, 58, 9095–9100 DOI: 10.1016/S0040-4020(02)01085-2
- <sup>41</sup> M.A. El-Atawy, F. Ferretii, F. Ragaini, Palladium-Catalyzed Intramolecular Cyclization of Nitroalkenes: Synthesis of Thienopyrroles, *Eur. J.*, **2017**, 14, 1902–1910 DOI: 10.1002/ejoc.201700165
- <sup>42</sup> B. Kaboudin, M. Khadamorady, Y. Abedi, A Practical and Convenient Method for the Synthesis of Some Benzimidazoles. *Org. Prep. Proced. Int.*, **2013**, 45, 162–167 DOI: 10.1080/00304948.2013.765294
- <sup>43</sup> A. Poloek, C. -W. Lin, C. -T. Chen, C. -T. Chen, High colour rendering index and colour stable hybrid white efficient OLEDs with a double emitting layer structure using a single phosphorescence dopant of heteroleptic platinum complexes, *J. Mater. Chem. C*, **2014**, 2, 10343–10356 DOI: 10.1039/c4tc01791a
- <sup>44</sup> X. Liu, X. Li, Y. Chen, Y. Hu, Y. Kishi, On Ni Catalysts for Catalytic, Asymmetric Ni/Cr-Mediated Coupling Reactions, *J. Am. Chem. Soc.*, **2012**, 134, 6136–6139 DOI: 10.1021/ja302177z
- <sup>45</sup> J. A. Berrocal, S. Albano, L. Mandolini, S. Di Stefano, A Cu<sup>I</sup>-Based Metallo-Supramolecular Gel-Like Material Built from a Library of Oligomeric Ligands Featuring Exotopic 1,10-Phenanthroline Units, *Eur. J. Org. Chem.*, **2015**, 34, 7504–7510 DOI: 10.1002/ejoc.201501201
- <sup>46</sup> H. Chen, X. Jia, Y. Yu, Q. Qian, H. Gong, Nickel-Catalyzed Reductive Allylation of Tertiary Alkyl Halides with Allylic Carbonates, *Angew. Chem. Int. Ed.*, **2017**, 56, 13103–13106 DOI: 10.1002/anie.201705521
- <sup>47</sup> R. A. Altman, S. L. Buchwald, 4,7-Dimethoxy-1,10-phenanthroline: An Excellent Ligand for the Cu-Catalyzed N-Arylation of Imidazoles, *Org. Lett.*, **2006**, 8, 13, 2779–2782 DOI: 10.1021/ol0608505
- <sup>48</sup> S. Makowski, Karbamoiłowe pochodne 2,2-dimetylo-1,3-dioksa-4,6-dionu w syntezie organicznej; aspekty aplikacyjne i mechanistyczne, (Habilitation) Gdańsk University of technology (**2013**)
- <sup>49</sup> N. E. Aksakal, H. H. Kazan, E. T. Eçika, F. Yuksel, A novel photosensitizer based on a ruthenium(II) phenanthroline bis(perylene-diimide) dyad: synthesis, generation of singlet oxygen and in vitro photodynamic therapy, *New J. Chem.*, **2018**, 42, 17538–17545 DOI: 10.1039/C8NJ02944J
- <sup>50</sup> R. J. Sundberg, F. A. Carey, *Advanced Organic Chemistry*, 4th Edition. Part B: Reactions and Synthesis, Kluwer Academic/Plenum Publishers: New York, **2001**
- <sup>51</sup> A. Biaggne, W. B. Knowlton, B. Yurke, J. Lee, L. Li, Substituent Effects on the Solubility and Electronic Properties of the Cyanine Dye Cy5: Density Functional and Time-Dependent Density Functional Theory Calculations, *Molecules*, **2021**, 26, 524 DOI: 10.3390/molecules26030524
- <sup>52</sup> M. L. Coote, 3.03 - Radical Reactivity by Computation and Experiment, *Polymer Science: A Comprehensive Reference*, **2012**, 3, 39–58 DOI: 10.1016/B978-0-444-53349-4.00062-5
- <sup>53</sup> S. Nsumiwa, D. Kuter, S. Wittlin, K. Chibale, T. J. Egan, Structure–activity relationships for ferriprotoporphyrin IX association and  $\beta$ -hematin inhibition by 4-aminoquinolines using experimental and ab initio methods, *Bioorg. Med. Chem.*, **2013**, 21, 3738–3748 DOI: 10.1016/j.bmc.2013.04.040
- <sup>54</sup> A. C. Kruger, D. L. Madigan, D. W. Beno, D. A. Batebenner, R. Carrick, B. E. Green, W. He, C. J. Maring, K. F. McDaniel, H. Mo, A. Molla, C. E. Motter, T. J. Pilot-Matias, M. D. Tufano, D. J. Kempf, Novel hepatitis C virus replicon inhibitors: synthesis and structure-activity relationships of

- fused pyrimidine derivatives, *Bioorg Med Chem Lett.*, **2012**, 22, 2212-2215 DOI: 10.1016/j.bmcl.2012.01.096
- <sup>55</sup> K. Shimizu, T. Shimizu, K. Kawakami, M. Nakoji, T. Sakai, Compound having tgf-beta inhibitory activity and pharmaceutical composition containing SAME, **2006**, EP1724268
- <sup>56</sup> S. R. Vippagunta, A. Dorn, H. Matile, A. K. Bhattachrjee, J. M. Karle, W. Y. Ellis, R. G. Ridley, J. L. Vennerstorm, Structural Specificity of Chloroquine–Hematin Binding Related to Inhibition of Hematin Polymerization and Parasite Growth, *J. Med. Chem.*, **1999**, 42, 4630–4639 DOI: 10.1021/jm9902180
- <sup>57</sup> S. Li, L. Hu, J. Li, J. Zhu, F. Zang, Q. Huang, L. Qiu, R. Du, R. Cao, Design, synthesis, structure-activity relationships and mechanism of action of new quinoline derivatives as potential antitumor agents, *Eur. J. Med. Chem.*, **2019**, 162, 666-678 DOI: 10.1016/j.ejmech.2018.11.048
- <sup>58</sup> Y. Hong, R.S. Kania, Novel quinoline derivatives, **2005**, WO2005063739
- <sup>59</sup> A. L. Ruchelman, J. E. Kerrigan, T. -K. Li, N. Zhao, A. Liu, L. F. Liu, E. J. LaVoie, Nitro and amino substitution within the A-ring of 5H-8,9-dimethoxy-5-(2-N,N-dimethylaminoethyl)-dibenzo[c,h][1,6]naphthyridin-6-ones: influence on topoisomerase I-targeting activity and cytotoxicity, *Bioorg. Med. Chem.*, **2004**, 12, 3731-3742 DOI: 10.1016/j.bmc.2004.03.076
- <sup>60</sup> C. Theeraladanon, M. Arisawa, A. Nishida, M. Nakagawa, A novel synthesis of substituted quinolines using ring-closing metathesis (RCM): its application to the synthesis of key intermediates for anti-malarial agents, *Tetrahedron*, **2004**, 60, 3017-3035 DOI: 10.1016/j.tet.2004.01.084
- <sup>61</sup> R. Boeckman, B. Boyce, L. Xiao, Z. Yao, F. H. Ebetino, Phosphonate-chloroquine conjugates and methods using SAME, **2017**, WO2017/79260
- <sup>62</sup> W. Devine, J. L. Woodring, U. Swaminathan, E. Amata, G. Patel, J. Erath, N. E. Roncal, P. J. Lee, S. E. Leed, A. Rodriguez, K. Mensa-Wilmot, R. J. Sciotti, M. P. Pollastrii, Protozoan Parasite Growth Inhibitors Discovered by Cross-Screening Yield Potent Scaffolds for Lead Discovery, *J. Med. Chem.*, **2015**, 58, 5522–5537 DOI: 10.1021/acs.jmedchem.5b00515
- <sup>63</sup> Y. Zhao, M. Antonietti, Visible-Light-Driven Conversion of Alcohols into Iodide Derivatives with Iodoform. *ChemPhotoChem*, **2018**, 2, 720–724 DOI: 10.1002/cptc.201800084
- <sup>64</sup> Z. Wang, R. Cao, X. Zhang, Z. Rong, X. Chen, X. Zhang, H. Huang, Z. Li, M. Xu, Z. Wang, J. Li, Z. Ren, Chloroxoquinoline derivative with anti-tumor activity, **2017**, CN105017145
- <sup>65</sup> G. -J. ten Brink, J. W. C. E. Arends, M. Hoogenraad, G. Verspui, R. A. Sheldon, Catalytic Conversions in Water. Part 23: Steric Effects and Increased Substrate Scope in the Palladium-Neocuproine Catalyzed Aerobic Oxidation of Alcohols in Aqueous Solvents, *Adv. Synth. Catal.*, **2003**, 345, 1341–1352 DOI: 10.1002/adsc.200303134
- <sup>66</sup> Y. Zhoua, W. Yana, D. Cao, M. Shao, D. Li, F. Wang, Z. Yang, Y. Chen, L. He, T. Wang, M. Shen, L. Chen, Design, synthesis and biological evaluation of 4-anilinoquinoline derivatives as novel potent tubulin depolymerization agents, *Eur. J. Med. Chem.*, **2017**, 138, 1114-1125 DOI: 10.1016/j.ejmech.2017.07.040
- <sup>67</sup> D. De, L. D. Byers, D. J. Krogstad, Antimalarials: Synthesis of 4-aminoquinolines that circumvent drug resistance in malaria parasites, *J. Heterocycl. Chem.*, **1997**, 34, 315-320 DOI: 10.1002/jhet.5570340149
- <sup>68</sup> Li Shuo; You Donghui; Tao Chuanyi; Li Na; Wang Mingqi, Triphenylamine-quinoline derivative and optical fiber sensor modified with triphenylamine-quinoline derivative and used for detecting oncogene-related G-quadruplexes, **2019**, CN109867625
- <sup>69</sup> I. P. J. Höglund, S. Silver, M. T. Engström, H. Salo, A. Tauber, H. -K. Kyyrönen, P. Saarenketo, A. -M. Hoffrén, K. Kokko, K. Pohjanoksa, J. Sallinen, J. -M. Savola, S. Wurster, O. A. Kallatsa, Structure–Activity Relationship of Quinoline Derivatives as Potent and Selective  $\alpha$ 2C-Adrenoceptor Antagonists, *J. Med. Chem.* **2006**, 49, 21, 6351–6363 DOI: 10.1021/jm060262x
- <sup>70</sup> C. Perez, J. Li, F. Parlati, M. Rouffet, Y. Ma, H.-J. Zhou, A. L. Mackinnon, T.-F. Chou, R.J. Deshaies, S. M. Cohen, Discovery of an Inhibitor of the Proteasome Subunit Rpn11, *J. Med. Chem.*, **2017**, 60, 3217–3217 DOI: 10.1021/acs.jmedchem.7b00390

- 
- <sup>71</sup> B. Koning, J.H. de Boer, A. Meetsma, R.M. Kellogg, Synthesis and complexation characteristics of phenanthroline and bipyridine diols, *Arkivoc*, **2004**, 2, 189-205 DOI: 10.3998/ark.5550190.0005.213
- <sup>72</sup> M. M. Nolasco, P. D. Vaz and L. D. Carlos, The role of 4,7-disubstituted phenanthroline ligands in energy transfer of europium(III) complexes: a DFT study, *New J. Chem.*, **2011**, 35, 2435–2441 DOI: 10.1039/c1nj20441f
- <sup>73</sup> C. Janiak, A critical account on  $\pi$ – $\pi$  stacking in metal complexes with aromatic nitrogen-containing ligands, *J. Chem. Soc. Dalton Trans.*, **2000**, 3885–3896 DOI: 10.1039/B003010O
- <sup>74</sup> C. Bhaskar, S. Chandrasekar, T. Mohandas, R.J. Butcher, Dibromidobis(3-bromobenzyl- $\kappa$ C)(4,7-diphenyl-1,10-phenanthroline- $\kappa^2$ N,N')tin(IV), *IUCrData*, **2019**, 4, x190336 DOI: 10.1107/S2414314619003365
- <sup>75</sup> K. -L. Zhong, G. -Q. Cao, W. Song, C. Ni, Tris(1,10-phenanthroline- $\kappa^2$ N,N')cobalt(II) bis(2,4,5-tricarboxybenzoate) monohydrate, *IUCrData*, **2019**, 4, x190059 DOI: 10.1107/S2414314619000592
- <sup>76</sup> R. Starosta, M. Puchalska, J. Cybińska, M. Barys, A. V. Mudring, Structures, electronic properties and solid state luminescence of Cu(I) iodide complexes with 2,9-dimethyl-1,10-phenanthroline and aliphatic aminomethylphosphines or triphenylphosphine, *Dalton Trans.*, **2011**, 40, 2459–2468 DOI: 10.1039/C0DT01284J
- <sup>77</sup> L. Viganor, O. Howe, P. McCarron, M. McCann, M. Devereux, The Antibacterial Activity of Metal Complexes Containing 1,10-phenanthroline: Potential as Alternative Therapeutics in the Era of Antibiotic Resistance, *Curr Top Med Chem*, **2017**, 17, 1280–1302 DOI: 10.2174/1568026616666161003143333
- <sup>78</sup> T. Okujima, A. Mifuji, J. Nakamura, H. Yamada, H. Uno, N. Ono, First Synthesis of Porphyrin-Fused 1,10-Phenanthroline–Ruthenium(II) Complexes, *Org. Lett.*, **2009**, 11, 18, 4088–4091 DOI: 10.1021/ol901510e
- <sup>79</sup> S. Chandraleka, K. Ramya, G. Chandramohan, D. Dhanasekaran, A. Priyadarshini, A. Panneerselvam, Antimicrobial mechanism of copper (II) 1,10-phenanthroline and 2,2'-bipyridyl complex on bacterial and fungal pathogens, *J. Saudi Chem. Soc.*, **2014**, 18, 953–962 DOI: 10.1016/j.jscs.2011.11.020
- <sup>80</sup> O. A. Dar, S.A. Lone, M. A. Malik, M. Y. Wani, A. Ahmad, A. A. Hashmi, New transition metal complexes with a pendent indole ring: insights into the antifungal activity and mode of action, *RSC Adv.*, **2019**, 9, 15151–15157 DOI: 10.1039/C9RA02600B
- <sup>81</sup> S. Ž. Durić, M. Mojicevic, S. Vojnovic, H. Wadepohl, T. P. Andrejević, N. Lj. Stevanović, J. Nikodinovic-Runic, M. I. Djuran, B. D. Glisica, Silver(I) complexes with 1,10-phenanthroline-based ligands: The influence of epoxide function on the complex structure and biological activity, *Inorganica Chim. Acta*, **2020**, 502, 1193572 DOI: 10.1016/j.ica.2019.119357
- <sup>82</sup> L. D. Ramos, L. H. de Macedo, N. R. S. Gobo, K. T. de Oliveira, G. Cerchiaro, K. P. M. Frin, Understanding the photophysical properties of rhenium(I) compounds coordinated to 4,7-diamine-1,10-phenanthroline: synthetic, luminescence and biological studies, *Dalton Trans.*, **2020**, 49, 16154–16165 DOI: 10.1039/D0DT00436G
- <sup>83</sup> A. Świetlicka, T. Klemens, B. Machura, E. Schab-Balcerzak, K. Laba, M. Lapkowski, M. Grucela, J. Nycz, M. Szala, M. Kania, Rhenium(I) complexes with phenanthrolines bearing electron-withdrawing Cl and electron-donating CH<sub>3</sub> substituents – synthesis, photophysical, thermal, and electrochemical properties with electroluminescence ability, *RSC Adv.*, **2016**, 6, 112908, DOI: 10.1039/c6ra23935h
- <sup>84</sup> H.-G. Zhanga, X.-T. TAO, K.-S. Chenb, C.-X. Yuana, M.-H. Jianga, Synthesis and photophysical properties of a new two-photon absorbing chromophore containing imidazo[4,5-f][1,10]phenanthroline, *Synthetic Metals*, **2011**, 161, 354–359, DOI: 10.1016/j.synthmet.2010.12.003
- <sup>85</sup> B. Feist, M. Pilch, J. E. Nycz, Graphene oxide chemically modified with 5-amino-1,10-phenanthroline as sorbent for separation and preconcentration of trace amount of lead(II), *Microchim Acta*, **2019**, 186, 91 DOI: 10.1007/s00604-018-3213-8

- 
- <sup>86</sup> F. Li, Z. Yang, H. Weng, G. Chen, M. Lin, C. Zhao, High efficient separation of U(VI) and Th(IV) from rare earth elements in strong acidic solution by selective sorption on phenanthroline diamide functionalized graphene oxide, *Chem. Eng. J.*, **2018**, 332, 340-350 DOI: 10.1016/j.cej.2017.09.038
- <sup>87</sup> A. T. Smith, A. M. LaChance, S. Zeng, B. Liu, L. Sun, Synthesis, properties, and applications of graphene oxide/reduced graphene oxide and their nanocomposites, *NMS*, **2019**, 1, 31-47 DOI: 10.1016/j.nanoms.2019.02.004
- <sup>88</sup> R. Sitko, E. Turek, B. Zawisza, E. Malicka, E. Talik, b J. Heimann, A. Gagor, B. Feista and R. Wrzalik, Adsorption of divalent metal ions from aqueous solutions using graphene oxide, *Dalton Trans.*, **2013**, 42, 5682-5689 DOI: 10.1039/C3DT33097D
- <sup>89</sup> N. S. Panina, V. N. Demidov, and S. A. Simanova, A DFT Study of 2,2'-Bi-1,10-phenanthroline and Its Reduced Form as a Potential Ligand for New Tetraaza Chromophore Complexes, *Russ. J.*, **2008**, 78, 913-918 DOI: 10.1134/S1070363208050137
- <sup>90</sup> S. S. Tan, S. Yanagisawa, K. Inagaki, M. B. Kassimabe. Y. Morikawa, Experimental and computational studies on ruthenium(II) bis-diimine complexes of *N,N'*-chelate ligands: the origin of changes in absorption spectra upon oxidation and reduction, *Phys. Chem. Chem. Phys.*, **2019**, 21, 7973-7988 DOI: 10.1039/c8cp05016c
- <sup>91</sup> M. Reiher, G. Brehm, S. Schneider, Assignment of Vibrational Spectra of 1,10-Phenanthroline by Comparison with Frequencies and Raman Intensities from Density Functional Calculations, *J. Phys. Chem. A*, **2004**, 108, 734-742 DOI: 10.1021/jp0366116
- <sup>92</sup> H. H. Perkampus, P. Muller, J. Knop, Dipole-Moments of Phenanthrolines, *Z. Naturforsch.*, **1970**, 26b, 83-86 DOI: 10.1515/znb-1971-0205
- <sup>93</sup> H. C. Longuet-Higgins, C. A. Coulson, 208. The electronic structure of some aza-derivatives of naphthalene, anthracene, and phenanthrene, *J. Chem. Soc.*, **1949**, 971-980 DOI: 10.1039/JR9490000971
- <sup>94</sup> Y. Shen, B. P. Sullivan, A Versatile Preparative Route to 5-Substituted-1,10-Phenanthroline Ligands via 1,10-Phenanthroline 5,6-Epoxyde, *Inorg. Chem.*, **1995**, 34, 6235-6236 DOI: 10.1021/ic00129a003
- <sup>95</sup> K. Binnemans, P. Lenaerts, K. Driesen, C. Görrler-Walrand, A luminescent tris(2-thenoyltrifluoroacetato)europium(III) complex covalently linked to a 1,10-phenanthrolinefunctionalised sol-gel glass, *J. Mater. Chem.*, **2004**, 14, 191 - 195 DOI: 10.1039/B311128H
- <sup>96</sup> P. G. Sammes, G. Yahiglu, 1,10-phenanthroline: A Versatile Ligand, *Chem. Soc. Rev.*, **1994**, 23, 327-334 DOI: 10.1039/CS9942300327
- <sup>97</sup> M. Yamada, Y. Tanaka, Y. Yoshimoto, S. Kuroda, I. Shima, Synthesis and properties of diamino-substituted dipyrido[3,2-a: 2',3'-c]phenazine, *Bull. Chem. Soc. Jpn.*, **1992**, 65, 1006-1011 DOI: 10.1246/bcsj.65.1006
- <sup>98</sup> R. D. Gillard, R. E. E. Hill, R. Maskill, Optically active coordination compounds. Part XX. Reactions of 1,10-phenanthroline coordinated to cobalt(III), *J. Chem. Soc. A*, **1970**, 0, 1447-1451 DOI: 10.1039/J19700001447
- <sup>99</sup> S. A. Miltsov, V. S. Karavan, V. A. Borin, Efficient Synthesis of 1,10-Phenanthroline-5,6-dione, *Russ. J.*, **2019**, 89, 1055-1057 DOI: 10.1134/S1070363219050281
- <sup>100</sup> R. Stranne, J. -L. Vasse, C. Moberg, Synthesis and Application of Chiral P,N-Ligands with *Pseudo-Meso* and *Pseudo-C<sub>2</sub>* Symmetry, *Org. Lett.*, **2001**, 3, 2525-2528 DOI: 10.1021/ol016193s
- <sup>101</sup> Y. -X. Peng, B. Hu, W. Huang, Oxidation for unsymmetrical bromo-1,10-phenanthrolines and subsequent hydroxylation, decarbonylation and chlorination reactions, *Tetrahedron*, **2018**, 74, 4495-4503 DOI: 10.1016/j.tet.2018.07.015
- <sup>102</sup> W. Z. Antkowiak, R. Antkowiak, On the Chlorine Addition to the C(5)-C(6) Bridge and the N-Oxidation of 1,10-Phenanthroline, *Heterocycles*, **1998**, 47, 893-909 DOI: 10.3987/COM-97-S(N)99
- <sup>103</sup> A. De Cian, E. DeLemos, J.-L. Mergny, M.-P. Teulade-Fichou, D. Monchaud, Highly efficient G-quadruplex recognition by bisquinolinium compounds, *J. Am. Chem. Soc.*, **2007**, 129, 1856-1857 DOI: 10.1021/ja067352b

- 
- <sup>104</sup> A. F. Larsen, T. Ulven, Efficient Synthesis of 4,7-Diamino Substituted 1,10-Phenanthroline-2,9-dicarboxamides, *Org. Lett.*, **2011**, 13, 3546–3548 DOI: 10.1021/ol201321z
- <sup>105</sup> M. Zhou, L. Yu, Electronically Neutral Metal Complexes as Biological Labels, **2016**, US2016146826,
- <sup>106</sup> A. C. Mkhohlakali, P. A. Ajibade; Synthesis, Photo Physical Studies and Evaluation of Ruthenium(II) Complexes of Polypyridyl Ligands as Sensitizer for DSSCs, *Int. J. Electrochem. Sci.*, **2015**, 10, 9907 – 9918
- <sup>107</sup> M. Yanagida, L. Singh, K. Sayama, K. Hara, R. Katoh, A. Islam, H. Sugihara, H. Arakawa, M. K. Nazeeruddin, M. Gratzel, *J. Chem. Soc., Dalton Trans.*, **2000**, 2817-2822 DOI: 10.1039/B002391O
- <sup>108</sup> L. R. Emerson, M. E. Nau, R. K. Martin, D. E. Kyle, M. Vahey, D. F. Wirth, Relationship between Chloroquine Toxicity and Iron Acquisition in *Saccharomyces cerevisiae* Antimicrobial Agents and Chemotherapy, **2002**, 46, 787-796 DOI: 10.1128/AAC.46.3.787-796.2002
- <sup>109</sup> R. Martins, J. Maier, A. -D. Gorki, K. V. M. Huber, O. Sharif, P. Starkl, S. Saluzzo, F. Quattrone, R. Gawish, K. Lakovits, M. C. Aichinger, B. Radic-Sarikas, C. -H. Lardeau, A. Hladik, A. Korosec, M. Brown, K. Vaahtomeri, M. Duggan, D. Kerjaschki, H. Esterbauer, J. Colinge, S. C. Eisenbarth, T. Decker, K. L. Bennet, S. Kubicek, M. Sixt, G. Superti-Furga, S. Knapp, Heme Drives Hemolysis-Induced Susceptibility to Infection via Disruption of Phagocyte Functions, *Nat. Immunol.*, **2016**, 17, 1361–1372 DOI: 10.1038/ni.3590
- <sup>110</sup> C. J. Chandler, L. W. Deady, J. A. Reiss, Synthesis of some 2,9-disubstituted-1,10-phenanthrolines, *J. Heterocyclic Chem.*, **1981**, 18, 599 – 601 DOI: 10.1002/jhet.5570180332
- <sup>111</sup> W. Lu, Z. Wei, Z. -Y. Gu, T. -F. Liu, J. Park, J. Park, J. Tian, M. Zhang, Q. Zhang, T. Gentle, M. Boscha, H. -C. Zhou, Tuning the structure and function of metal–organic frameworks via linker design, *Chem. Soc. Rev.*, **2014**, 43, 5561-5593 DOI: 10.1039/C4CS00003J
- <sup>112</sup> S. Zhang, W. Shi, P. Cheng, The coordination chemistry of *N*-heterocyclic carboxylic acid: A comparison of the coordination polymers constructed by 4,5-imidazoledicarboxylic acid and 1*H*-1,2,3-triazole-4,5-dicarboxylic acid/Coordination Chemistry Reviews, **2017**, 352, 108–150 DOI: 10.1016/j.ccr.2017.08.022
- <sup>113</sup> J. Meisenheimer, Ueber Reactionen aromatischer Nitrokörper, *Liebigs Ann. Chem.*, **1902**, 323, 205-246 DOI: 10.1002/jlac.19023230205
- <sup>114</sup> D. Andrade-Acuna, J. G. Santos, W. Tiznado, A. Canete, M. E. Aliaga, Kinetic study on the aromatic nucleophilic substitution reaction of 3,6-dichloro-1,2,4,5-tetrazine by biothiols, *J. Phys. Org. Chem.*, **2014**, 27 670–675 DOI: 10.1002/poc.3316
- <sup>115</sup> R. O. Al-Kaysi, I. Gallardo, G. Guirado, Stable Spirocyclic Meisenheimer Complexes, *Molecules*, **2008**, 13, 1282-1302 DOI: 10.3390/molecules13061282
- <sup>116</sup> G.V. Salmoria, E. Dall'Oglio, C. Zucco, Aromatic nucleophilic substitutions under microwave irradiation, *Tetrahedron Lett.*, **1998**, 39, 2471-2474 DOI: 10.1016/S0040-4039(98)00308-6
- <sup>117</sup> Y. Zhao, R. Duan, J. Zhao, C. Li, Spin-Orbit Charge Transfer Intersystem Crossing in the Perylenemonoimide-Phenothiazine Compact Electron Donor-Acceptor Dyads, *Chem. Commun.*, **2018**, 54, 12329-12332 DOI: 10.1039/C8CC07012A
- <sup>118</sup> K. Błaziak, W. Dankiewicz, M. Mąkosza, How Do Aromatic Nitro Compounds React with Nucleophiles? Theoretical Description Using Aromaticity, Nucleophilicity and Electrophilicity Indices, *Molecules*, **2020**, 25, 4819 DOI: 10.3390/molecules25204819
- <sup>119</sup> M. Mąkosza, Nucleophilic Substitution of Hydrogen in Nitroarenes: A New Chapter of Aromatic Chemistry. *Synthesis*, **2011**, 15, 2341–2356 DOI:10.1055/s-0030-1260668
- <sup>120</sup> M. Mąkosza, J. Winiarski, Vicarious nucleophilic substitution of hydrogen, *Acc. Chem. Res.*, **1987**, 20, 282-289 DOI: 10.1021/ar00140a003
- <sup>121</sup> N. J. Lawrence, O. Lamarche, N. Thurrab, The facile synthesis of -aryl- -hydroxy esters via one-pot vicarious nucleophilic substitution and oxidation, *Chem. Commun.*, **1999**, 689–690 DOI: 10.1039/A900986H

- 
- <sup>122</sup> M. Makosza, K. Stalinski, Oxidative Nucleophilic Substitution of Hydrogen in Nitroarenes with Phenylacetonitrile Derivatives, *Tetrahedron*, **1998**, 54, 8797–8810 DOI: 10.1016/S0040-4020(98)00472-4
- <sup>123</sup> J. Engel-Andreasen, B. Shimpukade, T. Ulve, Selective copper catalyzed aromatic N-arylation in water, *Green Chem.*, **2013**, 15, 336-340 DOI: 10.1039/C2GC36589H
- <sup>124</sup> T. E. Kokina, Yu. P. Ustimenko, M. I. Rakhmanova, L. A. Sheludyakova, A. M. Agafontsev, P. E. Plyusnin, A. V. Tkachev, S. V. Larionov, Luminescent Complexes of Zn(II) and Cd(II) with Chiral Ligands Containing 1,10-Phenanthroline and Natural Monoterpenoids (+)-3-Carene or (+)-Limonene Fragments, *Russ.*, **2019**, 89, 87–95 DOI: 10.1134/S107036321901016X
- <sup>125</sup> L. -Y. Zheng, Y. -H. Chi, Y. Liang, E. Cottrill, N. Pan, J. -M. Shi, Green and mild oxidation: from acetate anion to oxalate anion. *J. Coord. Chem.*, **2018**, 71, 3947–3954 DOI:10.1080/00958972.2018.1543870
- <sup>126</sup> R. Mondal, A. K. Mallik, Recent Applications of Potassium Carbonate in Organic Synthesis, *Org. Prep. Proced. Int.*, **2014**, 46, 391–434 DOI:10.1080/00304948.2014.944402
- <sup>127</sup> M. Sandroni, Synthesis and Characterization of Heteroleptic Copper(I) Complexes for Solar Energy Conversion (Ph.D. thesis) Université de Nantes, **2012**
- <sup>128</sup> R. Rabie, M. M. Hammouda, K. M. Elattar, Cesium carbonate as a mediated inorganic base in some organic transformations, *Res. Chem. Intermed.*, **2017**, 43,1979–2015 DOI: 10.1007/s11164-016-2744-z
- <sup>129</sup> G. -G. Shan, H. -B. Li, H. -T. Cao, D. -X. Zhu, Z. -M. Su, Y. Liao, Synthesis, structure and photophysical properties of cationic Ir(III) complexes, *J. Organomet. Chem.*, **2012**, 713, 20-26 DOI: 10.1016/j.jorganchem.2012.04.018
- <sup>130</sup> C. Ulbricht, B. Beyer, C. Friebe, A. Winter, U. S. Schubert, Recent Developments in the Application of Phosphorescent Iridium(III) Complex Systems, *Adv.*, **2009**, 21, 4418-4441 DOI: 10.1002/adma.200803537
- <sup>131</sup> Z. -J. Yu, H. Chen, A. J. J. Lennox, L. -J. Yan, X. -F. Liu, D. -D. Xu, F. Chen, L. -X. Xu, Y. Li, Q. -A. Wu, S. -P. Luo, Heteroleptic copper(I) photosensitizers with carbazole-substituted phenanthroline ligands: Synthesis, photophysical properties and application to photocatalytic H<sub>2</sub> generation, *Dyes Pigm.*, **2019**, 162, 771–775 DOI: 10.1016/j.dyepig.2018.10.067
- <sup>132</sup> C. Yang, K. Wu, S. Gong, L. Zhan, Thermal activation delayed fluorescence material containing 1,10-phenanthroline unit and application of material, **2016**, CN105859714
- <sup>133</sup> M. A. El-Atawy, F. Ferretti, F. Ragaini, Palladium-Catalyzed Intramolecular Cyclization of Nitroalkenes: Synthesis of Thienopyrroles, *Eur. J. Org. Chem.*, **2017**, 1902–1910 DOI: 10.1002/ejoc.201700165
- <sup>134</sup> F. Ferretti, E. Gallo, F. Ragaini, Nitrogen ligands effects in the palladium-catalyzed carbonylation reaction of nitrobenzene to give N-methyl phenylcarbamate, *J. Organomet. Chem.*, **2014**, 771, 59–67 DOI: 10.1016/j.ica.2017.05.014
- <sup>135</sup> F. Ferretti, F. Ragaini, R. Lariccia, E. Gallo, S. Cenini, Palladium-Catalyzed Intramolecular Cyclization of Nitroalkenes: Synthesis of Thienopyrroles, *Organometallics*, **2010**, 29, 1465–1471 DOI: 10.1002/ejoc.201700165
- <sup>136</sup> S. Mukherjee, M. Pal, Quinolines: a new hope against inflammation, *Drug Discov. Today*, **2013**, 18, 389-398 DOI: 10.1016/j.drudis.2012.11.003
- <sup>137</sup> P. Zajdel, A. Partyka, K. Marciniec, A. J. Bojarski, M. Pawłowski, A. Wesółowska, Quinoline- and isoquinoline-sulfonamide analogs of aripiprazole: novel antipsychotic agents?, *Future Med. Chem.*, **2014**, 6, 57-75 DOI: 10.4155/fmc.13.158
- <sup>138</sup> M. O. Puskullu, B. Tekiner, S. Suzan, Recent Studies of Antioxidant Quinoline Derivatives, *Mini-Rev. Med. Chem.*, **2013**, 13, 365 DOI : 10.2174/1389557511313030005
- <sup>139</sup> R. Musioł, M. Serda, S. Hansel-Bielówka, J. Polański, Quinoline-Based Antifungals, *Curr. Med. Chem.*, **2010**, 17, 1960 DOI: 10.2174/092986710791163966

- 
- <sup>140</sup> N. Ahmed, K. G. Brahmabhatt, S. Sabde, D. Mitra, I. P. Singh, K. K. Bhutani, Synthesis and anti-HIV activity of alkylated quinoline 2,4-diols, *Bioorg. Med. Chem.*, **2010**, 18, 2872-2897 DOI: 10.1016/j.bmc.2010.03.015
- <sup>141</sup> J. Jampilek, M. Dolezal, J. Kunes, V. Buchta, Quinaldine Derivatives Preparation and Their Antifungal Activity, The 8th International Electronic Conference on Synthetic Organic Chemistry, **2004** DOI: 10.3390/ecsoc-8-01976
- <sup>142</sup> A. A. Al-abbasi, Theoretical study of the inhibition and the adsorption properties of N-containing aromatic compounds as corrosion inhibitors of mild steel in hydrochloric acid, The 1st International Conference on Chemical, Petroleum, and Gas Engineering, **2016**
- <sup>143</sup> V. Prachayasittikul, S. Prachayasittikul, S. Ruchiwarat, V. Prachayasittikul, 8-Hydroxyquinolines: a review of their metal chelating properties and medicinal applications, *Drug Des Devel Ther.*, **2013**, 7, 1157-1178 DOI: 10.2147/DDDT.S49763
- <sup>144</sup> A. Albert, D. Magrath, The choice of a chelating agent for inactivating trace metals; derivatives of oxine (beta-hydroxyquinoline), *Biochem.*, **1947**, 41, 534-545 DOI: 10.1042/bj0410534
- <sup>145</sup> J. McElroy, The treatment of pulmonary tuberculosis by intravenous injections of chinosol with formaldehyde, *The Lancet*, **1910**, 176, 1408-1409 DOI: 10.1016/S0140-6736(01)08447-1
- <sup>146</sup> A. G. Dalecki, C. L. Crawford and F. Wolschendorf, Copper and Antibiotics: Discovery, Modes of Action, and Opportunities for Medicinal Applications, *Adv. Microb. Physiol.*, **2017**, 70, 193-260 DOI: 10.1016/bs.ampbs.2017.01.007
- <sup>147</sup> L. Gunatilaka, Chapter 1 Alkaloids From Sri Lankan Flora, *Alkaloids: Chem. Biol.*, **1998**, 52, 1-101 DOI: 10.1016/S0099-9598(08)60025-5
- <sup>148</sup> J. E. Nycz, G. J. Małecki, Synthesis, spectroscopy and computational studies of selected hydroxyquinoline carboxylic acids and their selected fluoro-, thio-, and dithioanalogues, *J. Mol. Struct.*, **2013**, 1032, 159-168 DOI: 10.1016/j.molstruc.2012.08.009
- <sup>149</sup> M. Szala, J. E. Nycz, G. Małecki, R. Sokolova, S. Ramesova, A. Switlicka-Olszewska, R. Strzelczyk, R. Podsiadly, B. Machura, Synthesis of 5-azo-8-hydroxy-2-methylquinoline dyes and relevant spectroscopic, electrochemical and computational studies. *Dyes Pigm.*, **2017**, 142, 277-292. DOI: 10.1016/j.dyepig.2017.03.043
- <sup>150</sup> M. Szala, Funkcjonalizacja wybranych pochodnych chinoliny w oparciu o reakcje typu aromatycznej substytucji elektrofilowej, PhD Thesis, **2017**
- <sup>151</sup> G. A. Ramann, B. J. Cowen, Recent Advances in Metal-Free Quinoline Synthesis, *Molecules*, **2016**, 21, 986 DOI: 10.3390/molecules21080986
- <sup>152</sup> C. Ludtke, A. Haupt, M. Wozniak, N. Kulak, Synthesis of fluorine-containing 1,10-phenanthrolines using mild versions of Skraup and Doebner-von Miller reactions, *J. Fluor. Chem.*, **2017**, 193, 98-105 DOI: 10.1016/j.jfluchem.2016.11.016
- <sup>153</sup> B. Bohanyi, J. Kaman, A concise synthesis of indoloquinoline skeletons applying two consecutive Pd-catalyzed reactions, *Tetrahedron*, **2013**, 69, 9512-9519 DOI: 10.1016/j.tet.2013.08.019
- <sup>154</sup> D. A. Klumpp, *Electrophilic Aromatic Substitution, Arene Chemistry*, Wiley, Hoboken, **2015**, 1-31 DOI: 10.1002/9781118754887.ch1
- <sup>155</sup> B. Galbov, D. Nalbantova, P. R. Schlayer, H. Schaefer, Electrophilic Aromatic Substitution: New Insights into an Old Class of Reactions, *Acc. Chem. Res.*, **2016**, 49, 6, 1191-1199 DOI: 10.1021/acs.accounts.6b00120
- <sup>156</sup> N. Grimblat, A. M. Sarotti, T. S. Kaufmana, S. O. Simonetti, A theoretical study of the Duff reaction: insights into its selectivity, *Org. Biomol. Chem.*, **2016**, 14, 10496-10501 DOI: 10.1039/C6OB01887D
- <sup>157</sup> J. Hine, J. M. Van der Veen, The Mechanism of the Reimer-Tiemann Reaction, *J. Am. Chem. Soc.* **1959**, 81, 24, 6446-6449 DOI: 10.1021/ja01533a028
- <sup>158</sup> P.M. Esteves, J. W. de M. Carneiro, S. P. Cardoso, A. G. H. Barbosa, K. K. Laali, G. Rasul, G. K. S. Prakash, G. A. Olah, Unified Mechanistic Concept of Electrophilic Aromatic Nitration:

---

Convergence of Computational Results and Experimental Data, *J. Am. Chem. Soc.*, **2003**, 125, 4836 DOI: 10.1021/ja021307w

<sup>159</sup> M. Shiri, M. A. Zolfigol, H. G. Kruger, Z. Tanbakochian, Advances in the application of N<sub>2</sub>O<sub>4</sub>/NO<sub>2</sub> in organic reactions, *Tetrahedron*, **2010**, 66, 9077-9106 DOI: 10.1016/j.tet.2010.09.057

<sup>160</sup> Z. -N. Lu, L. Wang, X. Zhang, Z. -J. Zhu, A selective fluorescent chemosensor for Cd<sup>2+</sup> based on 8-hydroxyquinoline-benzothiazole conjugate and imaging application, *Spectrochim. Acta A Mol. Biomol.*, **2019**, 213, 57-63 DOI: 10.1016/j.saa.2019.01.041

<sup>161</sup> K. V. Sashidhara, A. Kumar, G. Bhatia, M. M. Khan, A. K. Khanna, J. K. Saxena, Antidyslipidemic and antioxidative activities of 8-hydroxyquinoline derived novel keto-enamine Schiff's bases, *Eur. J. Med. Chem.*, **2009**, 44, 1813-1818 DOI: 10.1016/j.ejmech.2008.08.004

<sup>162</sup> L. W. Deady, S. M. Devine, M. L. Rogers, A convenient procedure for indirect oxidation of aromatic methyl groups to aldehydes and carboxylic acid, *Org Prep Proced Int.*, **2003**, 35, 627-630 DOI: 10.1080/00304940309355366

<sup>163</sup> S. Malancona, M. Donghi, M. Ferrara, J. I. M. Hernando, M. Pompei, S. Pesci, J. M. Ontatria, U. Koch, M. Rowley, V. Summa, Allosteric inhibitors of hepatitis C virus NS5B polymerase thumb domain siteII: Structure-based design and synthesis of new templates, *Bioorg. Med. Chem.*, **2010**, 18, 2836-2848 DOI: 10.1016/j.bmc.2010.03.024

<sup>164</sup> V. P. Boricha, S. Patra, Y. S. Choahan, P. Sanavada, E. Suresh, P. Paul, Synthesis, Characterisation, Electrochemistry and Ion-Binding Studies of Ruthenium(II) and Rhenium(I) Bipyridine/Crown Ether Receptor Molecules, *Eur. J. Inorg. Chem.*, **2009**, 9, 1256-1267 DOI: 10.1002/ejic.200801099

<sup>165</sup> N. Garelli, P. Vierling, Synthesis of new amphiphilic perfluoroalkylated bipyridines, *J. Org. Chem.* **1992**, 57, 3046-3051 DOI: 10.1021/jo00037a019

<sup>166</sup> O. Buriez, E. Labbe, Disclosing the redox metabolism of drugs: The essential role of electrochemistry, *Curr Opin Electrochem*, **2020**, 24, 63-68 DOI: 10.1016/j.coelec.2020.07.002

<sup>167</sup> J. Hwang, J. I. Son, Y. -B. Shim, Electrochromic and electrochemical properties of 3-pyridinyl and 1,10-phenanthroline bearing poly(2,5-di(2-thienyl)-1H-pyrrole) derivatives, *Sol. Energy Mater Sol. Cells.*, **2010**, 94, 1286-1292 DOI: 10.1016/j.solmat.2010.03.027

<sup>168</sup> B. Lim, S. -Y. Han, S. -H. Jung, Y. J. Jung, J. M. Park, W. Lee, H. -S. Shim, Y. -C. Nah, Synthesis and electrochromic properties of a carbazole and diketopyrrolopyrrole-based small molecule semiconductor, *J. Ind. Eng. Chem.*, **2019**, 80, 93-97 DOI: 10.1016/j.jiec.2019.07.035

<sup>169</sup> R. Sokolova, J. E. Nycz, S. Ramesova, J. Fiedler, I. Degano, M. Szala, V. Kolivoska, M. Gal, Electrochemistry and Spectroelectrochemistry of Bioactive Hydroxyquinolines: A Mechanistic Study, *J. Phys. Chem. B.*, **2015**, 119, 6074 DOI: 10.1021/acs.jpcc.5b00098

<sup>170</sup> B. A. Frontana-Urbe, R. D. Little, J. G. Ibanez, A. Palma, R. Vasquez-Medrano, Organoelectrosynthesis: A promising green methodology in organic chemistry, *Green Chem.* **2010**, 12, 2099-2119 DOI: 10.1039/c0gc00382d

<sup>171</sup> N. K. Shee, S. G. Patra, M. G. B. Drew, L. Lu, E. Zangrando, D. Datta, Electrochemical behaviour of tris(1,10-phenanthroline)ruthenium(II) at a surface modified electrode. Electrocatalytic reduction of dioxygen, *Inorganica Chim.*, **2017**, 466, 349-357 DOI: 10.1016/j.ica.2017.05.074

<sup>172</sup> S. Musumeci, E. Rizzarelli, I. Fragala, S. Sammartano, R.P. Bonomo, Low valence state of metal chelates. I. Complexes of iron (II) perchlorate with 1,10-phenanthroline, 3,7-dimethyl- 1,10-phenanthroline and 4,7-diphenyl-1,10-phenanthroline, *Inorganica Chim. Acta*, **1973**, 7, 660-664 DOI: 10.1016/S0020-1693(00)94905-3

<sup>173</sup> H. Yi, A. Jutand, A. Lei, Evidence for the interaction between Terc-BuOK and 1,10-phenanthroline to form the 1,10-phenanthroline radical anion: a key step for the activation of aryl bromides by electron transfer, *Chem. Commun.*, **2015**, 51, 545-548 DOI: 10.1039/c4cc07299e

<sup>174</sup> M. V. Mirifico, E. L. Svartman, J. A. Caram, E. J. Vasini, Partial electrooxidation of nitrogenated heterocycles: novelsynthesis of 1,10-phenanthroline-5,6-quinone by electrooxidationof 1,10-phenanthroline, *J. Electroanal. Chem.*, **2004**, 566, 7-13 DOI: 10.1016/j.jelechem.2003.11.007



- 
- <sup>175</sup> P. Gayathri, A. S. Kumar, Electrochemical behavior of the 1,10-phenanthroline ligand on a multiwalled carbon nanotube surface and its relevant electrochemistry for selective recognition of copper ion and hydrogen peroxide sensing, *Langmuir*, **2014**, 30, 10513–10521 DOI: 10.1021/la502651w
- <sup>176</sup> K. Alwair, J. Girmshaw, Electrochemical reactions. Part XV. Factors which determine the rate of carbon–halogen bond fragmentation in radical anions illustrated by some halogenated derivatives of quinoline, quinoxaline, and phenazine, *J. Chem. Soc., Perkin Trans. 2*, **1973**, 1811–1815 DOI: 10.1039/P29730001811
- <sup>177</sup> R. Sokolova, S. Giannarelli, N. Fanelli, L. Pospisil, Electrochemical bond cleavage in pesticide ioxynil. Kinetic analysis by voltammetry and impedance spectroscopy, *Bulg. Chem. Commun.*, **2017**, 49, 134–138
- <sup>178</sup> A. A. Isse, G. Berzi, L. Falciola, M. Rossi, P. R. Mussini, A. Gennaro, Electrocatalysis and electron transfer mechanisms in the reduction of organic halides at Ag, *J. Appl. Electrochem.*, **2009**, 39, 2217–2225 DOI: 10.1007/s10800-008-9768-z
- <sup>179</sup> A. A. Isse, L. Scarpa, C. Durante, A. Gennaro, Reductive cleavage of carbon–chlorine bonds at catalytic and non-catalytic electrodes in 1-butyl-3-methylimidazolium tetrafluoroborate, *Phys. Chem. Chem. Phys.*, **2015**, 17, 31228–31236 DOI: 10.1039/C5CP04142B
- <sup>180</sup> D. G. Peters, in *Organic Electrochemistry*, ed. O. Hammerich and B. Speiser, Taylor & Francis, London, 5th edn, **2015**, 5, 939–977
- <sup>181</sup> J. Casanova and V. P. Reddy, in *The Chemistry of Halides, Pseudohalides and Azides*, ed. S. Patai and Z. Rappoport, John Wiley & Sons, New York, **1995**, 18, 1003
- <sup>182</sup> B. Huang, A. A. Isse, C. Durante, C. Wei and A. Gennaro, Electrocatalytic properties of transition metals toward reductive dechlorination of polychloroethanes, *Electrochim. Acta*, **2012**, 70, 50–61 DOI: 10.1016/j.electacta.2012.03.009
- <sup>183</sup> O. Scialdone, C. Guarisco, A. Galia and R. Herbois, Electroreduction of aliphatic chlorides at silver cathodes in water, *J. Electroanal. Chem.*, **2010**, 641, 14–22 DOI: 10.1016/j.jelechem.2010.01.018
- <sup>184</sup> M. Zhang, Q. Shi, X. Song, H. Wang, Z. Bian, Recent electrochemical methods in electrochemical degradation of halogenated organics: a review, *Environ. Sci. Pollut. Res.*, **2019**, 26, 10457–10486 DOI: 10.1007/s11356-019-04533-3
- <sup>185</sup> K. Lam, S.J. Van Wyck, W.E. Geiger, One-electron oxidation of chloroquine, cymanquine, and related aminoquinolines in nonaqueous media, *J. Electroanal. Chem.*, **2017**, 799, 531–537 DOI: 10.1016/j.jelechem.2017.06.041
- <sup>186</sup> R. Liu, Y. Li, Q. Xiao, J. Chang, H. Zhu, Synthesis and luminescent properties of carbazole end-capped phenylene ethynylene compounds, *J. Lumin.*, **2012**, 132, 191–197 DOI: 10.1016/j.jlumin.2011.08.032
- <sup>187</sup> J. Lu, S. Zhu, H. Su, Y. Li, H. Zhu, Synthesis, luminescence and excited state absorption properties of conjugated D- $\pi$ -A and D- $\pi$ -D phenothiazine compounds, *J. Lumin.*, **2019**, 205, 158–166 DOI: 10.1016/j.jlumin.2018.09.001
- <sup>188</sup> J. Ji, F. Sajjad, Q. You, D. Xing, H. Fan, A. G. K. Reddy, W. Hu, S. Dong, These groups are successfully used as substituents in many types of compounds that are later tested for luminescent and biological properties, *Arch. Pharm.*, **2021**, 354, 2000449 DOI: 10.1002/ardp.202000449
- <sup>189</sup> W. Liu, Y. Ma, Y. Yin, Y. Zhao, Anodic Cyanation of 1-Arylpyrrolidines, *Bull. Chem. Soc. Jpn.*, **2006**, 79, 577–579 DOI: 10.1246/bcsj.79.577
- <sup>190</sup> J. F. Ambrose, R. F. Nelson, Anodic Oxidation Pathways of Carbazoles, *J. Electrochem. Soc.* **1968**, 115, 1159–1164 DOI: 10.1149/1.2410929
- <sup>191</sup> W. Lamm, F. Pragst, W. Jugelt, Untersuchungen zum anodischen Verhalten von Carbazolen und Indolo[3,2-b] carbazolen in Acetonitril. *Journal f. prakt. Chemie.* **1975**, 317, 995–1004 DOI: 10.1002/prac.19753170616
- <sup>192</sup> K. Karon, M. Lapkowski, Carbazole electrochemistry: a short review, *J. Solid State Electrochem.*, **2015**, 19, 2601–2610 DOI 10.1007/s10008-015-2973-x

- 
- <sup>193</sup> A. N. Pankratov, I. M. Uchaeva, A. N. Stepanov, Chemical and electrochemical oxidation of phenothiazine, *Can. J. Chem.*, **1993**, 71, 674-677 DOI: 10.1139/v93-091
- <sup>194</sup> K. Mielech-Łukasiewicz, H. Puzanowska-Tarasiewicz, A. Panuszko, Electrochemical Oxidation of Phenothiazine Derivatives at Glassy Carbon Electrodes and Their Differential Pulse and Square-wave Voltammetric Determination in Pharmaceuticals, *Anal. Lett.*, **2008**, 41, 789-805 DOI: 10.1080/00032710801935038
- <sup>195</sup> B. Blankert, H. Hayen, S. M. van Leeuwen, U. Karst, E. Bodoki, S. Lotrean, R. Sandulescu, N. Mora Diez, O. Dominguez, J. Arcos, J. -M. Kaufmann, Electrochemical, Chemical and Enzymatic Oxidations of Phenothiazines, *Electroanalysis*, **2005**, 17, 1501-1510 DOI: 10.1002/elan.200403253
- <sup>196</sup> N. Urasaki, S. Yoshida, T. Ogawa, K. Kozawa, T. Uchida, Oxidation Potentials and Absorption Spectra of Phenothiazine Derivatives I. Benzophenothiazines and Triphenodithiazine, *Bull. Chem. Soc. Jpn.*, **1994**, 67, 2024-2030 DOI: 10.1246/bcsj.67.2024
- <sup>197</sup> J. E. Nycz, **J. Wantulok**, R. Sokolova, L. Pajchel, M. Stankevic, M. Szala, J. G. Małecki, D. Swoboda, Synthesis and electrochemical and spectroscopic characterization of 4,7-diamino-1,10-phenanthrolines and their precursors, *Molecules*, **2019**, 24, 4102 DOI: 10.3390/molecules24224102
- <sup>198</sup> **J. Wantulok**, R. Sokolova, J. Nycz, I. Degano, Oxidation and Reduction of Selected 1,10-Phenanthrolines; PROCEEDINGS OF INTERNATIONAL CONFERENCE MODERN ELECTROCHEMICAL METHODS XXXIX., International Conference on Electrochemical Methods XXXIX. Jetricovice, Czech Republic, May 20-24, **2019**, 240-243; ISBN 978-80-905221-3-8
- <sup>199</sup> **J. Wantulok**, I. Degano, M. Gal, J. E. Nycz, R. Sokolova, IR spectroelectrochemistry as efficient technique for elucidation of reduction mechanism of chlorine substituted 1,10-phenanthrolines, *J. Electroanal. Chem.* **2020**, 859, 113888 DOI: 10.1016/j.jelechem.2020.113888
- <sup>200</sup> P. M. S. Monk, R. J. Mortimer, D. R. Rosseinsky, *Electrochromism and Electrochromic Devices*, Cambridge University Press, Cambridge, **2007**
- <sup>201</sup> P.S. Yang, M.T. Tsai, M.H. Tsai, C.W. Ong, The regioselective homocoupling of methoxyhydroxypyridines with hypervalent iodine(III), *Chem. Asian J.*, **2015**, 10, 849-852 DOI: 10.1002/asia.201403359
- <sup>202</sup> S. Musumeci, E. Rizzarelli, I. Fragala, S. Sammartano, R. P. Bonomo, Low valence state of metal chelates. I. Complexes of iron (II) perchlorate with 1,10-phenanthroline, 3,7-dimethyl-1,10-phenanthroline and 4,7-diphenyl-1,10-phenanthroline, *Inorganica Chim. Acta*, **1973**, 7, 660-664 DOI: 10.1016/S0020-1693(00)94905-3
- <sup>203</sup> R. Sokolova, S. Giannarelli, N. Fanelli, L. Pospisil, Electrochemical bond cleavage in pesticide ioxynil. Kinetic analysis by voltammetry and impedance spectroscopy, *Bulg. Chem. Commun.*, **2017**, 49, 134-138
- <sup>204</sup> A. J. Bard, L. R. Faulkner, *Electrochemical Methods, Fundamentals and Applications*, 2<sup>nd</sup> ed. John Wiley & Sons, Inc, New York, **2001**
- <sup>205</sup> C. H. Hamann, A. Hamnett, W. Vielstich, *Electrochemistry*, 2<sup>nd</sup> ed. Wiley-VCH, Weinheim, **2007**
- <sup>206</sup> R. S. Patil, V. A. Juvekar, V. M. Naik, Oxidation of chloride ion on platinum electrode: dynamics of electrode passivation and its effect on oxidation kinetics, *Ind. Eng. Chem. Res.*, **2011**, 50, 12946-12959 DOI: 10.1021/ie200663a
- <sup>207</sup> K. Wu, T. Zhang, L. Zhan, C. Zhong, S. Gong, Z. -H. Lu, C. Yang, Tailoring Optoelectronic Properties of Phenanthroline-Based Thermally Activated Delayed Fluorescence Emitters through Isomer Engineering, *Adv. Optical Mater.*, **2016**, 4, 1558-1566 DOI: 10.1002/adom.201600304
- <sup>208</sup> **J. Wantulok**, R. Sokolova, I. Degano, V. Kolivoska, J. E. Nycz, The effects of 4,7-di(pyrrolidin-1-yl) substituents on the reduction and oxidation mechanisms of 1,10-phenanthrolines: new perspectives in tailoring of phenanthroline derivatives, *Electrochimica Acta*, **2021**, 137674 DOI: 10.1016/j.electacta.2020.137674
- <sup>209</sup> J. -M. Savéant, *Elements of Molecular and Biomolecular Electrochemistry. An Electrochemical Approach to Electron Transfer Chemistry*, John Wiley and Sons, Inc., New Jersey, **2006**

- 
- <sup>210</sup> W. Liu , Y. Ma , Y. W. Yin , Y. F. Zhao , Anodic Cyanation of 1-arylpiperidines, *Bull. Chem. Soc. Jpn.*, **2006**, 79,577-579 DOI: 10.1246/bcsj.79.577
- <sup>211</sup> S. S. Libendi , Y. Demizu , O. Onomura , Direct electrochemical alpha-cyanation of N-protected cyclic amines, *Org. Biomol. Chem.*, **2009**, 7, 351-356 DOI: 10.1039/B816598J
- <sup>212</sup> T. Golub , J. Y. Becker, Electrochemical oxidation of amides of type Ph<sub>2</sub>CHCONHAr, *Org. Biomol. Chem.*, **2012**, 10, 3906-3912 DOI: 10.1039/C2OB06878H
- <sup>213</sup> P. Zuman , *Substituent Effects in Organic Polarography*, Plenum Press, New York, **1967**
- <sup>214</sup> R. Sokolova, M. Gal, M. Valasek, New proton donors in electrochemical mechanistic studies in non-aqueous solution dimethyl sulfoxide: chlorinated hydroxybenzonnitriles, *J. Electroanal. Chem.*, **2012**, 685, 33–36 DOI: 10.1016/j.jelechem.2012
- <sup>215</sup> **J. Wantulok**, R. Sokolova, I. Degano, V. Kolivoska, J. E. Nycz, J. Fiedler, Spectroelectrochemical properties of 1,10-phenanthroline substituted by phenothiazine and carbazole redox-active units, *ChemElectroChem*, **2021**, 8, 2935-2943 DOI: 10.1002/celec.202100835
- <sup>216</sup> E. T. Seo, R. F. Nelson, J. M. Fritsch, L. S. Marcoux, D. W. Leedy, R. N. Adams, Anodic Oxidation Pathways of Aromatic Amines. Electrochemical and Electron Paramagnetic Resonance Studies, *J. Am. Chem. Soc.*, **1966**, 88, 3498-3503 DOI: 10.1021/ja00967a006
- <sup>217</sup> K. Y. Chiu, T. X. Su, J. H. Li, T. H. Lin, G. S. Liou, S. H. Cheng, Novel trends of electrochemical oxidation of amino-substituted triphenylamine derivatives, *J. Electroanal. Chem.*, **2005**, 575, 95-101 DOI: 10.1016/j.jelechem.2004.09.005
- <sup>218</sup> L. Kortekaas, F. Lancia, J. D. Steen, W. R. Browne, Reversible Charge Trapping in Bis-Carbazole-Diimide Redox Polymers with Complete Luminescence Quenching Enabling Nondestructive Read-Out by Resonance Raman Spectroscopy, *J. Phys. Chem. C*, **2017**, 121, 14688-14702 DOI: 10.1021/acs.jpcc.7b04288
- <sup>219</sup> J. C. Imbeaux, J. M. Saveant, Convolutive potential sweep voltammetry: I. Introduction, *J. Electroanal. Chem.*, **1973**, 44, 169-187 DOI: 10.1016/S0022-0728(73)80244-X
- <sup>220</sup> T. Pajkossy, Analysis of quasi-reversible cyclic voltammograms: Transformation to scan-rate independent form, *Electrochem. Commun.*, **2018**, 90, 69-72 DOI: 10.1016/j.elecom.2018.04.004
- <sup>221</sup> J. B. Flanagan, S. Margel, A. J. Bard, F. C. Anson, Electron transfer to and from molecules containing multiple, noninteracting redox centers. Electrochemical oxidation of poly(vinylferrocene), *J. Am. Chem. Soc.*, **1978**, 100, 4248-4253 DOI: 10.1021/ja00481a040
- <sup>222</sup> F. Ammar, J. M. Saveant, Convolution potential sweep voltammetry: II. Multistep nernstian waves, *J. Electroanal. Chem.*, **1973**, 47, 215-221 DOI: 10.1016/S0022-0728(73)80448-6
- <sup>223</sup> N. Das, A. M. Arif, P. J. Stang, M. Sieger, B. Sarkar, W. Kaim, J. Fiedler, Self-Assembly of Heterobimetallic Neutral Macrocycles Incorporating Ferrocene Spacer Groups: Spectroelectrochemical Analysis of the Double Two-Electron Oxidation of a Molecular Rectangle, *Inorg. Chem.*, **2005**, 44, 5798-5804 DOI: 10.1021/ic0481834
- <sup>224</sup> C. Wang, L. Lystrom, H. Yin, M. Hetu, S. Kilina, S. A. McFarland, W. Sun, Increasing the triplet lifetime and extending the ground-state absorption of biscyclometalated Ir(III) complexes for reverse saturable absorption and photodynamic therapy applications, *Dalton Trans.*, **2016**, 45, 16366-16378 DOI: 10.1039/C6DT02416E
- <sup>225</sup> L. Calucci, G. Pampaloni, C. Pinzino, A. Prescimone, Transition metal derivatives of 1,10-phenanthroline-5,6-dione: Controlled growth of coordination polynuclear derivatives, *Inorganica Chim. Acta*, **2006**, 359, 3911-3920 DOI: 10.1016/j.ica.2006.04.040
- <sup>226</sup> A. S. Touchy, S. M. A. H. Siddiki, W. Onodera, K. Kona, K.-I. Shimizu, Hydrodeoxygenation of sulfoxides to sulfides by a Pt and MoO<sub>x</sub>-co-loaded TiO<sub>2</sub> catalyst, *Green Chem.*, **2016**, 18, 2554-2560 DOI: 10.1039/C5GC02806J
- <sup>227</sup> C. Hiort, P. Lincoln, B. Norden, DNA binding of Δ- and Λ-[Ru(phen)<sub>2</sub>DPPZ]<sup>2+</sup>, *J. Am. Chem. Soc.*, **1993**, 115, 3448-3454 DOI: 10.1021/ja00062a007

- 
- <sup>228</sup> A. Itoh, Y. Masaki, Synthesis and Application of New Phenyl-Functionalized Zeolites as Protection Against Radical Bromination at the Benzylic Position, *Synlett*, **1997**, 12, 1450-1452 DOI: 10.1055/s-1997-1070
- <sup>229</sup> Th. Curtius, E. Quedenfeldt, Ueber symmetrisches Dibenzylhydrazin, *J. Prakt. Chem.*, **1898**, 58, p. 369-392 DOI: 10.1002/prac.18980580118
- <sup>230</sup> G. Hardy, J. King-Underwood, G. Hardy, P. J. Murray, G. J. Williams, T. S. Onions, J. Gareth, Pyrazole p38 map kinase inhibitors, , **2013**, US2013029990A1
- <sup>231</sup> G. Moutiers, J. Pinson, F. Terrier, R. Goumont, Electrochemical Oxidation of  $\sigma$ -Complex-Type Intermediates in Aromatic Nucleophilic Substitutions, *Chem. Eur. J.*, **2001**, 7, 1712–1719 DOI: 10.1002/1521-3765(20010417)7:8<1712::AID-CHEM17120>3.0.CO;2-G
- <sup>232</sup> I. Gallardo, G. Guirado, J. Marquet, Nucleophilic Aromatic Substitution of Hydrogen: A Novel Electrochemical Approach to the Cyanation of Nitroarenes, *Chem. Eur. J.*, **2001**, 7, 1759-1765 DOI: 10.1002/1521-3765(20010417)7:8<1759::AID-CHEM17590>3.0.CO;2-F
- <sup>233</sup> H. Wynberg, The Reimer-Tiemann reaction. *Chem. Rev.*, **1960**, 169–184 DOI: 10.1021/cr60204a003
- <sup>234</sup> J. A. González-Vera, E. Luković, B. Imperiali, Synthesis of Red-Shifted 8-Hydroxyquinoline Derivatives Using Click Chemistry and Their Incorporation into Phosphorylation Chemosensors. *J. Org. Chem.*, **2009**, 74, 7309–7314 DOI: 10.1021/jo901369k
- <sup>235</sup> X. Ding, F. Zhang, Y. Bai, J. Zhao, X. Chen, M. Ge, W. Sun, Quinoline-based highly selective and sensitive fluorescent probe specific for Cd<sup>2+</sup> detection in mixed aqueous media, *Tetrahedron Lett.*, **2017**, 58, 3868–3874 DOI: 10.1016/j.tetlet.2017.08.068
- <sup>236</sup> S. S Mahajan, M. Scian, S. Sripathy, J. Posakony, U. Lao, T. K. Loe, V. Leko, A. Thalhoffer, A. D. Schuler, A. Bedalov, J. A. Simon, Development of Pyrazolone and Isoxazol-5-one Cambinol Analogues as Sirtuin Inhibitors, *J. Med. Chem.*, **2014**, 57, 3283–3294 DOI: 10.1021/jm4018064
- <sup>237</sup> B. Machura, J. Mišek, J. Kusz, J. Nycz, D. Tabak, Reactivity of oxorhenium(V) complexes towards quinoline carboxylic acids. X-ray structure of [ReOCl<sub>2</sub>(hquin-7-COOH)(PPh<sub>3</sub>)]·OPPh<sub>3</sub>, [ReOBr<sub>2</sub>(hquin-7-COOH)(PPh<sub>3</sub>)] and [ReOX<sub>2</sub>(hmquin-7-COOH)(PPh<sub>3</sub>)]. DFT and TD-DFT calculations for [ReOCl<sub>2</sub>(hquin-7-COOH)(PPh<sub>3</sub>)], *Polyhedron*, **2008**, 27, 1121-1130 DOI: 10.1016/j.poly.2007.12.006
- <sup>238</sup> S. Lytton, B. Mester, I. Dayan, H. Glickstein, J. Libman, A. Shanzer, Z. Cabantchik, Mode of action of iron (III) chelators as antimalarials: I. Membrane permeation properties and cytotoxic activity, *Blood*, **1993**, 81, 214–221 DOI: 10.1182/blood.V81.1.214.214
- <sup>239</sup> J. Phillips, The Reactions Of 8-Quinolinol, *Chem. Rev.*, **1956**, 56, 271–297 DOI: 10.1021/cr50008a003
- <sup>240</sup> B. Szpakiewicz, M. Grzegozek, Vicarious nucleophilic amination of nitroquinolines with 4-amino-1,2,4-triazole. *Can. J. Chem.*, **2008**, 86, 682–685 DOI: 10.1139/v08-051
- <sup>241</sup> E. A. Bocharova, L. M. Gornostaev, N. P. Gritsan, T. N. Gurova, Amination of 3,5-dibromo-4-nitrosoanilines and 3-halo-4-nitrosophenols. *Russ. J. Org. Chem.*, **2010**, 46, 1639–1644 DOI: 10.1134/S1070428010110047
- <sup>242</sup> A. J. Nicholls, A. S. Batsanov, I. R. Baxendale, Copper-Mediated Nitrosation: 2-Nitrosophenolato Complexes and Their Use in the Synthesis of Heterocycles. *Molecules*, **2019**, 24, 4154 DOI: 10.3390/molecules24224154
- <sup>243</sup> G. Malecki, J. E. Nycz, E. Ryrych, L. Ponikiewski, M. Nowak, J. Kusz, J. Pikies, Synthesis, spectroscopy and computational studies of some biologically important hydroxyhaloquinolines and their novel derivatives. *J. Mol. Struct.*, **2010**, 969, 130–138 DOI: 10.1016/j.molstruc.2010.01.054
- <sup>244</sup> M. Szala, J. E. Nycz, G. J. Malecki, R. Sokolova, S. Ramesova, A. Switlicka-Olszewska, R. Strzelczyk, R. Podsiadly, B. Machura, Synthesis of 5-azo-8-hydroxy-2-methylquinoline dyes and relevant spectroscopic, electrochemical and computational studies, *Dye. Pigment.*, **2017**, 142, 277–292 DOI: 10.1016/j.dyepig.2017.03.043
- <sup>245</sup> I. Gaussian 09, Revision A.02, Frisch M. J., Trucks G. W., Schlegel H. B., Scuseria G. E., Robb M. A., Cheeseman J. R., Scalmani G., Barone V., Petersson G. A., Nakatsuji H., Li X., Caricato M.,

---

Marenich A., Bloino J., Janesko B. G., Gomperts R., Mennucci B., Hratchian H. P., Ortiz J. V., Izmaylov A. F., Sonnenberg J. L., Williams-Young D., Ding F., Lipparini F., Egidi F., Goings J., Peng B., Petrone A., Henderson T., Ranasinghe D., Zakrzewski V. G., Gao J., Rega N., Zheng G., Liang W., Hada M., Ehara M., Toyota K., Fukuda R., Hasegawa J., Ishida M., Nakajima T., Honda Y., Kitao O., Nakai H., Vreven T., Throssell K., Montgomery J. A. Jr., Peralta J. E., Ogliaro F., Bearpark M., Heyd J. J., Brothers E., Kudin K. N., Staroverov V. N., Keith T., Kobayashi R., Normand J., Raghavachari K., Rendell A., Burant J. C., Iyengar S. S., Tomasi J., Cossi M., Millam J. M., Klene M., Adamo C., Cammi R., Ochterski J. W., Martin R. L., Morokuma K., Farkas O., Foresman J. B., and D. J. Fox, Gaussian, Inc., Wallingford CT, **2016**.

<sup>246</sup> A. D. Becke, Density-functional thermochemistry. III. The role of exact exchange, *J. Chem. Phys.*, **1993**, 98, 5648-5652 DOI: 10.1063/1.464913

<sup>247</sup> C. Lee, W. Yang, R. G. Parr, Development of the Colle-Salvetti correlation-energy formula into a functional of the electron density, *Phys. Rev. B*, **1988**, 37, 785-789 DOI: 10.1103/PhysRevB.37.785

<sup>248</sup> M. Krejčík, M. Danek, F. Hartl, Simple construction of an infrared optically transparent thin-layer electrochemical cell: Applications to the redox reactions of ferrocene,  $\text{Mn}_2(\text{CO})_{10}$  and  $\text{Mn}(\text{CO})_3(3,5\text{-di-}t\text{-butyl-catecholate})^-$ , *J. Electroanal. Chem.*, **1991**, 317, 179-187 DOI: 10.1016/0022-0728(91)85012-E

<sup>249</sup> D. Wang, D. Kuang, F. Zhang, C. Yang, X. Zhu, Room-Temperature Copper-Catalyzed Arylation of Dimethylamine and Methylamine in Neat Water, *Adv. Synth. Catal.*, **2015**, 357, 714–718 DOI: 10.1002/adsc.201400785

<sup>250</sup> C. J. Whiteoak, O. Planas, A. Company, X. Ribas, A First Example of Cobalt-Catalyzed Remote C–H Functionalization of 8-Aminoquinolines Operating through a Single Electron Transfer Mechanism, *Adv. Synth. Catal.*, **2016**, 358, 1679–1688 DOI: 10.1002/adsc.201600161

<sup>251</sup> M. Gasiorowska, J. Typek, J. A. Soroka, M. J. Sawicka, E. K. Wróblewska, N. Guskos, G. Zolnierkiewicz, Spectroscopic and magnetic properties of solvatochromic complex of  $\text{Cu}^{2+}$  and novel 3*H*-indolium derivative, *Spectrochim. Acta A*, **2014**, 124, 300–307 DOI: 10.1016/j.saa.2014.01.007

<sup>252</sup> H. Fiedler, Synthesis of methyl-8-hydroxyquinoline aldehydes, *Arch. Pharm.*, **1960**, 293, 609–621 DOI: 10.1002/ardp.19602930606

<sup>253</sup> D. Prema, A. V. Wiznycia, B. M. T. Scott, J. Hilborn, J. Despera, C. J. Levy, Dinuclear zinc(II) complexes of symmetric Schiff-base ligands with extended quinoline sidearms, *Dalton Trans.*, **2007**, 4788–4796 DOI: 10.1039/B709454J

<sup>254</sup> H. Junzo, M. Hiroyuki, H. Kenji, Z. Kiyoshi, A ratiometric fluorescent chemosensor, 1,10-phenanthroline-4,7-dione, for anions in aqueous–organic media. *Tetrahedron Lett.*, **2007**, 48, 4861–4864 DOI: 10.1016/j.tetlet.2007.05.045

<sup>255</sup> M. F. Belian, H. J. Batista, A. G. S. Bezerra, W. E. Silva, G. F. de Sá, Jr. S. Alves, Eu(III) complex luminescence behavior upon chlorine substitution in the 1,10-phenanthroline ligand: A theoretical and experimental study, *Chem. Phys.*, **2011**, 381, 29–34 DOI: 10.1016/j.chemphys.2011.01.005

<sup>256</sup> A. C. Edwards, C. Wagner, A. Geist, N. A. Burton, C. A. Sharrad, R. W. Adams, R. G. Pritchard, P. J. Panak, R. C. Whitehead, L. M. Harwood, Exploring electronic effects on the partitioning of actinides(III) from lanthanides(III) using functionalised bis-triazinyl phenanthroline ligands, *Dalton Trans.*, **2016**, 45, 18102–18112 DOI: 10.1039/C6DT02474B

<sup>257</sup> A. Maroń, J. E. Nycz, B. Machura, Jan. G. Małecki, Luminescence properties of palladium(II) phenanthroline derivative coordination compounds, *ChemistrySelect*, **2016**, 1, 798-804 DOI: 10.1002/slct.201600143

<sup>258</sup> A. C. Edwards, A. Geist, U. Müllich, C. A. Sharrad, R. G. Pritchard, R. C. Whitehead, L. M. Harwood, Transition metal-free, visible-light mediated synthesis of 1,10-phenanthroline derived ligand systems, *Chem. Commun.*, **2017**, 53, 8160–8163 DOI: 10.1039/C7CC03903D

<sup>259</sup> G. Zucchi, V. Murugesan, D. Tondelier, D. Aldakov, T. Jeon, F. Yang, P. Thuéry, M. Ephritikhine, B. Geffroy, Solution, solid state, and film properties of a structurally characterized highly luminescent molecular europium plastic material excitable with visible light, *Inorg. Chem.*, **2011**, 50, 4851–4856 DOI: 10.1021/ic2000415

- 
- <sup>260</sup> M. Li, L. Li, H. Ge, Direct C-3-Alkenylation of Quinolones via Palladium-Catalyzed C-H Functionalization, *Adv. Synth. Catal.*, **2010**, 352, 2445-2449 DOI: 10.1002/adsc.201000364
- <sup>261</sup> D. Ding, H. Jiang, X. Ma, J. J. Nash, H. I. Kanttamaa, Effects of the Distance between Radical Sites on the Reactivities of Aromatic Biradicals, *J. Org. Chem.*, **2020**, 85, 13, 8415–8428 DOI: 10.1021/acs.joc.0c00658
- <sup>262</sup> C. Wen, R. Zhong, Z. Qin, M. Zhao, J. Li, Regioselective remote C5 cyanoalkoxylation and cyanoalkylation of 8-aminoquinolines with azobisisobutyronitrile, *Commun. Chem.*, **2020**, 56, 9529-9532 DOI: 10.1039/D0CC00014K
- <sup>263</sup> N. D. Heindel, C. J. Ohnmacht, 2-methyl-1,10-phenanthroline: A direct and a serendipitous synthesis, *J. Heterocycl. Chem.*, **1968**, 5, 869-870 DOI: 10.1002/jhet.5570050623
- <sup>264</sup> N. A. Voloshin, A. V. Chernyshev, S. O. Bezuglyi, A. V. Metelitsa, E. N. Voloshina, V. I. Minkin, Spiropyrans and spirooxazines 4. Synthesis and spectral properties of 6 ‘-halo-substituted spiro[indoline-2,2’-2H-pyrano[3,2-h]quinolines], *Russ. Chem. Bull. Int. Ed.*, **2008**, 57, 151–158 DOI: 10.1007/s11172-008-0022-y
- <sup>265</sup> K. Skonieczny, G. Charalambidis, M. Tasiar, M. Krzeszewski, A. Kalkan-Burat, A. G. Coutsolelos, D. T. Gryko, General and Efficient Protocol for Formylation of Aromatic and Heterocyclic Phenols, *Synthesis*, **2012**, 44, 3683–3687 DOI: 10.1055/s-0032-1317500
- <sup>266</sup> B. Bobranski, Über den Oxy-6-chinolin-aldehyd-5 und einige daraus dargestellte 5,6-substituierte Chinolinabkömmlinge, *J. Prakt. Chem.*, **1932**, 134, 141–152 DOI: 10.1002/prac.19321340403
- <sup>267</sup> C. Sen, T. Sahoo, H. Singh, E. Suresh, S. C. Ghosh, Visible Light-Promoted Photocatalytic C-5 Carboxylation of 8-Aminoquinoline Amides and Sulfonamides via a Single Electron Transfer Pathway, *J. Org. Chem.*, **2019**, 84, 9869–9896 DOI: 10.1021/acs.joc.9b00942
- <sup>268</sup> A.V. Müller, L. D. Ramos, K. P. M. Frin, K. T. De Oliveira, A. S. Polo, A high efficiency ruthenium(ii) tris-heteroleptic dye containing 4,7-dicarbazole-1,10-phenanthroline for nanocrystalline solar cells. *RSC Adv.*, **2016**, 6, 46487–46494 DOI: 10.1039/C6RA08666G